Proactive Optimisation of Intelligent Wells under Uncertainty

Morteza Haghighat Sefat

Submitted for the degree of Doctor of Philosophy

Heriot-Watt University

School of Energy, Geoscience, Infrastructure and Society

Institute of Petroleum Engineering

October 2016

Abstract

The number of installations of intelligent well (I-well) completions, which are providing layer-by-layer monitoring and control capability of production or injection, is growing. However, the number of available techniques for optimal control of I-wells is limited. Currently, most of the I-wells which are equipped with Interval Control Valves (ICVs) are operated to enhance the short-term production and to resolve problems associated with breakthrough of the unfavourable phase. This reactive strategy is unlikely to deliver the long-term optimum production targets. On the other side, the proactive control strategy of I-wells, with its ambition to provide the optimum control for entire well's production life, has a potential to maximize the cumulative oil production and/or reduce the cumulative water production. This strategy, however, results in a high dimensional optimisation problem with a computationally demanding and uncertain objective function based on one or more simulated reservoir model(s).

This thesis investigates the challenging proactive optimisation problem and its solution for detailed modelling of I-wells. The desire is to develop algorithm and guidelines that could be readily used by engineers to solve proactive optimisation problems for large real field models with limited computational resources. The black-box characteristics of most of the commercial reservoir simulators has limited the use of gradient-based algorithms despite their efficiency in solving large-scale optimisation problems. Stochastic estimation of the (steepest) gradient by simultaneous perturbation of all control variables is proposed in this thesis and shown to provide a fast and efficient solution to the I-well proactive optimisation problem.

A novel framework for robust proactive optimisation of ICVs under reservoir's description uncertainty, quantified by multiple model realisations, is developed. A small representative ensemble of model realizations that performs in an equivalent manner to all available realizations is systematically selected. A utility function is then calculated accounting for both the expectation and variance of the objective function so as to account for both the field development value and risk.

The proposed robust proactive optimisation framework has been tested on several case-studies. The practicality of the developed framework is illustrated by optimising a real North Sea intelligent field development with a single high-end workstation.

Dedication

I dedicate this thesis to my beloved mother (Zhaleh) and my father (Mohsen) for their prayers, support and encouragement.

Acknowledgment

I would like to express my sincere appreciation to all those who made this thesis possible.

I owe a special gratitude to my supervisors Prof. David Davies and Dr. Khafiz Muradov for their patience and continuous help and support during my PhD study. I also thank Dr. Ahmed Elsheikh for the valuable advice and support during this research.

I wish to thank the examiners Profs Jan Dirk Jansen, Geir Nævdal and Dr. Vasily Demyanov for their time and valuable comments.

I am thankful to my colleagues: Dr. Ivan Grebenkin, Dr. Reza Malakooti, Faraj Zarei, Dr. Mojtaba Moradi, Ehsan Nikjoo, Dr. Yousef Rafiei and other members of "Value from Advanced Wells" (VAWE) Joint Industry Project for their invaluable discussion and moral support.

I thank sponsors of the "VAWE" JIP at Heriot-Watt University for the financial support and feedback. I am also especially grateful to Dr. Steve Todman, Dr. Andrew Carnegie, Jeremy Rhodes, Ross Waterhouse, Craig Durham and Dr. Alexander Kuznetsov for their comments and data provided for research.

Last but not least, I sincerely thank my father (Mohsen) and my mother (Zhaleh) for their continuous support, patience and encouragement during all my life. I would also like to thank my sisters (Sara & Sahar), other family members and friends for their moral support during this period.

ACADEMIC REGISTRY

Research Thesis Submission

Name*:*	Morteza Haghighat Sefat		
School:	Energy, Geoscience, Infrastructure and Society		
Version: *(i.e. First, Resubmission, Final)*	Final	Degree Sought:	PhD in Petroleum Engineering

Declaration

In accordance with the appropriate regulations I hereby submit my thesis and I declare that:

1) the thesis embodies the results of my own work and has been composed by myself
2) where appropriate, I have made acknowledgement of the work of others and have made reference to work carried out in collaboration with other persons
3) the thesis is the correct version of the thesis for submission and is the same version as any electronic versions submitted*.
4) my thesis for the award referred to, deposited in the Heriot-Watt University Library, should be made available for loan or photocopying and be available via the Institutional Repository, subject to such conditions as the Librarian may require
5) I understand that as a student of the University I am required to abide by the Regulations of the University and to conform to its discipline.
6) I confirm that the thesis has been verified against plagiarism via an approved plagiarism detection application e.g. Turnitin.

* *Please note that it is the responsibility of the candidate to ensure that the correct version of the thesis is submitted.*

Signature of Candidate*:*		Date:	

Submission

Submitted By *(name in capitals):*	MORTEZA HAGHIGHAT SEFAT
Signature of Individual Submitting:	
Date Submitted:	

For Completion in the Student Service Centre (SSC)

Received in the SSC by *(name in capitals):*			
Method of Submission *(Handed in to SSC; posted through internal/external mail):*			
E-thesis *Submitted (**mandatory for final theses)***			
Signature:		Date:	

Table of Contents

Nomenclature

Symbols

a	=	tuning parameter controlling search step
A_c	=	cross-section area of the constriction
A_p	=	cross-sectional area of the pipe
$\mathbb{A}$	=	SPSA tuning parameter
A	=	tuning constant in utility function
b	=	annual discount rate
c	=	tuning parameter controlling perturbation step
c_k	=	perturbation step
C_v	=	dimensionless flow coefficient for the valve
d	=	average dissimilarity
D_p	=	pipe diameter
D	=	distance measure functions
e	=	absolute roughness
E	=	expected value
f	=	Fanning friction factor
f_w	=	fractional flow of water
$\mathcal{F}$	=	objective function
g	=	standard (finite-difference) gradient
$\hat{g}$	=	stochastically estimated gradient
$\overline{\hat{g}_k}$	=	average stochastically estimated gradient
h	=	data dimension (low)
H	=	data dimension (high)
$H_{v,out}$	=	outlet velocity head
$H_{v,in}$	=	inlet velocity head
I	=	instantaneous objective function
ℓ_∞	=	infinity norm
L_p	=	pipe length
m_i	=	reservoir simulator input space
n_e	=	number of ensembles
n_x	=	number of control parameters
N_c	=	number of clusters

N_{copt}	=	optimum number of clusters
N_p	=	number of production wells
N_r	=	number of realisation
N_z	=	number of production zones
O_i	=	reservoir simulator output/response space
p	=	dimension of the state vector
q	=	average rate
q_m	=	mixture flow rate
Q	=	production potential
r	=	price/cost
$\mathbb{R}$	=	real numbers
R_e	=	Reynolds number
S	=	total number of simulation steps
Sil	=	Silhouette value
$\overline{Sil}$	=	average Silhouette value
t	=	time
t_n	=	cumulative time up to simulation step n
u	=	random direction of directional derivative
U	=	matrix of perturbed control variables for all ensembles
$\mathcal{U}$	=	utility function
$\mathbb{U}$	=	high-dimensional original space
$\mathbb{u}$	=	low-dimensional mapped space
w	=	mass flow rate
x	=	vector of control parameters
y	=	state vector of the reservoir
Y	=	matrix of objective values for all ensembles
α_k	=	search step
∂	=	partial derivative
ϑ	=	SPSA tuning parameter
γ	=	SPSA tuning parameter
τ	=	locations of the clusters centre
δ	=	dissimilarity (distance)
δP_f	=	frictional pressure drop
δP_a	=	acceleration pressure drop

δP_{cons}	=	pressure drop due to the constriction
δt^n	=	length of the nth simulation step
Δ	=	vector of random variables
θ_r	=	reservoir state vector for realisation r
θ_{r_0}	=	initial reservoir state vector for realisation r
ρ	=	fluid density
v	=	fluid velocity
$\emptyset$	=	constraint term
∇	=	Jacobian operator

Subscripts

0	=	initial value
g	=	gas
k	=	iteration index
l	=	liquid
min	=	minimum value
max	=	maximum value
o	=	oil
pw	=	produced water
r	=	model realization
w	=	water
∞	=	infinity

Superscripts

n	=	simulation step index
T	=	transpose
-1	=	inverse

Abbreviations

AICD	=	Autonomous Inflow Control Device
AFCD	=	Autonomous Flow Control Device
AFI	=	Annular Flow Isolation
AWC	=	Advanced well completion
BHP	=	Bottom Hole Pressure
CDF	=	Cumulative Distribution Function

CPU	=	Central Processing Unit
EnOpt	=	Ensemble-based Optimization
EnKF	=	Ensemble Kalman Filter
ft	=	feet
GA	=	Genetic Algorithms
GPS	=	Generalized Pattern Search method
GUF	=	Gas-lift Utilisation Factor
GOR	=	Gas-Oil-Ratio
HJ	=	Hooke-Jeeves
ICD	=	Inflow Control Device
ICV	=	Interval Control Valve
IV	=	Infinitely Variable
I-field	=	Intelligent field
I-wells	=	Intelligent wells
LSDF	=	Line-Search Derivative Free
mD	=	millidarcy
MILP	=	Mixed-Integer Linear Programming
MM	=	Million (10^6)
MDS	=	Multi-Dimensional Scaling
NM	=	Nelder-Mead
NPV	=	Net Present Value
PCA	=	Principal Component Analysis
PDF	=	Probability Distribution Function
PSC	=	Passive Stinger Completion
PSO	=	Particle Swarm Optimization
ROM	=	Reduced Order Model
SA	=	Simulated Annealing
SAS	=	Stand Alone Screen
SCF	=	Standard Cubic Feet
SGSD	=	Stochastic Gaussian Search Direction
Sm^3	=	Standard cubic meter
SPSA	=	Simultaneous Perturbation Stochastic Approximation
STB	=	Stock Tank Barrel
SQP	=	Sequential Quadratic Programming
THP	=	Tubing Head Pressure
VFP	=	Vertical Flow Performance
WC	=	Water-Cut
SIM	=	Reservoir simulator function
$	=	US dollar

Publications by the Candidate

Journal papers:

1. Haghighat Sefat, M., Elsheikh, A. H., Muradov, K. M. & Davies, D. R. 2015. Reservoir uncertainty tolerant, proactive control of intelligent wells. Computational Geosciences, 1-22.

2. Haghighat Sefat, M., Muradov, K. M., Elsheikh, A. H. & Davies, D. R. 2016. Proactive Optimization of Intelligent Well Production Using Stochastic Gradient-Based Algorithms. SPE Reservoir Evaluation & Engineering.

Conference presentations:

1. Haghighat Sefat, M., Muradov, K. M. & Davies, D. R. 2013. Field Management by Proactive Optimisation of Intelligent Wells - A Practical Approach. SPE Middle East Intelligent Energy Conference and Exhibition. Dubai, UAE.

2. Haghighat Sefat, M., Muradov, K. M., Elsheikh, A. H. & Davies, D. R. 2014. Reservoir Uncertainty-tolerant, Proactive Control of Intelligent Wells. ECMOR XIV - 14th European conference on the mathematics of oil recovery Italy: EAGE.

3. Haghighat Sefat, M., Muradov, K. M., Elsheikh, A. H. & Davies, D. R. 2014. Optimisation of Intelligent Oil Wells using Stochastic Algorithms. 20th Conference of the International Federation of Operational Research Societies, Spain.

4. Haghighat Sefat, M., Muradov, K. M. & Davies, D. R. 2016. "Optimal Field Development and Control Yields Accelerated, More Reliable, Production: A North Sea Case Study", SPE Intelligent Energy International, September 2016, Aberdeen.

Chapter 1– Introduction

Intelligent wells (I-wells) add downhole (zonal) control and monitoring capabilities to the traditional conventional wells. Downhole control provides the opportunity to reduce the number of wells to be drilled and to accelerate oil production by commingled production from different reservoir layers (zones). Moreover, the optimal control of zonal production (or injection) can reduce the production of unwanted fluids, and increase oil recovery. However, the risks associated with a non-optimum control increases at the same time due to possible production loss compared to the no control case. Several types of downhole control devices have been developed suitable for different reservoir types and well functions. The maximum control flexibility is provided by using multiple, downhole, Interval Control Valves (ICVs) installed across the well completion intervals. The ICV control strategy can be:

1. Short-Term, Reactive Control strategy to achieve instantaneous goals; e.g. maximise oil production, minimise unwanted fluids production, manage tubing and production network performance, etc.
2. Long-Term, Proactive Control strategy to improve long-term objectives e.g. Net Present Value (NPV) or cumulative oil production.

Currently, most I-wells are operated to enhance current production and to resolve recognised problems. Reactive strategy alone requires solving a relatively simple nonlinear optimisation problem describing current condition of the production system. By contrast, the proactive control strategy has the ambition to provide optimum control for the entire well's production life; results in the necessity to find solution to a high-dimensional, nonlinear and uncertain optimization problem. The complexity of proactive optimisation substantially increases when it is applied to large oil and gas fields with multiple I-wells each equipped with multiple ICVs. Currently available, commercial optimisation software cannot achieve this.

1.1. Thesis Motivations and Objectives

With the number of I-field developments increasing, for example to provide an economic field development scenario in low oil price by comingled production from

multiple reservoirs, the need for a robust optimal framework to control these fields increases. This thesis develop an efficient framework for robust optimal control of I-fields with the focus on immediate real field, industrial applications.

Following are the main objectives of this study and the key findings in each area,

a. Understand the nature of the proactive optimisation problem. Previous studies (Holmes et al., 1998) investigated the detailed, realistic modelling of I-wells. One of the novel aspects of this thesis is investigating the impact of the modelling approach on the proactive optimisation problem. It is shown that, a detailed modelling approach results in a more complicated optimisation problem while it is a better representation of reality. The optimisation framework is developed considering the realistic modelling of I-wells.

b. Develop criteria for simplification of the proactive optimisation problem with only a minor loss in "added-value" by inclusion of engineering and mathematical understanding. The novel idea of a combined proactive and reactive approach for control of I-fields is scrutinised in this thesis. It is shown that plateau period with oil rate constraint in the most important period for proactive optimisation due to: (1) extra production capacity is available, therefore it is possible to improve sweep efficiency by manipulating the production without sacrificing current oil production (2) interaction between the control variables during this period, while the optimum value of one variable depends on the value of other variables, therefore all variables should be optimised simultaneously. A fast reactive control can optimise the production after the plateau period mostly by enhancing the outflow performance while reducing water production. The proposed combined approach reduces the computation time significantly and make optimization of real fields possible with limited computational resources.

c. Develop a fast, efficient, yet robust, framework to provide optimal proactive control of ICVs while recognising reservoir uncertainty. The search space in a proactive optimisation problem with detailed I-well model is investigated in this study. Previous studies investigated the search space in history matching (Oliver et al. (2008), Oliver and Chen (2011)) and in the production optimization (Jansen et al., 2009, van Essen et al., 2011, Fonseca et al., 2014). The search space in all these high-dimensional problems

is characterised by several local optima with objective values close to the global optimum. This characteristic of the search space and the fact that the objective function is calculated using a black-box commercial reservoir simulator makes stochastic gradient-based algorithm a suitable choice. Simultaneous Perturbation Stochastic Approximation (SPSA) is shown a good performance in several case studies.

A novel framework is developed to select a small ensemble of reservoir model realisations to account for the uncertain geological condition. The framework present an efficient combination of the standard projection and clustering methods with the focus on immediate application by an engineer with limited computational resources. A dissimilarity distance measure tailored to the subsequent proactive optimisation objectives is shown the best performance when projecting the realisations onto 2D space using multi-dimensional-scaling (MDS). Representative realisations are then selected from each cluster recognised using k-means clustering in the 2D space.

The so-called robust optimisation approach has been introduced in the petroleum engineering by Yeten et al. (2003) for well location optimisation, Bailey and Couet (2005) for maximising asset value in a gas field, and van Essen et al. (2013) for production and injection optimisation in conventional wells. The mean-variance approach to robust optimisation has been previously employed in history matching (Chen et al., 1999). This thesis investigates the performance of the mean-variance approach on proactive optimisation of I-wells, while the uncertainty is represented by a small number of realisations selected using the developed framework. It is shown that optimising an adjustable utility function, calculated using selected realisations by the developed framework can achieve a globally acceptable performance while significantly reduces the computation time. Generally, larger number of realisations need to be selected when the focus of optimisation is on reducing the variance (i.e. a risk averse control scenario).

Another novel aspect of this thesis is the application of the developed framework to a real North-sea intelligent field development case study. It efficiently handled the large number of control variables, the high computation time and the numerical instabilities, frequently experienced in proactive optimization of large, real-field simulation models. Reducing the number of wells to be drilled via an I-well development scenario resulted

in an increased, early-time, NPV. It may also accelerates field development and plateau production by speeding up the drilling process. The proactive optimization of ICVs extended the oil production plateau in all reservoir model realisations, ensuring that the early NPV gain was maintained. The robust control strategy of ICVs provides maximum expected added-value (i.e. increasing mean), while at the same time reducing the uncertainty in the operation (i.e. reducing the variance).

1.2. Thesis outline

Proactive optimisation of I-wells under reservoir uncertainty is investigated in this thesis as follows:

Chapter 2 starts with a literature review of advanced well completion technology. Available inflow control devices are presented and their control flexibility are compared with the main focus on ICVs. Realistic modelling of the advanced well completions is required in order to evaluate/compare performance of different inflow control devices and define appropriate optimum control strategy. The impact of the modelling approach on the proactive optimisation is investigated

Chapter 3 investigates the characteristic of the proactive optimisation problem by analysing the behaviour of the objective function and the correlation between the control variables. The objective is to reduce the number of proactive optimisation control variables by discarding variables of lower importance. This process simplifies the problem with a minimum loss in added-value. This is particularly important in computationally expensive field models with multiple I-wells each equipped with multiple ICVs. Two criteria are proposed to reduce the number of control variables by limiting the proactive optimisation period and reducing the control frequency.

Chapter 4 starts with the mathematical formulation of the proactive optimisation problem. It is shown how the search space can be visualised in a proactive optimisation problem to provide insight into its characteristics. The large number of control variables, and the observed fact that the search space is typically characterised by several local optima with values close to the global optimum ((Oliver et al., 2008, Oliver and Chen, 2011, Jansen et al., 2009, van Essen et al., 2011, Fonseca et al., 2014) and also Section 4.3), make gradient-based algorithms a good choice for proactive

optimisation of the ICVs. However, commercial reservoir simulators are a black-box to most users; limiting access to the data required for the efficient calculation of the gradients using the adjoint method. An alternative approach is the stochastic gradient approximation methods. The Simultaneous Perturbation Stochastic Approximation (SPSA) and the Ensemble-based optimisation (EnOpt) are evaluated in terms of convergence performance, parallel processing capabilities and the nature of the obtained control scenario from an operational point of view. Guidelines are provided for tuning of the corresponding parameters.

Chapter 5 addresses the problem of proactive optimisation under reservoir description uncertainty. The objective function is substituted with an augmented objective function (utility function) calculated using an ensemble of simulated reservoir model realisations. The reservoir model realisations are generated to quantify the uncertainty in the reservoir's description. The utility function accounts for both the expectation and the variance of the Net Present Value (NPV) by modifying the objective function when considering different reservoir model realizations.

Chapter 6 investigates robust optimisation of multiple reservoir model realisations. Consideration of all available model realizations is usually a prohibitively expensive option. By contrast, choosing a small ensemble of model realizations is computationally less demanding, but is subject to bias during the selection process. K-means clustering is applied for selecting an ensemble of model realizations to acceptably represent all available realizations. A distance measure, tailored to the proactive optimization application, is proposed and used to define the similarity/dissimilarity of the different realizations.

Chapter 7 applies some of the developed concepts to a real North-sea field with 3 intelligent and 8 conventional production wells. The impact of proactive optimisation of ICVs has also been investigated under different operational conditions (e.g. different water injection strategies, different control frequency). I-well development scenario with and without robust proactive control of ICVs is compared with a conventional well development scenario.

Chapter 8 summarises the thesis conclusions and provides recommendations for future work.

Chapter 2 – Modelling and Optimisation of Advanced Well Completions

2.1. Introduction

This chapter starts with a literature review of advanced well completion technology. The development of advanced well completions will be briefly reviewed followed by a short description of the available inflow control devices and their applications. The devices have varying levels of control flexibility, some of which limit the choice of control strategy. Two major control strategies (i.e. Reactive and Proactive) are described followed by a discussion of their advantages and disadvantages. Realistic modelling of the advanced well completions is required in order to evaluate/compare performance of different inflow control devices and define the appropriate optimum control strategy. The impact of the chosen modelling approach on optimum control is investigated.

2.2. Advanced Well Completions

Advances in the drilling technology have allowed the design of long and complex well trajectories that increase well production rates and recovery. However, developing such wells with a conventional completion generally fails to provide the ultimate added-value because they are prone to early breakthrough of unwanted fluids into an (often) limited section of the completion. Advanced well completions (AWCs) address this problem and showed great potential to improve production by providing flexible control of in/out flow from different zones in various well types. AWCs that provide downhole flow control and monitoring capabilities (Figure 2-1), generally known as Intelligent wells, are an integral element of intelligent oil and gas fields (a.k.a. I-fields, smart fields) (Robinson, 2003). Their ultimate aim is to improve reservoir management and reduce the number of wells to be drilled and deliver increased oil recovery while decreasing the required number of well interventions.

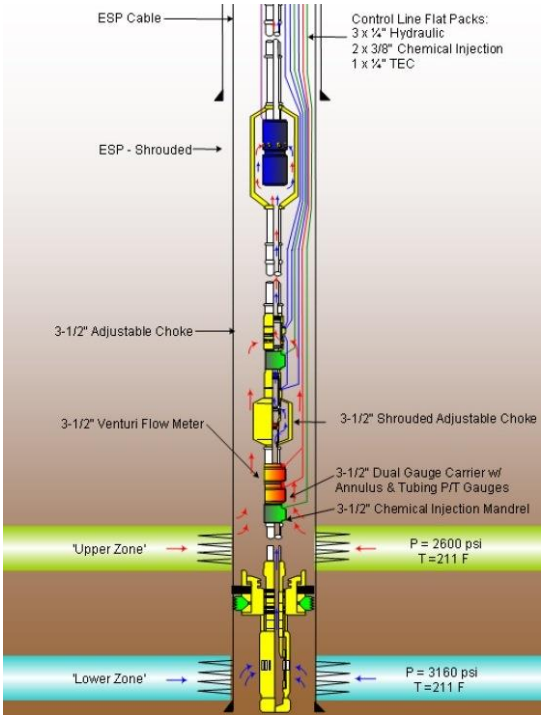

Figure 2-1: A two-zone I-well with control and monitoring capabilities (Courtesy of Baker Hughes, from (Vachon and Lee, 2007) with modification).

The major advanced well completion components can be classified as:

1. **Downhole flow control devices.** These devices enhance flow control flexibility by providing control of production/injection along the length of the completion zone in real time. By contrast conventional wells only provide surface control. Different downhole flow control devices are available and research is ongoing to develop new devices. The downhole flow control can be fixed (e.g. Inflow Control Devices (ICDs)), or variable. The latter is operated either intermittently using wireline or frequently via surface controlled Interval Control Valves (ICVs). Section 2.4 briefly explains the operation principles of the most common devices with the focus on ICVs which provide the active flow management required to implement the results from this study.
2. **Downhole monitoring devices.** Sensors provide zonal information to aid reservoir characterization, make decisions for flow control, and validate the applied control. Zonal pressure and temperature are the most common parameters measured. In this study monitoring devices are required to validate the applied control (i.e. change in the ICV flow area) during optimum proactive

control scenario. The current downhole single point pressure sensors provide an accuracy of ± 3 psi (Da Silva et al., 2012). The accuracy is thus normally sufficient to confirm that an ICV has been successfully operated.

The estimated zonal liquid production rate and water-cut is required for reactive control of ICVs. The current downhole Multi-Phase Flow Meters provide an accuracy of ± 5% of measurement of two-phase flow rate and water-cut (Da Silva et al., 2012). Zonal pressure and temperature data can also be translated into zonal liquid production rate, water-cut, etc. via virtual flow-metering with lower accuracy (Kawaguchi et al., 2013). The impact of measurement accuracy of flow rate and water-cut on reactive control of ICVs need further investigation. Detailed information about calculating zonal properties using downhole measured temperature and pressure data can be found in (Muradov, 2010) and (Malakooti, 2015).

3. **Annular flow isolation devices.** These annular isolation devices prevent undesirable flow between the advanced completions production zones. Advanced completions are frequently installed to manage comingled production when there is a contrast in zonal deliverability (permeability, pressure, water-cut) by imposing an extra pressure drop on some of the zones. Preventing annular flow allows the ICV to control the flow of the chosen zone and maximise the expected added-value. Annular Flow Isolation (AFI) is thus an integral part of an I-well completion. Packers and gravel packs are two common forms of AFI. Packers are the most common form of AFI, since installing gravel pack just for AFI seriously increase the complexity of the completion installation. Various types of packers are available with different setting mechanisms, costs, strength, etc. Al-Khelaiwi (2013) provides further background information on the different types of packers used in I-wells. Determining the number and placement of packers is another challenge in advanced well completions (Moradidowlatabad et al., 2014). A larger number of packers provides better isolation of the different zones; but also increases the cost and complexity of the completion as well as the installation risks. In this study we assume that adequate AFI is installed to provide acceptable annular isolation between the zones.

2.3. History of Advanced Well Completions

The first application of advanced well completions, with the objective of enhancing performance of the Troll Field production wells while using downhole flow control, goes back to the 1990s (Lien et al., 1991, Haug, 1992). The Troll field a giant gas field in the North Sea with a thin oil column (4-27 meters) above an aquifer. Initially the field was developed as a gas field while production of the thin oil column was deemed to be uneconomical using vertical wells. Advances in the drilling technology allowed a 500 m long horizontal well to be drilled in the thin-oil-column and subsequent long-term tests showed significant oil production potential (Lien et al., 1991). Production logging of these early horizontal wells showed that ~80% of the wells' length was initially open to flow. The unproductive 20% was thought to be due to insufficient clean-up, though some of these intervals were expected to gradually become productive (Lien et al., 1991). It was also observed that ~75% of the inflow originated from the first half (heel) of the completion interval due to the frictional pressure loss along the horizontal section being of the same order of magnitude as the reservoir drawdown. This phenomenon, known as the heel-toe effect, has an increasing impact on the completion's performance as the well length increases. Three different completion options were proposed to overcome this problem.

1. A Passive Stinger Completion (PSC). This is an extension of the tubing into the horizontal completion section that shifts the inflow into the production tubing from the heel of the well to a point near the middle of the well. This results in additional pressure drop for the produced fluid from the heel section; consequently reducing the production contribution at the heel and providing a greater opportunity for toe clean-up and production.
2. Variable density perforation. The well is perforated with a higher shot density in the toe section (to increase production from toe) and a lower shot density in the heel. The required perforation pattern is selected to equalise the well inflow. Well inflow calculations are performed with the objective of choosing a perforation density along the well that will achieve as near as possible uniform inflow along the length of the completion.
3. A downhole device to control inflow. This was the first generation of passive Inflow Control Devices (ICDs) (Figure 2-2) with adjustable length labyrinths

embedded in a sleeve surrounded by a pre-packed liner (Brekke and Lien, 2013). The produced fluid from each section passed through the labyrinth before entering the production string. Ten different channel lengths could be chosen depending on the pressure drop required at each location to balance the flow along the well length. The well in-flow is balanced by imposing an additional pressure drop on the higher production rate intervals due to (1) employing a device with more restrictive configuration (Figure 2-3) or (2) employing a device with a pressure drop that is proportional to flow rate.

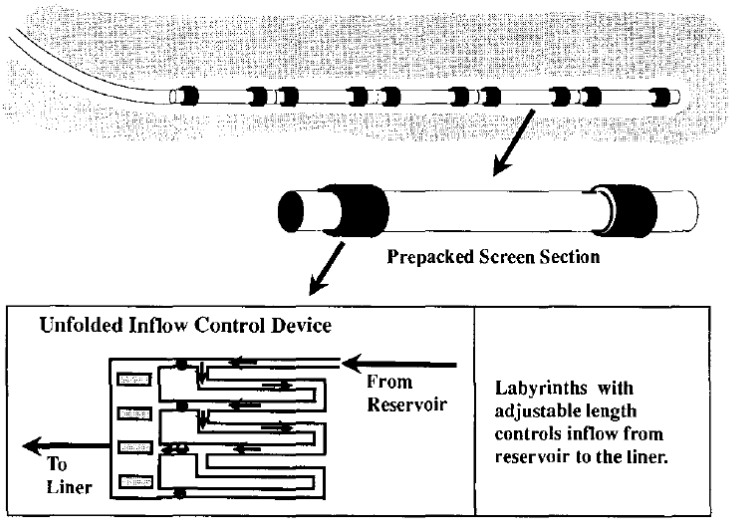

Figure 2-2: Schematic diagram of the first ICD (from (Brekke and Lien, 2013))

2.4. Downhole Flow Control Devices and Their Published Applications

An I-well downhole control device provides a restriction to flow that locally reduces the flow rate. They can be classified into 3 groups based on their reaction to the fluid flow.

2.4.1 Passive flow control: ICDs

These devices provide a single position, fixed, pre-determined flow restriction. The pressure drop along these devices changes with changing flow composition and rate. However, the flow area cannot be adjusted after the device has been installed. Optimum implementation of these devices requires a good knowledge of the reservoir

heterogeneity (and the expected production from each zone) as the device imposed restriction to each zone cannot be modified.

ICDs have also been used for various other applications requiring alleviating the zonal flow discrepancy from reservoir heterogeneity. ICD applications are illustrated by the following selected case studies.

a. Alleviating heel-toe effects:

ICDs were employed to mitigate the heel-toe effect in the longest horizontal well (~3600 m) of the Troll field (Ratterman et al., 2005). The well was completed with Stand Alone Screen (SAS) equipped with ICDs. Five different strengths of ICDs were used (Figure 2-3, ICD-5 highest strength, ICD-1 lowest strength) with the highest strength ICDs (i.e. the ones with maximum pressure drop) (blue in Figure 2-3) being installed at the heel and SAS (Screen-1, yellow, in Figure 2-3), with a negligible pressure drop, at the toe. The results showed a balanced production inflow and prevented water coning.

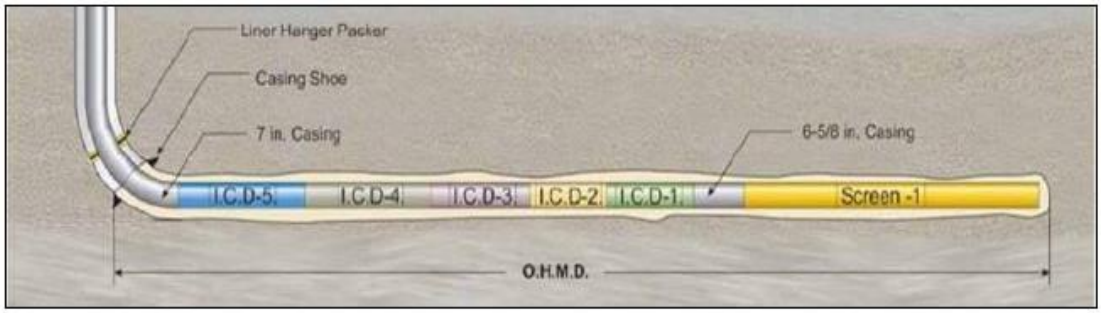

Figure 2-3: ICD configuration to balance heel-toe effect (from (Ratterman et al., 2005)). Colours show ICDs with different strengths. ICD-5 (blue) highest strength. ICD-1 (green) lowest strength. Screen (yellow) negligible pressure drop.

b. Improving production in heterogeneous reservoirs

b1. Short-term production strategy (a.k.a. "Snapshot" flow control completion design)

This application employs a snapshot of the characteristics of the system (e.g. near well-bore permeability, or instantaneous production rate profile) at a particular time to design the ICD completion to balance the production along the well bore at that particular time [e.g. (Least et al., 2013, Das et al., 2012)].

b2. Long-term recovery strategy (a.k.a. "Lifecycle" flow control completion design)

Here long-term objectives (e.g. NPV, cumulative oil production) are considered to develop an optimum ICD completion design. Generally, an optimisation algorithm is employed to find the optimum ICD strength profile while a numerical reservoir simulation model is used to calculate the long-term objective function for the specified ICD completion scenario (Alghareeb et al., 2009).

2.4.2 Autonomous flow control: AICDs

Autonomous Flow Control Devices (AFCDs) are the next generation of ICDs to substitute the passive, or fixed, flow control with a self-adjusting restriction, which reacts to the flow characteristics (e.g. changes in the density/viscosity) of the produced fluid. This self-adjusting restriction provides improved downhole flow control by a pre-designed, fluid-dependent, flow control action. Moreover, a relatively greater added-value is expected in reservoirs with uncertainty, where unexpected breakthrough of the unfavourable phase in a zone has a high probability of occurring. Autonomous Inflow Control Device (AICD) is a member of this group. Different types of AICDs with various design concepts have been proposed (Eltaher et al., 2014). Commercially successful design concepts have been developed, in which the changing effective flow area is based on the characteristics of the flowing fluid (e.g. (Fripp et al., 2013, Halvorsen et al., 2012)).

2.4.3 Active flow control: ICVs

These devices are offering flow restriction with multiple positions that provide flexible flow control managed by actuation from the surface. ICVs are providing high level of control flexibility and the potential to achieve the ultimate expected improvement under uncertain operational/reservoir conditions. ICVs power and control can employ hydraulic, electric or electro-hydraulic systems (Shaw, 2011). Battery powered ICVs eliminate the need for a control line, but do require a downhole source of power or have a limited operational life. The control commands are then transmitted using wireless signals (e.g. (Tendeka, 2013)) or by circulating electrical chips (e.g. (Snider and Fraley, 2007)).

3 classes of ICVs are available based on the number of control positions (or flow area options).

1- ON/OFF ICVs only provide fully-open and fully-closed positions.
2- Discrete ICVs provide a limited number of positions (up to 10, including the fully open and fully closed positions). Each position, represents a different flow area, has to be chosen during the ICV design stage. This is normally based on the desired flow rate and pressure drops. The flow area of many designs changes exponentially between adjacent positions. An optimal design ensures that an incremental change in the pressure drop or flow rate is achieved at all ICV positions. For example, when the objective of installing ICVs is to control zonal gas breakthrough a design with more positions with small area and fewer positions with larger area is preferred (Al-Khelaiwi, 2013). By contrast, control of zonal water breakthrough often employs a uniform logarithmic change in the area between the fully open and fully closed positions. This dependency on the fluid composition can be explained using Eq. 2-8 where the pressure drop across an ICV is proportional to the density of the produced fluid.
3- Infinitely Variable ICVs, provide continuous control of the flow area between the fully open and fully close positions (e.g. (Rubbo and Littleford, 1998)).

The control flexibility increases by moving from group 1 to group 3. However, this results in a more complex completion, which will generally have an increased chance of

failure, though recent advances in the ICV technology with an improved reliability have been reported (Rahman et al., 2012).

The ICV's flexible flow control capability allows implementation of new, more effective production scenarios, which would increase the economic viability of the field. These scenarios can also respect constraints defined by the installed equipment and the operator's management strategy. However, finding the optimal control scenario for ICVs is a challenging optimisation problem which is the subject of this thesis.

It should be noted that, the ICV's ability of being controlled from the surface dictates a limitation on the maximum number of ICVs which can be installed in a well [i.e. 5 using current technology for hydraulic ICVs; for example see (Carvajal et al., 2014)]. This results in a coarse scale zonation as compared to ICDs and AICDs which can be installed at every completion joint (~ 12 meters), hence extra consideration are required to achieve optimal zonation by installing ICVs in their optimum location. Recent development with electric ICVs allows a greater number of devices (over 20 valves controlled with a single downhole cable) to be installed in each well (Campbell, 2015, Potiani and Eduardo, 2014). Potiani and Eduardo (2014) provided a brief comparison among hydraulic, electric-hydraulic and all-electric systems and concluded that all-electric system is as reliable as hydraulic system and more reliable than electric-hydraulic systems. The all-electric system is still operational in their case study after around 10 years of installation and is shown to be more cost effective and reliable when water depth exceeds 10000 ft.

2.5. Modelling of Advanced Wells

The simulation of advanced wells in a reservoir simulator requires a sophisticated well model, which provides a detailed description of the fluid flow in the wellbore. The pressure losses (hydrostatic, friction, acceleration) will vary along a complex well structure. This is accounted for by discretising the well model into a number of segments, where each segment is defined using 4 independent variables: fluid pressure, total flow rate and water and gas fractions. The well equations are solved fully implicitly and coupled to the reservoir model. A steady-state well model results in a simpler problem as the dynamics of the well flow versus reservoir flow might be quite

different. This approach is known as multi-segment well model (Holmes et al., 1998) and is available in several commercial reservoir simulators (e.g. Eclipse Reservoir Simulator (ECLIPSE, 2012)). It should be noted that segment temperature is considered as another independent variable when thermal modelling is also performed.

The impact of fluid production from multiple completion zones can be modelled realistically using a multi-segment well model. This includes variations in the zonal production rate due to changes in the pressure loss as a result of production changes from other zones or the crossflow between zones. Complex crossflow might occur in advanced wells (between different zones in a lateral or between different laterals). The multi-segment well modelling approach allows local flow conditions to be accurately determined including the extent and composition of any crossflow. This is in contrast to the traditional approaches to wellbore modelling in which average fluid properties are considered.

A multi-segment well model is a collection of segments arranged in a gathering tree topology. Each segment consists of nodes and a flow path. The pressure is calculated at segment nodes while the nodes are connected to neighbouring nodes and/or grid blocks. Each segment is characterised by its length, diameter, roughness, area and volume, which are used for calculating segment storage and pressure drop. Figure 2-4 is a schematic diagram of a multi-segment well. It represents the flow from reservoir grid blocks (RG1 to RG10) to the annulus, along the annulus (segment number 16-20 and 21-25), from the annulus to the tubing through Flow Control Devices (Segment 14 and 15), along the tubing (segments 4-13) and to the main wellbore (segments 1-3).

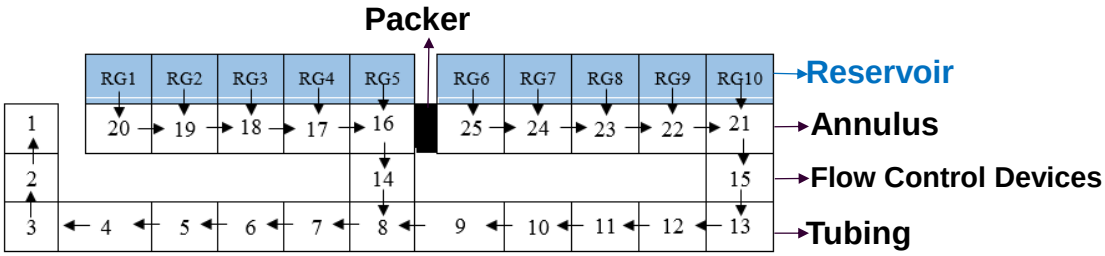

Figure 2-4: Schematic of the multi-segment well model

The pressure drop across each segment can be calculated using any of the following methods. The employed method depends on the role of each segment, the expected flow regime and the available information for that segment.

- *Fluid flow models*, Homogenous flow model assumes there is no slip between the phases therefore all phases flow with the same velocity. The hydrostatic component of pressure loss (or gain) (δP_h) is calculated using a weighted average density of the existing phases.

$$\delta P_h = \rho\, g\, L_p \,.\sin(\theta) \tag{2-1}$$

where ρ is the mixture density, g is the acceleration of gravity, L_p is the segment length and θ is the segment angle with horizontal. Frictional pressure losses are calculated as follows,

$$\delta P_f = 2f \,.\frac{L_p}{D_p} \,.\rho \,.v^2 \tag{2-2}$$

where δP_f is the frictional pressure drop, D_p is the pipe diameter, f is the Fanning friction factor, and v is the fluid velocity. The Fanning factor depends on the Reynolds number R_e. For laminar flow ($R_e < 2000$), $f = \frac{16}{R_e}$. For $R_e >$ 4000,

$$\sqrt{\frac{1}{f}} = -3.6\, log_{10}(\frac{6.9}{R_e} + \left(\frac{e}{3.7D_p}\right)^{\frac{10}{9}}) \tag{2-3}$$

where e is the absolute roughness of the tubing and has the same unit as D_p. For $2000 < R_e < 4000$ the value of f is calculated by linear interpolation between $R_e = 2000$ and $R_e = 4000$.

Acceleration component of pressure loss (or gain) occurs when there is a change in the flow velocity due to a change in the flow geometry (e.g. expansion, contraction or bend) or phase changes and calculated as follows,

$$\delta P_a = H_{v,out} - \sum_{inlets} H_{v,in} \tag{2-4}$$

where δP_a is the acceleration pressure loss across a segment which is the difference between outlet velocity head ($H_{v,out}$) and summation of all inlet velocity heads ($H_{v,in}$). The velocity head is calculated as follows:

$$H_v = \frac{1}{2}\,\rho\, v^2 = \frac{1}{2}\,\frac{w^2}{A_p^2\,\rho} \qquad 2\text{-}5$$

where A_p is the cross-section area and w is the mass flow rate.

Total pressure drop (δP) is then calculated as summation of all the pressure drop components:

$$\delta P = \delta P_h + \delta P_f + \delta P_a \qquad 2\text{-}6$$

In this study the homogenous flow model is used to calculate pressure drop in all segments without a flow control device because of the small volume of free gas in these segments. Table 2-1 shows an example of contribution of different components of pressure drop to total pressure drop for 2 selected segments in the multi-segment well model shown in Figure 2-4 using 4 in. tubing. The acceleration component is negligible in both segments as there is no change in the flow velocity.

Table 2-1: Example of contribution of different components of pressure drop for 2 selected segments in the multi-segment well model shown in Figure 2-4

	δP_h (% of δP)	δP_f (% of δP)	δP_a (% of δP)
Horizontal Segment (No. 5)	0	100	0
Vertical Segment (No. 2)	99.5	0.5	0

A “Drift-flux” model (Zuber and Findlay, 1965) should be used when two or more phases flowing in the segment and they tend to flow at different in-situ velocities. Generally, the phase that is less dense flows faster and causes a "slip" effect between the phases. In this condition liquid holdup can be significantly different from the input liquid fraction resulting in a different in-situ mixture density (ρ) and mixture viscosity (μ) and therefore a different pressure drop.

- *Models for specific flow control devices,* Equations have been developed and built into the simulator's code to represent the pressure drop across a specific design of flow control devices. This study used the built-in model of sub-critical flow through a valve to represent the performance of an ICV segment [see WSEGVALV keyword in (ECLIPSE, 2012)].

  The following equations are used for calculating the pressure drop across an ICV:

$$\delta P = \delta P_{cons} + \delta P_f \tag{2-7}$$

$$\delta P_{cons} = C_u \frac{\rho q_m^2}{2\, C_v^2 A_c^2} \tag{2-8}$$

$$\delta P_f = 2\, C_u\, f\, \frac{L_p}{D_p}\, \rho\, \frac{q_m^2}{A_p^2} \tag{2-9}$$

  where δP is the total pressure drop, δP_{cons} is the pressure drop due to the constriction, δP_f is the pressure drop due to the friction, C_u is the unit conversion constant, ρ is the mixture density, q_m is the mixture flow rate, C_v is the dimensionless flow coefficient for the valve, A_c is the cross-sectional area of the valve constriction, L_p is the additional pipe length in the segment, A_p is the cross-sectional area of the pipe. This study used a small value of L_p (≈ 0) to represent a valve segment. The segment frictional pressure drop is thus negligible compared to the pressure drop due to flow through the constriction.

- Pre-calculated pressure drop tables. Multiple tables define the pressure drop as a function of outlet pressure, flow rate, water-cut and gas-oil-ratio similar to the Vertical Flow Performance (VFP) tables. The segment pressure drop is then calculated by linear interpolation from the tables. One of the advantages of this method is that tables can be generated using more sophisticated multiphase flow models in a separate software. Moreover, this method can be employed for modelling pressure drops across specific flow control devices (e.g. recently developed Autonomous Flow Control Devices) for which there are no equation currently built into the simulator. The flow performance data for new devices can be obtained from laboratory experiments.

Only one of these options can be used to calculate the pressure drop of a segment at a specific time step; thought it is possible to use a combination of these options for different segments within the well. Employing the correct option for modelling each segment ensures that the well model is a good representation of reality. Moreover, the well model should be run for enough number of iterations to ensure convergence. The impact of well modelling errors (uncertainty) on optimal design and control of advanced wells is not considered in this study.

Two further approaches are employed in the literature for modelling zonal control in the I-wells in addition to the multi-segment well model. The first approach ignores the well flow processes and controls the zonal production/injection rate at the sand face. For example Chen and Oliver (2009) employed this approach to show the value of downhole zonal control in improving the reservoir sweep efficiency; however this simplified modelling approach generally fails to represent reality since the individual zonal production rate will be affected by production from other zones. Moreover, Section 2.9 shows that interaction among zonal productions due to a rate dependent frictional pressure drop in the tubing results in a different, and possibly more complicated, optimisation problem.

The second approach involves integration of the reservoir model and well model. Initially this approach models the reservoir and wells separately. During the production period these models communicate with one another at a predefined, or adaptive, frequency. This approach offers the most powerful modelling due to the freedom to independently model the wells and the reservoir. However, the integration might results in an unstable process with convergence problems which increases the modelling error and the computation time. This is mainly due to introduction of extra constraints (i.e. boundary conditions) in models already optimising large number of wells/zones with various production constraints (e.g. field total oil rate constraints, gas lift optimisation). Grebenkin and Davies (2012) modelled an intelligent field using the integrated approach which is then employed for implementing reactive optimisation of the ICVs. They discussed the problems associated with integrated modelling and proposed solutions to alleviate these problems. The Multi-segment well model will be used for this thesis.

2.6. Optimum Control of the Downhole Flow Control Devices

Brouwer and Jansen (2004) were the first who developed a systematic approach for optimal control of the downhole flow control devices based on the optimal control theory. Significant research efforts continue to be devoted to the development of methodologies for optimising production and injection parameters during the different stages of production (e.g. Peters et al. (2010) presents several optimisation methods on the Brugge benchmark case study). These approaches can be classified as optimising either short-term objectives [reactive optimisation (Naus et al., 2006, Grebenkin and Davies, 2012)] or long-term objectives [proactive optimisation (Alghareeb et al., 2009, Almeida et al., 2010, Haghighat Sefat et al., 2013)]. ICVs provide real time, adjustable zonal flow control which allows implementation of both a reactive and/or a proactive optimisation approach to increase the economic viability of the field while respecting the defined constraints by equipment and operator. This is in contrast to ICDs and AICDs, whose fixed design can only be optimised at the installation stage.

2.6.1 Reactive Optimization

Reactive optimization aims to find a control strategy for the current condition of the system so as to optimize the chosen short-term (instantaneous) objective, subject to any active constraints. This strategy, in its simplest form, starts with the measurement of a parameter followed by its comparison with predetermined thresholds and possible reactions if the threshold(s) being exceeded. This relatively simple type of control is suitable for real-time, decision making and reacting to unexpected situations. However, it often fails to provide the optimum long-term (or even short-term) field management strategies.

Examples of reactive control include Jansen et al. (2002) who employed a Smart Stinger Completion (SSC), that is an extension of the Passive Stinger Completion (PSC) with actively controlled ICV, to not only reduce the heel-toe effect but also reactively control coning. The ICV pressure drop set point was multiplied by a factor greater than one when more than 25% WC or more than 5% increase in GOR was detected downhole. Moreover, they employed Inflow Switching Process (ISP) in a multi-zone completion to control coning. The segments are closed as soon as water or gas breakthrough happens.

Drawdown is increased to maintain the production rate, until all segments are close. The cycle repeats with all segments open and a lower gas rate constraints to ensure a gradually decreasing drawdown over life of the reservoir. These simple reactive control strategies provided improvement in current production through coning control however, the economic profitability highly depends on reservoir parameters and production constraints.

Naus et al. (2006) employed a more systematic approach using Sequential Linear Programming (SLP) to periodically optimise ICV settings during commingled production of an I-well with the objective to maximise the oil production rate. This short-term optimisation resulted in accelerated oil production however in some cases a lower ultimate recovery was observed. Guyaguler and Byer (2008) employed a piecewise linear controls and Mixed-Integer Linear Programming (MILP) to solve the production allocation problem in large number of conventional wells. These techniques resulted in accurately capturing nonlinearities and handling multiple dependent operational constraints while maximizing real-time objectives. Grebenkin and Davies (2012) proposed a fast and simple reactive strategy for controlling large number of multi-zone vertical I-wells with immediate application to a full-field problem. A critical water cut criterion was developed to determine which offending zones should be shut-in. Their approach (Grebenkin and Davies, 2012) was shown to be fast and stable in comparison to current commercial alternatives. It provided an increase in oil production under the condition of limited outflow performance.

2.6.2 Proactive Optimization

Proactive optimization of well control should be started during the early production life of a well to mitigate forecast problems and/or to optimise longer-term objectives (e.g. ultimate economical profit or oil recovery). Numerical reservoir models are used to calculate the production forecast to evaluate the optimisation objective function.

2.7. Formulation of the Problem of I-well Proactive Control

Proactive optimization of ICVs begins with a formulation of the multiphase flow in the reservoir. This formulation is in reality only as good as the assumptions (e.g., Darcy flow) behind its construction. This study is independent of the choice of

formulation/solution approach and considers the following short form of the reservoir simulation process:

$$\frac{dy_r}{dt} = SIM(y_r, x, t), \qquad y_r(t_0) = y_{r0}, \tag{2-10}$$

where, $y_r \in \mathbb{R}^p$ is the p-dimensional state vector of the reservoir (e.g. saturations, pressure field) for a certain model realization r, $SIM: \mathbb{R}^p \times \mathbb{R}^{n_x} \times \mathbb{R}^1 \to \mathbb{R}^p$ is the reservoir simulation operation and $x \in \mathbb{R}^{n_x}$ is the vector of n_x control variables discretized over the field production time (t). The initial state of the system is defined by y_{r_0} at time t_0. Differential equation 2-10 can be solved using implicit or explicit method. Therefore, the production performance under a certain control scenario for a single model realization y_r is evaluated using a general, scalar objective function of the form (Speyer and Jacobson, 2010):

$$\mathcal{F}(x, y_r) = -\int_{t_0}^{t_f} \emptyset(y_r(t), x(t), t)dt + \int_{t_0}^{t_f} I(y_r(t), x(t), t)dt\,, \tag{2-11}$$

where $\emptyset: \mathbb{R}^p \times \mathbb{R}^{n_x} \times \mathbb{R}^1 \to \mathbb{R}^1$ is a constraint term and $I: \mathbb{R}^p \times \mathbb{R}^{n_x} \times \mathbb{R}^1 \to \mathbb{R}^1$ is the instantaneous objective function. In the current formulation the class of control functions x is limited to the class of bounded piecewise constant functions where the control variables are only optimized at discretized control steps during the simulation period and are kept constant between two steps. This is a first-order, step-like discretization of the continuous optimization problem to reduce the number of control variables. Besides, in real-life ICV positions are often changed at regular time intervals either during planned operations or due to the limited number of cycles an ICV can experience during its life. The solution to the optimal control problem is to find the $x(.) \in \mathbb{R}^{n_x}$ that minimizes (or maximizes) the function $\mathcal{F}$ subject to the differential Equation 2-10. Additional constraints on the control variables *x* may also be applied.

The constraint term in Equation 2-10 ($\emptyset$) is handled by the reservoir simulator to respect the defined well/field production limits in this study. (I.E. The reservoir simulator controls the well Bottom Hole Pressure (BHP) to achieve the defined liquid production rate). Kourounis et al. (2014) showed that this heuristic constraint handling procedure can outperform the formal constraint handling approach (i.e. constraints are enforced by

the optimization algorithm) in challenging cases of large model with large number of control variables. Although formal constraint handling procedure is theoretically superior, its efficiency decreases due to the existence of local optima and complexity of solving constrained optimization problems with large number of control variables. Moreover, the piecewise constant assumption converts the integral term into a summation over the discretized control steps. This results in a standard simplified Net Present Value (NPV) formula used by Brouwer and Jansen (2004) and utilized in this thesis. The objective is to find an ICV control scenario that maximizes the NPV during the reservoir's production life. NPV in this study, which only considered oil and water production, is defined as:

$$\mathcal{F}(x) = \sum_{n=1}^{S} \left[\sum_{j=1}^{N_p} \left(r_o q_{o,j}^n - r_{pw} q_{w,j}^n - r_{opex} q_{l,j}^n \right) \right] \frac{\delta t^n}{(1+b)^{t_n}}, \qquad 2\text{-}12$$

where S is the total number of simulation steps; N_p is the number of production wells. The costs constants r_o, r_{pw} and r_{opex} (in \$/sm^3) are the oil price, the water handling cost and the operating cost respectively. Variables $q_{o,j}^n$, $q_{w,j}^n$ and $q_{l,j}^n$ are the oil, water and liquid production rates of well j at time step n in sm^3/day. The discount rate b is in decimal and δt^n is the length of the n^{th} simulation step and t_n is the cumulative time up to that simulation time step in years. This NPV definition reflects a simplified description of the "Added Value" from intelligent completions since it ignores many items, in particular the associated capital cost.

2.8. Challenges in Optimum Control of the Downhole Flow Control Devices

The following challenges are observed in the reactive and proactive optimisation of the downhole flow control devices.

2.8.1 Reactive Optimization

The following challenges of the reactive optimisation are important in this study for future comparison with the developed proactive optimisation approach.

a. Limited application period and possible control oscillation

Reactive optimisation control is triggered when the objective function starts deteriorating. Optimum control, from a reactive optimisation point of view, is do-nothing prior to this stage being reached. The algorithm must be robust in order to eliminate oscillations in the control of a fast dynamic system (i.e. where control actions result in a fast change to the system). Control oscillations in reactive optimisation are not uncommon [(Grebenkin, 2013)].

b. Accounting for reservoir and operational uncertainties

The reactive nature of control provides a flexible response to unexpected incidents. In principle, this eliminates the need to include reservoir description uncertainties during the development stage of the reactive optimisation algorithm. Grebenkin (2013) tested his reactive optimisation algorithm under static (porosity and permeability distribution) and dynamic (relative permeability, oil-water contact, gas-oil contact and aquifer strength) reservoir description uncertainties. He confirmed that an optimum reactive control adds value by increasing the expected mean and reducing the variance of the objective function. Birchenko et al. (2008) performed a probabilistic comparison of the recovery from (i) a conventional well, (ii) an I-well with an ICD completion designed to achieve a reasonable level of inflow equalisation (Section 2.4.1-b) and (iii) an I-well with an ICV completion managed by reactive control to limit production from zones with high water cut. They found that the expected recovery from ICD completion is higher than conventional completion. However, the variance was almost the same (Green line in Figure 2-5). The ICV completion (Red line in Figure 2-5) showed both a higher expected recovery and a lower variance compared to the conventional completion.

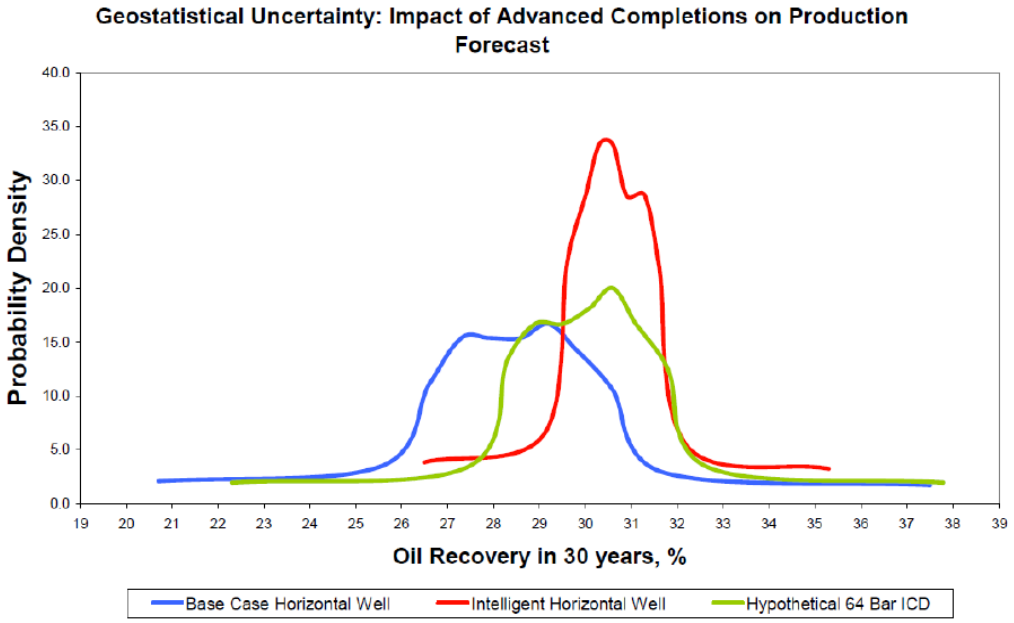

Figure 2-5: Probabilistic comparison of oil recovery in conventional, ICD and ICV completions (Birchenko et al., 2008) – This result was based on a limited number of Gaussian random realisations

2.8.2 Proactive Optimization

The major challenges presented by proactive optimization are:

- Uncertain objective function
- Large number of control variables
- Computationally expensive objective function

The following sections briefly explain these challenges and review the main approaches available in the literature to address them.

a. Uncertain objective function

The limited geological knowledge of the field available at time that the reservoir simulator's geological model was built results in the reservoir model's forecast having a normally high level of uncertainty. Model uncertainty can be quantified using an ensemble of models to evaluate the range of possible forecasts. Therefore the objective function (Equation 2-12) is in fact a function of the uncertainties,

$$\mathcal{F}(x, y_r) = \sum_{n=1}^{S} \left[\sum_{j=1}^{N_p} \left(r_o q_{o,j}^n - r_{pw} q_{w,j}^n - r_{opex} q_{l,j}^n \right) \right] \frac{\delta t^n}{(1+b)^{t_n}}, \qquad 2\text{-}13$$

A fixed set of control vector (x) will produce a different objective function value ($\mathcal{F}$) when applied to each one of the model realizations (y_r).

The uncertainty can be reduced by introduction of a closed-loop reservoir management process, where the model(s) is continuously updated by changing the model to "history match" the field's actual, measured production data (see Wang et al. (2009) and Jansen et al. (2009) for a detailed discussion of the components of a closed-loop, reservoir management process). History matching is another challenging optimization problem (Oliver et al., 2008, Oliver and Chen, 2011). Once completed, it requires repeating the production optimization of the updated model(s).

Some production optimization studies (e.g. (Lorentzen et al., 2006, Almeida et al., 2010, Pinto et al., 2012)) employ a single realization of the reservoir model. This is typically either the most probable realization or a randomly selected model from the ensemble of all available realizations. The resulting control scenario from proactive optimization of a single reservoir model realization will not be robust since the actual reservoir might be very different from that of the chosen model. van Essen et al. (2013) proposed to reduce the risk associated with the geological uncertainty by substituting the objective function with the expectation of the objective function calculated from a set of reservoir model realizations. They performed robust optimization of conventional wells using 100 geological realizations of the reservoir model and concluded that the resulting robust control scenario provided a higher mean of the objective value as well as reduced the variance when compared to the single realization optimization. Chen and Oliver (2009) applied robust optimization using all available model realizations to closed-loop reservoir management of (outflow independent) multi-zone production and injection wells in the Brugge field.

It is generally accepted that performing robust optimization while considering all available model realizations is the best way to capture the geological uncertainty. Unfortunately, it rapidly becomes computationally expensive when applied to full-field models. Choosing a small ensemble of model realizations for robust optimization that

are representative of all available models is computationally less demanding, but is also subject to bias during the selection process. Chen et al. (2011) repeated the earlier (Chen and Oliver, 2009) study by performing robust optimization for the Brugge field with 11 realizations distributed uniformly based on the objective function value from 104 available realizations while considering both short-term and long-term objectives. They successfully reduced the computational cost.

Haghighat Sefat et al. (2014) employed a similar approach to reduce the computation time of the robust optimization approach. However, these studies employed random sampling for selecting a subset of realizations for robust optimization. Unfortunately, random sampling does not guarantee that the underlying model uncertainties are fully captured. The preferred alternative is to employ a methodology for systematic selection of a subset of realizations (Park, 2011, Scheidt and Caers, 2013). The developed methodology for realization selection is demonstrated in Chapter 6.

b. Large number of control variables

In proactive optimisation the total number of control variables (n_x) is equal to the number of controlled elements multiplied by the number of control steps. Therefore, the total number of control variables increases proportionally with increase in the number of controlled elements or by an extension of the control period. The non-linear proactive optimisation problem is more difficult to solve with a larger number of control variables.

Variable interaction is also observed in the proactive optimisation problem. This means that when the value of a given variable changes, the value of the other variables should be changed in a unique way to get the optimum results. Two types of interaction might exist among decision variable in an optimisation problem (Tiwari and Roy, 2002):

1- Inseparable function interaction, in this type the effects of one variable on the objective function depend on the value of the other variable however there is not a defined functional relationship between the two variables. Figure 2-6(a) shows a schematic example of a problem with no interaction between the control variables (X1 and X2). The optimum value of control variable X1 (i.e. b) does not change by changing the control variable X2. While Figure 2-6(b) shows

interaction between control variables X1 and X2. The optimum value of X1 changes when the value of X2 is changed. This effect is further investigated in Section 3.2.

2- Variable dependence, in this type one variable in a function of other variable and the functional relationship is known. For example X2 = g (X1,…), where X1 and X2 are control variables and g is the functional relationship. There is no variable dependence in proactive optimisation of ICVs. However, this type of variable dependence might be observed in complex full field optimisation problems (e.g. optimisation of well production rate and gas lift injection rate in a field where wells are equipped with gas lift and produced gas is used for gas lift). This type of interaction is not considered in this thesis.

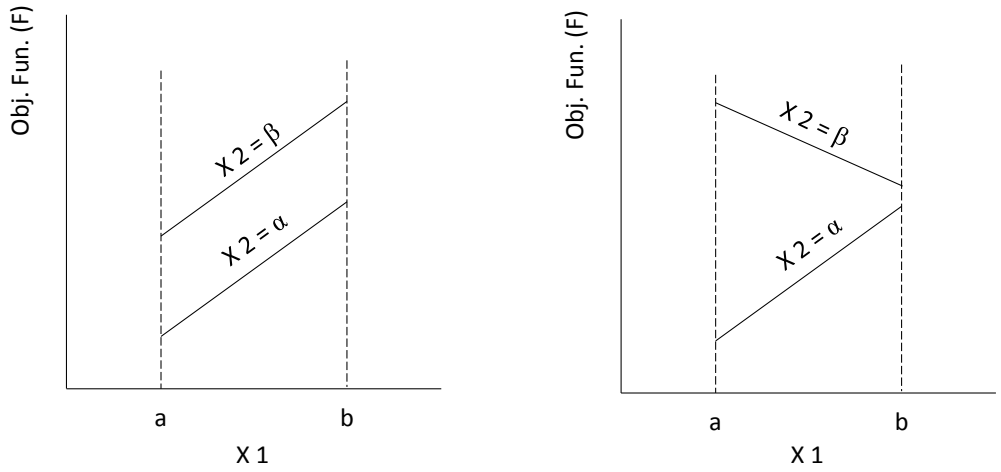

(a) (b)

Figure 2-6: Schematic examples of inseparable function interaction (a) No interaction (b) Interaction between X1 and X2

Two approaches are available to address the large number of control variables: (1) simplifying the problem to reduce the number of variables, (2) employing a more efficient optimisation algorithm. Published work (Brouwer and Jansen, 2004, Sarma et al., 2006, Suwartadi et al., 2009, Alghareeb et al., 2009, Almeida et al., 2010) and ongoing research tries to enhance the proactive optimisation process by improving one or both of these. Following subsections summarises the previous studies on proactive optimisation of intelligent and conventional wells classified based on the employed optimisation approach. The maximum number of control variables that are successfully handled by each optimisation algorithm is shown.

Gradient-based optimization: one option is to use the adjoint gradient of the forward model in an effective proactive algorithm. This is especially beneficial, when the dimension of the simulated model (y_r in Equation 2-10) is much higher (usually orders of magnitude) than the number of control variables (x in Equation 2-10). The adjoint approach is then computationally less expensive than finite difference based gradient estimation (Giles and Pierce, 2000, Jansen, 2011). Review and development of adjoint-based optimisation with the application in reservoir simulation is available in (Jansen, 2011). The major advantage of applying the adjoint algorithm to the I-well control problem is the fact that the cost of the gradient estimation is approximately one additional simulation run, regardless of the number of control variables. Unfortunately, the required data for the adjoint calculation is not available in most commercial reservoir simulators, though several studies have used adjoint-based algorithms for proactive optimization of I-wells in conjugation with an in-house reservoir simulator (Brouwer and Jansen, 2004, Sarma et al., 2006, Suwartadi et al., 2009, van Essen et al., 2011). Sarma et al. (2006) and Brouwer and Jansen (2004) found that the algorithm to be efficient at finding a local optimum for a large number of control variables. Asadollahi and Naevdal (2009) used an adjoint optimizer in a commercial reservoir simulator (ECLIPSE, 2012) for field-scale production and injection optimization of a field developed with 20 production and 10 injection wells, each of which was selectively completed on three reservoir layers. This resulted in more than 3000 control variables during the 30-year production period. They found the algorithm to be very sensitive to the (arbitrary) starting point of the optimization process and the algorithm was converging to different local optima using different starting points due to the employed gradient-based search algorithm.

Gradient-based methods are also employed to efficiently solve well location optimisation problem (i.e. a discrete optimisation problem). Zandvliet et al. (2013) introduced the concept of pseudo-wells surrounding the actual wells whose locations have to be optimised. These pseudo-wells while producing (or injecting) at very low rate, to have negligible effect on the actual wells, enable calculation of the gradient of the objective function w.r.t. the flow rates in the pseudo-wells. The gradient is employed to iteratively improve well location by moving the well in the direction of the best pseudo-well to increase the objective function value. The pseudo-wells with zero

rate are eliminated from the model. Zandvliet et al. (2013) employed an adjoint method developed in an in-house reservoir simulator, Forouzanfar et al. (2010) employed adjoint optimizer in a commercial reservoir simulator (ECLIPSE, 2012) to calculate the gradient for subsequent well location optimisation using the concept of pseudo-wells. A local optimum is expected due to using a gradient-based algorithm. Zandvliet et al. (2013) suggested to consider several initial well location to alleviated this problem.

Meta-heuristic optimization: algorithms have also been used to solve the proactive optimization problem. Genetic Algorithm (GA), a popular member of this group, was first introduced by Holland (1992). GA is based on the principal of natural evolution and survival of the fittest (See (Mohaghegh, 2000) for a description of the algorithm). The popularity of GA is due to its: (1) Simplicity of implementation (it treats the system as a black-box whose only input and output information is required) and (2) Efficiency in solving problems with a limited number of control variables. Alghareeb et al. (2009), Almeida et al. (2010) and Pinto et al. (2012) used GA for proactive optimization of I-wells. Further, they simplified the problem to limit the number of control variables to a maximum of 100. Despite this, the number of simulation runs required varied from 1,000 to more than 10,000; depending on the number of control variables.

Particle Swarm Optimisation (PSO) is a popular member of the next generation of meta-heuristic optimisation algorithms. PSO was developed by Eberhart and Kennedy (1995) inspired by the social behaviour of bird flocking. Zhao et al. (2011a) employed PSO for production and injection optimisation of conventional wells and compared the performance with stochastic gradient-based optimisation. Several meta-heuristic optimisation algorithms are available and new algorithms are developing. The search mechanism of the population based algorithms as compared to the gradient-based algorithms is discussed in the comparative study subsection.

Derivative-free optimization: methods offer another approach for proactive optimization. Asadollahi et al. (2014) evaluated four derivative-free optimization methods [Hooke-Jeeves (HJ), Generalized Pattern Search method (GPS), Nelder-Mead (NM) and Line-Search Derivative Free (LSDF)] for production optimization of an oil field developed with conventional wells. They also compared these four methods with the gradient-based Sequential Quadratic Programming (SQP). They found that:

- LSDF is an efficient algorithm to solve the reservoir optimisation problem despite its nonlinearity.
- GPS is capable of searching more globally, providing a rapid improvement towards an optimum during early iterations while showing a slow rate of convergence at later stages.
- HJ performed better than GPS. It provided a combination of the exploratory and pattern search.
- NM was very slow and was not recommended.
- SQP performed efficiently at early steps. However, the convergence rate deteriorated at later iterations because of the noisy gradient calculated using finite difference method with relatively large perturbation step. Asadollahi et al. (2014) observed that selecting a larger perturbation step provides better total performance by alleviating the problem of zero gradients for some optimisation variables.

Routine application of these methods to large I-field reservoir models requires that the model performs efficiently with a greater number of control variables. Note that (Asadollahi et al., 2014) also limited the optimization problem to a maximum of 54 control variables. Hence they proposed stochastic estimated gradient-based methods as the most appropriate option for solving this problem.

Stochastically estimated gradient-based optimization: take advantage of the gradient-based algorithms efficiency in large-scale optimization problem (Zingg et al., 2008), when use of an adjoint code is not available (as in most commercial reservoir simulators). A stochastic estimate of the gradient is found by using a small ensemble of simultaneously perturbed control variables (i.e. the reservoir simulator is treated as a black-box). The most popular stochastic methods employed in reservoir engineering are the Ensemble-based Optimization (EnOpt) method (Chen et al., 2009), the Ensemble Kalman Filter (EnKF) method (Lorentzen et al., 2006) and the Simultaneous Perturbation Stochastic Approximation (SPSA) method (Spall, 1992).

Do and Reynolds (2013) provided a theoretical and numerical comparison of solution of a set of test problems of the performance of EnOpt, a SPSA-type algorithm and a doubly smoothed simplex gradient algorithm. They showed that the expectation of the

gradient obtained by the three methods represented a first-order approximation of the true gradient pre-multiplied (i.e. smoothed) by a squared covariance matrix. Haghighat Sefat et al. (2015) provides a comprehensive comparison of the performance of SPSA and EnOpt methods for proactive optimization of I-wells (Also described in detail in Chapter 4 of this thesis). They found that both methods provided similar performance for medium ensemble sizes; with SPSA being frequently able to bypass local optima due to Bernoulli perturbation. Moreover, major differences were observed in the optimum solution obtained by the two methods.

Approaches based on stochastically estimated gradients have been successfully applied to optimize control parameters of conventional production and injection wells (Wang et al., 2009, Zhao et al., 2011b, Do and Reynolds, 2013). Chen and Oliver (2009) employed EnOpt for optimizing production and water injection completion rates using the Brugge field as the test case. They employed a simplified model of an I-well which considered independent zonal production from different zones, though they ignored the effect of hydraulic communication within the wellbore.

Comparative studies: Zingg et al. (2008) compared the performance of GA and Adjoint gradient-based algorithm in an aerodynamic optimization problem with 9, 19 and 35 control variables. The GA was 6 to 200 times slower than the Adjoint approach. This depended on the number of control variables, the complexity of the optimization problem and the degree of convergence required. They found the computation time of the gradient-based approach to scale linearly with the number of control variables while the computation time for the GA increased more rapidly. SPSA has also been compared with various meta-heuristic optimization algorithms including Simulated Annealing (SA), Particle Swarm Optimization (PSO) and GA (Spall et al., 2006, Zhao et al., 2011a, Zhao et al., 2013, Haghighat Sefat et al., 2013). A brief comparison of SPSA and a commercially available GA for solving proactive optimisation problems is provided in (Appendix B) of this thesis. SPSA was shown to give faster convergence to a near-optimal solution compared to meta-heuristics optimization algorithms, presumably due to meta-heuristics algorithms being designed to effectively explore the search space rather than achieve a rapid improvement to a near-optimum solution. Using gradient information provides faster convergence to a local optimum solution however the

exploration capability is reduced compared to meta-heuristics optimization algorithms which discover the search space mostly using several populations.

Multi-scale approach: the number of control variables can also be reduced by using a multiscale approach (Lien et al., 2008, Oliveira and Reynolds, 2015). The optimization starts with a very coarse representation of the control variables but as the optimization proceeds and approaches the optimum solution, the resolution is gradually increased. The upscaling can be performed in time (i.e. zonal control settings remain constant over a time period) or space (i.e. multiple zones are grouped and treated as one). Lien et al. (2008) found that using a multiscale approach can obtain solutions with similar or even better performance than the ordinary fine-scale approach.

This study address the large number of control variables by using an efficient optimization algorithm (Chapter 4) and also by development of criteria to reduce the number of control variables by eliminating the less important ones (Chapter 3). Multiscale approach is not considered in this study however could complement the framework developed in this thesis and speed-up the optimisation process or used as an alternative to the developed variable reduction components.

c. Computationally expensive objective function

Reservoir models are generally computationally expensive which is often exacerbated by numerical issues arising from numerical dispersion of the discretization method employed as well as convergence failures of the nonlinear solvers. Several studies attempt to substitute some, or all, of the objective function evaluations required during the optimisation process with a cheaper alternative. This approach uses a surrogate model as an approximation function that mimics the original system behaviour that can be evaluated much faster. Surrogate models, also known as Meta or proxy models, can be divided into two main categories based on their approximation strategy:

(1) Model driven or physics based approach. These Reduced Order Models (ROM) aim to approximate the original equations with lower order equations and hence reduce the computational cost (e.g. (van Doren et al., 2006, Wilson and Durlofsky, 2013, Rousset et al., 2014)). Application of these approaches

requires access to the reservoir simulator source codes; a requirement which is generally impossible when using a commercial reservoir simulator.

(2) Data driven approaches. These consider the system as a black-box, generating the surrogate model using only input data and output responses (e.g. (Christie et al., 2006, Mohaghegh et al., 2012)). Such data driven models meet the objectives of this thesis, which aims to develop methodologies that are independent of the choice of the reservoir simulator employed. Golzari et al. (2015) developed a novel surrogate modelling approach that performed efficiently in production optimisation problems with a large number of control variables.

Surrogate modelling assisted optimisation was not considered in this study, which addresses a problem with a large number of control variables and an uncertain objective function. However, it is expected that a suitable surrogate modelling approach could complement the framework developed in this thesis and speed-up the optimisation process.

2.9. Impact of I-well modelling on the optimization process

Various previous studies [e.g. (Chen and Oliver, 2009)] employed a simplified model of an I-well, which considered independent zonal production from different zones, while ignoring hydraulic communication within the wellbore. However, in reality the production from an individual zone of an I-well is often affected by the production from other zones; an interaction, which can only be captured by coupled modelling of the outflow (wellbore model) in conjunction with the inflow (reservoir model). A multi-segment well model (ECLIPSE, 2012) can efficiently capture these effects (See Section 2.5). This section discuss the impact of using a multi-segment well model on the subsequent analysis.

A simple box-shaped model was employed to investigate the correlation of zonal productions and its impact on proactive optimisation. Only two phase (oil and water) is considered in this example however similar behaviour is expected in three phase problems as well. The test reservoir model has a square layout of 10×10×1 grid blocks in x, y and z direction, respectively. Each grid block has $\Delta x=\Delta y=120$ m and thickness of

3 m. This reservoir consisted of a high (100 millidarcy, mD) and a low (40 mD) permeability region (red and blue, respectively in Figure 2-7). The reservoir was developed by one horizontal injector and one intelligent, 2-zone producer. Water is injected at a constant rate of 1400 stb/day and the production well operates at a constant Bottom Hole Pressure (BHP) of 600 psi.

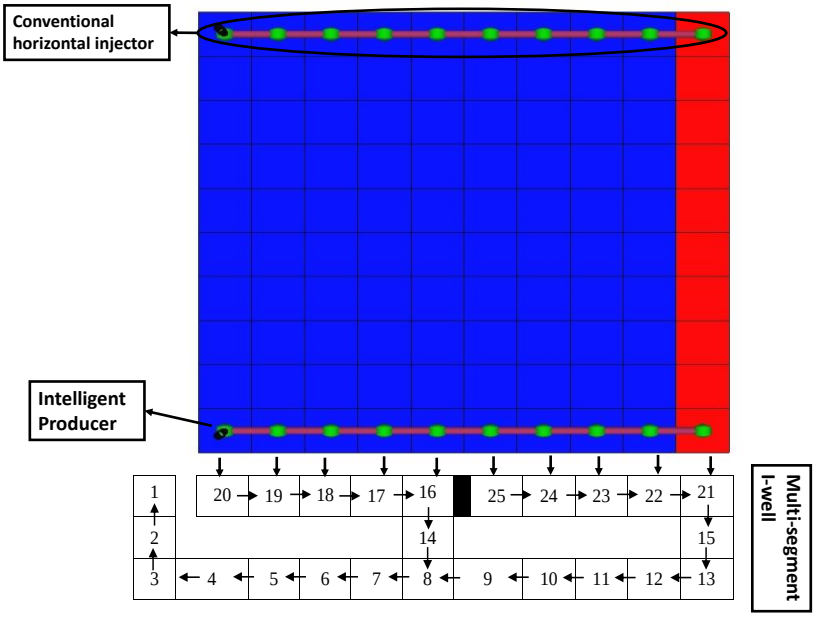

Figure 2-7: Top view of the test box-shaped reservoir model. Colour shows the permeability (red=100 mD; blue=40 mD). A schematic network flow diagram of the multi-segment I-well

Figure 2-7 also shows a network diagram of the flow paths in the multi-segment I-well. Segments 14 and 15 correspond to the ICVs controlling the production from two different zones of the reservoir. Segments 1 to 13 correspond to the tubing, while numbers 16 to 25 are segments representing the annulus. Fluid flows from the reservoir grids to the connected annulus segments. It then flows along the annulus and through the ICVs into the tubing. The flow direction in the annulus and tubing is always from a higher segment number to a segment with a lower number. The hydrostatic pressure component is negligible for all segments. Note, that there are two sets of pressure drop components associated with the ICV segments in Eclipse: (1) the housing segment (similar to a tubing or annulus segment) and (2) the restriction. A good practice is to eliminate the components corresponding to the housing segment by considering a small segment length then the pressure drop is only controlled by the restriction properties.

Two cases are considered:

1- A rate dependent frictional pressure drop exists in the annulus and tubing segments. This effect is considered by assuming a small (~2 in) internal diameter for the tubing and a similar annulus equivalent diameter.
2- Frictional pressure drop is negligible in the annulus and tubing segments. A small friction factor and large segment diameters are used to reduce the frictional pressure drop in the model.

This work will compare two identical well and completion configurations with the only difference being the correlation among zonal productions due to the rate dependent frictional pressure drop in Case-1.

Figure 2-8 compares the liquid production rate from fully-open ICV-15 versus ICV-14 (segments 14 and 15) while Figure 2-9 shows the liquid production rate form ICV-14 and ICV-15 versus production time for case-1 and case-2. Greater production is achieved from ICV-15 in case-2, no frictional pressure drop, since it is located in the high permeability region. Liquid production rates from both ICVs are decreased proportionally over the 40 day of production period due to reservoir depletion (a linear plot in Figure 2-8).

However, production from ICV-15 in Case-1 is smaller than ICV-14 during the initial production period. This is due to the larger frictional pressure drop as a result of high rate, plus the fluid from ICV-15 flows from the toe prior to evacuation. The impact of the frictional pressure drop decreases with time due to the flow rate decreasing. The ratio of the production rate from ICV-15 compared to ICV-14 is thus rate dependent. Hence the frictional pressure drop is the cause of the non-linear shape of case-1 data plotted in Figure 2-8.

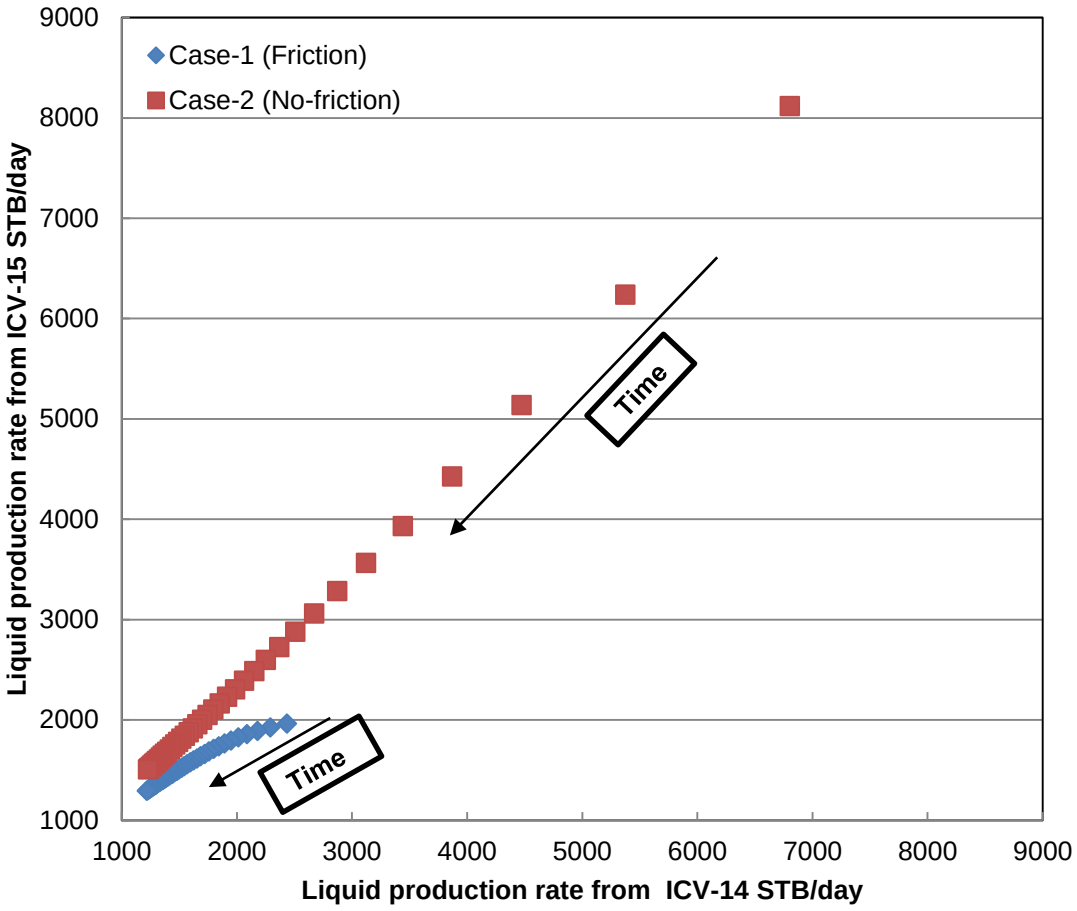

Figure 2-8: Liquid production rate from fully-open ICV-14 and ICV-15 over 40 day period for case-1 and case-2

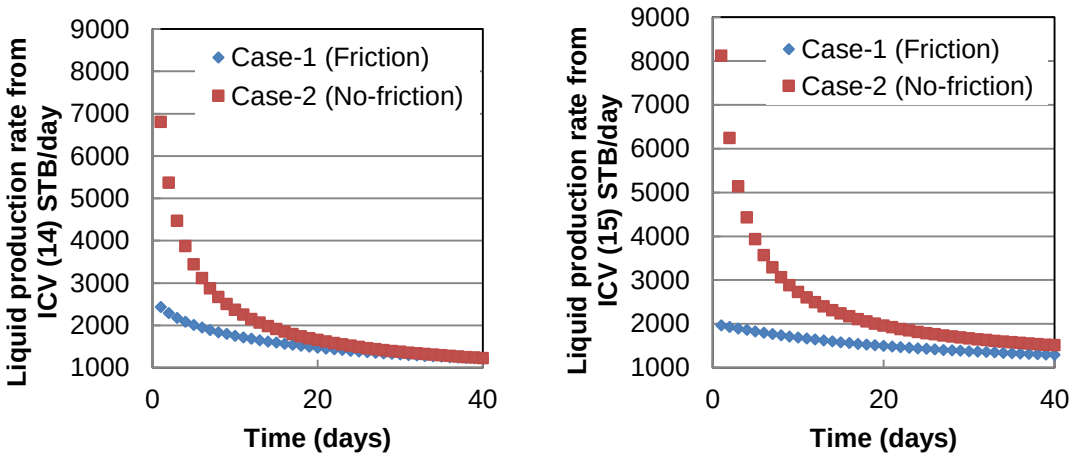

(a) (b)

Figure 2-9: Liquid production rate from fully-open (a) ICV-14 and (b) ICV-15 over 40 days period for case-1 and case-2

Further testing was performed by varying ICV-14's open area at the first time step with 10 steps (1%, 10%, 20%, …, 90%) while monitoring the liquid production rate from ICV-14 and ICV-15 at the first time step in case-1 and case-2 (Figure 2-10). The production from ICV-14 decreases by reducing the opening area. This results in a reduction in the frictional pressure drop along the tubing and an increase in the liquid production from ICV-15 in case-1. By contrast, in case-2 only minor changes are observed in liquid production from ICV-15 due to weaker correlation between zonal production rates resulting from a small frictional pressure drop along the tubing. Note that larger change in ICV-14 production in case-2 is due to greater base-case production in that case.

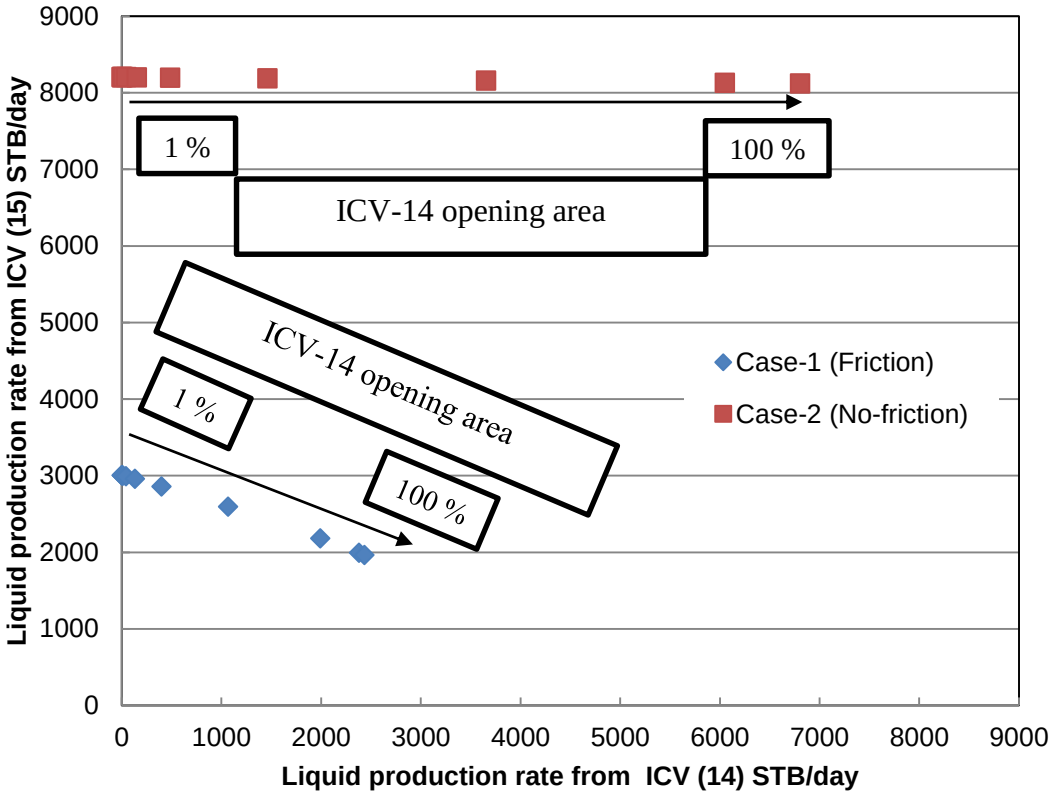

Figure 2-10: The zonal liquid production rate at first time step as a result of controlling ICV-14 opening area at first time step in case-1 and case-2 (arrows show the direction of increasing ICV-14 opening area)

The test was repeated while varying ICV-15's open area at the first time step with 10 steps (1%, 10%, 20%, …, 90%) and monitoring the liquid production rate from ICV-14 and ICV-15 at the first time step in case-1 and case-2 (Figure 2-11). Similar tests were repeated while varying ICV-14 or ICV-15 opening area at different time steps. The

same trend of stronger correlation between zonal productions in case-1 compared to case-2 was observed.

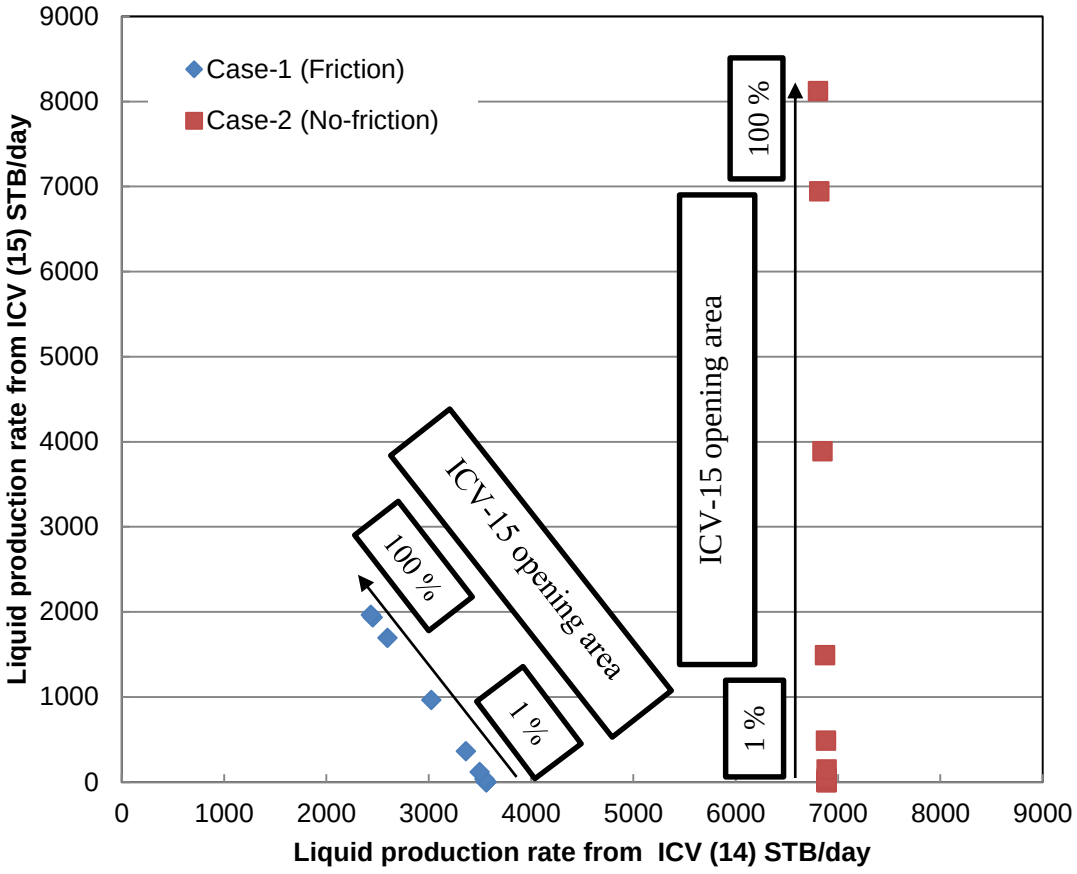

Figure 2-11: The zonal liquid production rate at first time step as a result of controlling ICV-15 opening area at first time step in case-1 and case-2 (arrows show the direction of increasing ICV-15 opening area)

Two other tests were performed while ICV-14 or ICV-15 is fully-closed at the first time step and then fully-opened for the rest of the production period (dashed lines in Figure 2-12 and Figure 2-13 respectively). Solid lines in Figure 2-12 and Figure 2-13 show liquid production rate versus time with fully-open ICVs (i.e. no control). In case-1 with friction, reduction in the liquid production rate from one ICV results in an increase in the liquid production rate from the other ICV at the same time step due to reduction in the frictional pressure drop along the wellbore (see Figure 2-12 (a) when ICV-14 is shut and Figure 2-13 (a) when ICV-15 is shut at the first time step). Moreover, reduction in the liquid production from an ICV during the first time step results in a proportional increase in the liquid production from the same ICV in the next time step.

Therefore, in case-1 with friction the control variables are not independent and changing one variable results in a change in the other variable.

In case-2 with no friction, reduction in the liquid production rate from an ICV during the first time step does no change the liquid production rate from the other ICV (see Figure 2-12 (b) when ICV-14 is shut and Figure 2-13 (b) when ICV-15 is shut at the first time step). In case-2 only a proportional increase in the liquid production from the same ICV is observed in the next time step (i.e. similar to Pressure Transient Testing). Therefore, in case-2 with no friction the control variables (zonal productions) are almost independent.

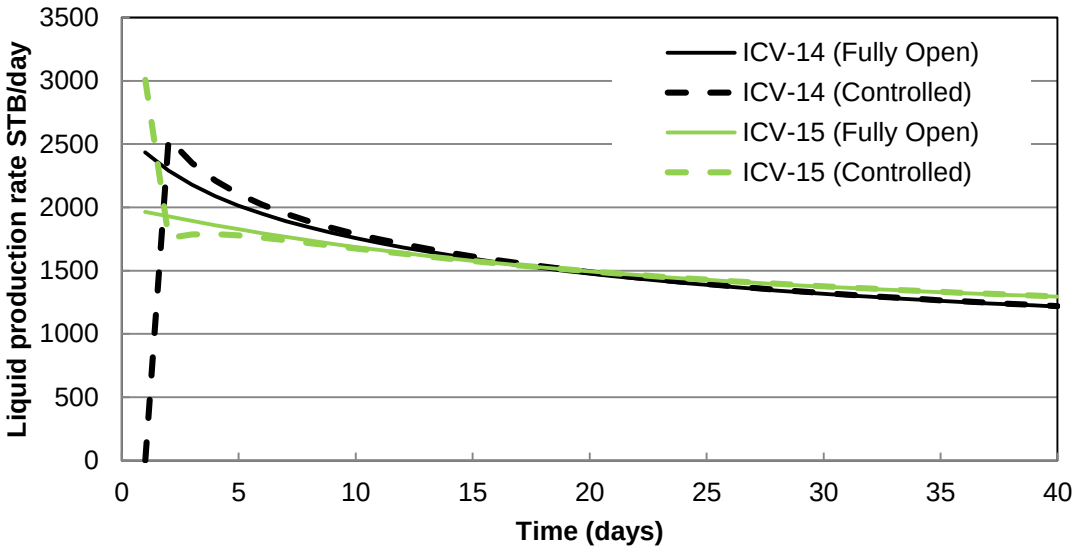

(a)

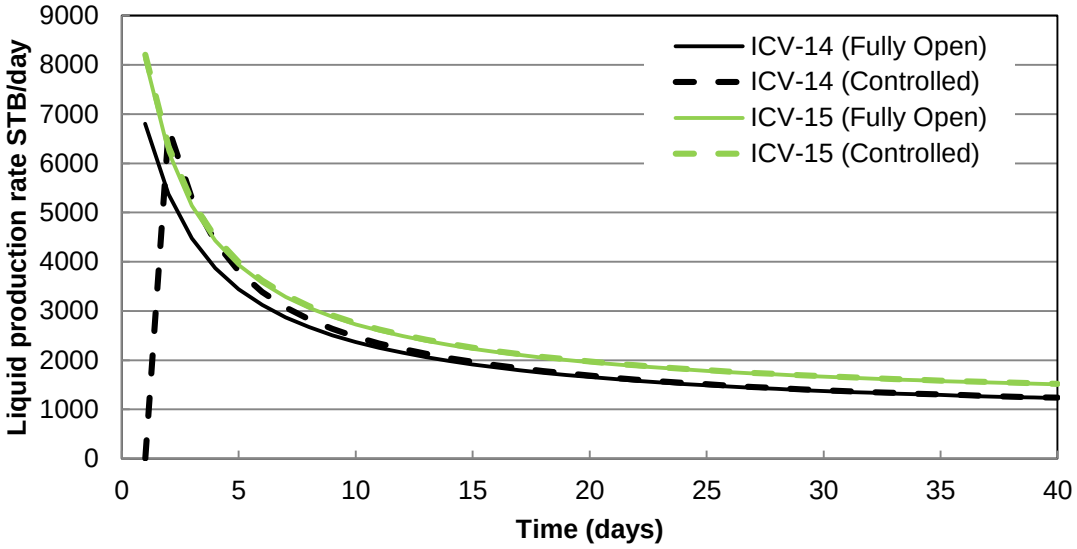

(b)

Figure 2-12: Zonal liquid production rates versus time as a result of closing ICV-14 at the first time step and then fully-open (Controlled) and fully-open during all time steps (Fully Open) for (a) case-1 with friction and (b) case-2 no friction

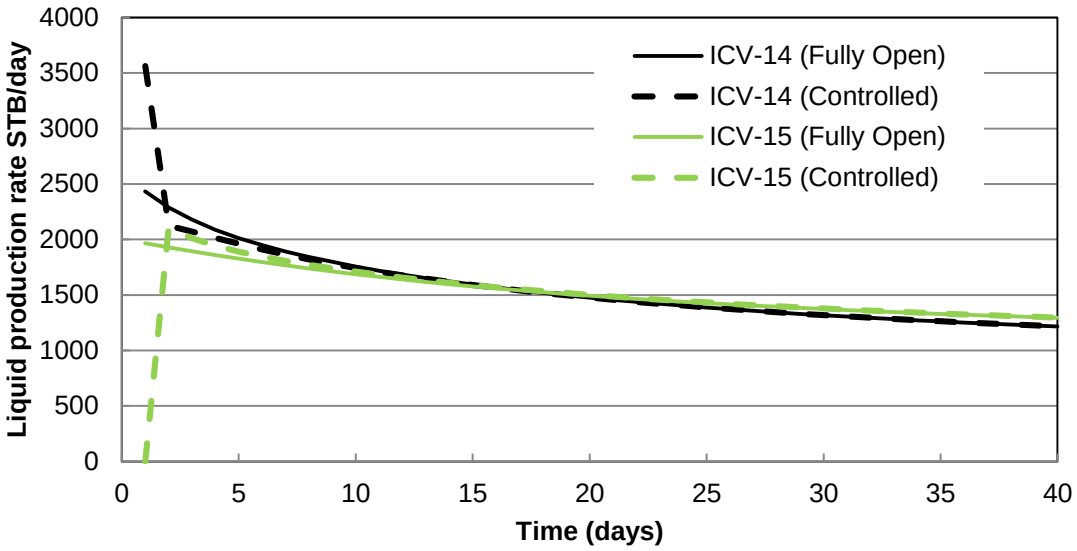

(a)

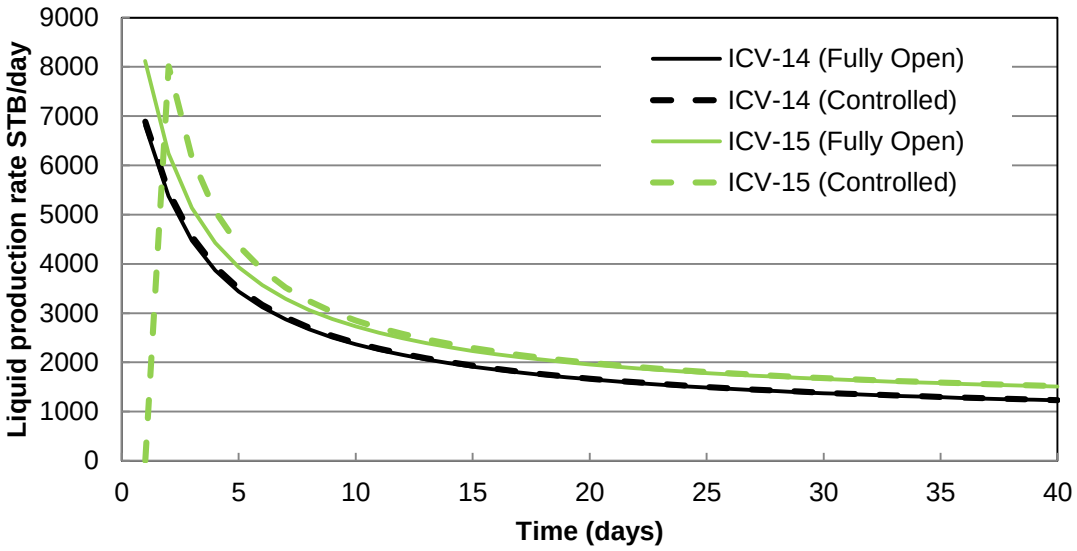

(b)

Figure 2-13: Zonal liquid production rates versus time as a result of closing ICV-15 at the first time step and then fully-open (Controlled) and fully-open during all time steps (Fully Open) for (a) case-1 with friction and (b) case-2 no friction

Proactive optimisation is performed using the I-well model developed in case-1 and case-2. The two ICVs are controlled during the 40 control steps of 1 day each (for detailed description of the employed gradient based optimisation algorithm see

Section 4.4.1). The optimisation starts from the same initial point in both cases and is performed for 100 iterations. Figure 2-14 compares the normalised improvement in both cases while 0% shows the initial point and 100% shows the optimum solution for each case. Faster convergence to the optimum solution is observed in case-2, with independent control variables, as compared to case-1, with dependent control variables. More accurate estimation of the gradient, defined as the first order partial derivate of the objective function w.r.t. control variables, is obtained with independent control variables. Therefore the employed gradient-based optimisation algorithm provides more accurate search steps and faster convergence. This shows that employing a more accurate, and also more representative, multi-segment well model creates a more challenging proactive optimisation problem which is addressed in this thesis. Different results might be obtained for other choices of the optimisation algorithms.

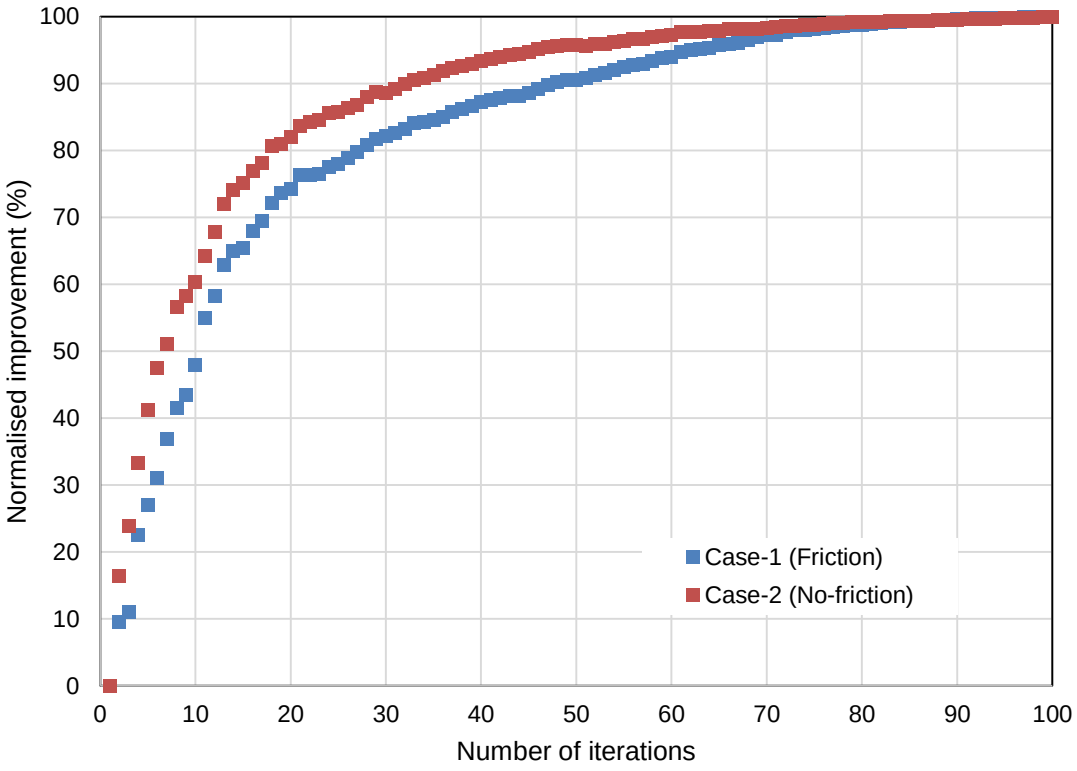

Figure 2-14: The optimisation performance during 100 iterations of the optimisation algorithm when the I-well is modelled using case-1 and case-2. (The data represents the average results from 5 independent runs.)

2.9.1 Summary

In this section the impact of modelling I-wells on the production prediction and subsequent optimisation process is investigated. It is observed that a multi-segment well modelling approach is used to accurately model downhole completion outflow, provides a different well and zonal production performance compared to the case when the outflow performance is ignored. The rate dependent frictional pressure drop component increases the interaction between zonal productions. Hence, increasing or decreasing the production from one zone not only changes the production from the other zones over the long-term (a reservoir effect); but also generates short-term (well effect) changes, which can only be captured by combined modelling of inflow and outflow. A strong interaction between zonal productions was observed in the considered case study. We also showed that this strong interaction between the control variables generates a more difficult proactive optimisation problem compared to the case with independent zonal production when using gradient-based optimisation algorithms. One novel aspect of this study is that it addresses the more challenging proactive optimisation problem of employing a more accurate, but also more representative, multi-segment well model.

Chapter 3 – Development of criteria for simplification of the problem of proactive control of ICVs

3.1. Introduction

This chapter describes how the proactive optimisation problem can be simplified in large real field industrial applications with limited computational resources. The challenges associated with proactive optimisation are described in Section 2.8.2. In this chapter we ignore the uncertainty associated with the modelling by considering a single reservoir model realisation ("Proactive Optimisation under Uncertainty" will be discussed in Chapter 5). A large number of control variables is the challenge to be addressed in this chapter. The objective is to reduce the number of proactive optimisation control variables by discarding the less important ones in order to simplify the problem with a minimum loss in added-value. This is particularly important in (1) computationally expensive field models with multiple I-wells each equipped with multiple ICVs (2) to employ the commercially available software to solve the problem with a reasonable efficiency. Two criteria for reducing the number of control variables are proposed and tested on the PUNQ-S3 model. Genetic Algorithm (GA) available in the MEPO software (SPTGroup, 2012) was used as the commercial optimiser however the developed criteria for simplification of the problem of proactive control of ICVs is independent of the choice of the optimization algorithm.

3.2. Limiting the length of the proactive optimisation period

An ideal proactive optimisation has the potential to deliver the ultimate improvement of the system by simultaneously considering all control variables during the optimisation process. However, this is subject to the availability of an efficient optimisation algorithm which can handle a large number of control variables and find the optimum solution. Generally the number of iterations required for convergence increases by increasing number of control variables in an optimisation problem, which is particularly important in proactive optimisation of large real field models with limited

computational resources. This Section proposed classifying the production period based on the control strategy employed.

The aim is to simplify the overall optimisation problem by limiting the proactive optimisation to the most important parts of the production period. Fast reactive control is expected to provide a reasonable performance for the rest of the production period with minor loss in the long-term objective function (e.g. NPV). A field's production life can be separated into two periods based on the effective control strategy:

1- Proactive only: This strategy can be used during the early, plateau production period, when the field has an excess fluid inflow capacity. Proactive optimisation of the production profile provides a better sweep and/or maximizes the NPV.
2- Proactive/reactive: Proactive optimisation is capable of finding the optimum control scenario throughout the life of the field. However, a simpler control strategy is generally sufficient after the plateau period, satisfying both short-term (production improvement) and long-term (NPV improvement) objectives. As a result, reactive strategy is good enough during this period even when considering long-term objectives. An example is during the decline period, when the well production is constrained by THP with multiple producing zones each controlled by ICV. The production is limited by tubing outflow; hence, a zone producing a large amount of water can reduce the well production rate and should be shut based on both the reactive and the proactive control strategy. It should be noted that, the importance of performing a proactive optimisation increases during this period, if ultimate recovery is the objective with a low discount factor and a small economic production rate (i.e. negligible operating cost).

Our goal is to recognise the production period associated with each group. This is achieved by investigating the optimisation objective function and constraints controlling the different stages of production. Moreover, a full-search study is performed on an optimisation problem and the control variables interactions are analysed to obtain the final conclusions.

3.2.1 Investigating the optimisation objectives and production constraints

The main intention of proactive strategy is to enhance long-term objectives by mitigating future undesired problems and/or states. The early, plateau period of field production is the ideal time for this control strategy, since it can be employed without cost to the short term objectives; assuming an optimal plateau rate is defined which is generally constrained by field fluid processing capacity and/or operator's production policy. As shown in Section 2.7, a simplified expression for NPV is used as the objective function for proactive optimization of a liquid (oil and water) producing well or field. Following is the formulation at zonal level, where ICV control is performed,

$$\mathcal{F}(x) = \sum_{n=1}^{S}\left[\sum_{j=1}^{N_z}\left(r_o q_{o,j}^n - r_{pw} q_{w,j}^n - r_{opex} q_{l,j}^n\right)\right]\frac{\delta t^n}{(1+b)^{t_n}}, \qquad 3\text{-}1$$

where S is the total number of simulation steps; N_z is the number of production zones. The costs constants r_o, r_{pw} and r_{opex} (in \$/sm^3) are the oil price, the water handling cost and the operating cost respectively. Variables $q_{o,j}^n$, $q_{w,j}^n$ and $q_{l,j}^n$ are the oil, water and liquid production rates of zone j at time step n in sm^3/day. The discount rate b is in decimal and δt^n is the length of the n^{th} simulation step and t_n is the cumulative time up to that simulation time step in years.

In contrast to proactive optimisation, instantaneous objective function at n^{th} simulation step (i.e. the internal summation of Equation 3-1) is the objective function of reactive optimisation of a liquid (oil and water) producing well or field as follows.

$$\mathrm{I}(x) = \sum_{j=1}^{N_z}\left(r_o q_{o,j}^n - r_{pw} q_{w,j}^n - r_{opex} q_{l,j}^n\right)\delta t^n . \qquad 3\text{-}2$$

Each zone is generating a term at the n^{th} simulation step (Equation 3-2). This term has a positive impact on $\mathrm{I}(x)$ at the beginning of production from a particular zone, but later on it decreases and can degrades $\mathrm{I}(x)$. The time of this change from a positive to a negative characteristic for a particular zone depends on the amount of oil and water production from that zone, the economic parameters and the constraints imposed on the total liquid production (oil and/or water) or pressures (BHP, THP) by the equipment or

management. The focus of this thesis is on optimisation of intelligent producers. It should be noted that, although intelligent injectors can be controlled proactively, by considering zonal injection rates as extra control variables (x), the optimal zonal injection control can never be reactive.

The aim is to find the time that a simple control strategy suffices to control zones with a negative impact and improve both instantaneous and long-term objectives. The reactive strategy is unable to provide any control scenario or is unlikely to find the optimum control scenario prior to this time. Figure 3-1 (a) shows an example of multi-zone production from a reservoir having two layers with different permeability separated by a partially sealed fault. There is a limit on the total liquid rate which can be produced from all zones (i.e. well liquid rate constraint). Keeping all ICVs open during the whole production period result in early water breakthrough in the high permeability zone and inefficient sweep of the low permeability layer (Figure 3-1 (b)). A reactive control strategy improves the instantaneous objective function (Equation 3-2) by reducing water production from higher water-cut (WC) zones, allowing an increase in the oil production at that time step. However, this reactive strategy fails to improve the long-term objectives (Equation 3-1), when it is not applied at appropriate time. The reduction in long-term objective is due to larger decrease in the instantaneous objective function (Equation 3-2) at $\ddot{n}^{\text{th}}$ simulation step ($\ddot{n} > n$) compared to the gain at n^{th} step. Figure 3-1 (c) shows water breakthrough in the neighbour zone as a result of reactive control. This therefore, shows that a proactive approach is required as long as the optimum decisions at a particular time step is affected with the decisions at future time steps. Section 3.2.2 investigates such an interaction between the control variables.

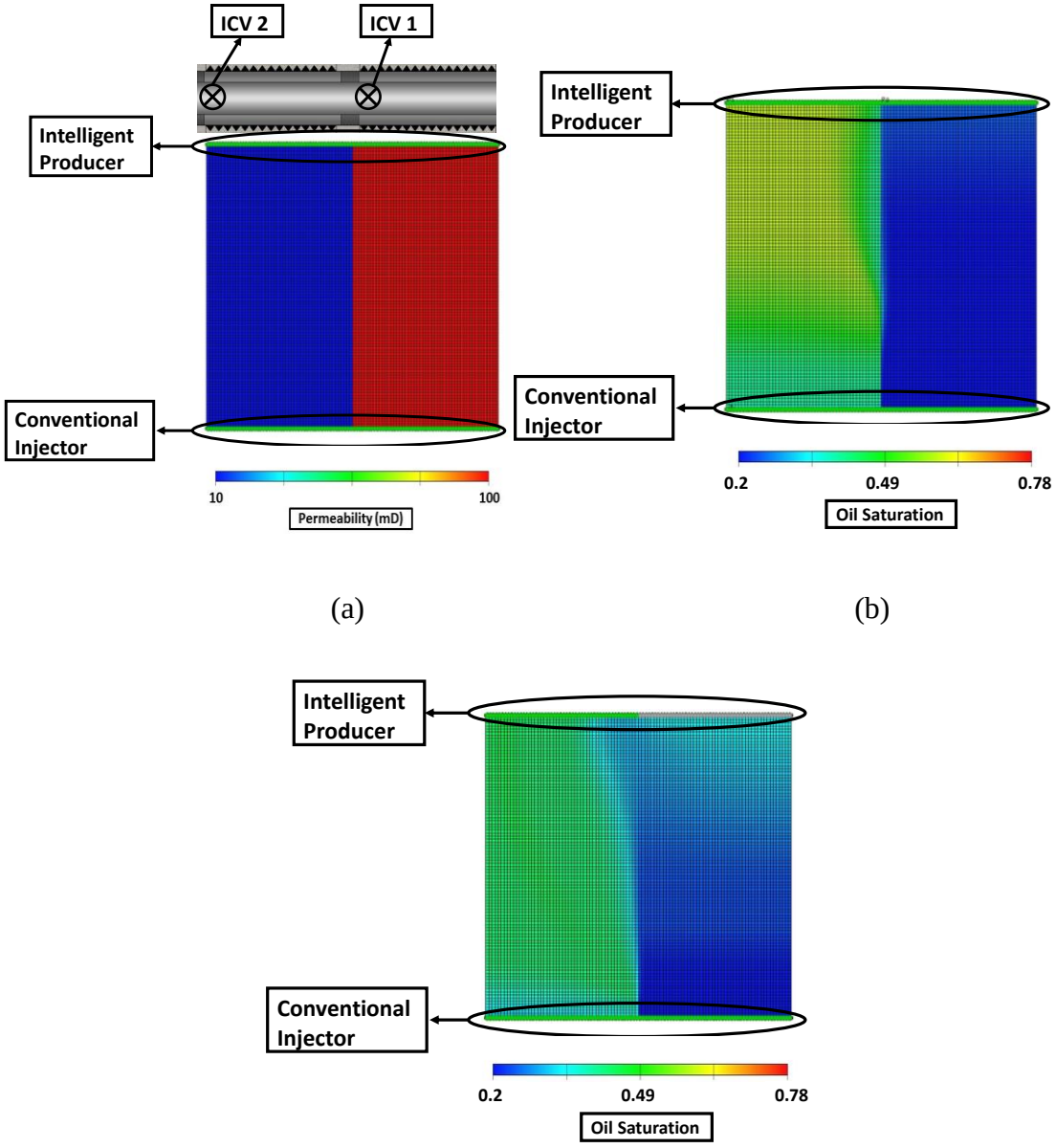

Figure 3-1: Example of situation that reactive control fails to provide optimum long-term objective (a) permeability distribution, well locations and completion (b) No-control (c) reactive control and water breakthrough in the neighbour zone due to partially sealed fault.

3.2.2 Analysing interaction between the control variables

Variable interaction in an optimisation problem was explained in Section 2.8.2-b. Inseparable function interaction between the control variables in a production optimisation problem is investigated in this section. The control variables are ICV areas discretised over the field production time, assuming 20 predefined control steps. This

study selected two control variables at different stages of the production period and performing a full-factorial search on these two variables while assuming all other variables are fixed at fully-open. The search is performed by varying the selected control variables (ICV areas) between fully-closed (i.e. 0) to fully-open (i.e. 1) in 25 steps. This assumes an infinitely variable ICV has been installed. The goal is to investigate if there is interaction between the control variables and how this characteristic is changed for variables corresponding to different production stages. This is achieved by investigating the changes in the optimum value of a given variable when the value of the other variable is changed (Figure 2-6).

Several cases are analysed where (i) both variables are during the plateau period, (ii) both variables are after the plateau period and (iii) one is during the plateau and another one after. For case (i) and (ii) control variables are always selected at two consecutive control steps in order to eliminate the effect of time difference on variable interactions. The study is performed on the PUNQ-S3 reservoir model developed with an intelligent producer in the optimum location. The details of the model are described in Section 4.5.2. The oil rate constraint with a maximum of 800 sm^3/day and a liquid rate constraint of maximum 900 sm^3/day are limiting the production from the field resulting in an oil rate plateau (until year 6) followed by a decline period (Figure 3-2).

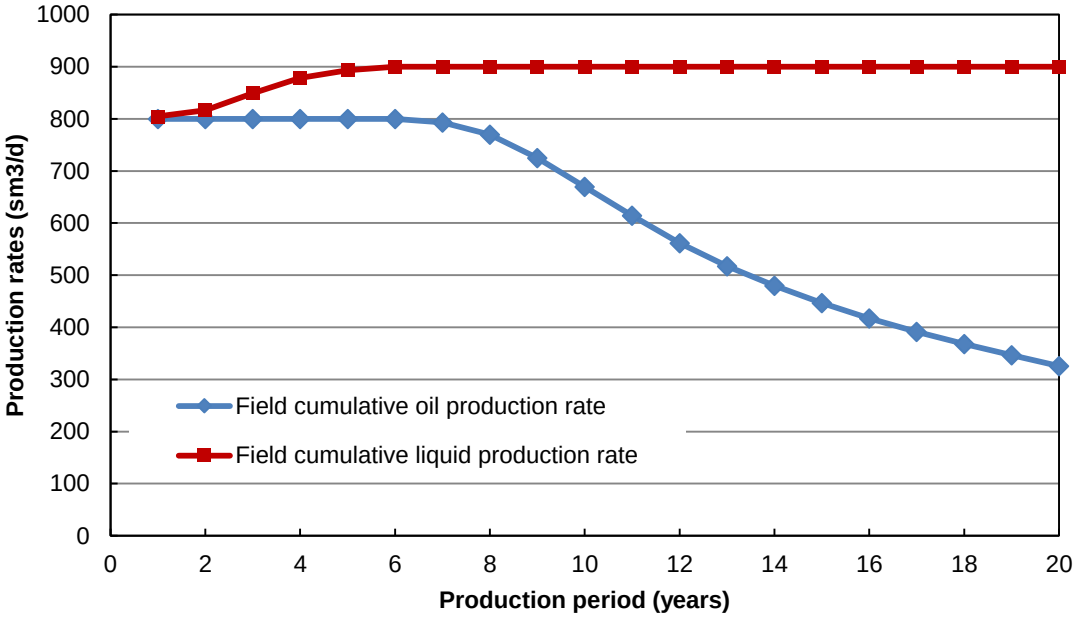

Figure 3-2: Oil production rate and liquid production rate during 20 years of production for PUNQ-S3 (constrained case)

Controlling an I-well equipped with 4 ICVs once every 12 months during 20 years of the production period (i.e. 20 control steps) results in 80 control variables. The test procedure was as follows:

1- Select an ICV (ICVx)
2- Select consecutive control steps (n, n+1)
3- Change flow areas of the selected ICV at the selected control steps ($A_{ICVx,n}$, $A_{ICVx,n+1}$) between 0 and 1 at 25 increments. Keep all the other control variable equal to 1 (i.e. fully-open).
4- Run 676 (26×26) experiments.
5- Find optimum value of $A_{ICVx,n+1}$ for each value of $A_{ICVx,n}$ (i.e. 26 values)
6- Find variance of the values of $A_{ICVx,n+1}$ from step 5
7- Repeat the process for another selection of ICVs and control steps.

The test was performed for all ICVs and similar results were observed in all cases. Following are the main characteristics of the response surface during different production stages presented using ICV4.

Figure 3-3 shows the 3D surface plot of the NPV versus normalised flow area of ICV4 at control step 2 ($A_{ICV4,2}$) and control step 3 ($A_{ICV4,3}$). It is observed that, the optimum value of $A_{ICV4,3}$ depends on the value of $A_{ICV4,2}$. When the value of $A_{ICV4,2}$ is small (0-0.4) the optimum value of $A_{ICV4,3}$ is fully open to improve NPV by extra oil production at step 3 to compensate lower production during step 2. When the value of $A_{ICV4,2}$ is large (0.7-1) the optimum value of $A_{ICV4,3}$ is fully closed to improve NPV by delaying water breakthrough to improve the sweep efficiency. However, the global optimum is obtained by $A_{ICV4,2}$ =0.4 and $A_{ICV4,3}$ = 0.64 resulting reduced production from this zone, rather than completely closing the zone. Here, the variance of the optimum value of $A_{ICV4,3}$ for different values of $A_{ICV4,2}$ is 0.13.

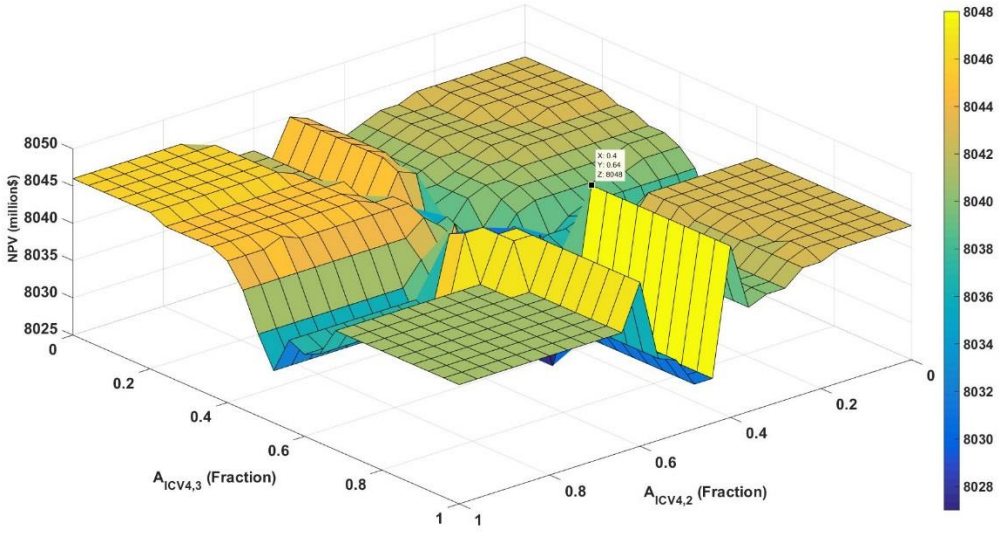

Figure 3-3: 3-D surface plot of NPV versus normalised flow area of ICV4 at control steps 2 & 3

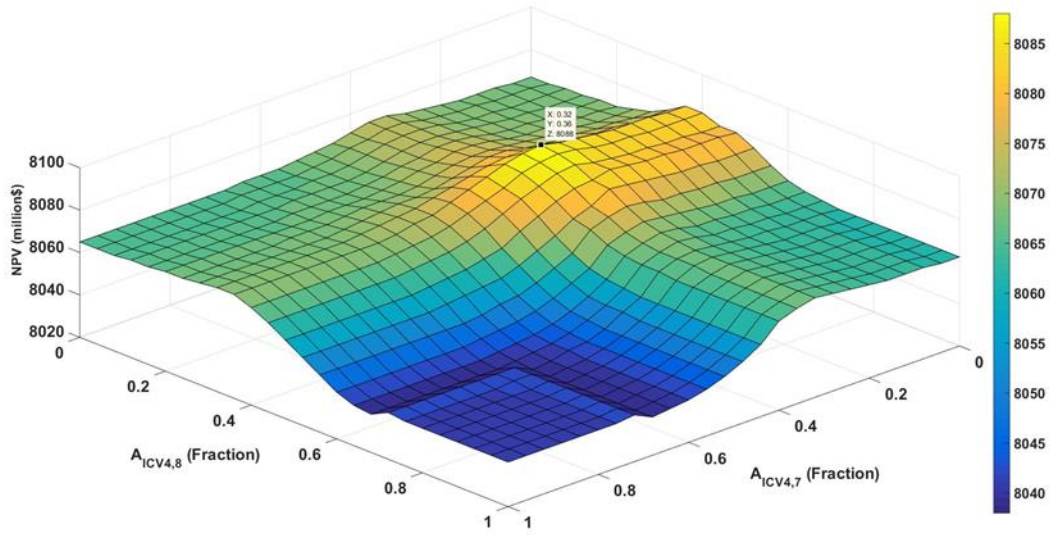

Figure 3-4: 3-D surface plot of NPV versus normalised flow area of ICV4 at control steps 7 & 8

Figure 3-4 shows the 3D surface plot of the NPV versus normalised flow area of ICV4 at control step 7 ($A_{ICV4,7}$) and control step 8 ($A_{ICV4,8}$). It is observed that, the optimum value of $A_{ICV4,8}$ is always in the range of 0.36 and does not depend on the value of $A_{ICV4,7}$. Here, the variance of the optimum value of $A_{ICV4,8}$ for different values of $A_{ICV4,7}$ is approximately zero (10^{-4}). The global optimum is obtained by $A_{ICV4,7}$ = 0.32 and $A_{ICV4,8}$ = 0.36. It should be noted that lower optimum flow area compared to step 2 and 3 (Figure 3-3) is mainly due to higher water production from this high permeability zone later in the production stage. However it is still economic to continue production from this zone rather than completely shut the zone.

The variables interaction during the plateau period is clearly observed by the response surface (Figure 3-3) and larger variance in the optimum value of $A_{ICV4,3}$ by changing value of $A_{ICV4,2}$. No interaction is observed between the control variables after the plateau period as shown by Figure 3-4 and close to zero variance. The variance of the optimum value of $A_{ICV4,n+1}$ by changing value of $A_{ICV4,n}$ for various consecutive control steps are shown in Table 3-1. A significant reduction in the variance is observed after control step 5 while the plateau period finishes at control step 6.

Table 3-1: Variance of optimum value of $A_{ICV4,n+1}$ by changing value of $A_{ICV4,n}$ for various consecutive control steps

Test #	1	2	3	4	5	6	7	8	9	10	11	12	13	14	15	16	17	18
1	0.126																	
2		0.13																
3			0.052															
4				0.004														
5					6×10^{-4}													
6						8×10^{-4}												
7							4×10^{-4}											
8								4×10^{-4}										
9									4×10^{-4}									
10																	0	

Table 3-2 shows the variance of the optimum value of $A_{ICV1,n+1}$ by changing value of $A_{ICV1,n}$ for various consecutive control steps. A significant reduction in the variance is observed after control step 8 which is delayed as compared to ICV4 (Table 3-1). This delay is mainly due to later water breakthrough in ICV1 producing from the low permeability zone.

Table 3-2: Variance of optimum value of $A_{ICV1,n+1}$ by changing value of $A_{ICV1,n}$ for various consecutive control steps

Test #	1	2	3	4	5	6	7	8	9	10	11	12	13	14	15	16	17	18
1	0.15																	
2		0.093																
3			0.068															
4				0.068														
5					0.068													
6						0.07												
7							0.07											
8								3×10^{-4}										
9									0									
10																	0	

Another test is performed when one variable is during the plateau period and another variable is after. Figure 3-5 shows the 3D surface plot of the NPV versus normalised flow area of ICV4 at control step 3 ($A_{ICV4,3}$) and control step 12 ($A_{ICV4,12}$). The variance of the optimum value of $A_{ICV4,12}$ for different values of $A_{ICV4,3}$ is zero and the variance of the optimum value of $A_{ICV4,3}$ for different values of $A_{ICV4,12}$ is approximately close to zero (10^{-4}). Therefore there is no interaction between the control variables during and after the plateau period.

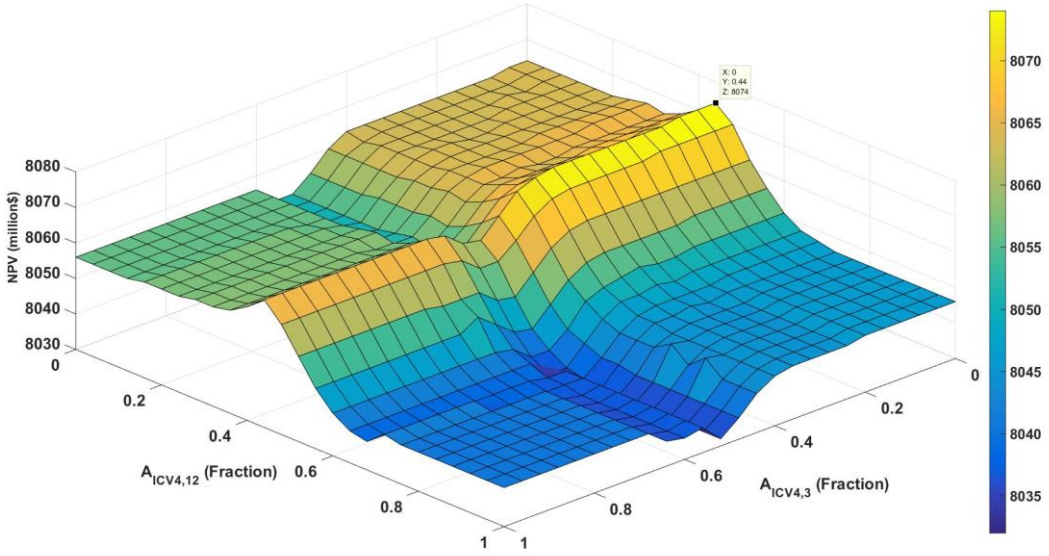

Figure 3-5: 3-D surface plot of NPV versus normalised flow area of ICV4 at control steps 3 & 12

The following main conclusions can be drawn:

I. The selected control steps are both during the plateau period: interaction is observed between the control variables. The optimum value of one variable thus depends on the value of the other; implying the control variables should be optimised simultaneously using a proactive approach during the plateau period.

II. The selected control steps are both after the plateau period: no or minor interaction is observed between the control variables; implying that the optimum value of one variable can be obtained independently from the other. This eliminates the need for simultaneous optimisation of the variables. A reactive approach can now find the optimum control after the plateau period as long as

the objective function of the reactive (short-term objectives) does not deviate considerably from the long-term objectives (Section 3.2.1).

III. One of the selected control steps is during the plateau period and the other one afterwards: the two variables show no, or only a minor, interaction. This means the proactive optimisation can be performed independent of the subsequent reactive optimisation and vice versa. This is particularly important for proactive optimisation, since it is performed early-on using a computationally expensive approach. Hence, having the option to eliminate the later reactive optimisation period from this calculation without experiencing a substantial loss, greatly reduces the complexity of the process.

3.2.3 Summary

This section investigated the behaviour of the objective function and variables interaction during the different stages of production. It is concluded that proactive is the best optimisation approach during the early production (plateau period) for a two phase production system with water as the unfavourable phase due to (1) generally, all zones are producing with a WC lower than a critical value (i.e. production from a zone does not degrade the instantaneous objective function Equation 3-2) hence reactive control will suggest a fully-open control scenario and cannot find the optimum long-term control strategy. (2) The optimal value of the control variables show substantial interaction with each other during this period and may be optimised simultaneously. Note that the active production constraint defines the way that proactive optimisation adds value at this stage. Proactive optimisation potentially improves the objective function during the whole production period when the well's production is controlled by an oil or a total liquid rate constraint. By contrast, proactive optimisation can only improve the long-term objective at the cost of sacrificing objectives during the short-term period when the well's production is controlled by a BHP or THP constraint. I.E. there is a penalty associated with proactive optimisation performed under a pressure constraint compared to a rate constraint due to the risk that the chosen control strategy may not prove to be optimum (Brouwer and Jansen, 2004).

One (or several) zones start to produce with WC higher than the critical value after the plateau period. Now production from one or several zones degrade the instantaneous

objective function (Equation 3-2). The reactive strategy of optimising the instantaneous objective function now has something to optimise. The resulting reactive control strategy provides a "close-to-optimum" long-term objective by removing the current negative term(s) from the objective function summation. The observation that the optimal value of the control variables after the plateau period show little or no interaction with value of the other control variables eliminate the need for all the variables to be optimised simultaneously.

Similarly, these guidelines can be extended to cases that other phases are produced (e.g. oil and gas) or when unfavourable phase is not water.

3.3. Limiting the control frequency of ICVs

The total number of variables increases rapidly in a proactive optimisation problem since the number of control elements is multiplied by the number of control steps that are planned for the expected production life of the well or field. Hence the control frequency plays an important role in defining the computational magnitude of the proactive optimisation problem. The control frequency is thus a variable that will benefit from optimal selection. Generally, a higher control frequency provides more flexibility in controlling production, potentially leading to an increased added-value. This is particularly true up to an optimal frequency however after this point the production cannot take advantage of this greater flexibility. For example: (1) reservoir flow dynamics react slowly compared to the rate of change in the zonal drawdown pressure when frequent changes in the ICV's flow area are made. (2) Proactive optimisation is frequently used to achieve an optimal sweep when water flooding a reservoir. The dynamics of the reservoir as a whole is much slower again (many months); hence a slow control frequency would be enough.

In order to investigate the impact of control frequency on proactive optimisation a test study is performed using the PUNQ-S3 reservoir model developed with an intelligent producer in the optimum location. The details of the model are described in Section 4.5.2. As previously (Section 3.2.2) an oil rate constraint of a maximum of 800 sm^3/day and a liquid rate constraint of a maximum of 900 sm^3/day limit the field's production resulting in an oil plateau followed by a decline period (Figure 3-2). This

model will be used to investigate the added-value of proactive optimisation at different control frequency for the ICV actions. Section 3.2 allowed the limitation of the length of the proactive optimisation period to only the plateau period. This reduced the computational demand. Six cases were considered where the control frequency was increased from once every 12, 6, 3, 2, 1 and 0.5 months. The optimisation was performed using the Genetic Algorithm (GA) option in MEPO (SPTGroup, 2012), a commercially available optimisation software. Several runs were performed for each optimisation using different values of the tuning parameters and a different random number generator; the aim being to ensure that the global optimum solution has been found in each case. The improvement w.r.t. the base case (no-control) is calculated for each case (Figure 3-6). We observed a substantial change in the added-value by decreasing the length of control steps from 12 months to 3 months. However, controlling the production more frequent than every 3 months did not show a significant improvement in the added-value. In this case greater control flexibility resulted in different solutions but no major change in the objective function value. Hence more frequent control of the ICVs for proactive optimisation cannot be justified for this case study.

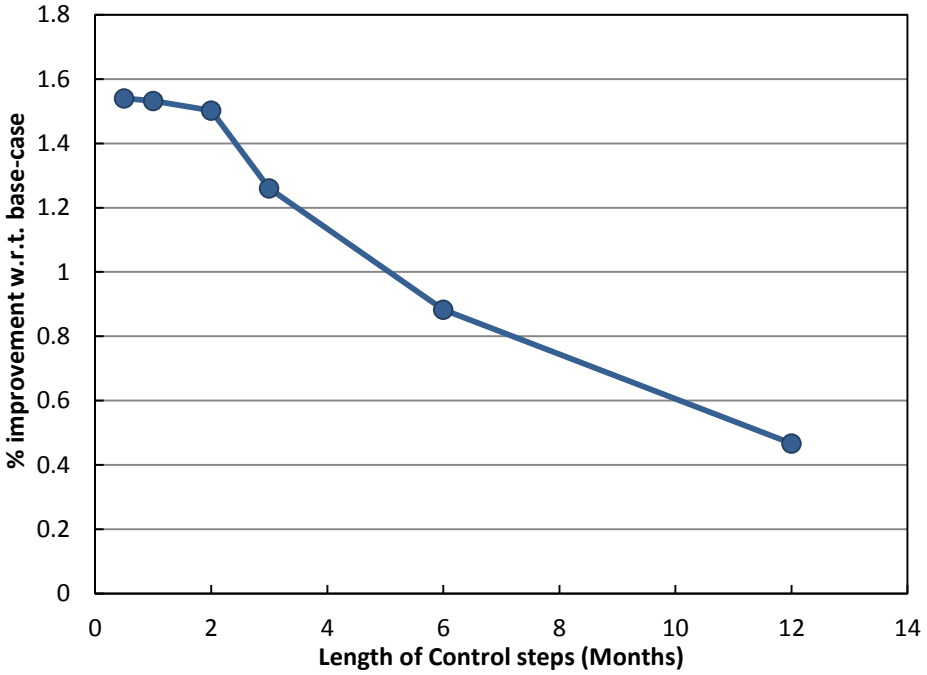

Figure 3-6: Improvement w.r.t. the base case for proactive optimisation performed using different control frequency of ICVs

Figure 3-6 shows the percent increase in NPV as the control frequency increases. Figure 3-7 shows the corresponding number of simulation runs as a function of the control frequency.

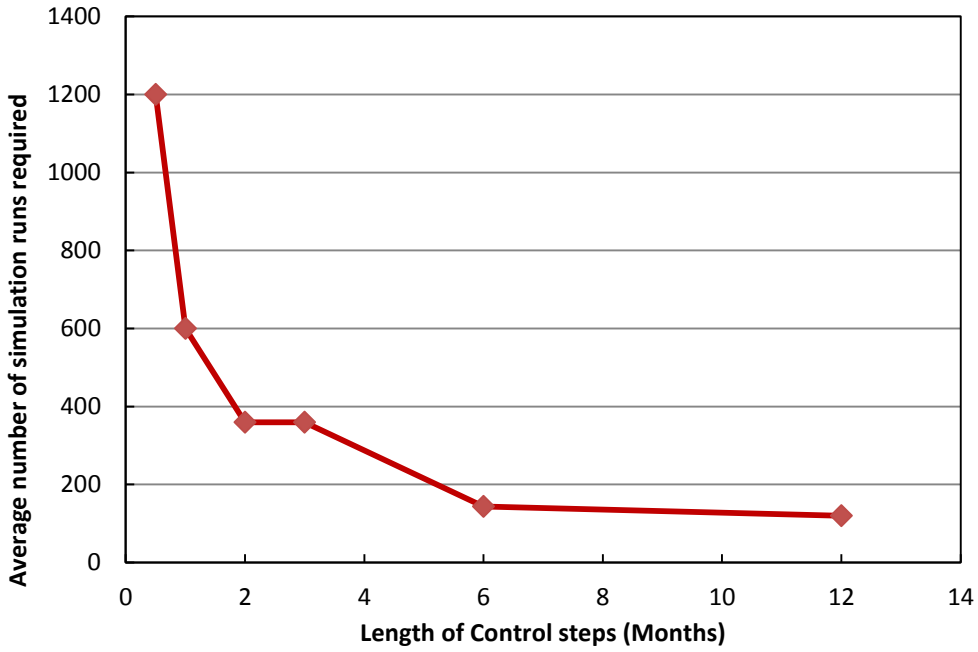

Figure 3-7: Average number of simulation runs required to find the optimum solution using different control frequency

Figure 3-6 and Figure 3-7 show that there is a conflict between higher added-value of more frequent control and the higher computation time due to increased number of control variables. Moreover, two other criteria need to be considered from an operational point of view:

1. In order to ensure the ICVs remain operable during their whole life, they need to be operated at least once (to prevent scale build-up, etc.) during a predetermined interval based on the chemistry of the produced fluids, the manufacture's recommendations and the operators' policy. It is of course possible to return the ICV to its original position after this operation, but this does provide a good opportunity to review whether the control scenario should be reviewed.
2. The life of the ICV may also be defined by an allowed maximum number of operations, which after performing the risk of ICV failure increases. Any such

constraints need to be taken into account as an extra constraint when designing the optimum control strategy.

The abovementioned criteria provide a guideline for defining the optimum control frequency of the ICVs to provide a balance between added-value, reliability and computation time required for optimisation. It is believed that this trend is general since same guidelines were found during the real field case study discussed in Chapter 7. Multiscale approach (Lien et al., 2008, Oliveira and Reynolds, 2015) discussed in section 2.8.2-b is an alternative approach to reduce the number of control variables while optimum control frequency might vary at different stages of the control period.

3.4. Conclusions

This chapter discussed guidelines for simplifying the proactive optimisation problem by reducing the number of control variables, while achieving the main added-value expected from the task. This is especially important when using commercial optimisers since they have been developed to address a wide range of applications and may not necessarily employ the most efficient method to solve our problem, the proactive optimisation of ICVs. Chapter 4 will develop an efficient optimisation algorithm for solving the proactive optimisation problem. The developed algorithm takes advantage of the proposed guidelines by efficient solution of the simplified proactive optimisation problem when there is computational constraints driven by the industrial applications.

Another important application of the developed guidelines is expected to be the proactive optimisation of real field models developed with many conventional wells and I-wells equipped with multiple ICVs. Note that both types of well can be controlled by the surface wellhead choke. Solution of this complex problem requires the use of the most efficient optimisation algorithm after problem simplification by implementation of the above guidelines. Chapter 7 presents such a case study.

Chapter 4– Development of a suitable algorithm for proactive optimisation of ICVs

4.1. Introduction

In this chapter, the search space of a proactive optimization problem is visualized to assist in selecting the most suitable proactive optimization approach that is state-of-the-art stochastic gradient approximation algorithms. The Simultaneous Perturbation Stochastic Approximation (SPSA) method (Spall, 1992) and the Ensemble-based Optimization (EnOpt) method (Chen et al., 2009) have all been implemented and evaluated. Additionally, we present a new derivation of EnOpt using the concept of directional derivatives.

Proactive optimization of an I-well control by the installed ICVs is performed with a detailed model of an I-well built within a commercial reservoir simulator. An I-well's zonal liquid production/injection rate cannot be controlled directly due to its direct hydraulic communication with the other zones. Instead, the ICV flow areas are used as control parameters. Moreover, there is a non-linear relationship between the ICV flow rate and its flow area and the physics of the valves flow performance. This integrated approach leads to more realistic models while resulting in a different and more challenging optimisation problem (See Section 2.9). Solution of the resulting constrained, non-linear optimization problem is addressed in this chapter. The optimization performance of the SPSA and EnOpt algorithms will be compared for different case studies while employing various sets of tuning parameters. Specific guidelines have been developed for setting the tuning parameters in the problem of proactive control of ICV based on the general guidelines suggested by e.g., Spall (1998). In addition, the well's operational problems normally result in the stochastic nature (smoothness) of the obtained ICV control scenario to be as important as its added-value.

4.2. Objective function in I-well proactive control

Following simplified Net Present Value (NPV) formula is considered as the objective function in proactive optimisation of ICVs, detailed formulation and definition of the variables was discussed in Section 2.7.

$$\mathcal{F}(x) = \sum_{n=1}^{S} \left[\sum_{j=1}^{N_p} \left(r_o q_{o,j}^n - r_{pw} q_{w,j}^n - r_{opex} q_{l,j}^n \right) \right] \frac{\delta t^n}{(1+b)^{t_n}}, \qquad 4\text{-}1$$

Only a single realisation of the reservoir model is considered in this chapter to develop and test the optimisation algorithms. For robust optimization, the objective function is substituted with another objective function as explained in Chapter 5 and Chapter 6.

4.3. Visualisation to assist investigation of the structure of the search space

Visualising the search space of an optimisation problem can provide a valuable insight into some inherent characteristics such as (i) the presence of local optima, (ii) the relative difference between the local optima and the global optimum in terms of the objective function value, (iii) the proximity of the control variables in the search space and (iv) the sensitivity of the objective function with respect to control variables. The area open to flow for each ICV at each control step is considered to be one dimension. The proactive optimisation is thus a high dimensional problem of up to thousands dimensions. Visualisation reduces the dimensionality of the data by projecting the data onto a 2D or 3D space while maintaining as much information as possible. High dimensional visualisation has already proved useful in several areas of petroleum engineering. Hajizadeh et al. (2012) compared the performance of the optimisation algorithms in history matching by visualising the optimisation process. Haghighat Sefat et al. (2013) showed that visualising the optimisation process can assist in quantifying the algorithm's tuning process. Fonseca et al. (2014) employed visualisation to aid in understanding the complex nature of the objective function surface and the performance of the optimization algorithm during robust ensemble-based multi-objective optimization.

Let $X = \{x_1, x_2, \dots, x_n\}$ be a set of H-dimensional data points with n instances defined on $\mathbb{R}^H$. A function δ: $\mathbb{R}^H \rightarrow \mathbb{R}$ is defined to calculate a proximity criterion where $\delta(x_i, x_j)$ is showing dissimilarity (distance) between two instances i and j. The goal is to project X into a lower (two for display) dimension space to have a set of points $Z = \{z_1, z_2, \dots, z_n\}$ with the same number of instances (n) defined on $\mathbb{R}^2$. Similarly a function $\hat{\delta}: \mathbb{R}^2 \rightarrow \mathbb{R}$ is defined to calculate the dissimilarity (Euclidian distance) between two points i and j in 2D space. $\alpha: X \rightarrow Z$ is the projection function from H-dimensional space to 2D. The goal is to preserve the distance relationship between the points given by the specified metric as much as possible i.e. make $\left|\delta(x_i, x_j) - \hat{\delta}(\alpha(x_i), \alpha(x_j))\right|$ approaches zero $\forall\, x_i, x_j \in X$. The degree to which the distance cannot be preserved is the projection error.

There are several approaches to solve this problem and reduce data dimensionality. Principal Component Analysis (PCA) is a widely known example which use statistical measures for dimensionality reduction. PCA operates by decomposing the covariance matrix of H-dimensional data into H eigenvectors with eigenvalues. The dimensionality reduction happens by selecting the first h eigenvectors (h<H) with the largest eigenvalues. The data variance is preserved even when h<<H. More information about PCA is available in (Jolliffe, 2002). A limitation of PCA is the Euclidean distance assumption in both high and low dimensional space. Multi-Dimensional Scaling (MDS) (Section 6.4), a more general approach, allows considering different types of distance measure for the high dimensional space is used in this thesis.

The search space in PUNQ-S3 (see Section 4.5.3) with an I-well in non-optimum location is investigated by generating 5000 experiments (each experiment is one control scenario with 80 variables) using Latin Hypercube Sampling (See (McKay et al., 1979) for more information about Latin Hypercube Sampling). NPV calculated using Equation 4-1 with the economical parameters provided in Table 4-1 is considered as the objective function. MDS is employed to reduce dimension of the generated control scenarios from its original 80D to 2D while Euclidean distance (Equation 6-5) is considered as the measure in the high dimensional and 2D space. Figure 4-1 shows the surface generated using 5000 experiments.

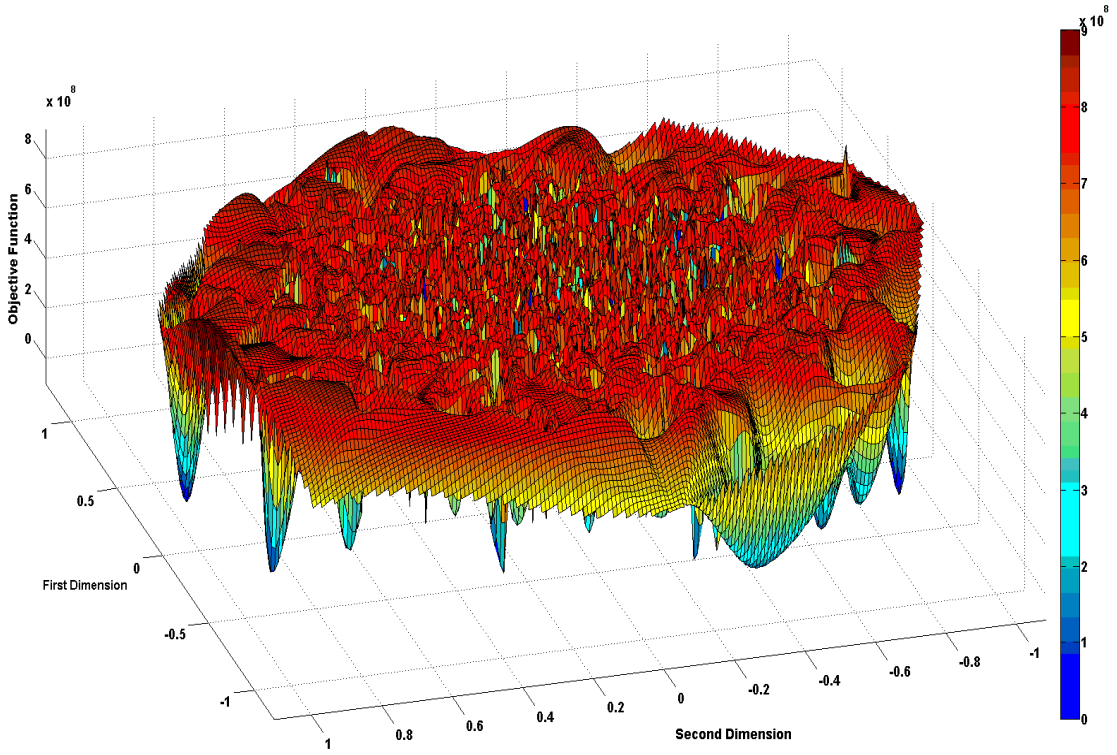

Figure 4-1: The 2D-projected search space in a proactive optimisation problem of PUNQ-S3. Surface generated using 5000 experiments, colour shows the objective function (NPV) (warm=high; cold=low)

Figure 4-1 reveals that there are several local optima with the objective value close to each other. Also in this case study a local optimum could achieve around 90% of the improvement obtained by the global optimum solution. A similar nature of the solution space was previously observed in high-dimensional history matching by (Oliver et al. (2008), Oliver and Chen (2011)) and in the production optimization of conventional wells by Fonseca et al. (2014). Jansen et al. (2009) and van Essen et al. (2011) observed similar behaviour during multi-objective short-term and long-term optimization, where degree of freedom (DOF) exists to improve one objective without sacrificing the other.

The global optimum (i.e. the best solution in the whole search space) is the preferred solution. However inferior local optima (i.e. best solutions in a neighbourhood of the search space) may be achieved due to time and/or algorithm limitations. Gradient-based algorithms, as a suitable choice for optimising large number of control variables, generally converge to a local optimum. This limitation is alleviated using some techniques such as injecting noise or starting the algorithm from different initial points. Besides, a small difference between a local optimum and the global optimum

improvement in proactive optimisation of ICVs can be tolerated by a field operator when quickly obtaining a profitable solution is already an achievement. This makes the gradient-based algorithms a reasonable choice for proactive optimisation of ICVs.

4.4. Stochastic gradient-based methods for proactive optimization of ICVs

Large number of control variables and the characteristics of the search space (see Section 4.3) during proactive optimisation of ICVs is the main motivation for choosing gradient-based methods as an appropriate optimisation algorithm. Efficiency of the gradient-based methods in solving large scale optimisation problem is also observed by (Zingg et al. (2008), Zhao et al. (2013)) . However calculating the gradient using standard finite-difference approaches is computationally unfeasible due to large number of control variables (up to thousands). Using an adjoint formulation is normally not possible as it is not widely implemented in most reservoir simulation packages.

In the current study, we use stochastic optimization methods where the gradient is estimated by perturbing all the control variables simultaneously (Spall, 2003). This is possibly a more efficient approach than the standard finite difference methods where the variables are perturbed one at a time. The following subsections present the details of the two algorithms under investigation.

4.4.1 Simultaneous Perturbation Stochastic Approximation (SPSA)

SPSA is a stochastic optimization method that uses an approximate steepest descent (or ascent) with a randomly selected stencil (Spall, 1992, Sadegh and Spall, 1998). Consider $\mathcal{F}(x_k)$ to be the value of the objective function where x_k is a vector of n_x control variables at iteration k ($x_k = \left[x_1, x_2, \dots, x_{n_x}\right]_k^T$). The gradient $g_k(x)$, calculated using standard (finite-difference) approximation method, is defined as the partial derivatives of the objective function: $g_k(x) = \frac{\partial\, \mathcal{F}(x)}{\partial\, x} = \left[\frac{\partial \mathcal{F}}{\partial x_1}, \frac{\partial \mathcal{F}}{\partial x_2}, \dots, \frac{\partial \mathcal{F}}{\partial x_{n_x}}\right]^T$ where $[.]^T$ denotes a column vector. The goal in the SPSA is to maximize $\mathcal{F}(x)$ iteratively using:

$$x_{k+1} = x_k + \alpha_k \hat{g}_k\,(x_k), \qquad 4\text{-}2$$

where $\hat{g}_k(x)$ is the stochastically estimated gradient.

Calculation of $\hat{g}_k(x)$, requires that $\Delta_k \in \mathbb{R}^{n_x}$ is defined as a vector of mutually independent, mean-zero random variables $[\Delta_{k1}, \Delta_{k2}, \dots, \Delta_{kn_x}]^T$ satisfying the following conditions:

$$\Delta_{ki}^{-1} = \Delta_{ki}, \tag{4-3}$$

$$E\left|\Delta_{ki}^{-1}\right| = E|\Delta_{ki}| = 0, \tag{4-4}$$

where *E* denotes the expected value. Usually, but not necessarily, Δ_{ki} is chosen from the Bernoulli (±1) symmetric distribution to respect the above conditions (Spall, 1992). Such n_x-dimensional column vector Δ_k and a positive scalar c_k can be used to evaluate $\mathcal{F}(x)$ for calculating the stochastic gradient:

$$\hat{g}_k(x_k) = \frac{\mathcal{F}(x_k + c_k\Delta_k) - \mathcal{F}(x_k - c_k\Delta_k)}{2c_k} \times \left[\frac{1}{\Delta_{k1}}, \frac{1}{\Delta_{k2}}, \dots, \frac{1}{\Delta_{kn_x}}\right]^T. \tag{4-5}$$

Equation 4-5 is similar to the central difference approximation of the Kiefer-Wolfowitz (Kiefer and Wolfowitz, 1952) or finite difference method. The only difference is the simultaneous perturbation of all control variables in Equation 4-5. Therefore SPSA-central requires only two evaluations of the objective function during each iteration. This should be contrasted with the classical forward-difference approach where (n_x+1) evaluations are required. For the rest of this thesis the short-form of SPSA refers to the SPSA-central formulation (Equation 4-5).

The constants α_k and c_k in Equations 4-2 and 4-5 are the SPSA algorithm's tuning parameters. The convergence of the SPSA iterations relies on the sequence of α_k and c_k. The importance of the tuning increases for computationally demanding objective functions. Spall (1998) proposed the following decaying sequences to estimate α_k and c_k to ensure a gradually refining search:

$$\alpha_k = \frac{a}{(\mathbb{A} + k + 1)^{\vartheta}}, \tag{4-6}$$

$$c_k = \frac{c}{(k+1)^{\gamma}}, \tag{4-7}$$

where a, c, $\mathbb{A}$, ϑ and γ are positive real numbers. For ensuring convergence of the algorithm the tuning parameters have to satisfy the following conditions (Spall, 1998):

$$\alpha_k > 0, \quad c_k > 0, \quad \alpha_k \to 0, \quad c_k \to 0, \quad \sum_{k=0}^{\infty} \alpha_k = \infty, \quad \sum_{k=0}^{\infty} \left(\frac{\alpha_k}{c_k}\right)^2 < \infty. \qquad 4\text{-}8$$

The constants ϑ and γ should also satisfy:

$$\vartheta - 2\gamma > 0, \qquad 3\gamma - 0.5\vartheta \geq 0. \qquad 4\text{-}9$$

This results in practical values for ϑ and γ of 0.602 and 0.101 respectively. The stability constant $\mathbb{A}$ is recommended to be about 5% - 10% of the allowed, or expected, number of search iterations (Spall, 2003). The constants a and c are defined by the user. The following subsections provide recommended guidelines for defining appropriate ranges for a and c in proactive optimization of ICVs while working in log-transformed space. These guidelines have recently been confirmed by an ICV-optimization visualization study (Haghighat Sefat et al., 2013). This sensitivity visualised the iterative values of the control variables in 2-dimensional space to quantify the impact of each tuning parameter on the search process.

An intuitive alternative approach to determine α_k is to use an approximate line-search method instead of Equation 4-6. SPSA with line search has been used in several studies (e.g. (Gao et al., 2007, Zhao et al., 2011b)). Gao et al. (2007) compared basic SPSA with SPSA equipped with a line search and observed that the basic SPSA achieves better final results despite the line search improving the initial convergence speed. This study uses basic SPSA where α_k is determined using Equation 4-6.

Tuning a. Increasing a up to some level can enhance the optimization performance if there is a large difference between the initial point and optimum solution and accurate gradient data is available. Do and Reynolds (2013) recommended choosing a such that at $k = 0$ we have $1 \leq \alpha_k = \alpha_0 \leq 3$. Equation 4-6 was solved for a after specifying $\mathbb{A}$ (set to 10% of the total allowed number of iterations), ϑ, α_0 and $k = 0$. Initial testing found that these choices resulted in an unstable optimization process when applied to the proactive optimization of ICVs. The systematic search had been converted into a

random search in the search space which was unable to converge to the optimum solution. This can be attributed to:

- Different local optima with similar objective values,
- A sharp change in the objective value resulting from a small change in the control (i.e. a large search step leads to an unstable optimization),
- Numerical convergence problem being experienced in some of the control scenarios.

A smaller a is required to compensate the gradient approximation error increase and to stabilize the search process. Spall (1998) reached the same conclusion when he recommended a smaller value of a together with a larger c value in a high-noise environment. The value of $0.1 \leq \alpha_k = \alpha_0 \leq 0.5$ was chosen for this study. The impact of this choice on the optimization process will be explained in the case studies (Section 4.5).

Tuning c. Spall (1998) suggested to set c at a level approximately equal to the standard deviation of the objective function measurement error. The standard deviation is calculated by making several measurements of $\mathcal{F}(x)$ at the initial guess x_0. A small, positive value of c should normally be chosen for a simulation-based optimization problem since when the objective function being evaluated by the numerical simulator has a zero measurement error. However, there are two problems associated with using small c in a simulation-based optimization: (1) the changes in the objective function can be significantly lower than round-off and/or convergence error within the simulator and (2) the estimated gradient will only capture the local variations of the objective function if the function is highly non-monotonic. Therefore, a small c can result in an inaccurate search step, oscillation and a low optimization performance.

The value of c was defined by setting $k = k_{max}$ then $c_k = c_{min}$ in this study. Equation 4-7 can then be solved for c by setting c_{min} as the minimum plausible perturbation size defined by the operational and design constraints of ICVs. The ICVs have been assumed to have a maximum of 10, 20 and 40 positions, with a logarithmic change in the fractional open-to-flow area between each position, during the perturbation stage for the initial guess. This translates into c_{min} being equal to 0.1, 0.05

and 0.025, respectively. It should be noted that these numbers of ICV positions have only been employed to define the size of the perturbation step, since the resulting optimum control setting of the ICVs is a continuous variable.

Average SPSA, The expectation of the stochastically estimated gradient ($\hat{g}_k(x_k)$), as calculated by the optimization algorithm, is the true gradient due to the random nature of Δ_k in Equation 4-5 (Spall, 1992, Gao et al., 2007). Spall (1992) and Wang et al. (2009) suggested to use an averaged stochastic gradient calculated from an ensemble of perturbation vectors to improve the estimation of the search direction. SPSA generates n_e independent samples of Δk during each iteration, resulting in $2 \times n_e$ objective function evaluations when using the central difference formulation for estimating the gradient. Consistency with EnOpt, which provides n_e independent samples of Δk from n_e objective function evaluations per iteration, was maintained by operating $n_e/2$ independent samples of Δk during each iteration of SPSA. The average stochastic gradient can then be calculated by arithmetic averaging of an ensemble of $n_e/2$ estimated gradients using:

$$\overline{\hat{g}_k\,(x_k)} = \frac{1}{n_e/2} \sum_{i=1}^{n_e/2} \hat{g}_i\,(x_k), \qquad 4\text{-}10$$

where $\overline{\hat{g}_k\,(x_k)}$ is the average stochastic gradient which is substituted for $\hat{g}_k\,(x_k)$ in Equation 4-2. The averaged stochastic gradient has been previously studied using an ensemble size of 2 and 4 (Spall, 1992) or 10 and 20 (Wang et al., 2009). Both studies concluded that the quality of the estimated gradient and the optimization performance is improved by increasing the ensemble size. However, an excessive increase in the ensemble size eliminates the stochastic effect in the obtained solution, but does not achieve a significant change in the final objective value. This study compares the optimisation process using ensemble sizes of 4 and 10.

4.4.2 Ensemble-based optimization (EnOpt)

This section discusses the EnOpt method (Chen et al., 2009, Chen et al., 2010). EnOpt is derived based on the definition of directional derivatives and stochastic estimation of the derivatives using an ensemble based method.

Directional Derivatives. Evaluation of the Jacobian $\nabla\mathcal{F}(x_k)$, which has the components $\partial_j\mathcal{F}(x_k)$, where $j = 1, \dots, n_x$, by a straightforward differentiating method is not feasible for high dimensional search spaces. Hence directional derivatives were employed with a random direction vector (of unit length) u, defined as:

$$\nabla_u\mathcal{F}(x_k) = \frac{\mathcal{F}(x_k + c_k u) - \mathcal{F}(x_k)}{c_k}, \tag{4-11}$$

where c_k is the step size. The directional derivative is related to the standard derivative as:

$$\nabla_u\mathcal{F}(x_k) = \nabla\mathcal{F}(x_k) \cdot u\,. \tag{4-12}$$

In the previous equations, $\nabla_u\mathcal{F}(x_k)$ is of size 1 and $\nabla\mathcal{F}(x_k)$ is of size $1 \times n_x$ and u is the perturbation vector of size $n_x \times 1$. Similarly, x_k is of size $n_x \times 1$.

Stochastic Ensemble Method. We use an ensemble of perturbations to approximate the gradient vector from an ensemble of directional derivatives as:

$$\nabla_U\mathcal{F}(x_k) = \nabla\mathcal{F}(x_k)U, \tag{4-13}$$

where $\nabla_U\mathcal{F}(x_k)$ is an ensemble of directional derivatives of size $1 \times n_e$ where n_e is the ensemble size (i.e., equal to the objective function evaluations here) and U is the perturbation matrix of size $n_x \times n_e$ used in estimating the directional derivatives. Multiply both sides from the right side with U^T one gets:

$$(\nabla_U\mathcal{F}(x_k))U^T = \nabla\mathcal{F}(x_k)(UU^T)\,. \tag{4-14}$$

From which, the standard derivative can be evaluated as:

$$\nabla\mathcal{F}(x_k) = [\nabla_U\mathcal{F}(x_k)]U^T(UU^T)^{-1}\,. \tag{4-15}$$

For each ensemble member i, the directional derivative around x_k is:

$$[\nabla_U\mathcal{F}(x_k)]_i = \frac{\mathcal{F}(x_k + c_k u_i) - \mathcal{F}(x_k)}{c_k}, \tag{4-16}$$

where u_i is a random normal perturbation in all components of x_k with zero mean and variance of 1. Note that u_i is multiplied by decaying c_k for gradual refining of the perturbation steps to ensure convergence of the algorithm. Value of c_k is calculated using the same equation employed in the SPSA (Equation 4-7). For the ensemble of directional derivatives, we can re-write the directional derivative in a matrix format as:

$$\nabla_U \mathcal{F}(x_k) = Y, \tag{4-17}$$

where Y is of size $1 \times n_e$ and each column i of Y corresponds to $[\mathcal{F}(x_k + c_k u_i) - \mathcal{F}(x_k)]/c_k$. The matrix form of Equation 4-15 is then

$$\nabla \mathcal{F}(x_k) = YU^T(UU^T)^{-1}. \tag{4-18}$$

Therefore the size of $\nabla \mathcal{F}(x_k)$ is $1 \times n_x$ where Y is of size $1 \times n_e$ and U is of size $n_x \times n_e$. Once the approximate gradient is obtained an iterative update equation can be formulated as:

$$x_{k+1} = x_k + \alpha_k \nabla \mathcal{F}(x_k)^T. \tag{4-19}$$

x_k, x_{k+1} and $\nabla \mathcal{F}(x_k)^T$ is of size $n_x \times 1$. A decaying sequence is defined for α_k using Equation 4-6 to ensure a gradually refining search. Moreover, $\nabla \mathcal{F}(x_k)^T = ((UU^T)^{-T} UY^T)$. Note that UU^T is a symmetric matrix and $(UU^T)^{-T} = (UU^T)^{-1}$. The inverse of the covariance matrix (N.B. $E(U)$=0 therefore UU^T is the covariance matrix) can be problematic as the ensemble size will be much smaller than the size of the control vector and the resulting covariance matrix will be rank deficient. Following the same argument proposed by Chen et al. (2009) the gradient is preconditioned by a matrix $(UU^T)^2$ to obtain a smoothed gradient. The updated equation of EnOpt is thus:

$$x_{k+1} = x_k + \alpha_k (UU^T)(UY^T). \tag{4-20}$$

Furthermore, the gradient is normalized with the ℓ_∞ (infinity norm)

$$x_{k+1} = x_k + \alpha_k \frac{(UU^T)(UY^T)}{\|(UU^T)(UY^T)\|_\infty}. \tag{4-21}$$

Equation 4-21 is then employed by the EnOpt algorithm for iteratively updating the control variables. The terms *U* and *Y* in our derivation are calculated using (x_k) and $\mathcal{F}(x_k)$ from the previous iteration (*k*). The alternative approach is to calculate *U* and *Y* using the mean of the ensembles from the current iteration. As a result, each column *i* of *U* and *Y* will be:

$$U_i = (u_i) - \frac{\sum_{j=1}^{n_e}(u_j)}{n_e}, \tag{4-22}$$

$$Y_i = \mathcal{F}(x_k + c_k u_i) - \frac{\sum_{j=1}^{n_e}\mathcal{F}(x_k + c_k u_j)}{n_e}. \tag{4-23}$$

The mean of extremely large number of ensembles will approach to the value from the previous iteration while a limited ensemble size will generate sampling errors. This was accounted for in the original EnOpt method by using the mean of the new ensembles. Both approaches has been applied to the problem of proactive optimization of ICVs and their performance compared. The approach employing the mean of the new ensembles showed a better performance and was more stable with limited size ensembles. This approach will be used for the rest of this study.

Fonseca et al. (2015) developed a methodology to quantify EnOpt ensemble size required to achieve a high-quality gradient in proactive optimization under uncertainty. A higher-quality gradient was obtained by increasing the ensemble size which is particularly important at later optimization iterations when the control variables approach the optimum solution. However, they observed that ensemble based methods, irrespective of ensemble size, always estimated the uphill direction. In this study, the same ensemble size (4 and 10) is used for EnOpt to provide a comparison with SPSA.

4.5. Case studies

SPSA and EnOpt have been compared by performing the same number of simulation runs per iteration for both algorithms using two ensemble sizes: 4 and 10. For example, with ensemble size of 10 (i.e., n_e=10), SPSA evaluates 5 random and independent instances of the gradient and uses their arithmetic average. EnOpt evaluates 10 random independent directional derivatives. On top of that, five independent runs were performed and the average results are compared in order to eliminate the effect of

random number generator employed in both SPSA and EnOpt. For all cases the optimization is terminated at 100 iterations (i.e., $k_{max} = 100$) in order to eliminate the effect of iteration number and provide a fair comparison of the different approaches. Decaying of α_k and c_k during the optimization iterations ensures convergence of the algorithm if it is allowed to run for a sufficient number of iterations.

The case studies will now be presented.

4.5.1 Case-1, a box-shaped reservoir model

This test case deals with a synthetic reservoir model with a square layout of 10×10×1 grid blocks in x, y and z direction, respectively. Each grid block has Δx = Δy = 120 m and Δx = 3 m. The reservoir (Figure 4-2) consists of a high (100 mD, red) and low (10 mD, blue) permeability regions. The reservoir is developed by one conventional injector and one intelligent, 2-zone producer. Water is injected at a constant rate of 40 sm^3/day while the production well operates at a constant Bottom Hole Pressure (BHP) of 70 bar. This example is designed to compare the performance of different algorithms on a production optimisation problem with a non-optimum, water injection strategy created by the water injector being located close to the producer in the high permeability zone.

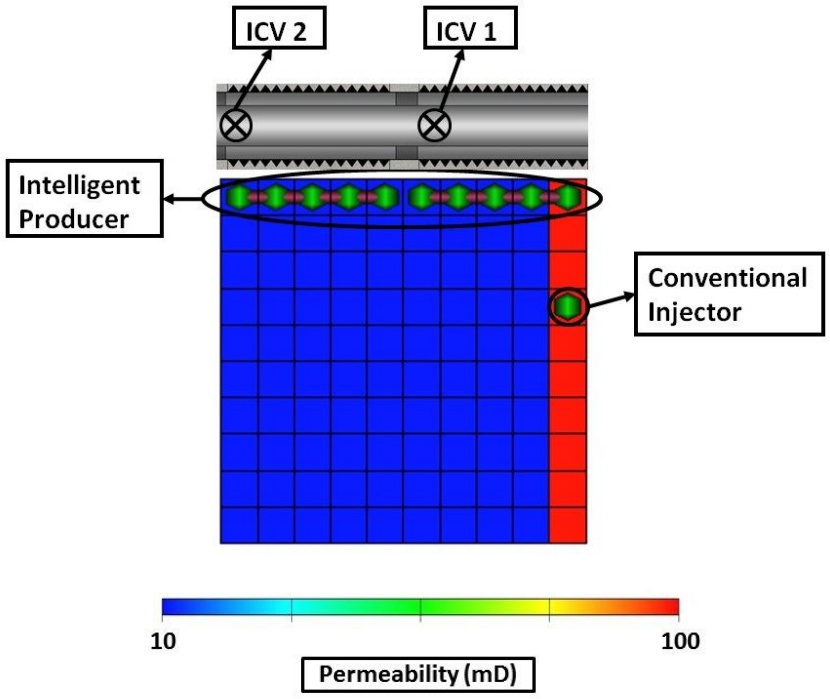

Figure 4-2: Top view of case-1's box-shaped reservoir model.

The production strategy (drive mechanism and production/injection constraints, etc.) determines how optimal control adds value and must be chosen prior to proactively optimising I-Well operation. Reducing the ICV's open area decreases both the pressure drawdown across the formation and the liquid (oil and water) production. Reducing the well's total liquid production rate under a constant BHP will only improve the NPV if:

1- Reducing production from a zone once its production becomes uneconomical due to excessive water production when the water processing cost is relatively high. The NPV is thus improved by reducing the cost of water handling. This scenario is a relatively simple optimisation problem.
2- A different situation occurs if production from all zones is economical. ICV choking now reduces both oil and water production, as well as the cash flow at that timestep. This reduction in the instantaneous objective function has to be justified by a future increase in the objective function due to resulting changes in the reservoir's flow behaviour (streamline manipulation). The discount rate used in the NPV calculation is often the key factor determining whether the current loss is lower than the future gain. The added value in this situation is due to the value of the increase in the discounted cumulative oil production (i.e. the water processing cost is relatively low compared to the oil price and the extra oil is produced relatively quickly compared to the field's producing life time). The solution of this optimisation problem is more difficult, as illustrated below.

The reservoir's production period was simulated for 40 time steps of 90 days each (total 3600 days) with the 2 ICVs being controlled at every timestep. The total number of control variables will then be 40×2=80. The objective function (NPV) was calculated using Equation 4-1 with the Table 4-1 economic data.

Table 4-1: Economic parameters

Parameter	Value
Oil revenue	377 \$/sm^3 oil
Water handling cost	6.3 \$/sm^3 water
Operating cost of the produced liquid	12.6 \$/sm^3 liquid
Discount rate	10 % / year

The optimisation starts from the initial point of fully-open ICVs at all control steps. Two values of c = 0.08 and c = 0.16 were chosen. This case study allows a relatively

higher value of a (a = 2, a = 5 and a = 10) while providing a better estimate of the gradient of case-1's simpler search space. This is not true for case-2 and case-3.

Figure 4-3 compares the results for an ensemble of size 10. EnOpt shows better performance compared to SPSA for the larger a-values. SPSA use of Bernoulli ±1 perturbation provides a rougher approximation of the gradient compared to the EnOpt's use of random normal perturbation. This rough estimation in SPSA aids bypassing local optima by providing a more global representation of the search space. However larger values of a degrades the search process by converting it into a random search of the search space. This case's simple optimum control scenario, reducing the production from the high permeability zone, generates a more monotonic search space characterised by few local optima. Hence SPSA showed almost the same performance as EnOpt with the best setting of $a = 2$ and $c = 0.16$. SPSA-forward (using following forward-difference formulation instead of Equation 4-5 for estimating the gradient) shows reduced performance. This is mainly due to the use of information from the previous iteration ($\mathcal{F}(x_k)$) when limited ensemble size result in sampling error with mean of the ensembles be significantly different with the value from the previous iteration (as explained earlier in Section 4.4.2 for EnOpt).

$$\hat{g}_k\,(x_k) = \frac{\mathcal{F}(x_k + c_k\Delta_k) - \mathcal{F}(x_k)}{c_k} \times \left[\frac{1}{\Delta_{k1}}, \frac{1}{\Delta_{k2}}, \dots, \frac{1}{\Delta_{kn_x}}\right]^T. \qquad 4\text{-}24$$

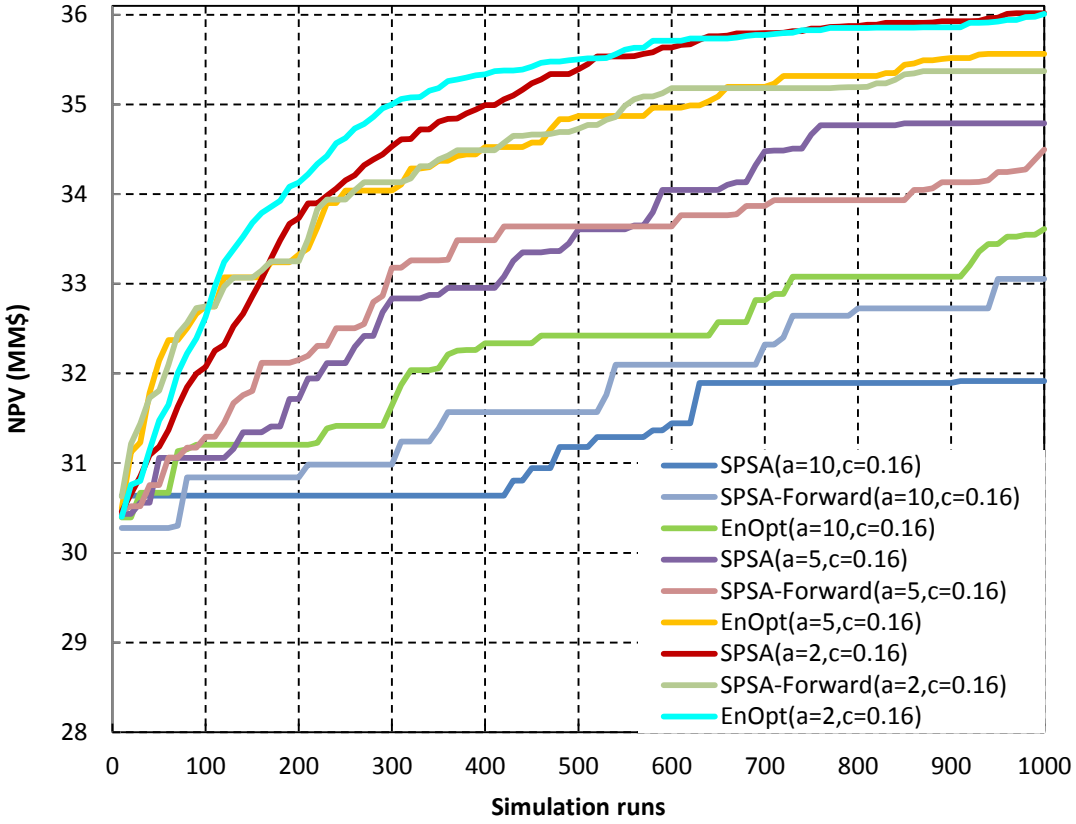

Figure 4-3: NPV versus number of simulation runs for SPSA, SPSA-forward and EnOpt for different values of *a* and *c* (ensemble of size 10, average results of 5 independent runs).

Figure 4-4 shows the standard deviation of 5 independent runs divided by the base-case with fully open ICVs to normalize the values. A reduction in the variance of the independent runs in the case with optimum value of the tuning parameters (Figure 4-4 a) shows convergence to the optimum solution in different runs. The variance between the independent runs is significantly lower than the total improvement w.r.t. the base case (i.e. 19%) showing 5 independent runs is enough to eliminate the random effect in this case study. A larger variance is observed in the cases with non-optimum tuning parameters (Figure 4-4 b and c) showing lack of convergence in independent runs.

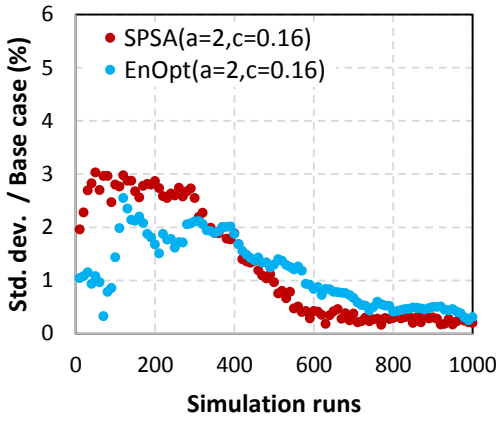

(a)

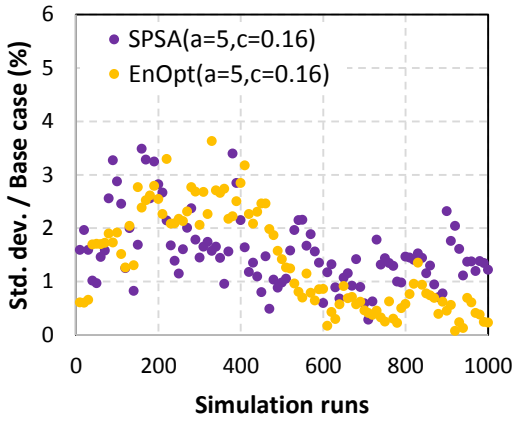

(b)

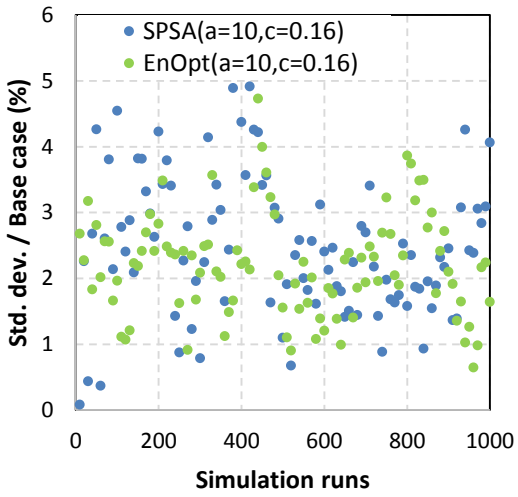

(c)

Figure 4-4: Standard deviation of 5 independent runs normalised by the base case versus simulation runs in SPSA and EnOpt for different value of *a* and *c* for ensemble of size 10

Figure 4-5 compares the performance of the algorithms for the ensemble of size 4. Generally, reducing the ensemble size degrades the quality of the estimated gradient and the performance of the optimisation algorithms. In this case, EnOpt is more robust since it provides a smoother gradient. Moreover, lower standard deviation is observed between the independent runs in EnOpt compared to SPSA (Figure 4-6) during the final simulation runs which is an indication of better convergence in EnOpt. Hypothesis testing (Neyman and Pearson, 1933) is performed to investigate the probability of better performance of EnOpt as compared to SPSA with ensemble of size 4. Average standard deviation of the last 50 simulation runs is considered (Figure 4-6). The null hypothesis (i.e. EnOpt does not provide better performance than SPSA) is only true after ~2

standard deviation away from the mean. Therefore EnOpt provides better performance than SPSA with a probability of around 95% (Figure 4-7).

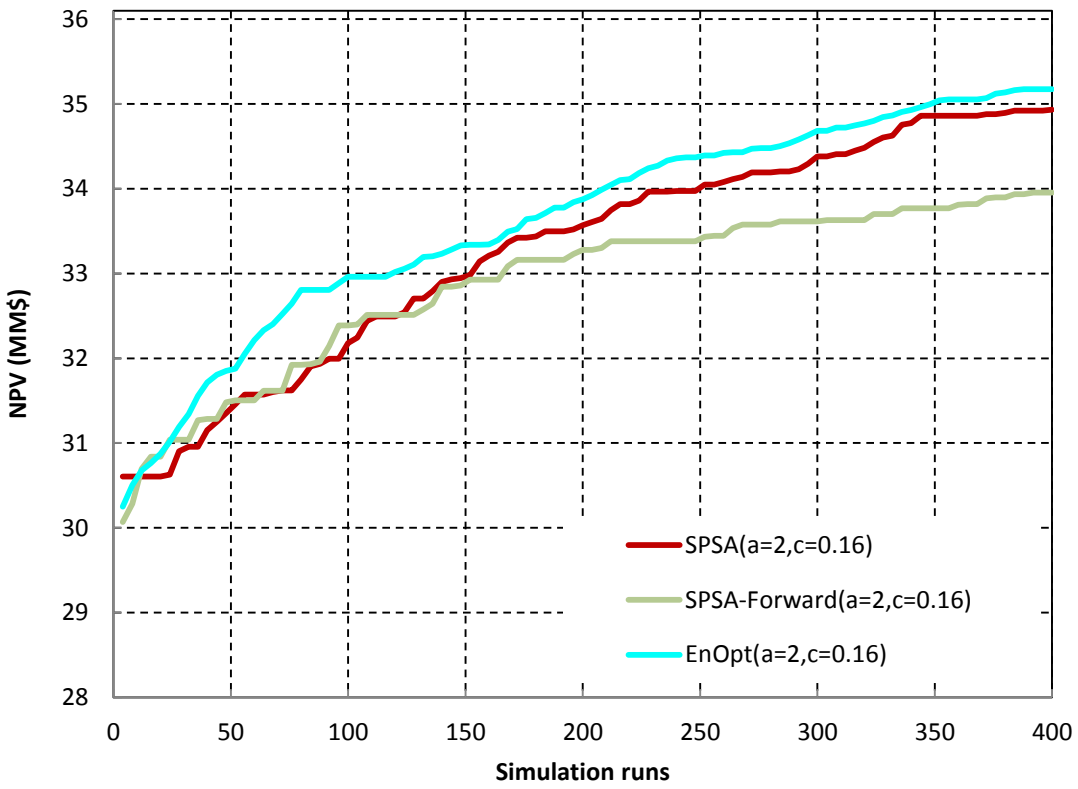

Figure 4-5: NPV versus number of simulation runs for SPSA, SPSA-forward and EnOpt (ensemble of size 4, average results of 5 independent runs)

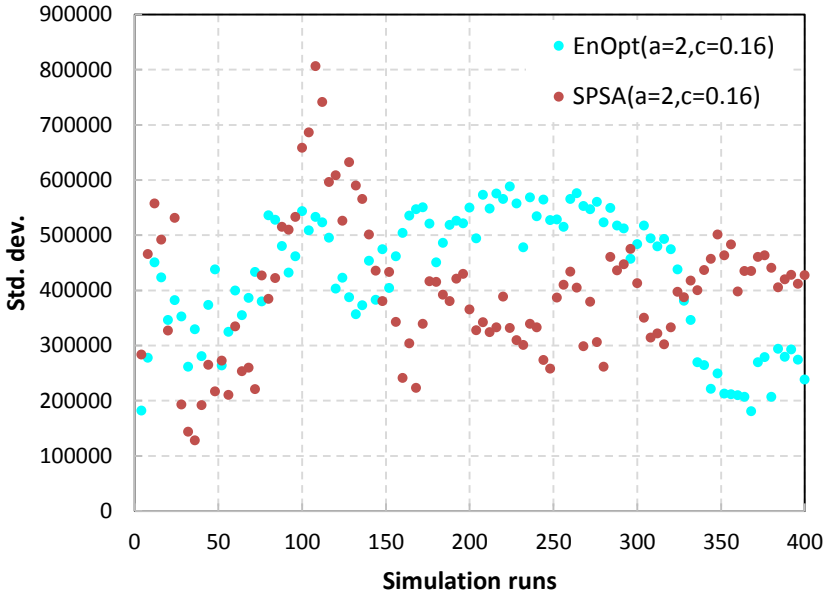

Figure 4-6: Standard deviation of 5 independent runs versus simulation runs for SPSA and EnOpt with ensemble of size 4

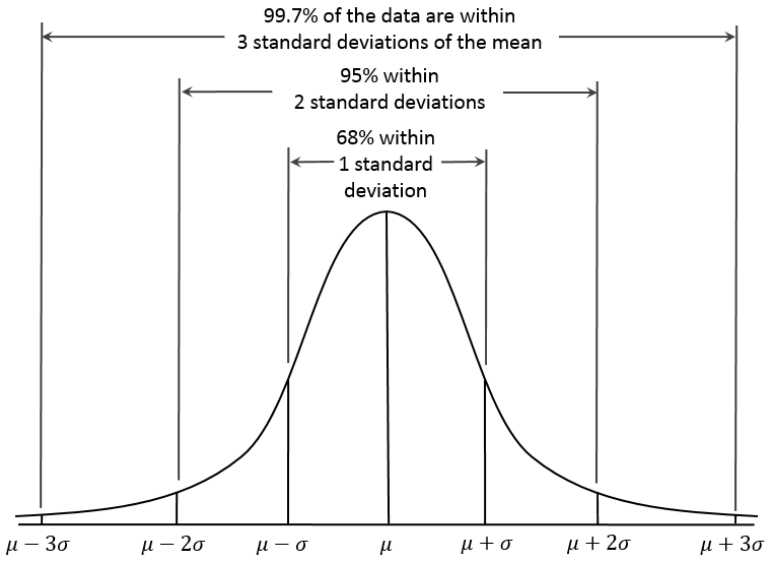

Figure 4-7: Probability of data being within particular standard deviation from the mean in a normal distribution (Kernler, 2014)

The best scenario shows a 19% improvement in NPV compared to the base case with fully-open ICVs at all control steps. Figure 4-8 shows the ICV-1 and ICV-2 open areas during the production period for the optimum scenario (SPSA with *a=2* and *c=0.16*). The area can change between 0.0127 ft^2 and 10^{-7} ft^2 in a logarithmic scale (10^{-7} ft^2 represents a closed ICV). The optimisation algorithm has closed ICV-1 after ~1 year, diverting the injection water from the side into the low permeability region zone 2. ICV-

1 is partially opened in the last time step to produce any remaining oil from the high permeability layer.

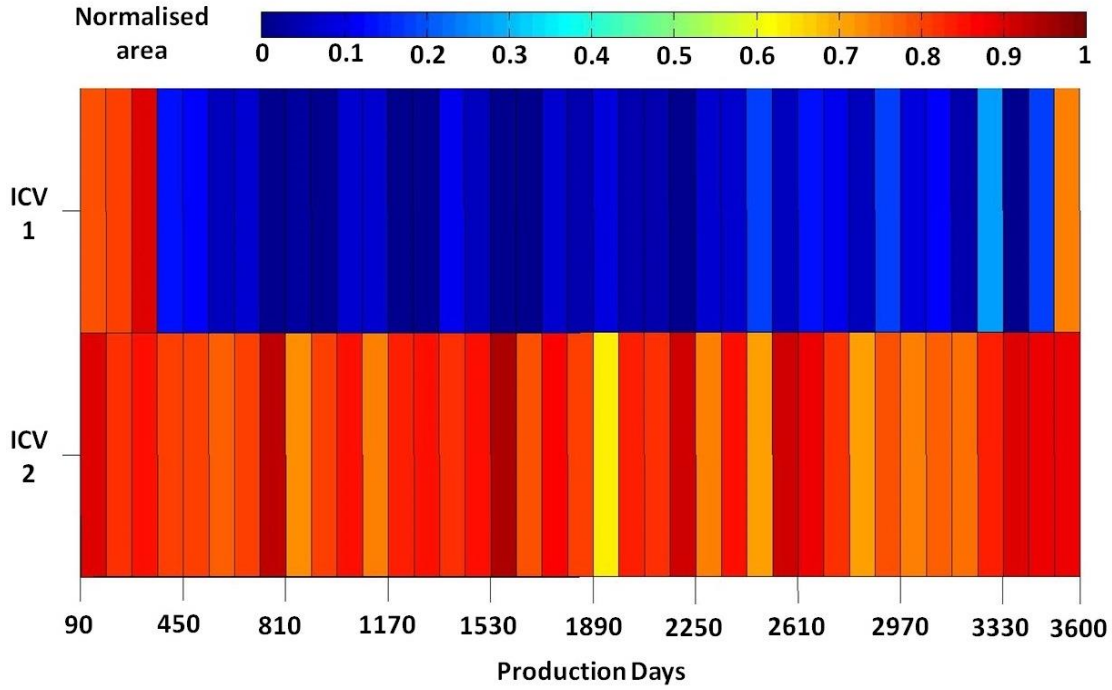

Figure 4-8: Optimal valve opening area during the production period obtained using SPSA

Figure 4-9 shows the early loss and late gain in NPV as a result of optimisation under BHP constraint. The effect of an increased discount rate, from 3%, 10% to 20%, on the optimum control scenario is also recorded. A higher discount rate reduces the early loss in the optimum scenario because of assigning lower weights to the late objectives compared to the early objectives.

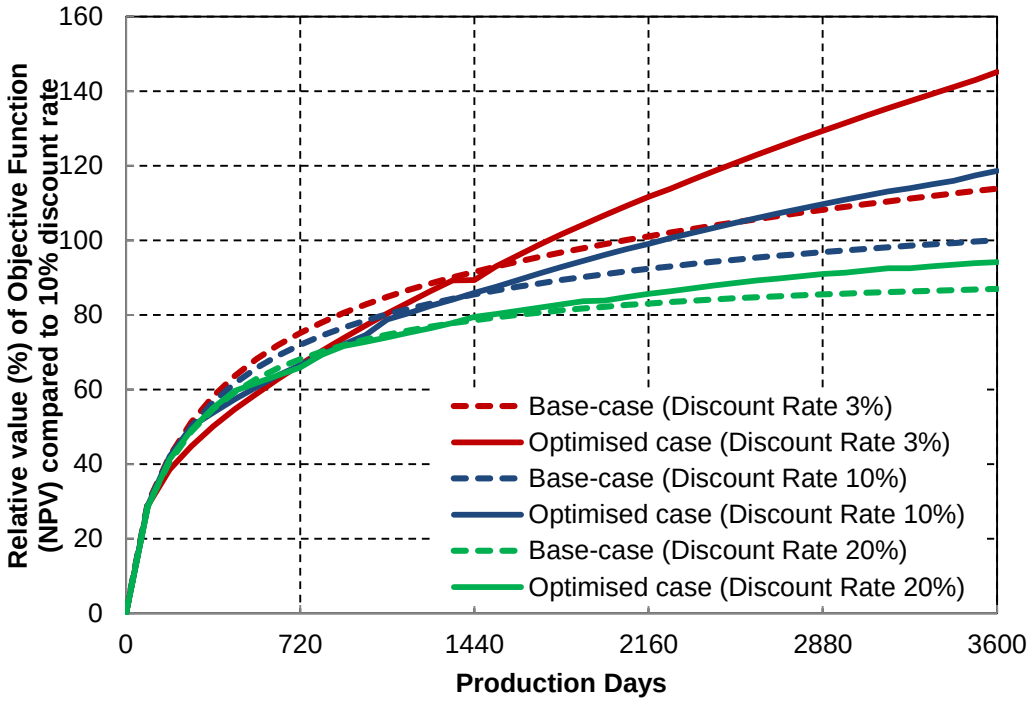

Figure 4-9: Change in relative value for the base and optimised case under BHP constraint with a varying discount rate – NPVs are normalised w.r.t. the Base-case (Discount rate 10%)

4.5.2 Case-2: PUNQ-S3 reservoir model with the I-well in an optimum location

The PUNQ-S3 model (Floris et al., 2001) which is a synthetic reservoir model, fairly typical of North Sea fault-bounded trap (Nikravesh et al., 2003), was used for case-2. The model consists of 19 × 28 × 5 grid blocks, of which 1761 blocks are active. The reservoir permeability is moderately heterogeneous despite the small scale of the model. This results in a model with a realistic, non-uniform water-front advance that is also computationally efficient; making it an appropriate choice for uncertainty and optimization studies. Figure 4-10 shows the permeability field for the top layer where the intelligent producer is located. The horizontal permeability (K_h) is equal to the vertical permeability (K_v). The model has two high permeability channels each surrounded by low permeability formation. The field is bounded by impermeable faults to the east and south with a strong aquifer in the north and west. There is a small gas cap at the centre of the field.

Figure 4-10 shows two vertical injectors in addition to the horizontal intelligent producer. Previous studies showed that the intelligent producer is near the optimum location. Thus only a small gain in production can be achieved by the optimal control of the production well. Case-3 investigates the optimal control of a production well in a far-from-optimum location. The multi-segment (ECLIPSE, 2012) well model considers the total pressure drop throughout the coupled well/reservoir model. Four ICVs control the production, one for each permeability region. The open flow area of each ICV is the variables to be optimally controlled. The reservoir simulator controls the BHP ≥ 100 bar to respect the well liquid production rate constraint of 1000 sm^3/day (See Section 2.7 for description of constraint handling). All produced gas is injected into the gas cap (gas separation/injection cost is ignored in the simplified objective function in this study, which only considered oil and water production Equation 2-12) and the water injector complements the aquifer support to maintain a constant reservoir pressure (further details about the reservoir and well model are available in (Grebenkin and Davies, 2010)). The injectors are operated under BHP control of 300 bar. The production period is 20 years with an ICV operational frequency of once per year. This results in an optimization problem with a total of 80 control variables.

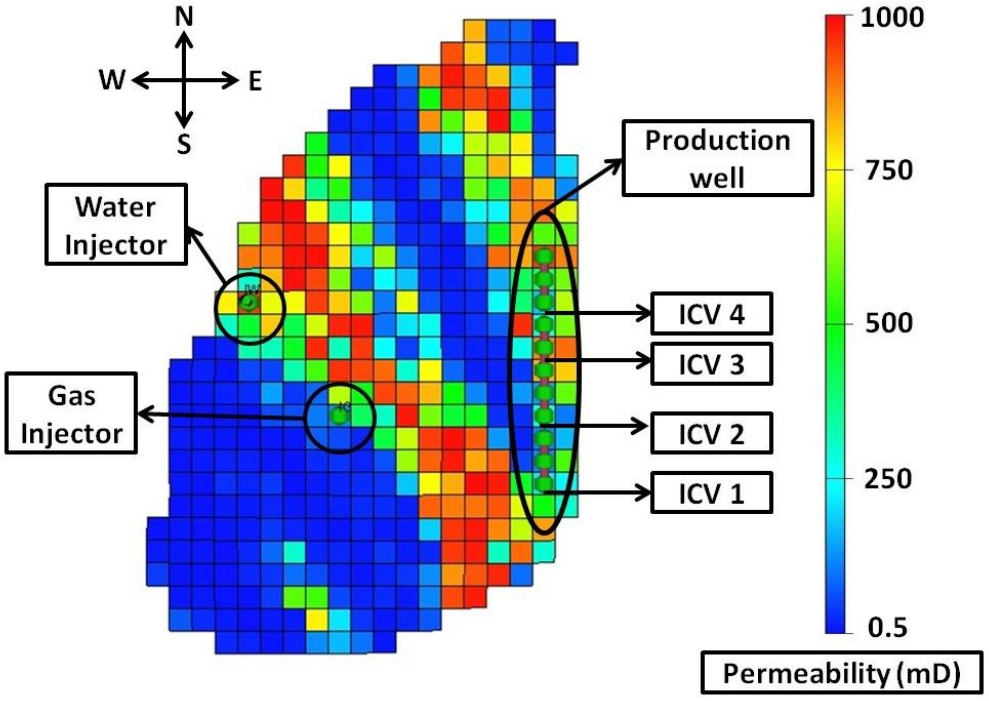

Figure 4-10: PUNQ-S3 reservoir model showing permeability distribution and well locations

The well liquid rate constraint of 1000 sm^3/day is smaller than the maximum well liquid production potential at all times. A well total liquid rate constraint allows the NPV to increase if the water production can be decreased and the oil production increased. Here the optimum scenario does not show a lower instantaneous cash flow with respect to the base-case (Figure 4-14).

The use of an estimated gradient can result in stepping into a non-optimum direction, decreasing the objective function value. This case study, with an optimum production well location and a liquid rate constraint, results in the fully-open scenario (i.e. the starting point of the optimization process) to be close to the optimum solution. Hence an unstable condition brought on by stepping in a non-optimum direction can be expected at an early iterations where a larger step size is employed. Spall (1997) suggested adding a blocking-stage to the search process in such unstable conditions. This blocking-stage, by checking an inequality at each iteration, prevents the algorithm behaving wildly and abruptly moving in a non-optimum direction. However, stochastic optimisation algorithms, by moving in the non-optimum directions, will explore the search space. This assists the algorithm to approach the global optimum. An appropriate tolerance should be thus considered to allow exploration of the search space while blocking abrupt changes. (Note that abrupt changes not only degrades the optimisation performance; but also increases the computation time by proposing unrealistic simulation cases which cause convergence problems).

The blocking-stage checks the following inequality at each iteration:

$$\mathcal{F}(x_{k+1}) \leq \mathcal{F}(x_k) - tolerance. \qquad 4\text{-}25$$

We have applied two implementations of the algorithms: (1) With-Blocking: by using a tolerance of 1% of $\mathcal{F}(x_k)$. (2) Without-Blocking: by allowing the algorithm update x at each iteration.

It should be noted that, the employed SPSA and EnOpt do not require evaluation of the objective function for the updated control variables at each iteration. As shown in the final formulation of SPSA (Equation 4-5) and EnOpt (4-22 and 4-23) only values of the objective function for the perturbed control variables at the current time step is required

($\mathcal{F}(x_k + c_k u_j)$) and it is not necessary to calculate the objective function for the updated control variable ($\mathcal{F}(x_{k+1})$). However, this objective function evaluation might be performed for visualising the performance or to check the convergence criteria. In contrast it is mandatory to evaluate the objective function for the updated control variable at each iteration, if the blocking stage is used. This increases the total computation time by the time required for one additional objective function evaluation per iteration.

The optimisation was performed for several choices of *a* and *c* within the recommended range (Sections 4.4.1). Small *a* and large *c* provide a better performance due to the small improvement potential and bypassing several local optima. As shown in Figure 4-11 SPSA and EnOpt show relatively similar performance. SPSA-forward shows reduced performance mainly due to the use of information from the previous iteration ($\mathcal{F}(x_k)$) when limited ensemble size result in sampling error (as explained earlier in Section 4.4.2 for EnOpt).

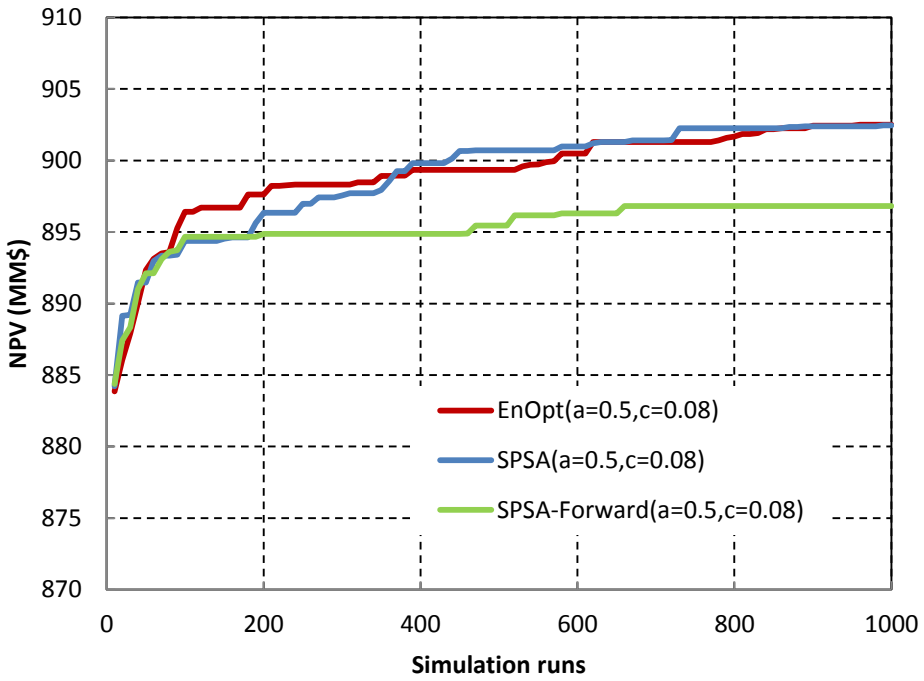

Figure 4-11: NPV versus number of simulation runs for SPSA, SPSA-forward and EnOpt without-blocking for best *a* and *c* (ensembles of size 10 per iteration, the average results of 5 independent runs)

Figure 4-12 shows the small difference in the performance of the algorithms with or without blocking. Blocking did increase the total computation time due to the one extra objective function evaluation per iteration being more computationally demanding than the reduction due to the elimination of the cases with convergence problems. Blocking did show improved performance for SPSA; mainly due to its rough approximate of the gradient.

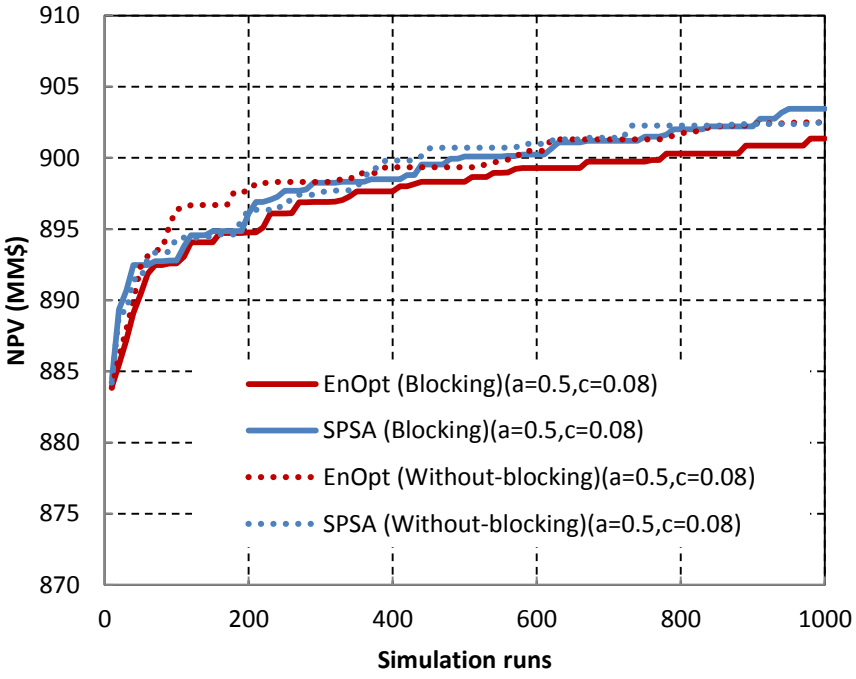

Figure 4-12: NPV versus number of simulation runs for SPSA and EnOpt with-blocking for best *a* and *c* (ensembles of size 10 per iteration, the average results of 5 independent runs)

The solution with maximum NPV is obtained by SPSA without-blocking, providing a 2.1% improvement w.r.t. the base-case. This is significantly higher than the standard deviation of 5 independent runs w.r.t. the base case (Figure 4-13) showing that both SPSA and EnOpt can find the optimum solution with a high probability (~100%). EnOpt shows a 2% improvement w.r.t. the base-case. The difference between the performance of SPSA and EnOpt is not statistically significant in this case study.

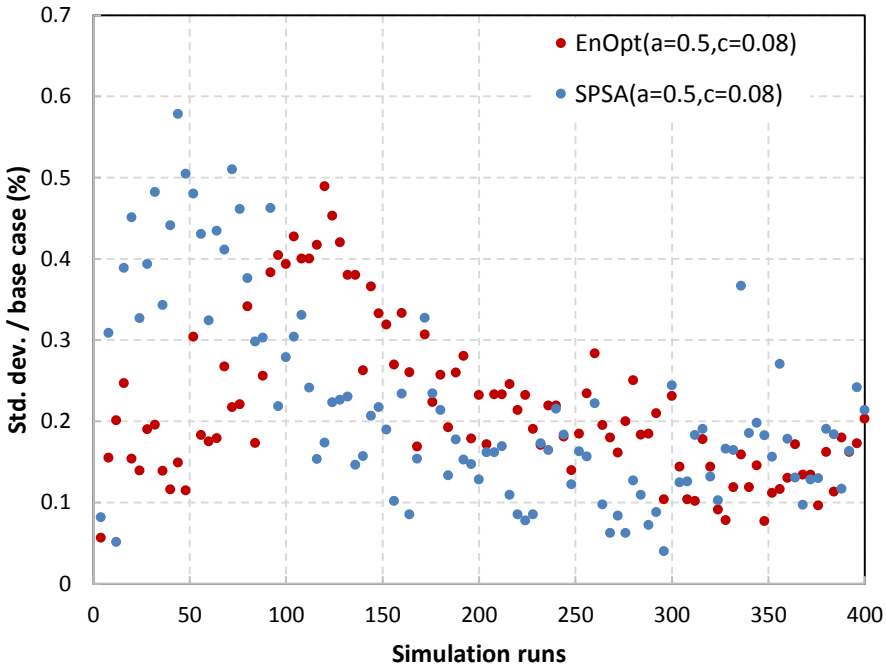

Figure 4-13: Standard deviation of 5 independent runs normalised by the base case versus simulation runs for SPSA and EnOpt without blocking for ensemble of size 10

The normalised NPV in the base-case and optimised-case and improvement w.r.t. the base case are shown in Figure 4-14 a and b, respectively. No loss in the NPV is observed in the optimum control scenario due to the liquid rate constraint in this case as compared to the BHP constraint in case-1. The improvement in NPV is due to extra oil production as a result of better sweep efficiency by decreasing production from the high permeability zone. Figure 4-14 (b) shows that the impact of better sweep efficiency is observed after around 2 years when the case with optimum control produces extra oil (and less water) as compared to the base case. No extra value is obtained after around 13 years as the reservoir is already swept. The optimum control only ensures that the extra added-value is not lost for example by extra water production (last part with zero slope in Figure 4-14 (b)).

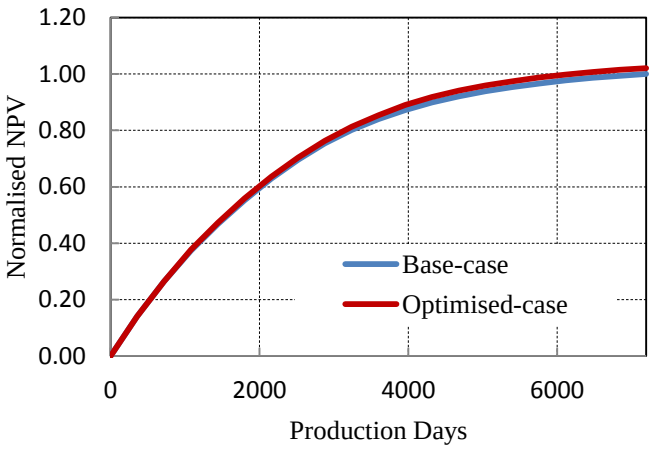

(a)

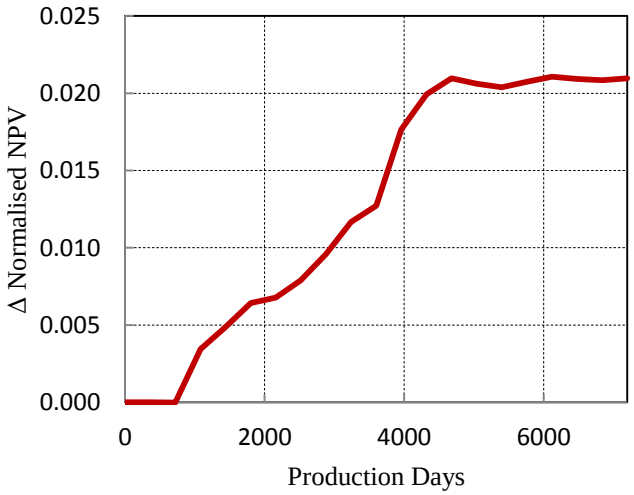

(b)

Figure 4-14: (a) NPV versus production days in the optimised-case obtained using SPSA and base-case, (b) improvement in NPV w.r.t. base case

Figure 4-15 shows the valve opening area for 4 ICVs for the best SPSA and EnOpt scenarios. The area is scaled between 0 (fully closed) and 1(fully open). Figure 4-16 shows the relative change in the cumulative oil production of each zone in the best scenario obtained by SPSA and EnOpt. As previously, the added-value is mainly obtained by decreasing the production from ICV-4 and from the high permeability region. An initial increase in the production is achieved from ICV-3 which is shown by positive slope in Figure 4-16-c. However, zone-3, due to its connection with zone-4, is also prone to the water breakthrough. This is alleviated in the optimum solution by a more uniform flood front being provided by a later reduction of production from ICV-3, as shown by zero slope in Figure 4-16-c. Both algorithms provide approximately the same level of improvement in the objective function value (Figure 4-14), despite the control scenarios being different since they have chosen two different local optimal solutions. The solution obtained by the SPSA shows larger changes being made to the valve area. This indicates a local convergence to a rough part of the control space in comparison to EnOpt.

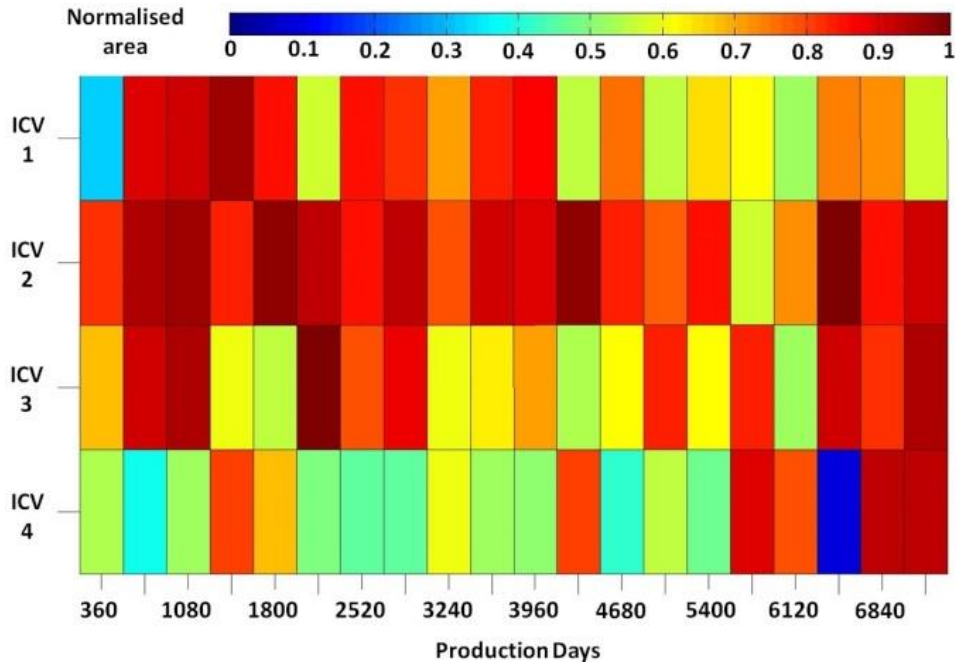

(a)

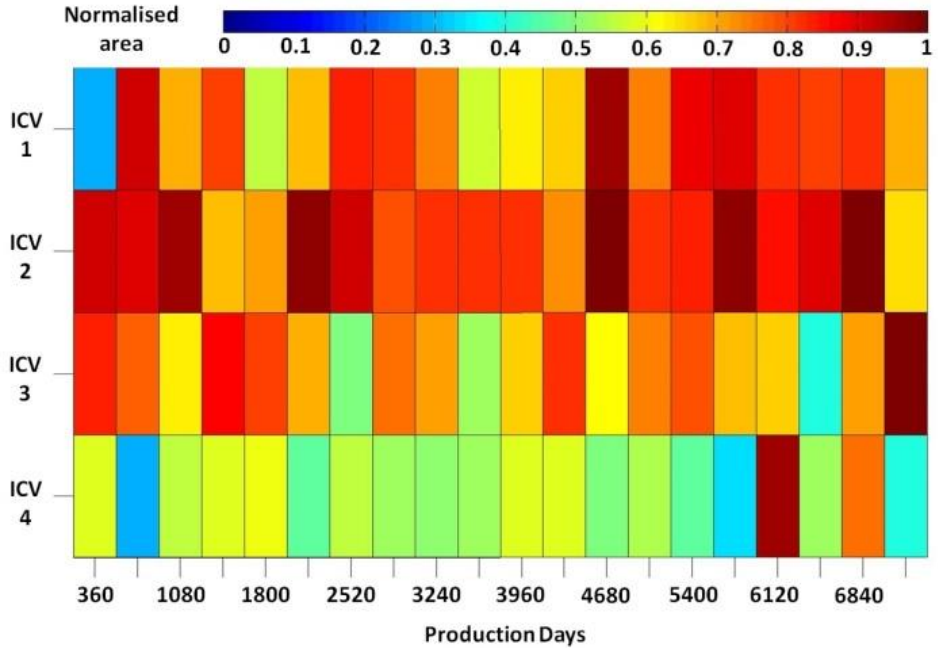

(b)

Figure 4-15: Valve opening area for the best case obtained by (a) SPSA (b) EnOpt

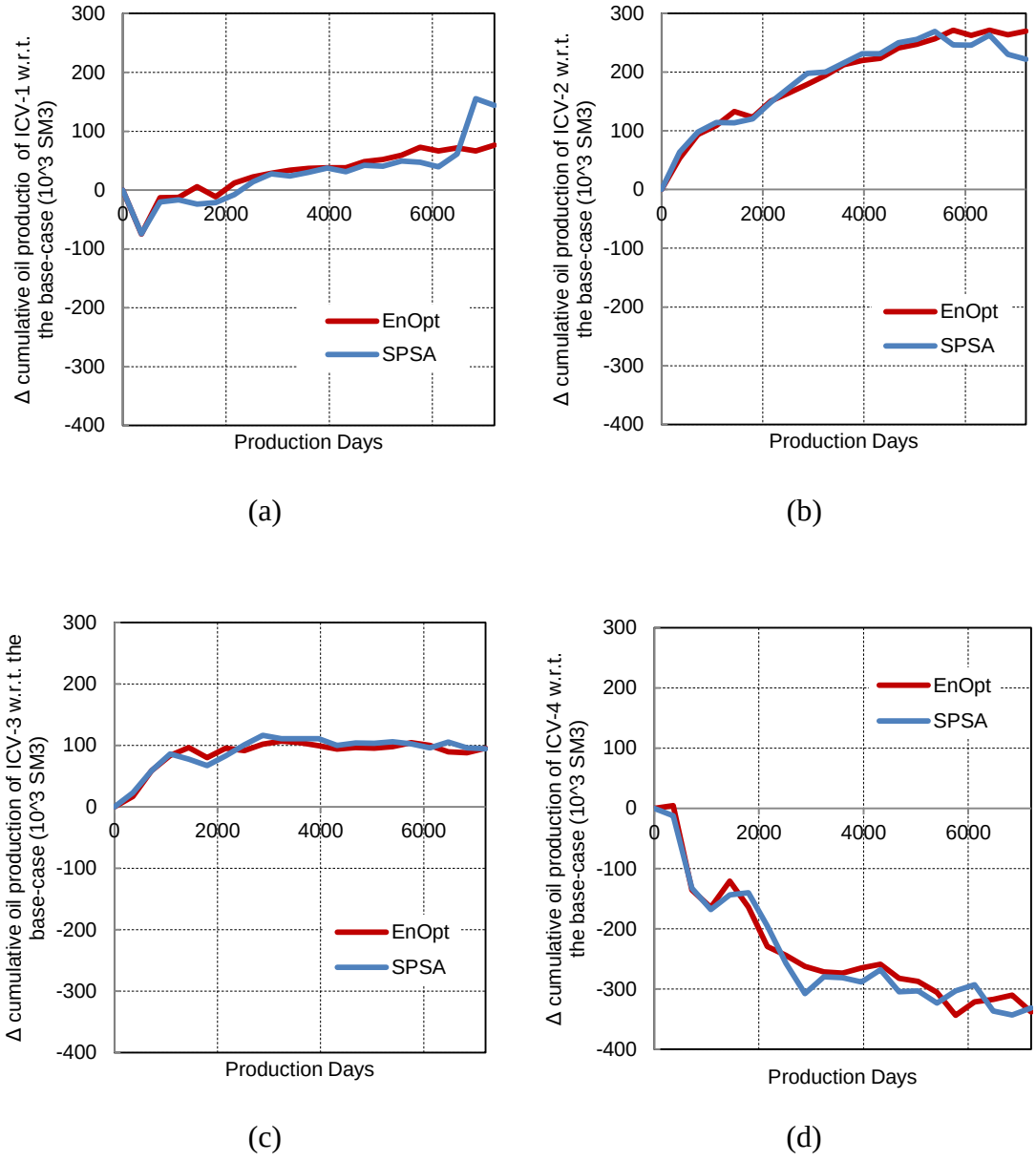

Figure 4-16- Relative change in the cumulative oil production of ICVs in the optimised scenario obtained by SPSA and EnOpt w.r.t. the base case: (a)ICV-1 (b)ICV-2 (c)ICV-3 (d)ICV-4

4.5.3 Case-3, PUNQ-S3 model with the I-well in a far-from-optimum location

The case-3 reservoir model is the same as in case-2, but now the intelligent production well is placed in a non-optimum location; a scenario representative of the incomplete knowledge about the reservoir properties (Figure 4-17).

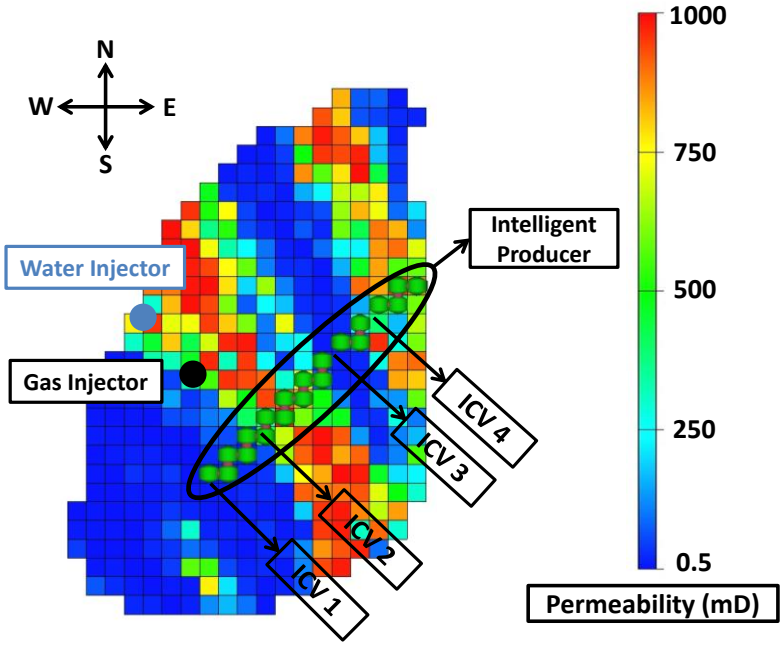

Figure 4-17: Top view of PUNQ-S3 reservoir model showing permeability distribution (Case-3, I-well in a far from optimum location)

Both algorithms converged to a low performance solution with a small c (c = 0.04) or large a (a = 5); while a value of c = 0.08 showed the best performance. Figure 4-18 compares the algorithms' performance for different values of a with this c = 0.08 value.

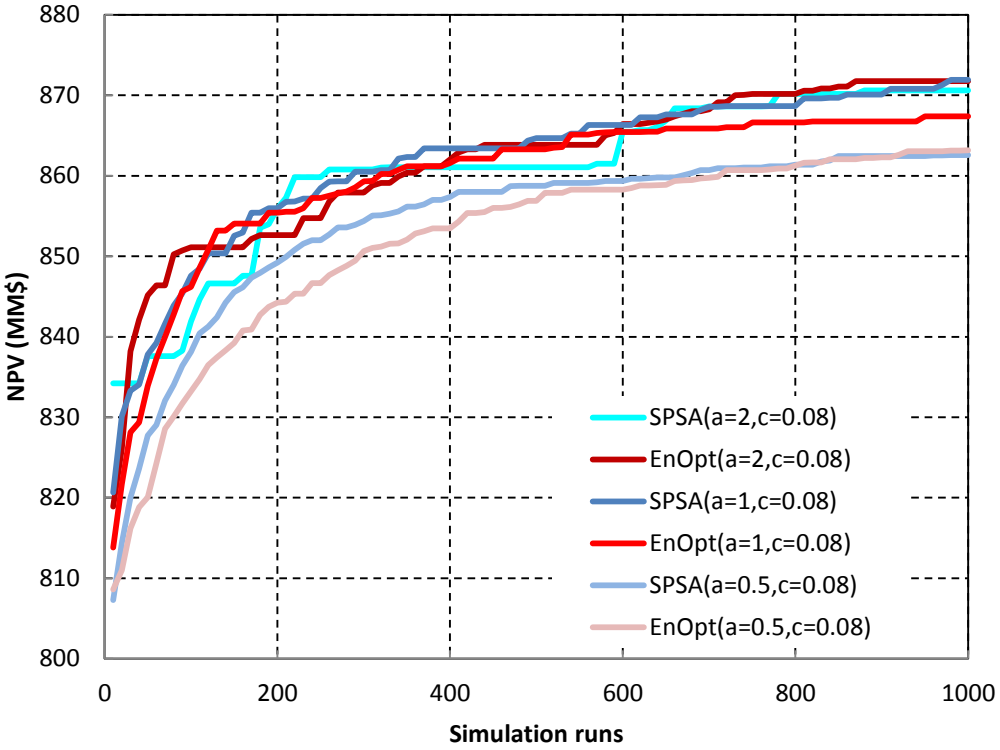

Figure 4-18: NPV versus number of simulation runs for SPSA and EnOpt, without-blocking (ensemble of size 10 per iteration, average results of 5 independent runs)

Here a larger value of *a* provides the optimum performance than was found for Case-2. This is due to the larger difference between the base-case and the optimum solution as a result of a non-optimum well location. The maximum value is obtained by SPSA (a=1, c = 0.08). The standard deviation between 5 independent runs in SPSA and EnOpt (Figure 4-19) is significantly lower than the improvement as a result of optimization showing the reliability of both algorithms to find the optimum solution despite random behavior of the algorithms. Hypothesis testing is performed to investigate the probability of better performance of SPSA as compared to EnOpt with (a=1, c = 0.08). Average standard deviation of the last 100 simulation runs is considered (Figure 4-19). The null hypothesis (i.e. SPSA does not provide better performance) is only true after ~4 standard deviation away from the mean. Therefore SPSA provides better performance than EnOpt with a probability close to 100%. No statistically significant difference is observed between SPSA and EnOpt with (a=2, c = 0.08).

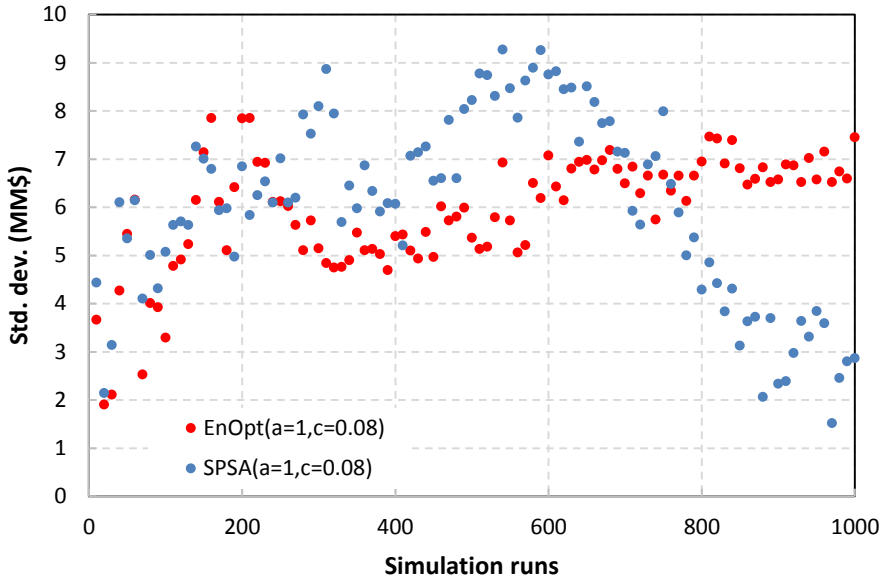

Figure 4-19: Standard deviation of 5 independent runs versus simulation runs for SPSA and EnOpt with ensemble of size 10

EnOpt outperforms SPSA using ensemble of size 4 (n_e=4) (Figure 4-20) with a probability of 68% calculated using hypothesis testing. In this case, SPSA use of Bernoulli ±1 perturbation provides a coarse approximation of the gradient which speeds up the convergence to the optimum solution during initial iterations (i.e. far from the optimum solution). However, better convergence is observed by EnOpt during later iterations (i.e. closer to the optimum solution) by providing a smoother and more accurate estimate of the gradient. Introducing a blocking stage for these cases showed a small improvement in the performance at the cost of an increased computation time.

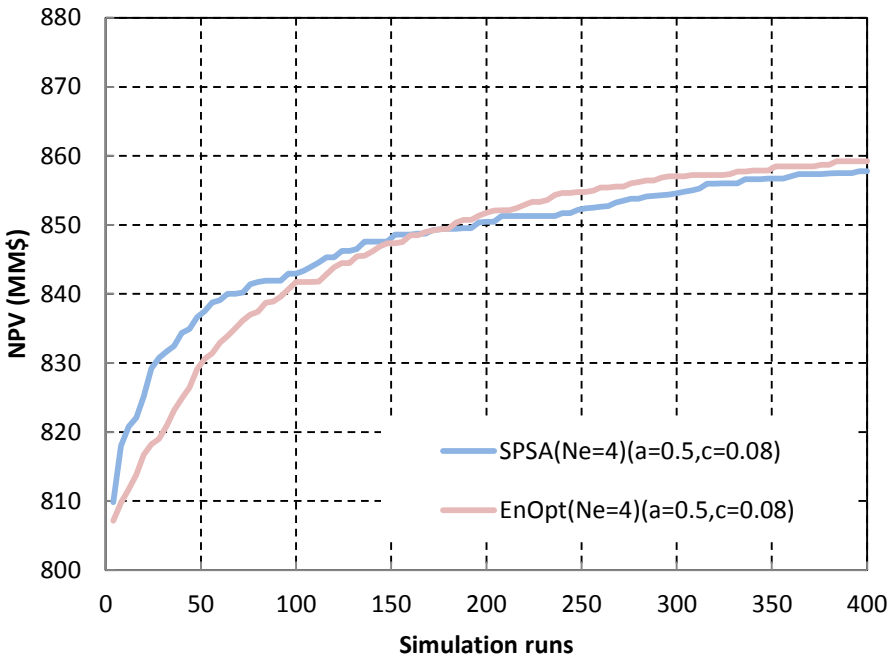

Figure 4-20: NPV versus number of simulation runs for SPSA and EnOpt, without-blocking (ensemble of size 4 per iteration, average results of 5 independent runs)

Figure 4-21 (a) and (b) shows the ICVs opening area for the best scenario obtained by SPSA and EnOpt, respectively. As previously, the area is scaled between 0 (fully closed) and 1 (fully open). Similar to case-2, the solution obtained by SPSA shows larger change in the valve area at two consecutive time steps as compared to EnOpt with smoother ICV operation. The added-value is mainly obtained by decreasing the production from the high permeability region (ICV-4) to provide better sweep of the reservoir.

4.5.4 Comparison of optimal proactive control with the I-well in an optimum and non-optimum location

The non-optimum well location resulted in proactive optimization delivering a greater improvement (~ 8.2% w.r.t. the base case) as compared to the improvement with the optimum well location (~ 2.1% w.r.t. the base case). It was observed that the ultimate value is obtained when the optimum control is applied to the optimally located well (i.e. the well whose production results in close to the maximum NPV without applying any control). Simultaneous optimization of the well location and control has been investigated in some recent studies (e.g., Forouzanfar et al., 2015).

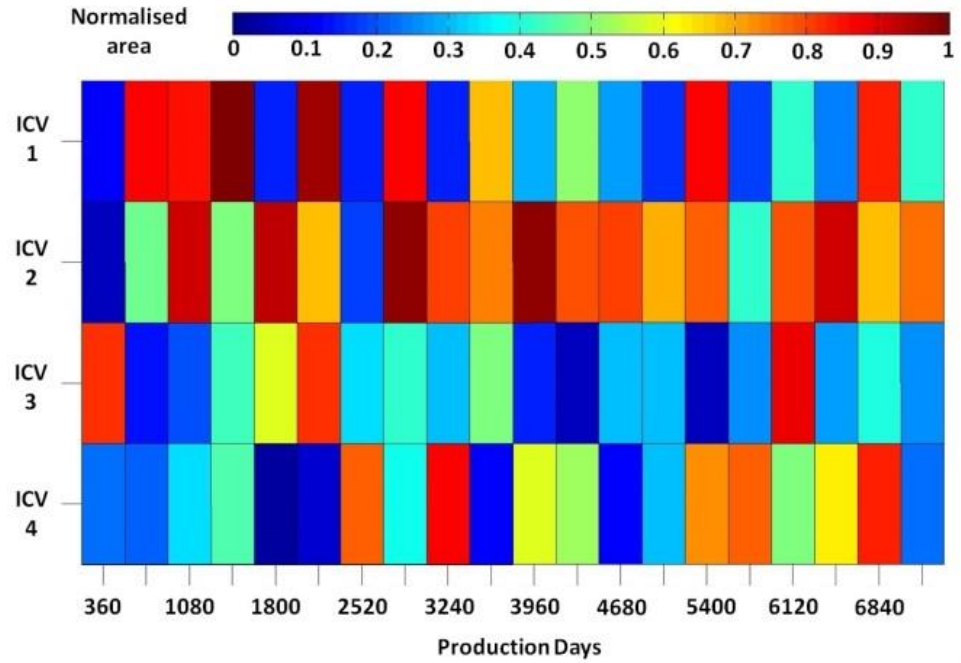

(a)

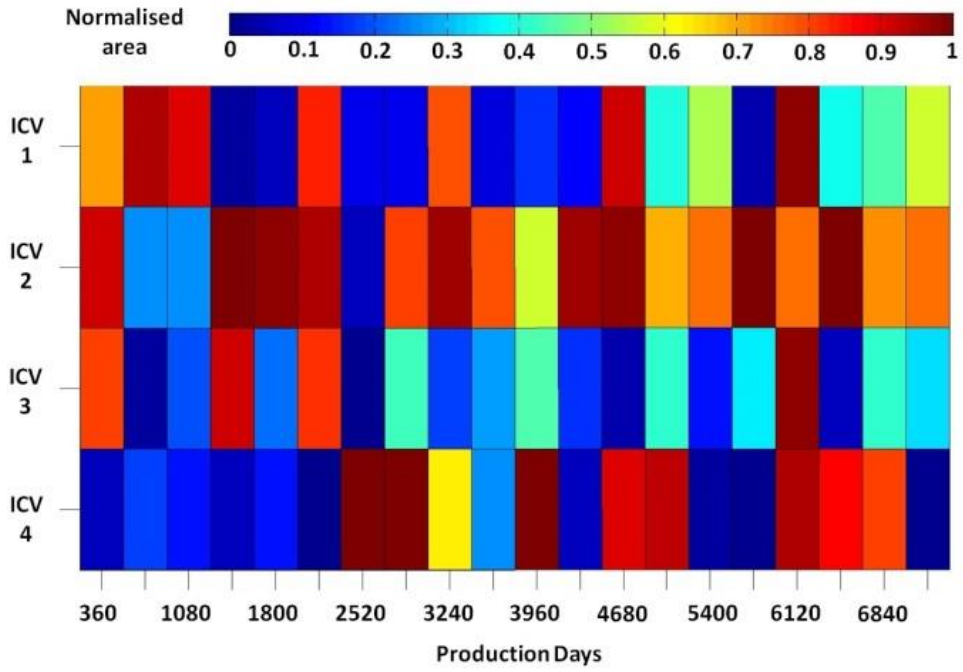

(b)

Figure 4-21: ICVs opening area during production period for the best case obtained by (a) SPSA (b) EnOpt

Comparing Figure 4-15 and Figure 4-21 highlights the difference between the optimum control scenarios obtained in case-2 (with optimum well location) and case-3 (with non-optimum well location). In case-2 the I-well is in the optimum location of an I-well with fixed, fully open ICVs. Hence, essentially fewer control of the zonal flow is required to improve the sweep performance. The extent of ICV's control is shown by the deviation from the fully open area while the same control frequency of ICVs is considered for both cases. Higher deviation from the no-control (fully-open) in case-3 is also confirmed by lower average flow area of the 4 ICVs at each control step in the optimum control scenario obtained as compared to case-2 (Figure 4-22).

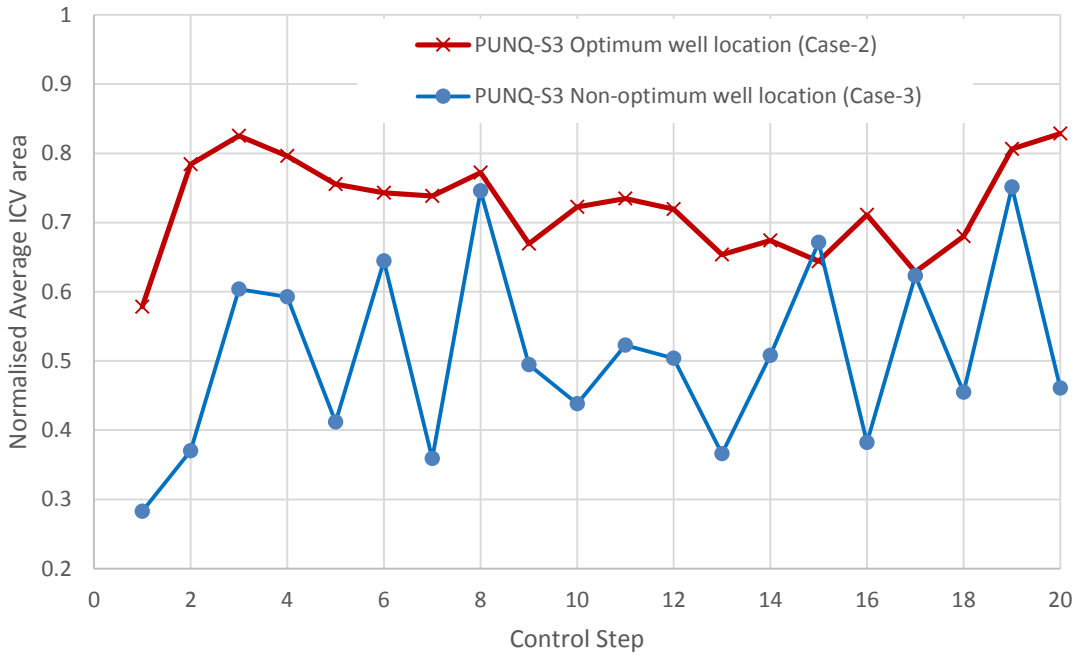

Figure 4-22: Normalised average area of 4 ICVs at each control step in the optimum control scenario obtained for PUNQ-S3 with optimum well location (Case-2) and PUNQ-S3 with non-optimum well location (Case-3)

Fluctuations are observed in the optimum control of individual ICVs obtained by both SPSA and EnOpt (Figure 4-15, Figure 4-21 and Figure 4-22). This might not be desirable from a practical point of view, as operator might prefer controls vary smoothly over time. A smoother control can be obtained by multiplying the gradient by a covariance matrix with a defined correlation length (e.g. (Do and Reynolds, 2013, Zhao et al., 2013)). The covariance function need to be applied on a zone by zone basis therefore, there is no correlation between controls of any two zones. The correlation

length is a function of the number of control steps over which we wish the zonal controls to be correlated. Increasing the correlation length forces the controls to be smoother. However, it is not always possible to obtain an optimal control, with a good level of improvement in NPV, with smooth controls for example when the optimal control shows bang-bang behaviour as in Wang et al. (2009). Further investigation on obtaining a smooth optimal control of ICVs is required.

4.6. Discussion and Conclusions

Two approaches based on stochastic estimation of gradient for the proactive optimisation of multiple ICVs that are independent of the choice of the reservoir simulator have been discussed. Moreover, the large number of control variables and the search space, which is characterised by several local optima with objective values close to the global optimum, are other reasons for suitability of the proposed approaches. Both approaches are employed to perform the optimisation on 3 representative case studies. These case studies are characterised with the following features in the search space:

- Case-1: a simple optimum control scenario with a low number of local optima.
- Case-2: the optimisation starting point is close to the optimum solution, but there are many local optima
- Case-3: the optimisation starting point is far from the optimum solution and there are many local optima.

Table 4-2 and the discussion below summarises the conclusions from these case studies and provides recommendations for future application of the algorithms.

Tuning. Optimum selection of the tuning parameters speeds-up the optimization process and/or improves the obtained solution, especially with a computationally demanding objective function. The previously published tuning guidelines have been modified for the application in proactive optimization of ICVs; though if time permits, it is recommended to select the best tuning parameters by testing the performance of the algorithm with multiple values taken from the defined range.

Algorithm selection. Both SPSA and EnOpt show good performance. The poorer performance of SPSA-forward when using a limited number of ensembles is due to employing information from the previous iteration. The recommended implementation of EnOpt uses the mean of the ensembles in the current iteration for the same reason. SPSA tends to outperform EnOpt with a larger ensemble size (10 here) due to its ability to bypass more local optima. However EnOpt provides better performance than SPSA for a smaller ensemble size and a limited number of simulation runs due to the smoother estimation of gradient (double smoothing in EnOpt see Equation 4-20).

An evaluation of the available resources is suggested for the algorithm selection stage. If parallel processing is not available we suggest to use EnOpt with a sufficiently small ensemble size (e.g. 4) in order to perform more iterations in a fixed number of simulation runs. However, nowadays with the increasing parallel processing capability (more than 4 CPUs) we recommend to use an ensemble size equal to the number of CPUs to take full advantage of the available resources. SPSA tends to outperform EnOpt under these conditions. Further, using an ensemble size larger than the number of CPUs is not recommended, following the same logic previously, since generally the optimization process takes advantage of the larger number of iterations. Additionally, EnOpt is more robust to the choice of the tuning parameters mainly due to its smoother estimation of the gradient.

Blocking. The blocking stage is not suggested when using SPSA and EnOpt formulation proposed in this study due to an increase in the computation time for a potentially small improvement in the performance. The computation time is affected by two conflicting behaviors, which are an additional objective function evaluation per iteration and eliminating simulation of the cases with convergence problems. Tuned first-order methods are showing a relatively stable process which reduces the cases with convergence problem, eliminating the need for adding the blocking stage. Moreover, moving in non-optimum direction during some iterations is considered as an injected noise helping the gradient-based optimization algorithm to discover the search space and approach the global optimum solution.

Characteristics of the solution. The case studies demonstrated that the difference between the two approaches is not only the level of improvement but also the

characteristics of the obtained optimal control strategy. SPSA use of Bernoulli ±1 perturbation provides a coarse approximation of the gradient and will generally approach to an optimum solution with sharper changes in the valve area at successive control steps when compared to EnOpt which provides a smoother operation (Figure 4-15, Figure 4-16 and Figure 4-21). Li and Reynolds (2011) proposed a modified version of the SPSA called Stochastic Gaussian Search Direction (SGSD) employing random normal distribution when calculating the gradient. This modification is not considered in this thesis. The characteristic of the solution is particularly important in order to satisfy the operators' preference to smoothly or abruptly control the ICV area (or zonal flow rates).

Table 4-2: Comparison of SPSA and EnOpt for proactive optimisation of ICVs

Cases and challenges	Production strategy	Optimisation algorithm	N° of ensembles	*a* value	*c* value	% Improvement w.r.t. base-case
Case-1 **Simple box model**	BHP	SPSA	10	2	0.16	19.7
			4			16.1
		SPSA-Forward	10	2	0.16	17.5
			4			12.7
		EnOpt	10	2	0.16	19.7
			4			16.9
Case-2 **PUNQ-S3** **Optimum well Location**	Liquid Rate	SPSA	10	0.5	0.08	2.1
		SPSA-Forward				1.4
		EnOpt				2
Case-3 **PUNQ-S3** **Non-Optimum well Location**	Liquid Rate	SPSA	10	1	0.08	8.2
				2	0.08	7.9
		EnOpt	10	1	0.08	7.5
				2	0.08	8.1

Chapter 5 – Robust proactive optimisation of ICVs under reservoir description uncertainty

5.1. Introduction

This chapter presents modifications to the proactive optimisation workflow in order to include reservoir description uncertainty. Assumptions made during the reservoir modelling process due to the limited knowledge of the field geology and its flow performance result in an uncertain model forecast. Uncertainty can be accounted for by generating multiple, equally-weighted model realizations that represent the range of potential production forecasts. These realizations need to be considered in the proactive optimisation process to ensure robustness of the obtained control scenario to provide "on-average" optimal performance in all realizations.

5.2. Problem formulation in proactive optimization under geological uncertainties

Following Section 4.2, the objective of proactive optimisation is to find a control scenario of ICVs that maximize NPV which is in fact a function of the uncertainties,

$$\mathcal{F}(x, y_r) = \sum_{n=1}^{S} \left[\sum_{j=1}^{N_p} \left(r_o q_{o,j}^n - r_{pw} q_{w,j}^n - r_{opex} q_{l,j}^n \right) \right] \frac{\delta t^n}{(1+b)^{t_n}}, \qquad 5\text{-}1$$

A fixed set of control vector (x) will produce a different objective function value ($\mathcal{F}$) when applied to each one of the model realizations (y_r).

A basic, proactive optimization approach (discussed in Chapter 4) performs the optimization using a single realization to obtain a control scenario that might show a sub-optimum effect when applied to other realizations, or even decrease the objective value with respect to the uncontrolled case. This reflects the undesired scenario when the I-wells are proactively controlled based on an inaccurate reservoir model, with this model not being properly updated.

The solution is to optimise an augmented objective function considering all or selected model realizations. The so-called robust optimisation approach has been introduced in the petroleum engineering by Yeten et al. (2003) for well location optimisation, Bailey and Couet (2005) for maximising asset value in a gas field, and van Essen et al. (2013) for production and injection optimisation in conventional wells. Several definitions for the augmented objective function, employed during the robust optimisation process, are developed in the literature which are briefly explained in the following subsections.

5.2.1 Mean-only

Substituting the objective function with the mean of the objective function values calculated over different realizations, i.e. the expectation, will potentially improve the robustness of the obtained solution. The new objective function is defined as:

$$\mathcal{U}(x, \hat{y}) = E(\mathcal{F}(x, \hat{y})) \quad 5\text{-}2$$

$$E(\mathcal{F}(x, \hat{y})) = \frac{\sum_{r=1}^{H} \mathcal{F}(x, y_r)}{H}, \quad 5\text{-}3$$

where $\hat{y}$ represents that a set of H nominated equally-weighted realizations (represented by the state vector y_r) are employed to calculate the expectation (mean) of the objective function value for each control scenario (x) during the robust optimization process. Various modifications of this approach have been previously applied by for example (van Essen et al., 2013, Chen et al., 2011, Wang et al., 2012, Fonseca et al., 2014, Mulvey et al., 1995, Capolei et al., 2013). The major drawback of this approach is that only the expected added-value (i.e. mean) but not the risk (i.e. variability) is considered during the robust optimisation process.

5.2.2 Mean-variance approach

This approach was developed to address the adverse effect of neglecting the variability of the objective function in the mean-only approach. The augmented objective function (a.k.a. Utility function) is now a combination of mean and variability of the uncertain objective function (NPV in this work) over a set of chosen model realizations. It was shown (Chen et al., 1999) that the mean-variance approach is capable of finding a robust solution. Their introduction of the variance term in the objective function

provided a flexible control of the level of risk. Petvipusit et al. (2014) employed mean-variance approach for robust optimisation of CO2 sequestration and showed that utility function can be adjusted based on the preference of the decision makers toward risk. They found that the mean-variance approach improves the worst case scenario as compared to mean-only approach. Capolei et al. (2015) employed mean-variance approach for proactive optimisation of conventional wells. They observed that introducing variance term in the objective function definition is able to reduce the risk significantly at the price of reduced mean profits. The following form of the utility function was employed in this study (Petvipusit et al., 2014, Capolei et al., 2015):

$$\mathcal{U}(x,\hat{y}) = E(\mathcal{F}(x,\hat{y})) - A\,\sigma^2\big(\mathcal{F}(x,\hat{y})\big), \tag{5-4}$$

$$E(\mathcal{F}(x,\hat{y})) = \frac{\sum_{r=1}^{H}\mathcal{F}(x,y_r)}{H}, \tag{5-5}$$

$$\sigma^2\big(\mathcal{F}(x,\hat{y})\big) = E\left(\mathcal{F}(x,\hat{y}) - E\big(\mathcal{F}(x,\hat{y})\big)\right)^2, \tag{5-6}$$

where $E(\mathcal{F}(x,\hat{y}))$ and $\sigma^2(\mathcal{F}(x,\hat{y}))$ are the mean and variance of the selected realizations, respectively. *A* is a tuning constant to define the allowable level of risk in the robust optimization process. The mean-variance dilemma is expected by using this approach while focus on reducing variance can result in a solution with very low mean. For example, consider the extreme case of fully-close control scenario with zero production in all realisations and therefore minimum (i.e. zero) variance, but also zero mean. This is similar to bias-variance dilemma in machine learning (Geman et al., 1992). The function of tuning constant, *A*, is to alleviate this problem by ensuring a balance between the weights of mean and variance in the augmented objective function (Equation 5-4). In this study the value of *A* is defined to provide the same order of magnitude for mean and variance term. The impact of *A* on the optimisation performance is investigated in Section 6.7.

Several other researches incorporate the variability in the objective function using the standard deviation instead of variance (Yeten et al., 2003, Bailey and Couet, 2005, Alhuthali et al., 2008). It is expected that the flexible tuning constant (*A*) is capable to define the weight of mean versus variance or standard deviation. Further study to

investigate the impact of mean-variance or mean-standard deviation objective function on the robust optimisation process is required.

5.2.3 Asymmetric approaches

One of the drawbacks of the mean-variance approach is the symmetric nature of the variance. Therefore variance might be reduced by penalising the upper tail (good cases) instead of increasing the lower tail (bad cases) of the objective function distribution. Robust optimisation approaches are developed to focus on the lower tail of the objective function distribution, for example: Worst-case Optimisation (WCO) or Conditional Value-at-Risk (CVaR) optimisation. WCO considers only the worst case and solve a max-min (or min-max) optimisation. The CVaR approach enhances the process by considering the average of a class of worst cases instead of a single case. The disadvantage in WCO and CVaR is that ignoring the mean could result in lower added-value. In the proactive optimisation of oil reservoirs mean-worst-case or mean-CVaR approach is employed (Siraj et al., 2015).

Siraj et al. (2015) and Capolei et al. (2015) compared asymmetric and symmetric (i.e. mean-variance) approaches to robust optimisation under uncertainty. They observed that mean-variance approach has a higher tendency to penalise good cases in order to minimise the variance as compared to the WCO and mean-CVaR.

Symmetric mean-only and mean-variance approaches are employed in this thesis while investigating the impact of realization selection on the robust optimisation process (Chapter 6).

5.3. Modifications to speed-up the robust optimisation process

The modified augmented objective function accounts for the uncertainty by considering a set of H nominated realizations. Naturally, the full ensemble of model realizations, the ideal approach, will identify the ultimate value, together with a significant increase in the computational costs, especially for full-field applications. Two possible approaches are described in the following subsections to alleviate this effect.

5.3.1 Prior reduction of the number of nominated realizations

Choosing a small ensemble of model realizations for robust optimization that are representative of all available models is computationally less demanding; but is also subject to bias during the selection process. The small ensemble of realisations may be selected randomly, as in (Chen et al., 2011) and (Haghighat Sefat et al., 2014). The randomly selected small ensemble of realizations are distributed uniformly based on the objective function value. An example application of this approach is presented in Section 5.4.

Employing random sampling for selecting a subset of the realizations for robust optimization cannot guarantee proper capturing of the underlying model uncertainties. It may also fail to provide optimal controls that generalizes well to the full ensemble of model realizations (Chapter 6). The preferred alternative is to employ a methodology to systematically select a subset of realizations that reflects the reservoir flow uncertainty of the full set (Park, 2011, Scheidt and Caers, 2013). Wang et al. (2012) used model input and output properties to cluster the model realizations and then select (based on this clustering) a small number of realizations for robust well location optimization. Park (2011) proposed to use a distance measure tailored to the subsequent application to measure the similarity/dissimilarity of all realizations. Similar realizations are grouped into a limited number of clusters from which a small number of realizations are selected. In this study the methodology developed by Park (2011) is modified to select a small number of realizations for robust proactive optimization of ICVs (Chapter 6).

This approach is independent of the choice of the optimization algorithm. The augmented objective function is evaluated using a smaller number of selected realizations (i.e. reducing the number of objective function evaluations) and then optimised using the chosen optimisation algorithm. This approach is employed for all robust optimizations in this thesis.

5.3.2 Estimating the Gradient from an ensemble of realizations

This approach can only be used when robust optimization is performed using ensemble based methods. Two sets of ensemble are considered during such robust optimization; the ensemble of (1) perturbed control variables (n_e) and (2) reservoir model realizations

(N_r). The normal implementation of ensemble based methods requires at least $n_e \times N_r$ objective function evaluations per iteration of robust optimization (i.e. all realizations are evaluated for each perturbed set of control variables).

A modified approach is to perform only n_e objective function evaluations per iteration in order to approximate the gradient (see (Stordal et al., 2014) for proof of gradient under geological uncertainty can be approximated using a different control variable for each reservoir model realization and example applications). In this approach each perturbed set of control variables is only applied to one realization (i.e. 1:1 ratio); making it computationally very attractive. However, the quality of the approximated gradient obtained using 1:1 ratio is not acceptable. This is especially true with a non-monotone objective function and when there is a large difference between employed realizations e.g. Raniolo et al. (2013) reported failure of the 1:1 ratio in optimization of polymer injection due to poor gradient estimates. They suggested using a small number of nominated realizations which approximately captures the uncertainty (see Section 5.3.1). The alternative is to improve the quality of the gradient using a ratio other than 1:1 while each realization is employed for evaluating larger number of perturbed control sets. For example Fonseca et al. (2014) used 1:20 ratio to alleviate this problem while nominated realizations are fixed during the whole optimization process. Li et al. (2013) suggested to randomly select a subset of realization at every iteration. Fonseca et al. (2015) proposed a modified ensemble-based robust formulation where gradient is calculated by considering value of each individual realisation at the current iteration step rather than a mean-shifted approach. They showed that, this modified approach can achieve a greater accuracy using a lower ratio.

Following limitations are associated with this approach:

- It can only be coupled with an ensemble based optimisation algorithm to reduce the computation time by evaluating each perturbation ensemble using only one, or a small number, of realisations
- All published studies (e.g. (Raniolo et al., 2013, Fonseca et al., 2014, Stordal et al., 2014)) consider mean-only objective function (Section 5.2.1). Calculation of variance, allowing employment of a mean-variance objective function (Section 5.2.2), is not representative using the 1:1 approach. The calculated

variance using 1:1 approach has the combined effect of difference in control and reservoir model realizations while the interest in mean-variance approach is to reduce the variance due to reservoir description uncertainty only.

5.4. Mean-only robust optimisation using randomly selected realizations based on the objective value

The PUNQ-S3 reservoir model with the Section 4.5.3 I-well configuration is used in this section. The uncertainty is quantified using 66 unique realizations of the porosity and permeability distribution ($N_r = 66$). They were generated by Grebenkin and Davies (2010) using a sequential Gaussian simulation algorithm based on real field data provided for the six original wells [see (Floris et al., 2001, Grebenkin and Davies, 2010) for the original well data). Figure 5-1 shows the distribution of NPV for the base case control scenario, fully open ICVs during the whole production period, for all realizations. Table 4-1 provides the economic parameters used for calculating the NPV.

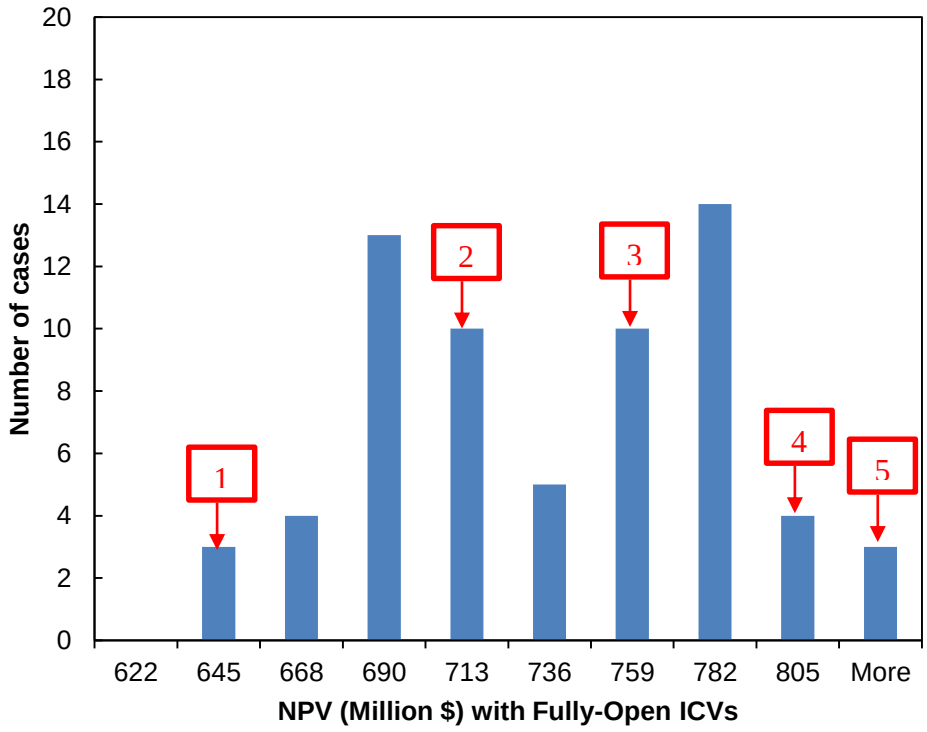

Figure 5-1: Distribution of NPV for the base case of all realizations and 5 randomly selected realisations

All realizations are sorted based on the NPV and five realizations were selected using a uniform random distribution (bins with a selected realization are shown in Figure 5-1). A random selection process does not guarantee to correctly capture the extent of the underlying uncertainty as for example in this case no realisation is selected from the NPV range with maximum probability (i.e. bin 782 Million $ in Figure 5-1). The permeability distribution and Oil-In-Place (OIP) in the selected realizations are shown in Figure 5-2. The small difference in OIP is because only permeability and porosity distribution are the uncertain parameters in this case study.

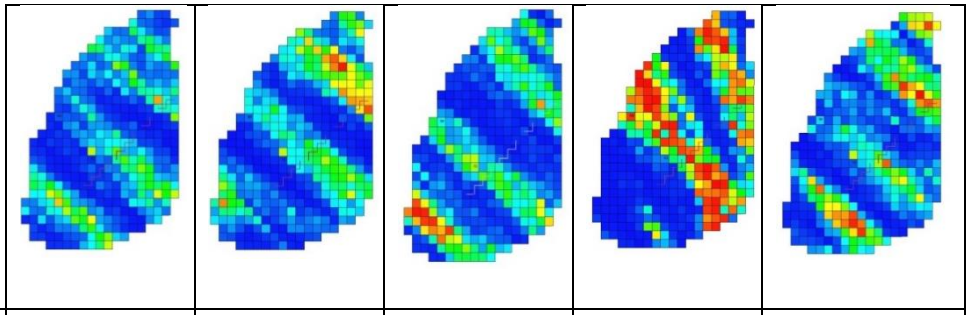

Realization Number	1	2	3	4	5
OIP (Million SM^3)	13.2	13.4	13.5	13.1	12.9

Figure 5-2: Top layer permeability distribution for 5 selected realizations

The objective function is evaluated using the mean-only approach (Equation 5-2) for these 5 selected realizations. SPSA is the optimization algorithm. It used an ensemble size of 10, performing 50 simulation runs per iteration to estimate the gradient. The objective function was evaluated for the updated control variables at each iteration. Visualisation and checking of the rate of convergence was made possible by adding 5 extra simulation runs per iteration.

Figure 5-3 shows the optimization performance. The objective value of the selected realisations for the obtained control scenario at each iteration is shown by dashed lines while the mean (i.e. the objective function) is shown by the red solid line. Robust optimization consistently increases the mean of the selected realizations with different levels of improvement being achieved for each realisation. Chapter 6 describes a

detailed comparison of the impact of robust optimisation on the mean and variance of the selected realisations as well as all realisations.

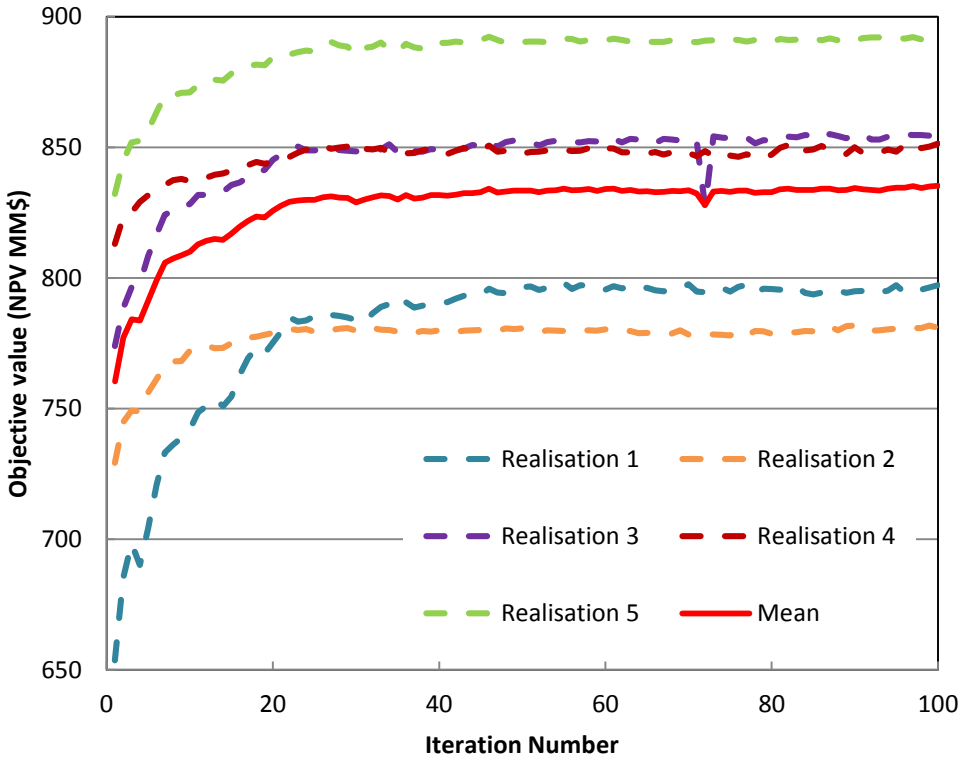

Figure 5-3: Objective values during the optimisation process using mean-only approach

5.5. Summary

A review of the approaches to robust optimization was provided in this Chapter. Generally, the objective function is modified to incorporate the underlying uncertainty. A greater flexibility to attain the added-value of interest from the robust optimization process is achieved by including both mean and variance in the robust objective function definition. An approach to reduce the computational cost of the robust proactive optimisation process by reducing the number of selected, representative realizations is independent of the choice of the optimization algorithm and the objective function definition.

Chapter 6–Realisation Selection in Robust Proactive Optimisation of ICVs

6.1. Introduction

Numerical reservoir models are used to calculate the oil production forecast and evaluate the optimisation objective function. The limited geological knowledge of the field requires that several assumptions have to be made during the numerical model's building process. This renders the model's forecast uncertain. This uncertainty is usually managed by creating an ensemble of equally-probable models to evaluate the range of the forecast uncertainty. Ideally, a robust proactive optimisation approach should consider all the available reservoir model realisations to completely capture the underlying uncertainty. Hundreds or thousands of the reservoir model realisations are available making this process computationally unfeasible. This chapter proposes an efficient methodology for selecting a small ensemble of the reservoir model realisations which are representative of all available ones.

The simplest approach to model selection is to randomly select a limited number of realisations form the ensemble of available realisations without any systematic method. Optimising a group of randomly sampled realisations does potentially improve the robustness of the solution when compared to single realisation optimisation. However, the extent of the underlying uncertainty is unlikely to be correctly represented by this random selection. The approach proposed in this thesis is to choose a few representative models by systematic screening and clustering of all available realisations. Reservoir models employ various properties (e.g. permeability, porosity, water saturation), corresponding to thousands or millions of grid blocks. As a result, each reservoir model is associated with a high-dimensional data set which exacerbates the screening and clustering process. One way to alleviate this problem is projecting the reservoir models onto a low dimensional metric space where visualisation and clustering can be performed efficiently.

Possible criteria for defining the distance between models to construct the metric space are discussed. A distance measure, tailored to the proactive optimization application, is used to define the similarity/dissimilarity of the different realizations which is then employed to perform the clustering operation. Multi-Dimensional Scaling (MDS) is

employed to convert all distances into an equivalent Euclidean value if necessary, followed by visualisation and analysis in a lower dimension. K-means clustering for selecting a representative ensemble of model realizations that performs in an equivalent manner to all available realizations has been chosen. A few more representative models may then be selected from the identified clusters to perform the subsequent robust proactive optimisation.

Moreover, we show that this robust proactive optimization process can either focus on the specific objective of increasing the mean or of reducing the variance (this is achieved via adjustable weights in the utility function). The relative importance of these conflicting objectives has to be taken into account during the model realization selection process to ensure the near-global success of the obtained control scenario. The proposed robust optimization framework has been tested on the PUNQ-S3 reservoir model.

6.2. Uncertainty quantification

Generally, uncertainty in a reservoir model is managed by creating an ensemble of equally probable model realizations. Let $m_i \in \mathbb{R}^{1\times p}$ be a vector of p elements representing i^{th} model realizations containing properties of all grid blocks (e.g. porosity, permeability). Usually hundreds of model realizations are generated covering the uncertainty associated with the reservoir description (Peters et al., 2010, Wang et al., 2012). The matrix $M \in \mathbb{R}^{N_r\times p}$ defines the high-dimensional, uncertainty space assuming the total number of available model realizations (N_r) is:

$$M = (m_1, m_2, \dots, m_i, \dots, m_{N_r})^T, \qquad 6\text{-}1$$

where, the vector m_i is the input to the reservoir simulator along with the defined control parameters x and $O(x, m_i)$ is the output of the reservoir simulator in-terms of integrated quantities of interest (e.g. oil production rate, water production rate). Unlike the high-dimensional input vector m_i, the output vector $O(x, m_i)$ has a low-dimension usually representing a time series at all simulation steps S during the field production time ($O(x, m_i) \in \mathbb{R}^{1\times S}$ for one output only). It should also be noted that later optimization might require calculating a cumulative value (e.g. cumulative oil production, NPV) from this time series as the final objective function. The objective of

modelling uncertainty is not the uncertainty itself; but its impact on the response from the model as discussed by Park (2011). Hence it is beneficial to capture the existing uncertainty in the high-dimensional input space m_i by the low-dimensional response space $O(x, m_i)$. Migrating to low-dimensional response space will not only simplify the screening and clustering process, but will also link them to the final application as explained in the following subsections.

6.3. Similarity/dissimilarity distance measure

The similarity/dissimilarity of reservoir model realizations can be defined by measuring the difference between the corresponding parameters of each realization. The difference can be measured as a distance by considering parameters from only the input space or only the response space or a combination of parameters from both input and response space as abstracted by Equations 6-2, 6-3 and 6-4 respectively.

$$Dm_{ij} = Dm(m_i, m_j), \tag{6-2}$$

$$DO_{ij} = DO(O_i, O_j), \tag{6-3}$$

$$DOm_{ij} = DOm([O_i, m_i], [O_j, m_j]). \tag{6-4}$$

The input space (m_i) is high-dimensional (10^3 to 10^6 dimensions) while the response/output space (O_i) is low-dimensional (10 to 10^3 dimensions). Dm, DO and DOm are the distance measure functions which can be any standard distance function, e.g. Euclidean, city-block, cosine (i.e. cosine of the angle between two vectors), etc. or any user-defined function.

6.3.1 Euclidean distance

The Euclidean distance between two data sets is defined as (e.g. from input space):

$$Dm(m_i, m_j) = \sqrt{\sum_{k=1}^{p} (m_{i,k} - m_{j,k})^2}\,. \tag{6-5}$$

The Euclidean distance has been used in several previous studies in the context of reservoir engineering, either by calculating the distance by considering parameters from

the input space (Tavakoli et al., 2014), the response space (Demyanov et al., 2014) or a combination of parameters from both the input and the response space (Wang et al., 2012).

6.3.2 Connectivity distance

In this study we modified the connectivity distance approach (Park, 2011), to generate a user-defined distance function for measuring dissimilarity in the response space (DO). The following criteria were considered when defining the distance function:

1. The distance has to be correlated with the dynamic response of the reservoir models;
2. The distance measure has to be tailored to capture the uncertainties of interest in the response parameters;
3. Evaluation of the function avoids a time consuming, full physics, reservoir simulation.

Park (2011) considered the summation of the differences in the fractional flow curves of all conventional production wells as the connectivity distance between models as follows.

$$DO(O_i, O_j) = \sum_{g=1}^{N_p} \int_{t=0}^{t_f} \left(f_w\left(O_i, t, w_p^g\right) - f_w\left(O_j, t, w_p^g\right) \right) dt, \qquad 6\text{-}6$$

where $f_w(O_i, t, .)$ is the fractional flow of water as a response of model i, w_p^g is the g^{th} production well, N_p is the total number of production wells, t_f is the final production time. The advantage of using fractional flow as a response parameter is that a good approximation of its value can be calculated via a (fast) streamline reservoir simulation (Thiele et al., 1996).

We have modified Park's (2011) formulation by considering the summation of differences in the fractional flow curves of all fully open ICVs as a proxy corresponding to the performance of the production zones.

$$DO(O_i, O_j) = \sum_{g=1}^{N_p} \sum_{z=1}^{N_z} \int_{t=0}^{t_f} \left(f_w(O_i, t, ICV_z^g) - f_w(O_j, t, ICV_z^g) \right) dt, \quad 6\text{-}7$$

where $f_w(O_i, t, .)$ is the zonal fractional flow as a response of model i, ICV_z^g is the z^{th} ICV in the g^{th} production well, N_z is the total number of ICVs (zones) in the g^{th} production well, N_p is the total number of production wells and t_f is the final production time.

The final objective of the proactive optimization in this study is to improve the NPV by controlling individual zonal production. This is often, but not always, closely related to a second, frequently employed objective of ensuring simultaneous water breakthrough in all zones. The zonal water fractional flow curves versus production time are expected to be an indicator of the variance in the optimal control scenario for different zones. A further advantage of using zonal fractional flow curves is that they reflect the zonal multi-phase flow dynamics, which is a particularly important parameter in the management of field oil-water production. An alternative choice is to use the variance of the NPV (Chapter 5). However, NPV provides aggregate global information on the behaviour of the whole system; while zonal information for subsequent zonal control is required for this study. Hence the clustering process has been tailored to the subsequent proactive optimization calculations with the fractional flow curve being calculated by considering the unfavourable phase (water) w.r.t. the favourable phase (oil). This study substitutes water-cut (WC), calculated by a full physics reservoir simulation, for the fractional flow curve. WC provides a similar (and possibly more accurate) behaviour to the fractional flow while satisfying criteria 1 and 2 above. The drawback of using WC is that it is calculated by a full-physics simulation which substantially increases the computation time (i.e. violating criterion 3). However, the WC was utilized in this study due to the use of a commercial reservoir simulator which did not provide quantitative, streamline information. The choice of using fractional flow or WC in the developed algorithm thus provides the additional flexibility of fast application when quantitative streamline information is available or slower application using the commercial reservoir simulators without streamline information.

6.4. Multi-Dimensional Scaling

Multi-Dimensional Scaling (MDS) is a statistical technique for mapping high-dimensional data (N_H) onto a low-dimensional space (N_L) while preserving the characteristics of the data as far as possible (Borg and Groenen, 2005). Generally, the distance measure between the data points is considered to be an indicator of similarity/dissimilarity. As a result, MDS performs the mapping such that the Euclidean distance between the points in the mapped low-dimensional space is as close as possible to the distance defined in the original space as follows.

$$\mathbb{U} \to \mathbb{u} \quad s.t.\ D(\mathbb{U}_i, \mathbb{U}_j) \cong D(\mathbb{u}_i, \mathbb{u}_j), \tag{6-8}$$

where $\mathbb{U} \in \mathbb{R}^{N_H}$ represents the data points in high-dimensional original space, $\mathbb{u} \in \mathbb{R}^{N_L}$ represents the data points in low-dimensional mapped space (usually 2 or 3 dimensions for the visualization purpose), $D(\mathbb{U}_i, \mathbb{U}_j)$ is the pairwise distance in the original space, calculated by using Equation 6-7 and $D(\mathbb{u}_i, \mathbb{u}_j)$ is the pairwise Euclidean distance between the mapped points. In this study, MDS is performed by eigenvalue decomposition of the dissimilarity matrix and then retaining the largest positive eigenvalues. Considering N_r as the total number of available model realizations the dissimilarity matrix has the dimension of $N_r \times N_r$ while elements of this matrix are pairwise distance between realizations corresponding to the row and the column of that element. The output matrix of the MDS has the dimension of $N_r \times N_L$, with each element representing the relative location of the N_r points in N_L dimensional space. In this study it is considered that $N_L = 2$, hence all model realizations will be mapped into a 2-dimensional space. MDS was previously used by (Scheidt and Caers, 2013) to map the high-dimensional data onto a lower dimension while preserving the similarity/dissimilarity of the different realizations.

6.5. K-means clustering

K-means clustering (Seber, 2004) is selected following previous works on the clustering in low-dimensional metric space (Caers and Park, 2008, Scheidt and Caers, 2013, Park, 2011, Wang et al., 2012). K-means clustering is fast and can achieve a good clustering accuracy especially when it is applied to a low-dimensional point set and therefore is

suitable for this study. K-means clustering routines provided by MATLAB is used in this study. All available realizations (N_r) are grouped into a small number of clusters (N_c) after mapping from N_H dimensional original space into 2-dimensional space. K-means clustering iteratively finds the locations of the clusters centre $\tau_{opt} = \{\tau_1, \tau_2, \dots, \tau_{N_c}\}$ of N_c clusters such that the summation of the distances for all N_r realizations from the nearest cluster centre is minimized. Formally, k-means clustering is an iterative algorithm that tries to solve the following optimization problem:

$$\tau_{opt} = arg \min_{\tau} \sum_{i=1}^{\mathrm{Nr}} \min_{j=1,\dots,N_c} \left\| \mathbb{u}_i - \tau_j \right\|^2, \quad 6\text{-}9$$

where $\tau_j \in \mathbb{R}^{N_L}$ is the centre for cluster j, $\mathbb{u}_i \in \mathbb{R}^{N_L}$ representing the mapped realization and $\|.\|$ represents the l2-norm. Each realization is assigned to the nearest cluster centre after determining the optimum cluster centres (τ_{opt}):

$$arg \min_{j=1,\dots,N_c} \left\| \mathbb{u}_i - \tau_{j,opt} \right\|. \quad 6\text{-}10$$

The Silhouette value (Rousseeuw, 1987) is calculated to evaluate how well a data point is assigned to a particular cluster.

$$Sil_i = \frac{b_i - a_i}{\max(a_i, b_i)}, \quad 6\text{-}11$$

$$a_i = d_{i,C(i)} \quad and \quad b_i = \min_{C \neq C(i)} d_{i,C}, \quad 6\text{-}12$$

$$d_{i,C} = \frac{1}{\#\ data\ points\ in\ cluster\ C} \sum_{l \in C} D(\mathbb{u}_i, \mathbb{u}_l), \quad 6\text{-}13$$

where Sil_i is the Silhouette value for data point i, $D(\mathbb{u}_i, \mathbb{u}_l)$ is the Euclidean distance between data point i and data point l, $d_{i,C}$ is the average dissimilarity of data point i with all other data points in cluster C, a_i is the average dissimilarity of data point i with all other data points within the same cluster. The value of a_i shows how well data point i is assigned to its own cluster. The value of b_i is the lowest average dissimilarity of point i with any point in any other cluster. This would be the neighbouring cluster which is the next best fit for point i. The maximum theoretical Silhouette value is +1, indicating points that are very distant from neighbouring clusters (e.g. an extreme case

with the number of clusters equal to the number of data points i.e. $a_i = 0$). The minimum theoretical Silhouette value is -1, indicating that there are points that have been assigned to the wrong cluster. A mid-range Silhouette value of zero, indicates the presence of points that are not distinctly in one cluster or another.

The average of the Silhouette value ($\overline{Sil}(N_c)$) for all data points evaluates the overall quality of the k-means clustering process with N_c clusters. This is calculated by:

$$\overline{Sil}(N_c) = \frac{1}{N_r} \sum_{i=1,\dots,N_r} Sil(i), \qquad 6\text{-}14$$

6.6. Realization selection in PUNQ-S3 with the I-well in a far-from-optimum location

The uncertainty of the PUNQ-S3 model containing a single I-well, discussed in Section 4.5.3, is quantified by 66 unique realizations of the porosity and permeability distribution ($N_r = 66$). An efficient selection workflow should provide the most robust control scenario while utilizing a minimum number of realizations. The robustness of the resulting control scenario will be evaluated by comparing the cases when a small ensemble of realizations is selected with either a systematic or a random process. Figure 6-1 shows the flow diagram employed for testing the different approaches in order to find the best approach to efficiently select a small ensemble of realizations to acceptably represent all the available realizations.

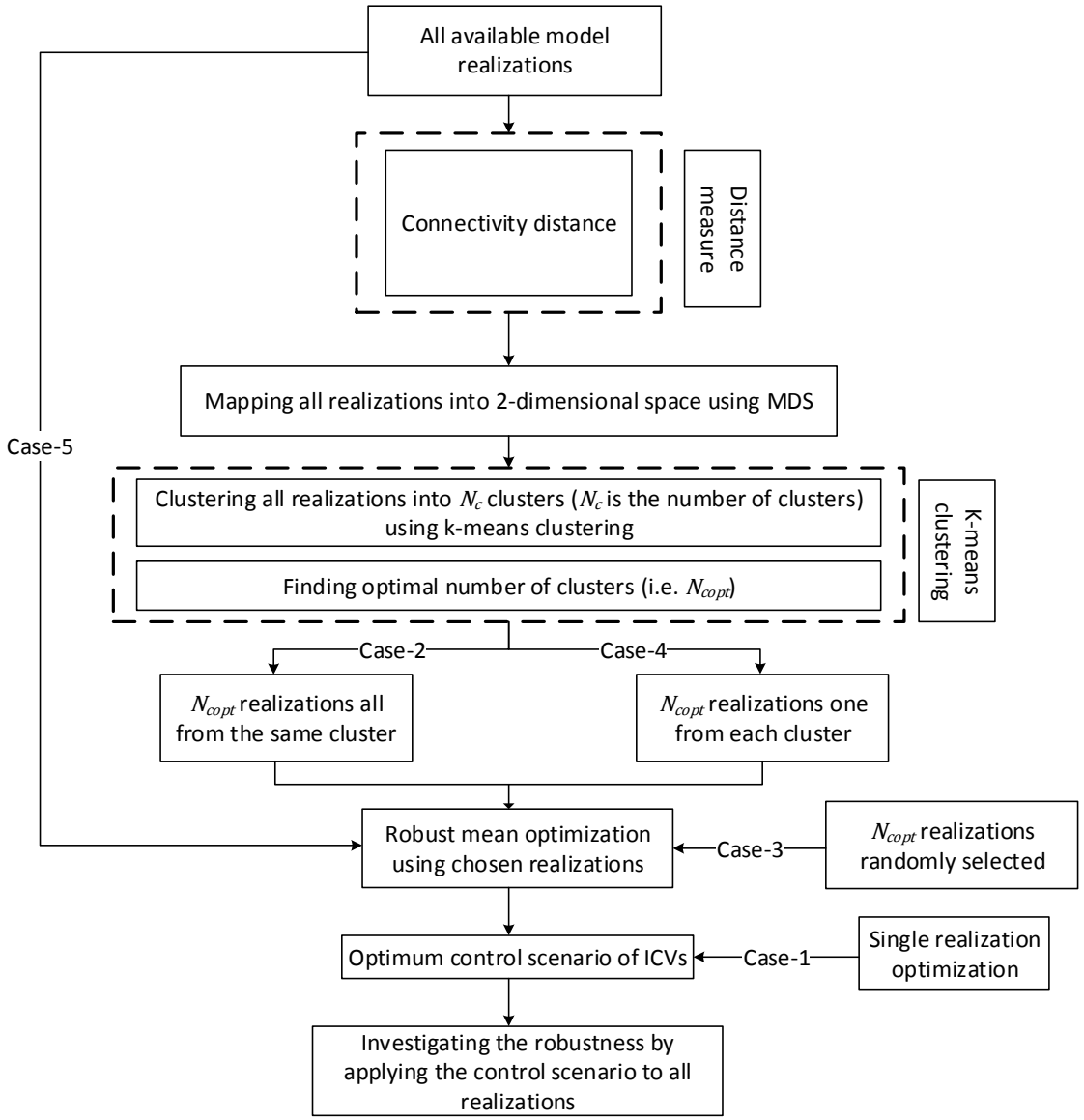

Figure 6-1: Flow diagram of the steps performed to investigate the performance of different approaches to realization selection

Different approaches could be used to measure the dissimilarity distance between realizations. The proxy for the distance between the realizations used for this study, follows Park (2011) recommendations for conventional wells. The proxy employs a modified connectivity distance formula (Equation 6-7) that measures the area between the zonal WC and the production time curves for different realizations. This value provides a good measurement of the similarity/dissimilarity of the different realizations due to the correlation of the distance measure employed with the dynamic response of the model and the objectives of the subsequent optimization. Figure 6-2, the individual WC curves for each of the four ICVs for all available realizations, illustrates how the

dynamic response of the different realizations is captured by the zonal WC curves. The calculated dissimilarity matrix is mapped into 2 dimensions using MDS (Figure 6-3).

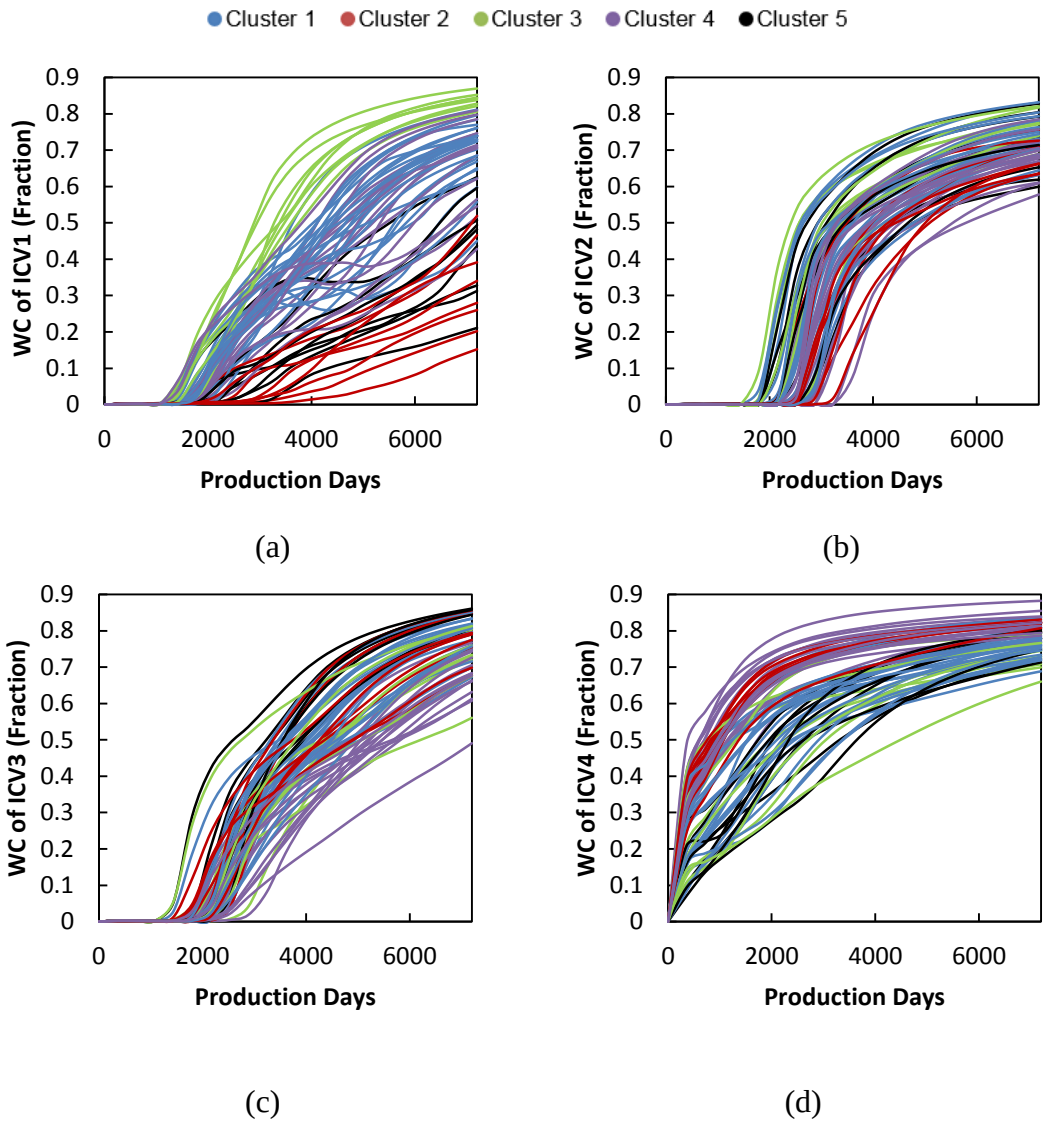

Figure 6-2: WC curves of 4 ICVs for all realizations, (a) ICV1, (b) ICV2, (c) ICV3, (d) ICV4. The colour shows the corresponding clusters.

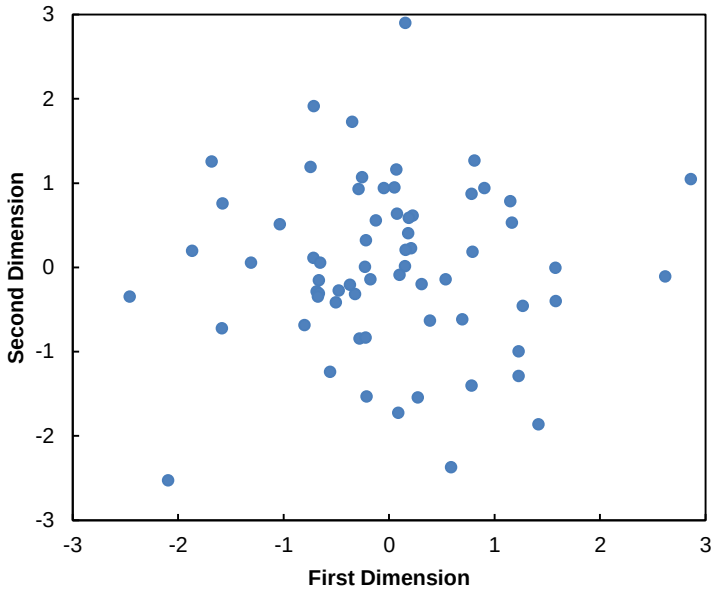

Figure 6-3: Mapping all realizations onto a two-dimensional space using MDS

K-means clustering is then employed to group the mapped data points. One of the major challenges in k-means clustering is to determine the optimal number of clusters (here N_{copt}). Various methods have been developed to address this challenge [e.g. (Ben-Hur et al., 2001)]. However, none of these methods guarantees finding an optimal solution in all cases. Determining the optimum number of clusters is an ill-posed problem and is mostly addressed by a combination of intuition supported by mathematical analysis. The approach used in this study is to calculate the average Silhouette value for all data points when k-means clustering is performed with different number of clusters (N_c) (Figure 6-4). The improvement in clustering (shown by a higher mean Silhouette value) as a result of increasing the number of clusters is divided into two regions (blue and red points in Figure 6-4) (Thorndike, 1953). The main improvement is achieved in the blue region (up to 6 clusters) while the rate of improvement slightly decreases in the red region (more than 8 clusters). The number of clusters was thus initially chosen to be six; as the minimum number of clusters that are representative of all 66 realisations.

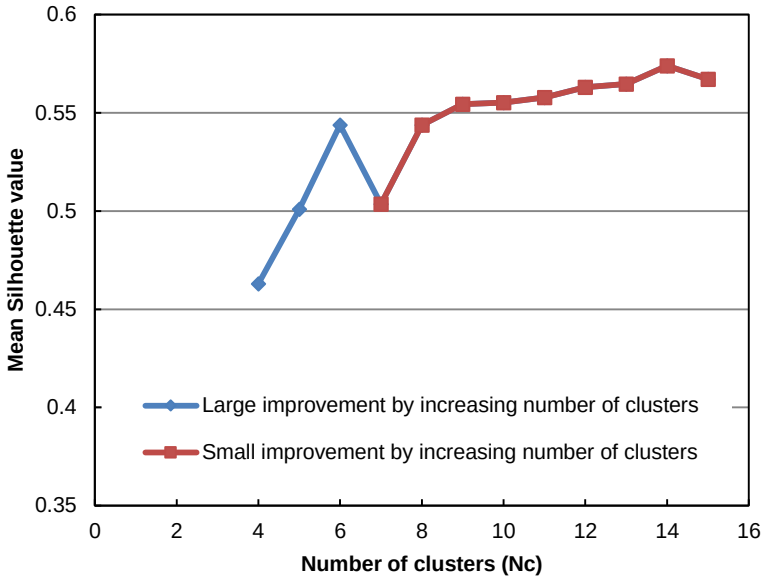

Figure 6-4: Mean Silhouette value of all data points calculated for different number of clusters in k-means

However, more detailed analysis showed that one of the clusters contained a single realization (cluster 6 in Figure 6-5 (b)). This is due to the significant difference in WC of ICV2 and ICV4 in this realisation as compared to other realisations (red curves in Figure 6-6 show the realisation in cluster 6). Hence the optimum number of clusters $N_{copt} = 5$ was chosen as the initial value for the subsequent optimization. Figure 6-2 shows the clustering results of Figure 6-5 (a) in the original space. However, due to the combined effects of different dimensions the distinct clusters in two dimensional space was not present in higher dimensional original space.

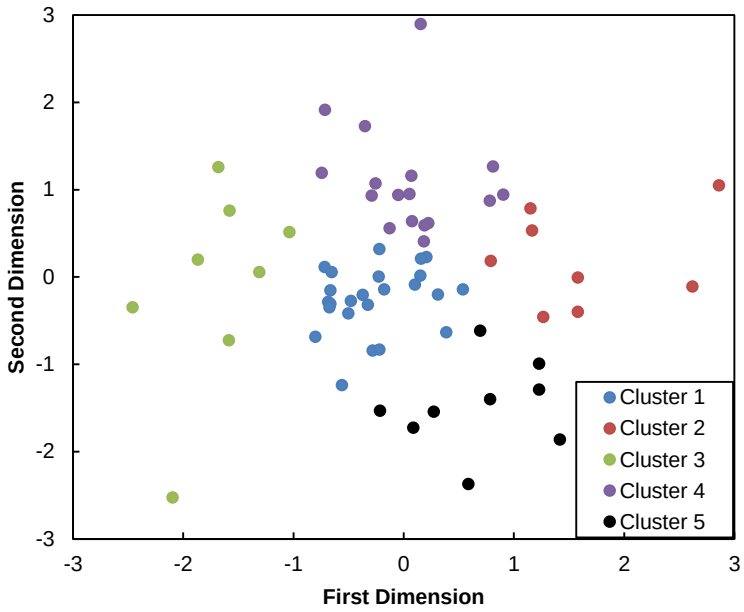

(a)

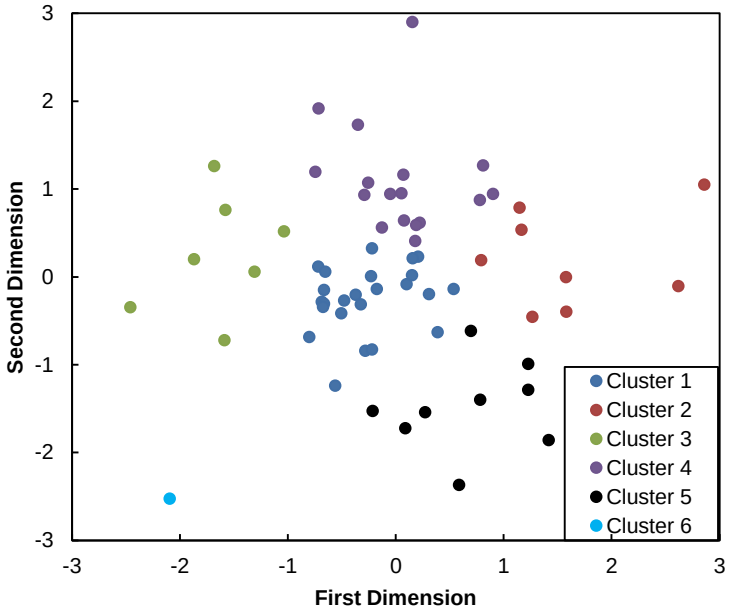

(b)

Figure 6-5: (a) K-means clustering considering 5 clusters (N_c=5) (b) K-means clustering considering 6 clusters (N_c=6)

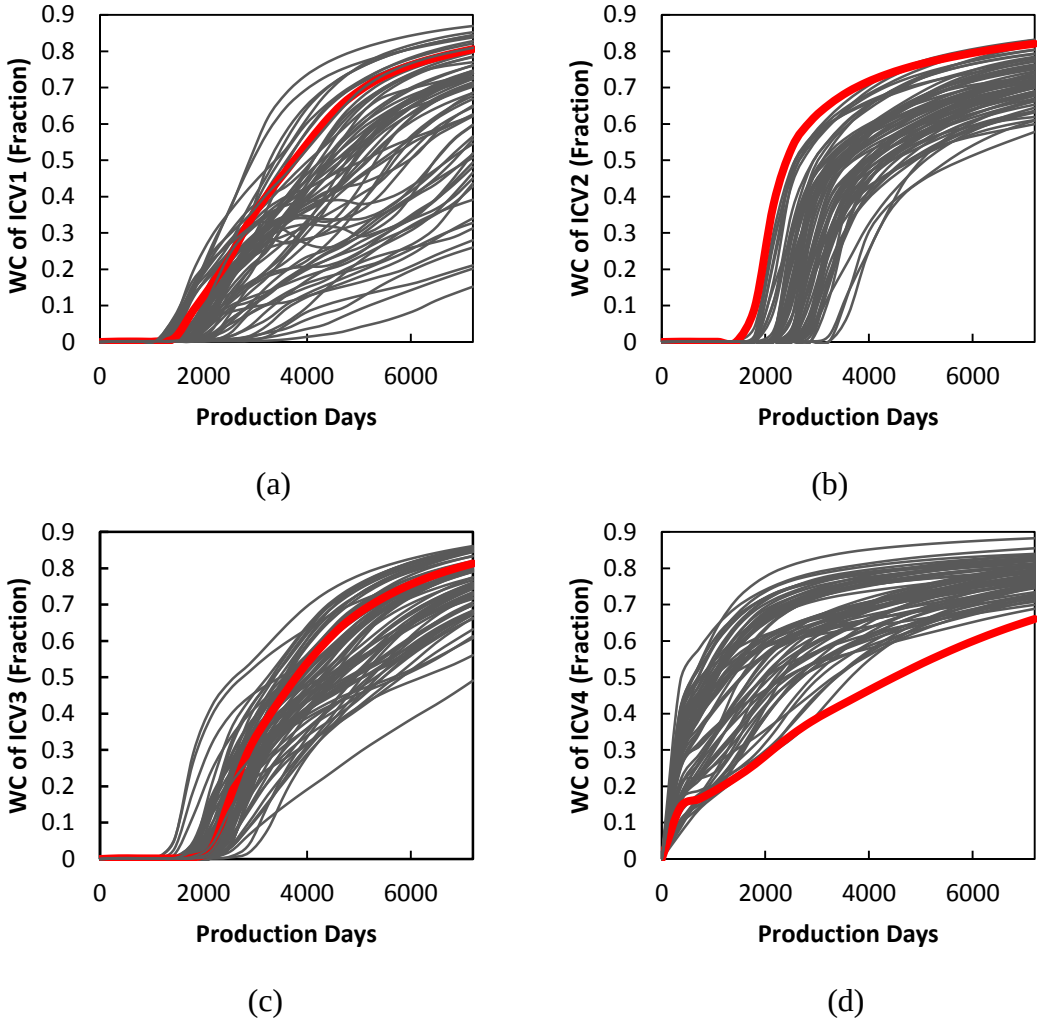

Figure 6-6: WC curves for the single realisation of cluster 6 (in red) as compared to other realisations, (a) ICV1, (b) ICV2, (c) ICV3, (d) ICV4.

Selecting one (or several) realizations from each cluster is another important decision that needs to be made prior to performing robust optimization. The minimum number of realizations are selected to minimize the computational cost of solving the robust optimization problem. A minimum number of 5 realizations have to be selected to account for the variability embedded in each cluster since all available realizations have been grouped into 5 clusters.

Five cases were considered where optimization was performed using: (1) randomly selected single realization, which corresponds to ignoring the model uncertainty in the optimization process. (2) Five realizations selected from the same cluster. This represents an ill-informed selection method. Several tests were performed where a single cluster is randomly selected and then 5 realizations were randomly selected from

this cluster. (3) Five realizations selected using a uniform random distribution based on the NPV (Section 5.4). (4) One realization is selected from each 5 clusters. This represents a well-informed selection method. The closest realization to the centre is selected as the representative realization of each cluster (Scheidt and Caers, 2013). (5) All available model realizations. The mean of the objective function of the chosen realizations (i.e. Equation 5-2) is optimized in all cases with multiple realizations. For all cases five independent runs were performed in order to eliminate the random effects originating from: (1) the random number generator employed in the SPSA, this affects all cases and (2) the random selection of the realizations in case 1, 2 and 3.

The obtained control scenarios from independent runs of the five cases are applied to all available realizations. The improvement in the expected NPV is compared in Figure 6-7 (a) w.r.t. the base case (i.e. average NPV of all realizations with fully open ICVs). Note that a reactive control was not chosen as the base case since a "do-nothing" base case is both unambiguous and simple to implement; allowing a relative comparison of the different robust proactive optimization approaches. Single realization optimization (case 1) provides the minimum robustness at a minimum computational cost while robust optimization considering all available realizations (case 5) provides the maximum improvement, at a possibly prohibitive, increase in the computation cost (Figure 6-7(c)). Here, the optimization was performed for 100 iterations for each case, while at each iteration the average stochastic gradient is calculated using 5 independent perturbations employing a central difference formulation. This results in 11 simulation runs per iteration for case (1); 55 simulation runs per iteration for case (2), (3) and (4); and 726 simulation runs per iteration for case (5).

Figure 6-7 (a) and (c) show that in this case study an acceptable improvement (~ 90% of the improvement using all realizations) is achieved within a reasonable computational time when clustering is performed and one realization is selected closest to the centre of each cluster. The lower mean in case 1, 2 and 3 is also due to the random selection of realisations in these cases which is also confirmed by larger variation of the random runs (Figure 6-7 (b)). Moreover, the normalised standard deviation (in case (4) and case (5)) is significantly lower than the normalised added-value showing that 5 independent runs are enough to eliminate the random effect of SPSA in this case study (Figure 6-7 (a) and (b)). The advantage of an approach with a low variance (e.g. case (4)) is higher

probability of achieving the optimum solution. Note that improved robust optimization due to prior clustering of realizations has also been observed by Wang et al. (2012) in an optimum well location study.

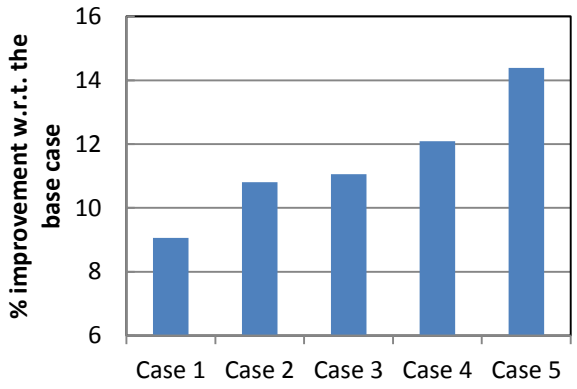

(a)

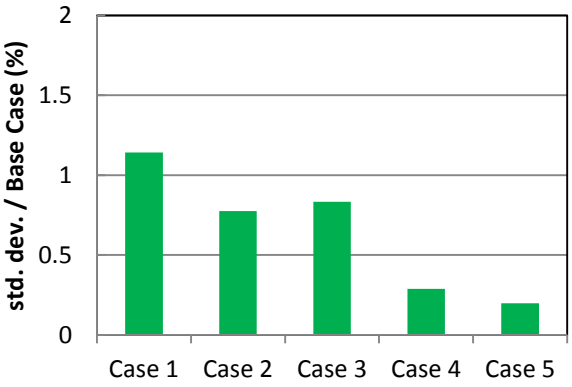

(b)

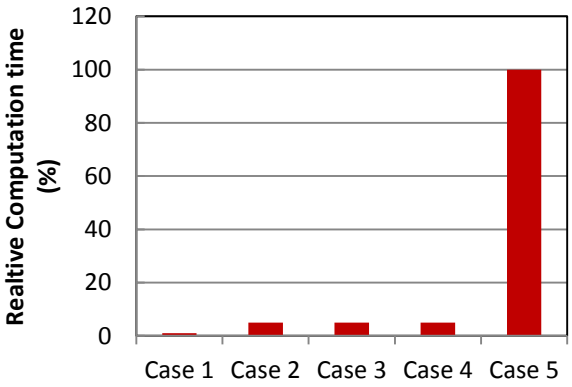

(c)

Figure 6-7: (a) The improvement in the expected NPV of all realizations w.r.t. the base case (b) the standard deviation of 5 random runs w.r.t. the base case (c) Relative computation time, as a result of performing optimization using different approaches: (case 1) single realization optimization, (case 2) 5 realizations are selected from the same cluster, (case 3) 5 realizations are randomly selected based on the objective value, (case 4) one realization is selected from each of the 5 clusters, (case 5) all available realizations are considered

6.7. Robust optimization using selected realizations

The framework developed for robust optimization is summarized in Figure 6-8, where the different steps required to efficiently select a small ensemble of realizations are detailed. A choice must then be made between the "mean" and "mean-variance" approaches for robust optimization. The effect of the random number generator employed in SPSA (Section 4.4.1) was eliminated here by performing five independent runs. Similar to previous cases the variance of independent runs is significantly lower than the obtained added-value. The best optimization run is then presented for three approaches below:

1. *Single realization optimization*: The optimization of this approach uses a single realization. The obtained controls are then applied to all other realizations with the test being repeated for each of the five cluster centres (Figure 6-5 (a)).
2. *Mean optimization:* The objective function is now the mean of the objective values of the five realizations (i.e. Equation 5-2 or Equation 5-4 with $A=0$). The cost of evaluating the objective function has increased from one to five simulation runs. The dashed lines in Figure 6-9 (a) shows the objective values for each five realizations while the solid red line is their mean value. Figure 6-9 (b) shows the impact of mean optimization on the variance.
3. *Mean and variance optimization:* The new objective function defined by Equation 5-4 was evaluated using two different values of A that provided the same order of magnitude for the utility function's mean and variance terms. In order to find the value of A we consider the objective values of the selected realizations at the starting point of the optimization process (i.e. fully-open ICVs). The utility function value is iteratively maximized (Figure 6-10 (c)). As expected, the case with a larger A *("Low Risk")* provides a control scenario that gives lower variance (Figure 6-10 (b)); reducing the uncertainty in the potential NPV at the cost of lowering the average expected NPV (Figure 6-10 (a)).

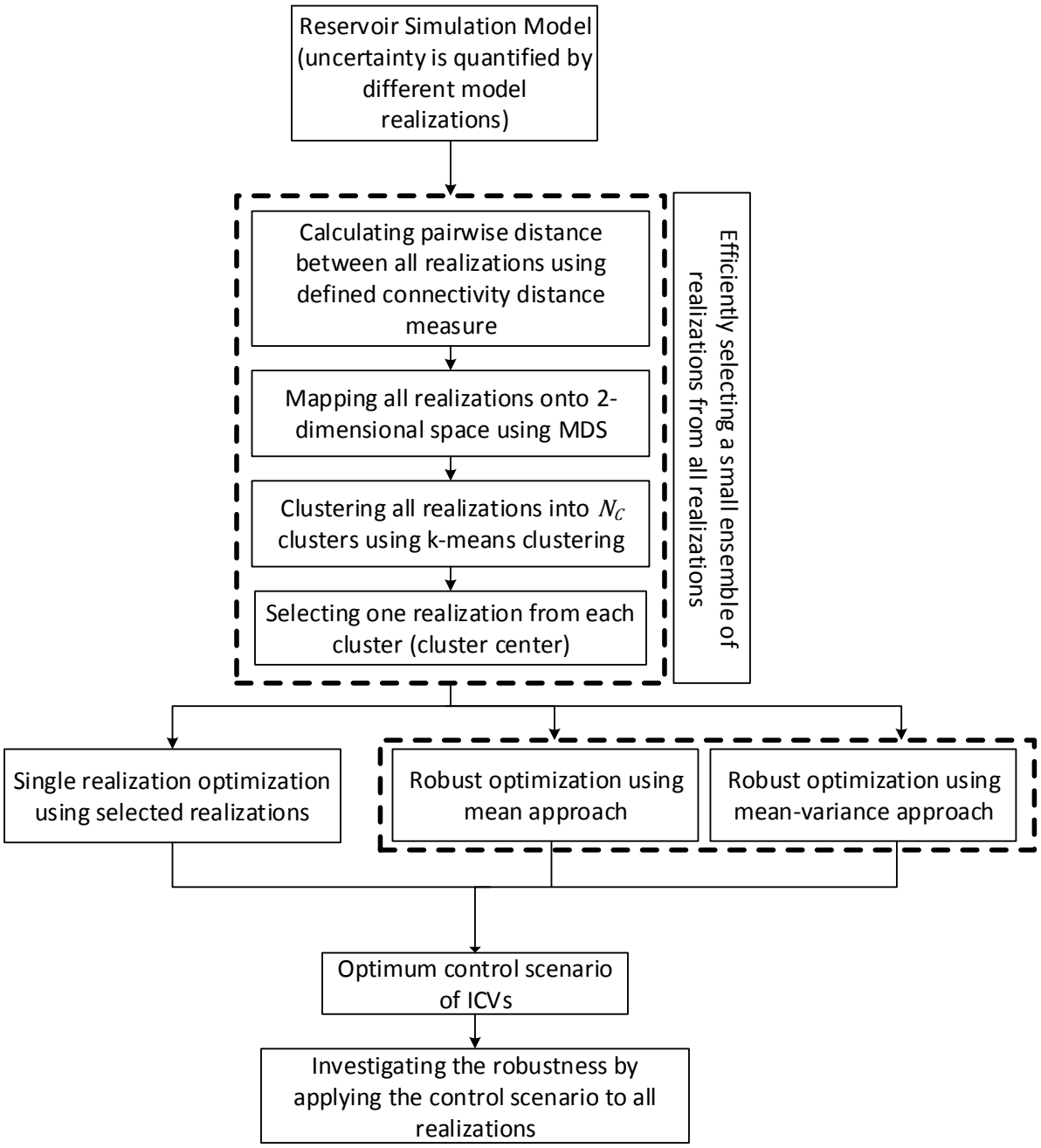

Figure 6-8: Flow diagram for the robust optimization framework

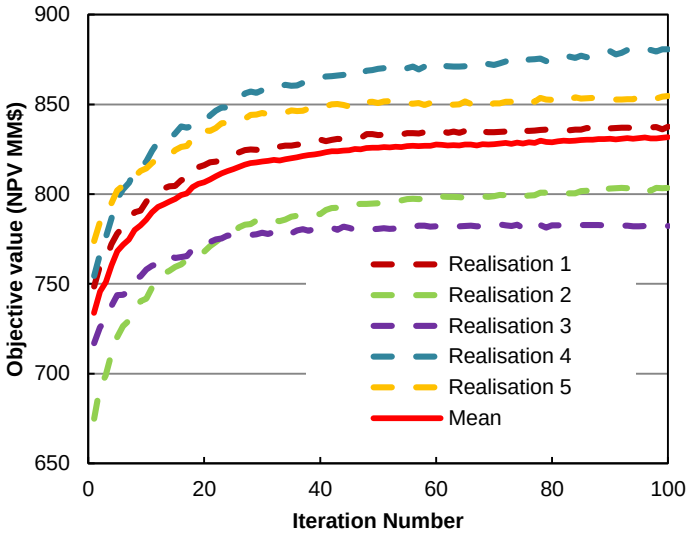

(a)

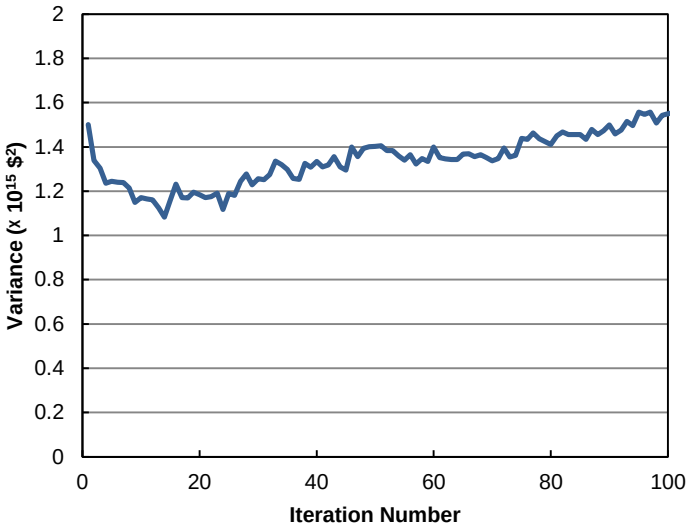

(b)

Figure 6-9: (a) Objective values during the optimization process using mean (A=0) as objective function (b) Variance during the optimization process

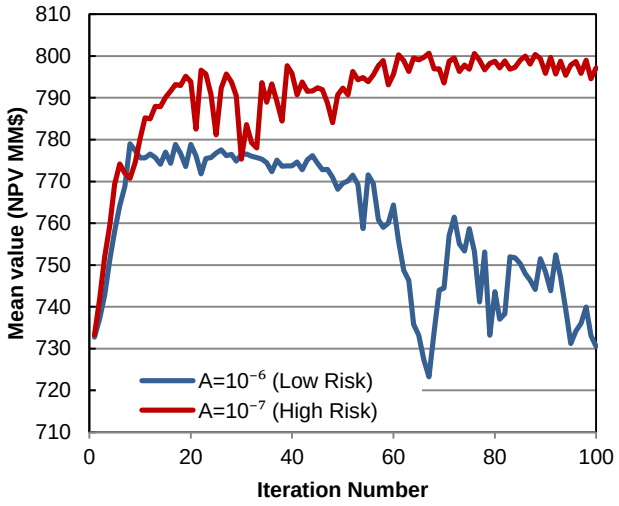

(a)

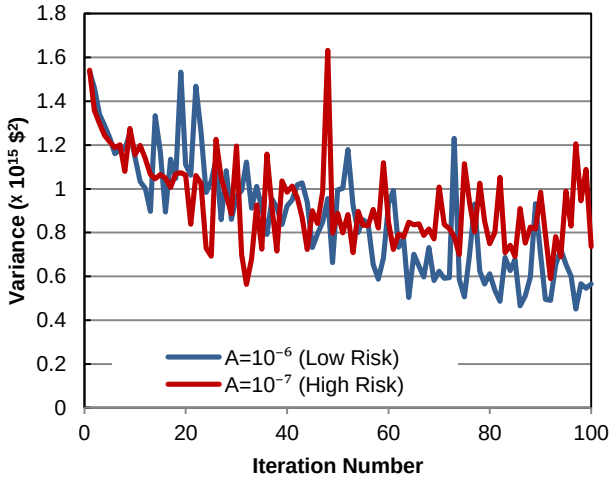

(b)

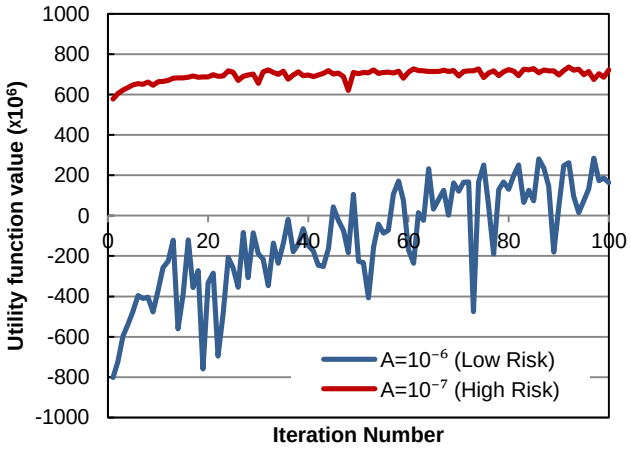

(c)

Figure 6-10: Mean and variance optimization approach using A=10^{-6} (low risk) and A=10^{-7} (High risk) - (a) Mean (added-value) (b) Variance (reliability) (c) Utility function value (objective function)

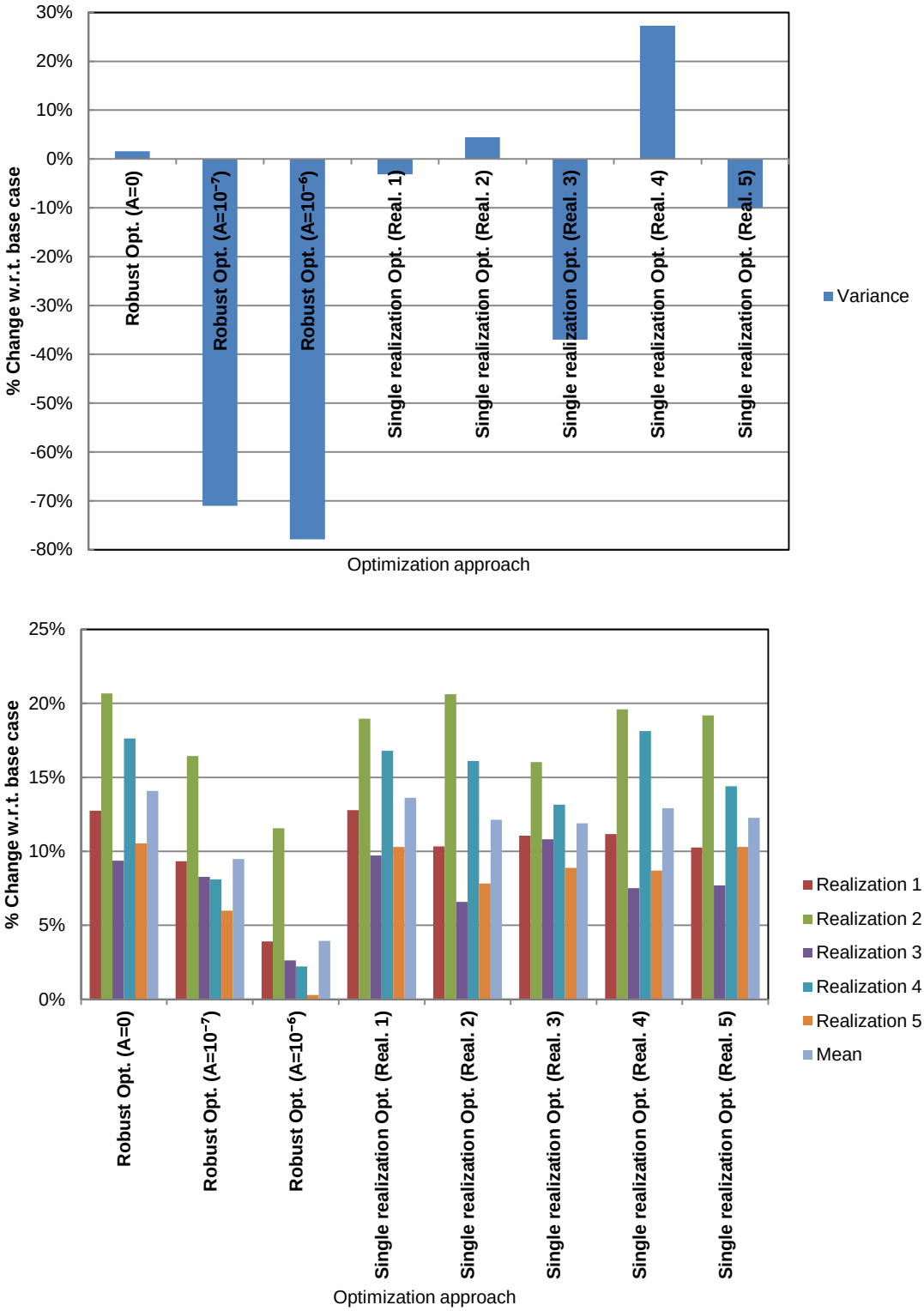

Figure 6-11: Changes in objective value of the selected realizations and their mean and variance using the Figure 6-8 different optimisation approaches. The mean and variance are calculated for the 5 selected realizations. The best case from performed independent runs.

The optimum solutions obtained by the three approaches are now applied to the selected 5 realizations. Figure 6-11 presents the percent changes in the objective value of each realization, mean and variance with respect to the base case. The control scenario obtained using a single realization optimization approach often provides the maximum improvement for that particular realization, but normally shows suboptimal performance for all other realizations; though it could, by chance, provide a significant global improvement (e.g. Single realization Opt. (Real. 1) in Figure 6-11). It certainly does not guarantee a robust control in all cases. Moreover, higher global improvement in single realization optimization as compared to the robust optimization might also be due to the convergence failure (or convergence to a local optimum) when using an estimated gradient-based optimization algorithm.

Figure 6-11 shows that robust optimization improves the reliability by using an ensemble of realizations. Robust optimization using the value (A=0) provided a maximum improvement of ~14% in the mean of the selected realizations; while a larger value (A=10^{-6}) provides the most reliable control scenario with a ~78% decrease in the variance, while at the same time delivering a ~4% improvement in the mean. The adverse effect of lower mean by introducing the variance in the objective function is due to the symmetric nature of the mean-variance optimisation approach as discussed in Section 5.2. An asymmetric approach (e.g.(Siraj et al., 2015)) is expected to alleviate this problem. Implementing a control scenario which reduces the variance (i.e. a reliable control scenario) enhances the confidence that a specific value will be achieved by operating the (real) well/field in the prescribed way.

The global performance of the obtained control scenario using each robust optimization approach was also been investigated by applying the resulting well controls to all available realizations. Table 6-1 shows the percent change in the mean and variance of all realizations w.r.t. the base case in contrast to Figure 6-11 which shows the result of applying the obtained control scenario to only the selected 5 realizations. The complete process is then repeated with an increased number of realization (10). Robust optimization (A=10^{-6}) is also repeated with an increased number of optimization iterations (400).

Table 6-1: The percent change in total mean and variance w.r.t. base case by applying the obtained control scenario using robust optimization approaches to all realizations

Total number of Iterations	Number of selected realizations	% Change	Robust (A =0)	Robust (A =10^{-7})	Robust (A =10^{-6})
100	5	**mean**	+14	+10	+4
		variance	-50	-54	-45
	10	**mean**	+13	+11	+9
		variance	-50	-56	-54
400	5	**mean**	-	-	+8
		variance	-	-	-47
	10	**mean**	-	-	+9.3
		variance	-	-	-57

Table 6-1 shows that the control scenario resulting from the mean optimization approach (A=0) reduces the variance when applied to all realizations. This agrees with earlier observations (Haghighat Sefat et al., 2015) and Chapter 4 of this thesis; that ICVs' flexible control improves the production performance relative to the base case. Hence, the realizations with less favourable base case performances show the greatest improvement. This effect, and the corresponding reduction in the gains achieved by ICV control of more favourable realizations inherently reduces the global variance in the mean optimization approach (Figure 6-12). However, this behaviour is not observed in all realizations (e.g. Figure 6-9 (a) realization 3 with a lower base case performance is showing less improvement than realization 5 with a better base case performance). It can thus be concluded that, the mean robust optimization approach (A=0) does not guarantee achieving the minimum variance.

The optimization algorithm aims to find a control scenario which provides a further reduction in the NPV variance when the value of A is increased in the utility function. However, the algorithm achieves this by no longer finding the absolute maximum of the mean NPV. Figure 6-11 confirms that the optimization algorithm achieves lower variance values, but with a reduction in the optimal mean NPV value, for these cases.

A discrepancy in the variance value was observed when investigating the global performance of the obtained control scenario using 5 selected realizations. Table 6-1 shows that robust optimization (A=10^{-6}) and 100 iterations failed to find a control scenario which provides minimum variance when applied to all realizations. This might be due to: (1) the selected realizations not being representative of all realizations when the objective of robust optimization is on constraining the variance. This is intuitive as the variance inherently depends on the degree of variability of all realizations; which can be captured by selecting a larger number of realizations. (2) The utility function becomes non-smooth when the value of A is increased [Figure 6-10 (c)]. A non-smooth objective function will degrade the performance of the stochastic gradient-based optimization algorithm used. The optimization algorithm could have been re-tuned e.g. by increasing c to bypass noise to overcome this problem.

The optimization process is repeated by dividing all realizations into 10 clusters and then selecting the realization closest to the centre of each cluster. Table 6-1 shows that increasing the number of selected realizations to 10 results in the maximum improvement for the case of robust optimization (A =10^{-6}), while showing a smaller improvement in the other two cases. Selecting 5 realizations is thus not fully representative of all realizations when the emphasis of robust optimization is on constraining the variance.

The optimization algorithm converged to an acceptable solution by increasing the number of iterations to 400 (i.e. $k_{max} = 400$) in the robust optimization (A =10^{-6}) case achieving the minimum variance. This shows that optimization with a risk-averse objective is a relatively harder to solve optimization problem which requires a larger number of iterations for convergence.

Figure 6-12 (a) shows the Probability Distribution Function (PDF) when the best control scenario obtained using robust optimization with A =0 and A =10^{-6} and single realization optimization are applied to all realizations compared to the base case. The probability values are calculated by considering a non-parametric kernel-smoothing distribution (Bowman and Azzalini, 1997). The single realization results correspond to a randomly selected realization from the full ensemble. Figure 6-12 (b) shows the corresponding Cumulative Distribution Function (CDF). The variance reduction

mechanism − resulted from larger improvement of realizations with poor base case performance and smaller improvement of realizations with good base case performance − is shown in Figure 6-12. The reduction in variance as a result of robust optimization with A =0 (i.e. mean-only optimization) is also observed by van Essen et al. (2013). A reactive control strategy might show lower performance than the single realization optimization (e.g. (van Essen et al., 2013)) or even lower than the base-case if it is not performed at the correct time (Section 3.2.1).

The impact of different optimization approaches on the obtained improvement from the worst-case realization (with minimum base-case NPV) and best-case realization (with maximum base-case NPV) is shown in Figure 6-13. All approaches show higher improvement of the worst-case compared to the best-case. Robust optimization (A=0), by maximising mean, provides the maximum improvement in both cases however, Robust optimization (A=10^{-6}) results in lower improvement in both cases while reducing the variance (symmetric nature of the mean-variance approach discussed in Section 5.2). The reduction in mean value by using mean-variance approach is also observed by Capolei et al. (2015). An asymmetric approach (Siraj et al., 2015) is expected to achieve better performance by providing higher improvement of the poor cases without reducing the improvement in the good cases.

The value of A ($A \geq 0$) in the robust optimization approach has to be decided based on the level of uncertainty (quantified by the variance calculated for the base case of all realizations) in the reservoir model and the need for a risk-averse control scenario based on engineering judgment or economic concerns. In this study only two values of A are considered to provide the same order of magnitude for mean and variance terms in Equation 5-4. A Pareto front can be generated by considering different value of A to help decision maker to select the preferred solution based on the risk preference. Capolei et al. (2015) considered Sharpe ratio (Sharpe, 1994), that is the ratio of added-value to risk ($Sh = E(\mathcal{F}(x,\hat{y})) \,/\, \sigma\big(\mathcal{F}(x,\hat{y})\big)$), as a measure to systematically choose a solution. The value of A that generates the final solution with the maximum Sharpe ratio (also called the market solution) can then be selected.

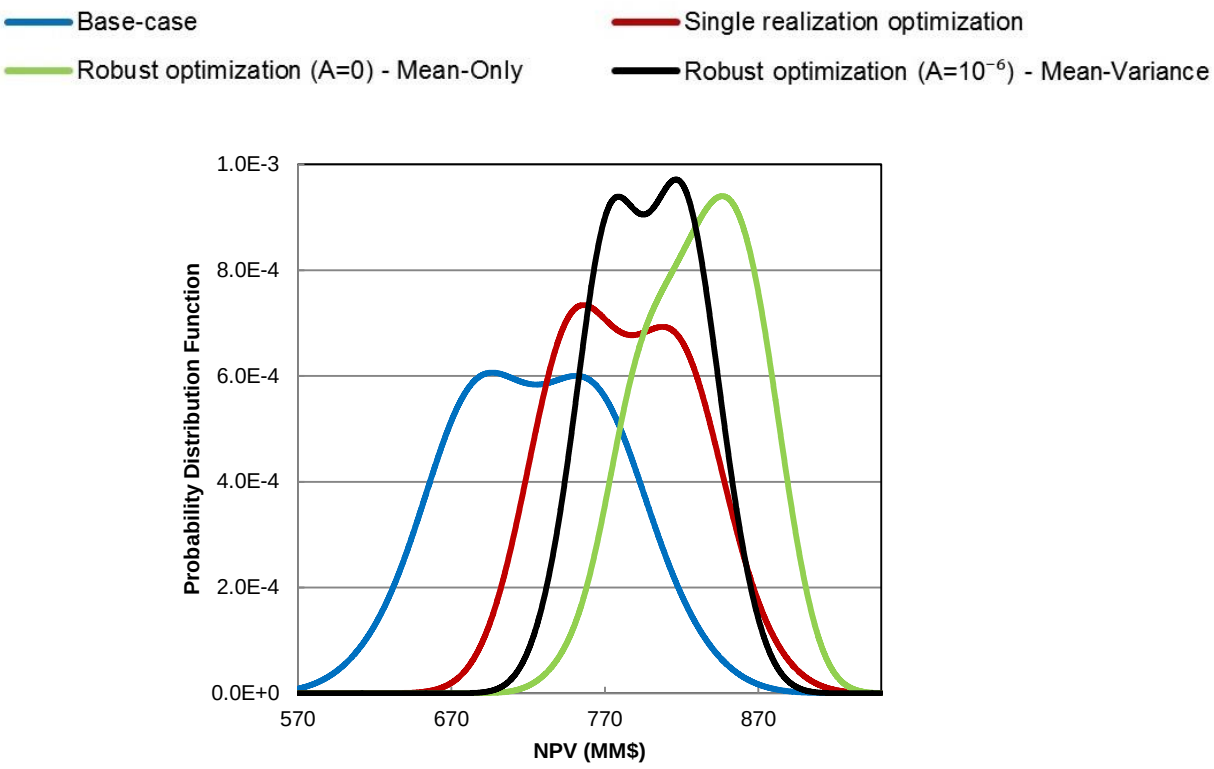

(a)

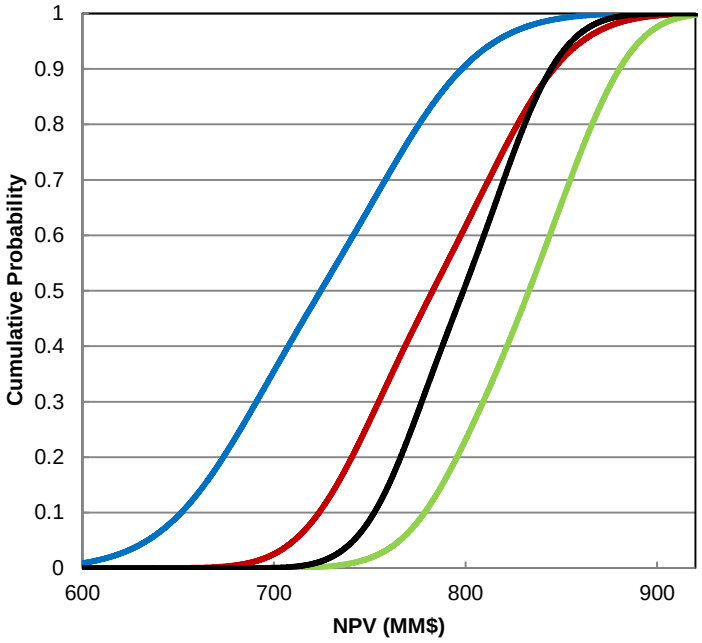

(b)

Figure 6-12: (a) PDF for the best cases obtained using different optimization approaches and base case (b) CDF for the best cases obtained using different optimization approaches and base case (Note: the peaks in (a) are as a result of fitting a kernel distribution with limited number of data points (i.e. 66 realizations here) – larger number of data points are required to investigate if the obtained distribution is multimodal)

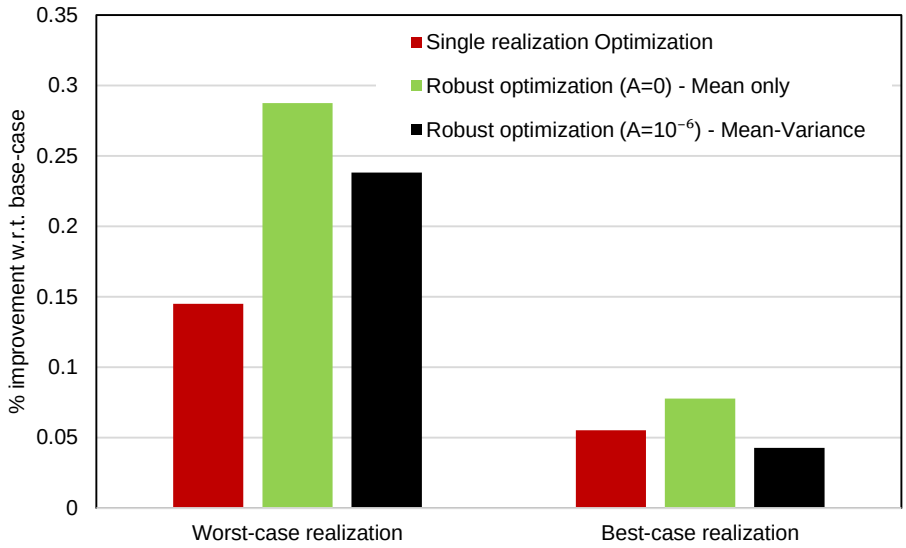

Figure 6-13: Impact of different optimization approaches on worst-case (min fully-open NPV) and best-case (max fully-open NPV) realizations

6.8. Weighted sampling

The above clustering approach resulted in clusters of dissimilar size (i.e. each cluster was made up of a different number of realizations) for the PUNQ-S3 case study. Table 6-2 shows the number of realizations in each cluster together with the weight of each cluster calculated from the number of realizations in each cluster divided by the total number of realizations. A weighted random sampling approach (Olken, 1993) using MATLAB's routine was introduced to address this issue. The sampling was performed 10 times with a different group of 5 realizations being selected from clusters each time according to the weight of each cluster (i.e. higher chance for realizations to be selected from the clusters with higher weights).

The results of robust mean optimization using each selected group are shown in Figure 6-14. It is worth noting that each iteration corresponds to 55 simulation runs since the average gradient is calculated by 5 independent perturbations using the central difference formulation. The best control scenario obtained from each optimization run was then applied to all realizations. Table 6-3 shows the corresponding increase in the mean and the reduction in the variance w.r.t. the base case when the obtained control scenario using different groups of realizations and different random number generator in

the SPSA is applied to all realizations. These results are similar to Figure 6-7(a) – Case 4 while here we use weighted random sampling instead of selecting the cluster centers.

Table 6-2: Weight of each cluster used in weighted sampling

Cluster name	Number of realizations	Weight
Cluster-1	24	0.36
Cluster-2	8	0.12
Cluster-3	8	0.12
Cluster-4	17	0.26
Cluster-5	9	0.14

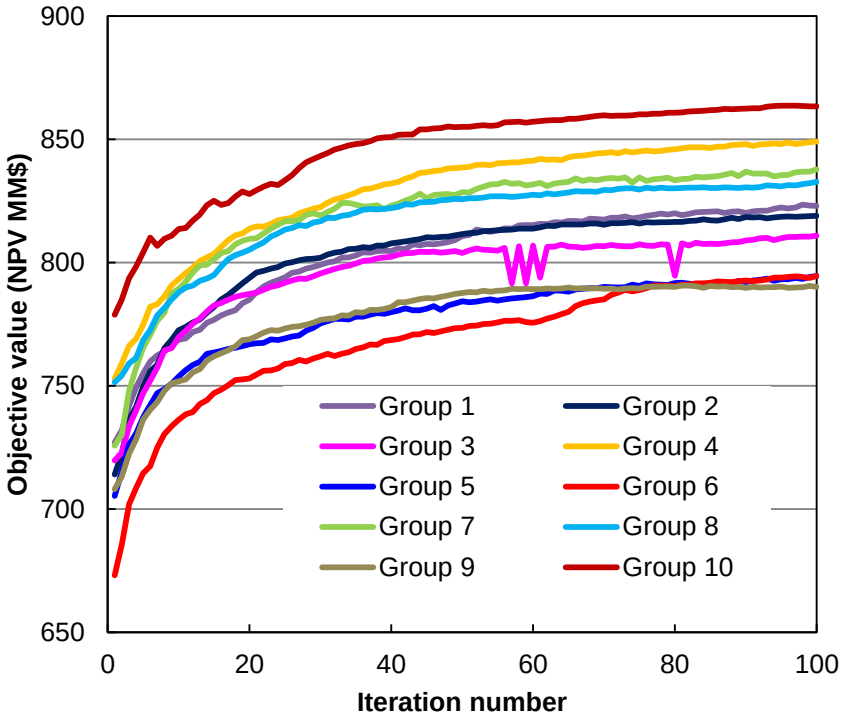

Figure 6-14: Robust mean optimization using 10 groups of realizations selected by weighted random sampling

We have thus achieved an improvement in the final optimization results by using a weighted random sampling approach rather than equal weights for all clusters and choosing cluster centers (compare average from Table 6-3 with Figure 6-7(a) case-4). The weighted sampling approach performs better than equal weights for all clusters with a probability of more than 95.4% calculated by the hypothesis testing using the standard deviation and mean from Table 6-3 and Figure 6-7 case-4. This can be due to

incorporating cluster weights which reduce the adverse effects of random realization selection. This result is particularly attractive when greater parallel processing computing resources are available since it provides the opportunity to perform robust optimization with an ensemble of realizations larger than the number of clusters.

Table 6-3: The percent change in total mean and variance of all realizations by applying the control scenario from different groups of realizations selected by weighted random sampling

Groups of selected realizations	**Mean (% change w.r.t. base case)**	**Variance (% change w.r.t. base case)**
Group-1	12.6	-44.6
Group-2	12.9	-52.4
Group-3	12.7	-53.3
Group-4	14.2	-46.6
Group-5	11.6	-48.5
Group-6	13.2	-49.7
Group-7	13.6	-50.0
Group-8	12.7	-47.6
Group-9	12.6	-56.5
Group-10	13.1	-50.3
Average	**12.9**	**-50.0**
Standard Deviation	**0.68**	**-**

6.9. Summary and conclusions

Proactive optimization of ICVs promises the maximum long-term objective value during the considered field life. However, the robustness of the optimized ICV control scenario depends on the reliability of the employed simulation model. The control scenario obtained using only a single model realization, while providing the maximum improvement for that particular realization, normally results in a sub-optimal performance when applied to the full ensemble of possible realizations. Chapter 6 has presented an efficient framework, integrating several previously developed components, for robust proactive optimization of I-wells. SPSA was chosen as the optimization algorithm based on the arguments presented in Chapter 4 however the framework is compatible with any optimization algorithm. Following main conclusions are obtained.

1. Robust optimized ICV controls are obtained when the objective function is substituted with an augmented function evaluated using an ensemble of realizations. Employing the full ensemble of model realizations is the ideal approach and should provide the ultimate value (van Essen et al., 2013). However, its use would significantly increase the computational costs. A workflow for smart selection of a smaller ensemble of realizations has been developed.
2. The recommended approach by Caers and Park (2008) for measuring the similarity/dissimilarity of the different realizations in response space prior to clustering is shown to perform successfully for I-wells. A connectivity distance measure tailored to the objective of the subsequent optimization is defined following Park (2011). It is observed that the distance calculated by summation of the differences in the WC curves of all ICV zones provides a suitable performance measure for use during clustering analysis when the objective of proactive optimization is to improve oil recovery by delaying early water breakthrough. This measure of connectivity distance is expected to change for other reservoir depletion strategies and drive mechanisms.
3. It is essential for success of the clustering algorithm to ensure that the chosen connectivity measure is projected onto a lower dimension (2-dimensional) space. MDS was used here to preserve the similarity/dissimilarity of the different realizations (Scheidt and Caers, 2013). K-means clustering was found to efficiently (i.e. fast and achieve a good clustering performance) group all realizations into a small number of clusters which may then be used to select a small ensemble for robust optimization.
4. Robust optimization by selecting realizations from different clusters (Wang et al., 2012) proportionally weighted with respect to the relative cluster size provides both an improvement close to the ultimate value as well as a substantial reduction in the computational cost. It provided ~ 90% of the ultimate value at a cost of only ~ 8% of the computational effort when compared to full ensemble optimization for the chosen case study.
5. The utility function approach (Chen et al., 1999, Petvipusit et al., 2014, Capolei et al., 2015) performed effectively with a reduced computation time when an objective-oriented realizations selection process is applied to ensure that the

selected realizations properly captured the required characteristics of all realizations. The chosen value of the utility function parameter, A, defines the manner in which the optimization provides robustness to the control scenario.

a. A value of A=0 (i.e. mean optimization) maximized the mean of the selected realizations. The flexible and optimal control provided by ICVs was observed to reduce the variance to some extent; despite the variance term having been ignored in the objective function's definition. This behaviours was also observed by van Essen et al. (2013) in robust optimization of conventional wells.
b. Higher values of A reduced the variance to give a more risk-averse control scenario. Conflict was not observed when attempting to individually increase the mean and reduce the variance during the early stages of optimization when the control variables were far from the optimum value. However, conflict did occur between these two objectives during the later stages of optimization when the optimum value of the augmented objective function is being approached. A risk tolerant control scenario, with a lower variance in the expected NPV, can thus be expected to show a relative decrease in the mean of the NPV (also reported by Capolei et al. (2015)). Asymmetric approaches are expected to show lower tendency of compromising the best cases in order to reduce the variance (Siraj et al., 2015).
c. A Pareto front can be generated by considering different value of A to help decision maker to select the preferred solution based on the risk preference. Capolei et al. (2015) considered Sharpe ratio (Sharpe, 1994), that is the ratio of the added-value to risk ($Sh = E(\mathcal{F}(x,\hat{y})) \,/\, \sigma\big(\mathcal{F}(x,\hat{y})\big)$), as a measure to systematically choose a solution. The value of A that generates the final solution with the maximum Sharpe ratio (also called the market solution) can then be selected.

Focusing robust optimization on the more risk-averse control scenario, with a larger value of A in the utility function, reduces the variance and also results in a more complicated optimization problem. Increasing the number of chosen realizations was

shown to address this problem. Increasing the number of iterations is also required to ensure convergence of the resulting non-smooth objective function.

Chapter 7 - A full-scale, simulation and robust proactive optimisation study of a real-field with 8 Conventional and 3 Intelligent Wells

7.1. Introduction

This chapter describes the testing of the developed concepts on a large, complex full-scale North-sea field simulated using a commercial reservoir simulator (ECLIPSE, 2012). A field development scenario employing advanced well completions as a potential substitute to a fully conventional development has been modelled. Each I-well is equipped with 4 Infinitely Variable (IV) ICVs controlling the production from the different reservoir layers. The I-wells were modelled using the Eclipse multi-segment well option. The developed criteria in Chapter 3 were employed to simplify the proactive optimisation problem in order to solve it in a reasonable time using limited computational resources (a single high-end workstation). The challenges associated with this simplification and the resulting sub-problems in a large field model are described and the best approach is proposed. The chosen simplified approach results in a sub-optimal solution however, the developed workflow ensures to achieve maximum added-value in a reasonable time with limited computational resources.

The developed workflow is employed to evaluate the impact of the water injection scenario on production from the reservoir and the added-value obtained from proactive optimisation of ICVs. Finally, the developed robust optimisation framework is applied to determine the added-value from the optimum ICV control scenario while the uncertainty is captured using available model realisations. The added-value of the partial I-well field development scenario is compared with that of a fully conventional development.

7.2. Model description

The N-field reservoir simulation model contains of two main reservoirs which partly overlay each other (Figure 7-1). Each reservoir is further divided into two heterogeneous layers which may or may not be hydraulically connected. The reservoirs

are moderately thick (tens of meters) with a typical permeability between a tenth and several Darcies (Figure 7-2). The reservoir simulation model is relatively large (200,000 active cells) and computationally expensive. The field is modelled at the beginning of the development stage; prior to any production history being available.

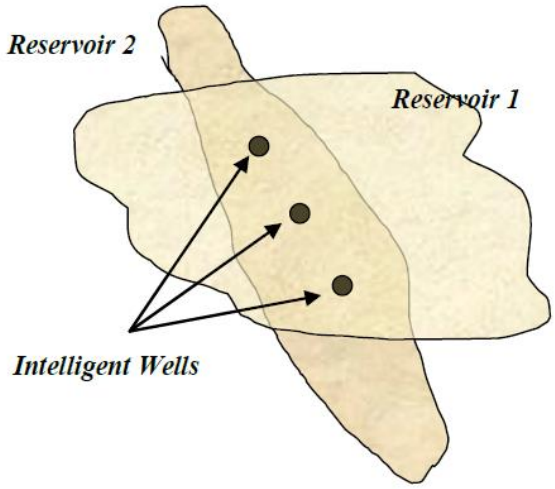

Figure 7-1: Schematic diagram of the N-field reservoirs from Grebenkin and Davies (2012)

Efficient aquifer pressure support is expected for the lower reservoir while there is no aquifer support for the upper reservoir. Similar fluids, a light oil with a moderate Gas-Oil-Ratio, are found in both reservoirs (detailed information about the reservoir cannot be presented due to confidentiality).

The conventional development plan is to drill 21 conventional wells (14 producers and 7 injectors). Six conventional producers are located in the overlap part of the field with 3 wells producing each reservoir. An alternative development scenario is proposed where 6 conventional producers in the overlapped area are substituted by 3 intelligent producers. This provides commingled production from 4 distinctive layers with each layer being monitored and controlled by ICV. Hence the total production well count is reduced to 11 including 3 I-wells and 8 conventional wells. Figure 7-2 shows production wells layout in the I-well development scenario. All wells are produced by gas lift with a maximum total lift gas supply limit for the field.

The initial ramp-up period is followed by the constrained maximum oil production plateau. The production declines after the plateau period and is constrained by a minimum THP limit. A higher THP limit is considered for producers far from the centre in order to transfer the produced fluid to the processing facilities located at the centre of the field. The resulting field oil and liquid production profiles for I-well development scenario with fully open ICVs are shown in Figure 7-3.

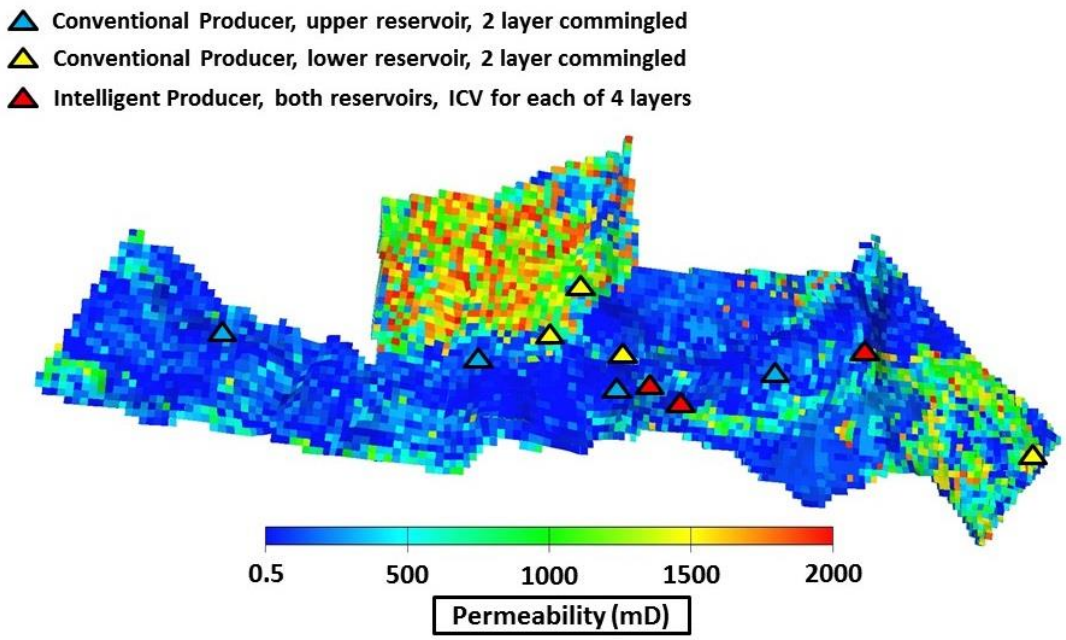

Figure 7-2: Permeability distribution and production wells layout in the I-well development scenario

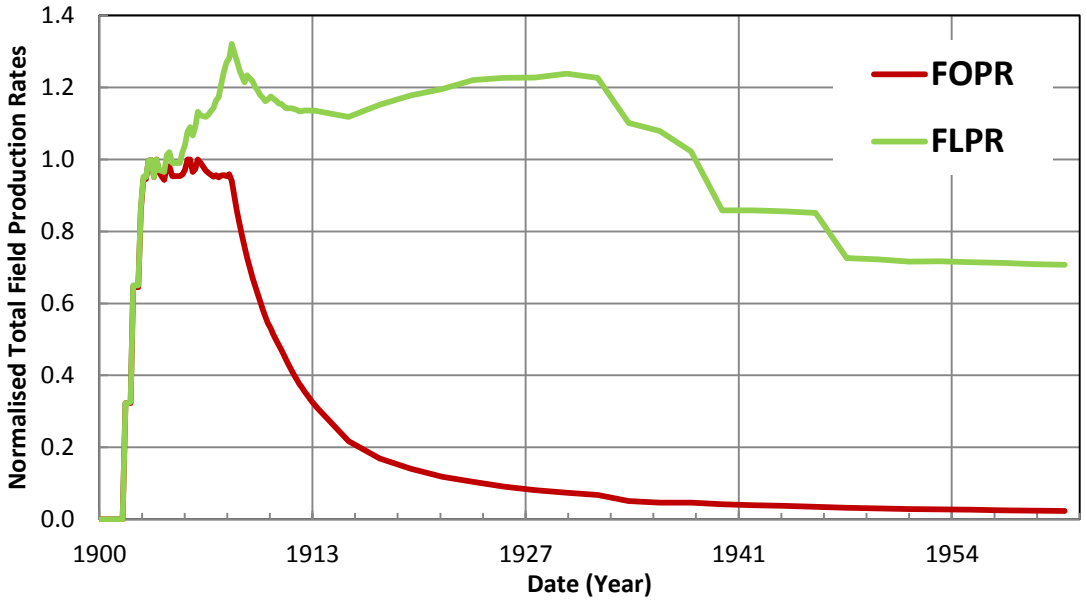

Figure 7-3: Field Oil Production Rate (FOPR) and Field Liquid Production Rate (FLPR) normalised to the plateau oil rate during whole production period for the N-field. (Dates are modified and provided for comparison purpose only.)

The field injection in the base-case is controlled to achieve a 100% voidage replacement while each individual injector is constrained by a limit on maximum injection rate and maximum BHP. Impact of employed injection scheme on the field production is discussed in Section 7.5.

7.3. Defining the suitable period for proactive optimisation

Following the conclusions from Chapter 3, the proactive optimisation is limited to the plateau period with oil rate constraint. Noted that, (1) reactive control is not an option during the plateau period, (2) due to interaction between the control variables during this period, they need to be optimised simultaneously, and (3) there is no loss in the current (or short-term) objectives (oil production) when a proactive optimisation is performed during this period to extend the plateau. Figure 7-4 shows how the production period is divided into the proactive (green) and the reactive (red) period. This chapter describes proactive optimisation process applied to the plateau and early decline (25% of the plateau period length) phases. A fast and efficient reactive control approach developed for this field was previously reported (Grebenkin, 2013).

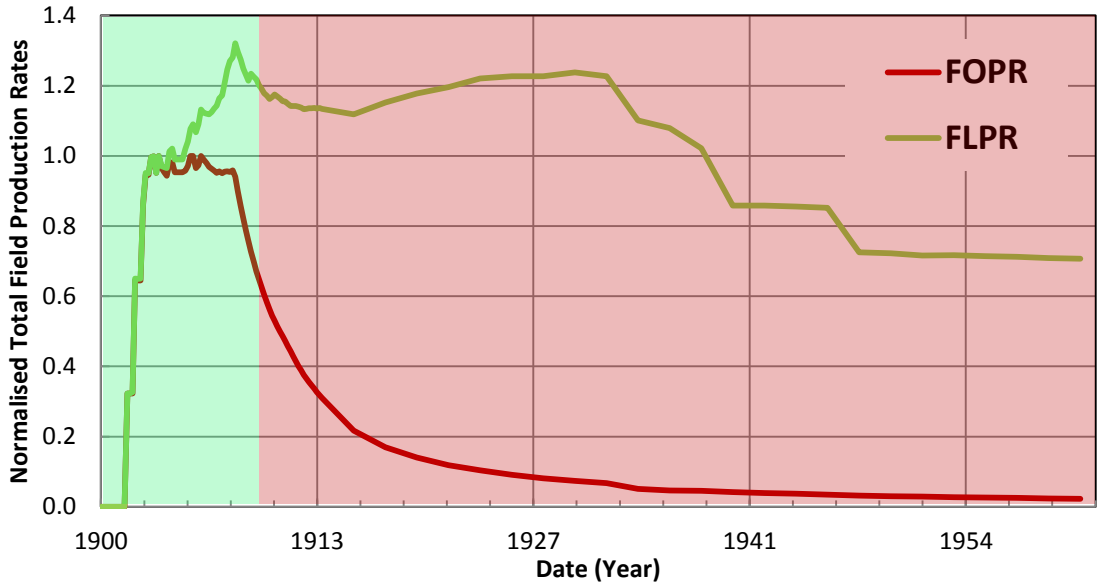

Figure 7-4: N-field Field Oil Production Rate (FOPR) and Field Liquid Production Rate (FLPR) normalised to the plateau oil rate. Proactive control strategy applied (green) followed by reactive control strategy (red).

7.3.1 Multi-level optimisation during plateau period

Proactive optimisation of production in fields developed with intelligent and conventional producers equipped with gas-lift results in large number of control variables. Optimising all the control variables simultaneously using a mathematical optimisation algorithm would be the ideal approach, but results in a very complex optimisation problem which is computationally demanding. The alternative approach is to reduce the number of control variables by breaking the optimisation problem into simpler sub-problems. Each problem may then be addressed separately, potentially by using different optimisation approaches. A sub-optimal solution is expected by solving this simplified problem however, the developed workflow ensures that maximum added-value is obtained in a reasonable time by using limited computational resources for this large field case study. This study used two optimisation loops:

1- Outer loop: Zonal production control using ICVs.
2- Inner loop: Allocating production among all producers to respect the defined oil rate constraint, allocating total available gas to gas lifted wells that can make the best use of it.

Outer loop optimisation was performed iteratively using the developed robust optimisation framework and discussed in Section 7.6. The objective function, NPV, was calculated using Equation 4-1 with the economic data employed previously (Table 4-1).

The inner loop is performed using Eclipse's built-in optimisation algorithms consecutively in one month frequency to ensure an optimal performance while outer loop control variables are set. The production allocation among all producers is explained in Section 7.3.2. The gas lift optimisation facility in Eclipse allocates lift gas increments to the wells based on the current Gas-lift Utilisation Factor (GUF), taking into account of any limits on the group production rate and supply of lift gas.

7.3.2 Production allocation during the plateau period

Production allocation among all available producers is the optimisation to be performed when limiting the proactive optimisation of ICVs to the plateau period with oil rate constraint since by definition the field has the potential to produce more oil than the defined rate constraint (Figure 7-5). Different approaches to select which wells are to be produced are explained in Appendix A. The logic behind each approach and the test on PUNQ-S3 (Appendix A) indicated that optimisation provides the maximum improvement compared to alternatives. However, the optimisation approach is computationally demanding for this case and becomes prohibitively expensive when combined with proactive optimisation of ICVs when only limited computing resources (a single, high performance PC) are available. The optimisation approach was not employed for N-field. The objective is to choose the best alternative approach, with maximum added-value, in order to decrease the deviation from the optimal solution (the best approach deviates only 0.2% from the optimal solution in PUNQ-S3 as shown in Appendix A).

Four cases are considered using prioritisation and group rate control approaches, assuming a direct (higher priority to high oil potential wells) or an inverse (higher priority to low oil potential wells) ratio. These cases were compared with the base-case of assigning a higher priority to the off-centre wells with a fixed (lower) priority for the central wells. Figure 7-6 compares the field's 10 year cumulative production with fully open ICVs. The 10 year production period was chosen as fully capturing the added-

value from extending the plateau and any adverse effects during the subsequent decline period. A reactive control strategy, not considered here, would be implemented during the subsequent field life.

Prioritising production from wells with a lower oil production potential (1/Qo) was found to increase the cumulative oil production. This was observed for both Prioritization (1/Qo) and Group Rate Control (1/Qo) (see Figure 7-6). The same trend has been previously observed in the PUNQ-S3 reservoir (Appendix A). Initiating the production from low oil rate potential wells rearranges the reservoir's flow behaviour due to increased production from reservoir areas with a lower sweep potential. Moreover, from production point of view, this provides a longer time for low oil potential wells to recover their potential reserves.

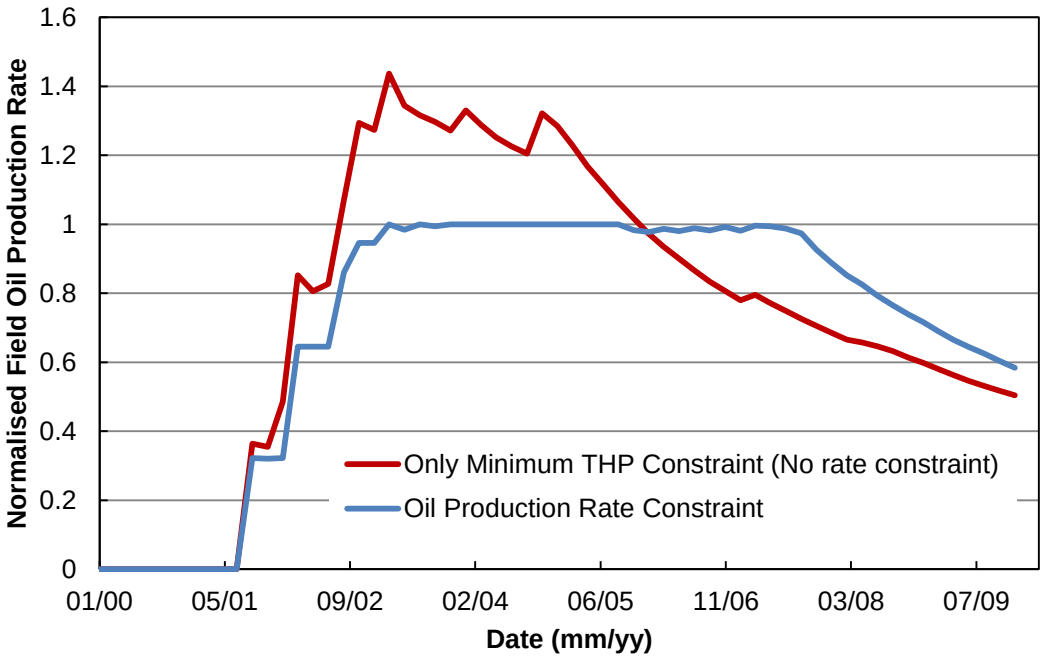

Figure 7-5: Normalised N-field oil production rate (normalised to the plateau oil rate) during the plateau and early decline period with (blue) and without (red) the constraint on oil production

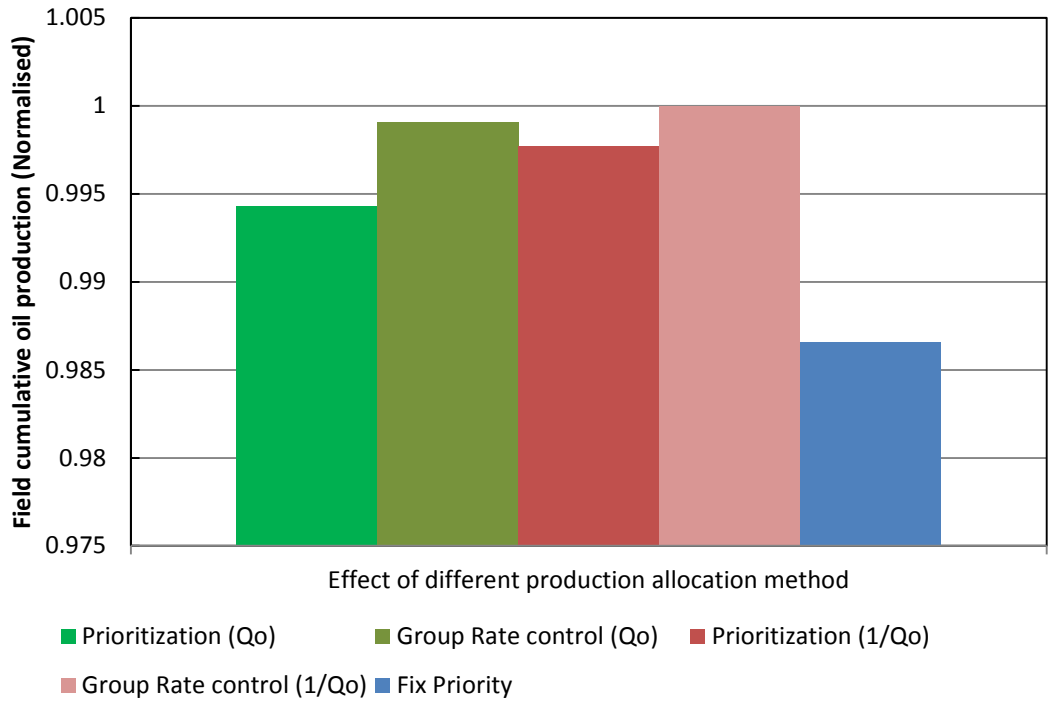

Figure 7-6: Normalised field cumulative oil production during plateau and early decline period utilising different well production allocation strategies

ON/OFF or continuous nature of the production control is another important decision. It is observed that a continuous control delivered by Group Rate Control provides a higher cumulative oil production in both cases (Qo and 1/Qo) (Figure 7-6). This is due to the fact that greater control flexibility is provided by a continuous control as compared to the ON/OFF control at the same control frequency. Greater control flexibility is required to improve the performance in non-optimum cases. A greater difference is thus observed between Prioritization (Qo) and Group Rate Control (Qo) (i.e. non-optimum) compared to the difference between Prioritization (1/Qo) and Group Rate Control (1/Qo). Moreover, continuous control maybe preferred from an operational point of view since stopping and (re)starting wells may impair the well's performance.

For the rest of this chapter Group Rate Control (1/Qo) is selected to allocate the production among all producers while proactive optimisation of ICVs is performed. An even higher added-value and more stable production are obtained using this approach.

7.4. Defining optimum control frequency of ICVs

Section 3.3 concluded that controlling ICVs at an optimum frequency

- Provides a good level of added-value
- Prevents a substantial increase in the number of control variables and the computational time
- Ensures the valves remain operable by operating them at a minimum required frequency defined by the producer and operator
- May reduce the risk of valve failure associated with the frequency of operation

Proactive optimisation of the N-field ICVs was performed at frequencies of 48, 24, 12, 6 and 3 months using NPV (Equation 4-1) as the objective function with Table 4-1 economic data. We observed that reducing the length of control steps increases the added-value by providing more flexible control (Figure 7-7). Note that the GA in MEPO (SPTGroup, 2012), a commercially available optimiser, failed to find the optimum solution for the 6 and 3 months control steps with more than 100 control variables. A control frequency of 48 months represent the case when the I-wells have been equipped with ICDs to give a constant flow area during the whole period.

A control step of 6 months will be used for the remainder of this chapter.

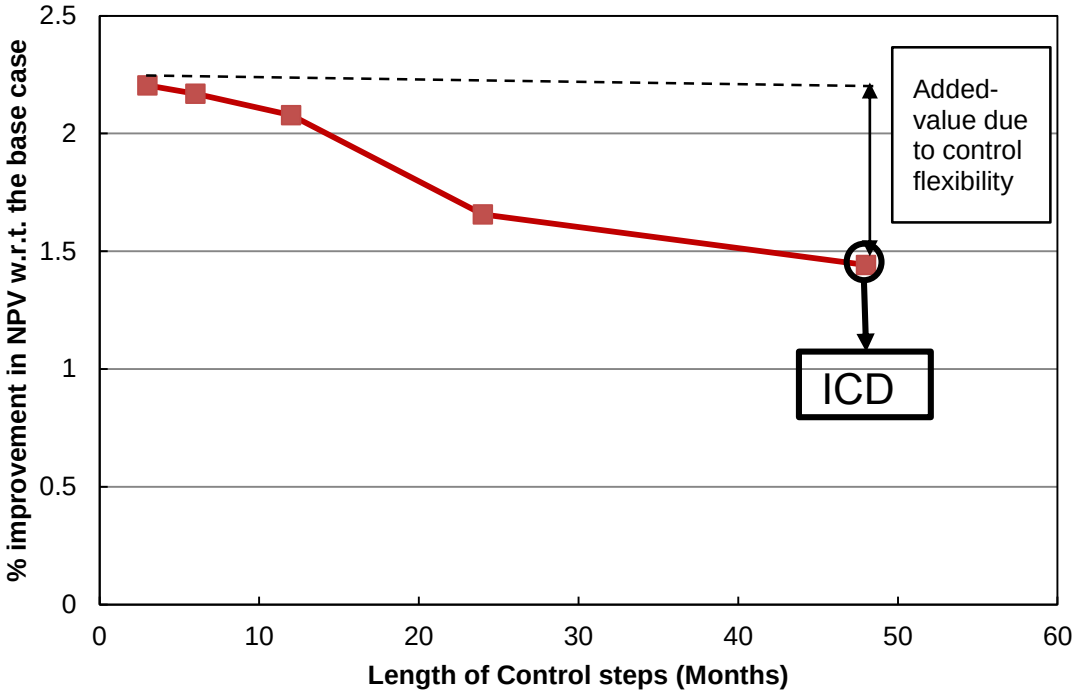

Figure 7-7: Percent improvement in NPV w.r.t. the base case (fully-open ICVs during whole production period) for the N-field ICVs controlled at different frequencies

7.5. Impact of water injection scheme on added-value from proactive optimisation of ICVs

N-field water injection is constrained by the total rate of available water for injection from two sources: (1) external source (e.g. sea water) with limited processing capacity and (2) produced water. As a result, more water is available for injection when water-cut increases during the later production stages. Five different injection regions have been previously defined (Figure 7-8). Two different water injection allocation schemes between these 5 reservoir regions will now be compared in order to allocate the total available water.

- Voidage replacement: this scheme tries to inject water in the group of injectors in each region equivalent to a fraction of the total production from the group of producers in the same region. The fraction is known as voidage replacement fraction which can be greater or smaller than 1. Optimal application of this

scheme requires identifying appropriate regions (assuming no hydraulic connections) and the corresponding production and injection well group. There is often hydraulic connectivity between the defined regions; hence the calculated production (or injection) from a particular region does not necessarily represents the fluid produced (or injected) in that region. The voidage replacement fraction for each region is usually tuned at several points during the production period to alleviate this problem. The main advantage of this scheme is that it results in reasonably stable water injection rates.

- Pressure maintenance: A target pressure (often equal to the initial reservoir pressure) is defined for each region. The algorithm tries to find the appropriate rate for the region's injection wells that meets this target pressure (ECLIPSE, 2012). A more stable and uniform regional pressure normally results from this approach and therefore provides a more robust control of injection while maintaining the initial reservoir pressure. However, there can be abrupt variations in the individual well injection rates.

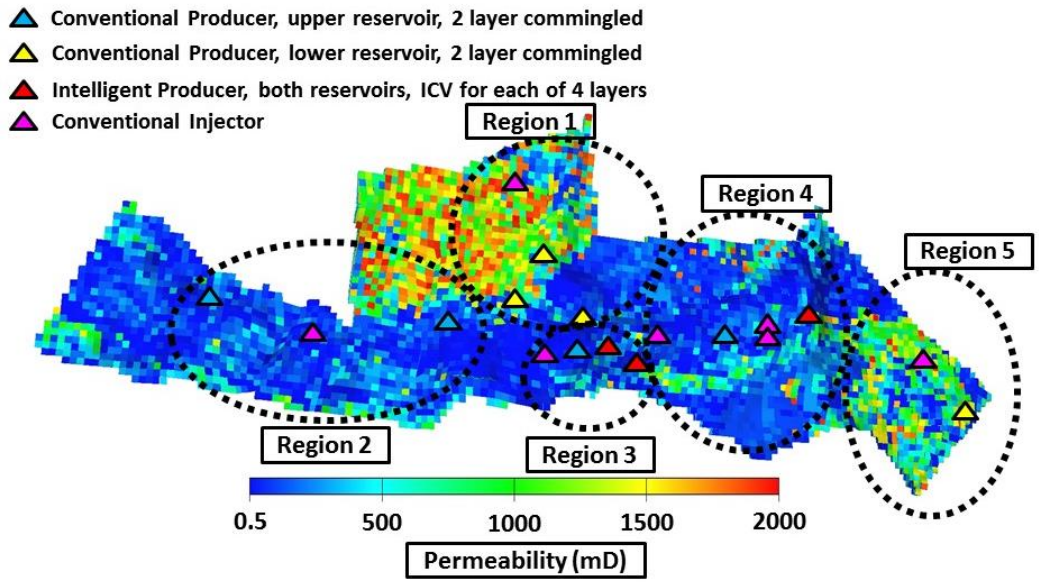

Figure 7-8: Defined regions with corresponding producers and injectors

Initially all ICVs are considered as fully open during the whole production period. Figure 7-9 (a-e) shows the average pressure in the 5 defined regions while Figure 7-10 shows the average reservoir pressure when N-field water injection is controlled using voidage replacement or pressure maintenance scheme. Bubblepoint pressure is around

1300 psi for all regions. Both water injection schemes are able to keep the regions and reservoir pressure above the Bubblepoint pressure. However, pressure maintenance provides improved control with the region pressures being maintained at values close to the initial reservoir pressure (Figure 7-10). Voidage replacement leads to significantly lower pressures in regions 1 and 5 (Figure 7-9 a, e) and over injection in regions 2 and 3 (Figure 7-9 b, c). An extended plateau is achieved by the pressure maintenance scheme (Figure 7-11). Figure 7-12 compares the difference in region cumulative oil and water production after the plateau (year 1911) in the pressure maintenance case w.r.t. voidage replacement. Lower cumulative oil and water production in region 2 is due to reduced injection in that Region in the pressure maintenance scheme. Reduced injection in region 3 results in lower water production in that region. However, the hydraulic connectivity between the regions results in increased oil production being observed. Increased injection in region 1 and 5 results in higher production in the neighbouring regions (3 and 4). Note that any extra water produced by the N-field will be re-injected into the reservoir which consequently keeps the reservoir pressure. Higher cumulative oil production is achieved by extending the plateau in the pressure maintenance scheme (Figure 7-13). No major difference in the oil production is observed after the plateau (Figure 7-13b) however higher water production in the pressure maintenance scheme results in a decrease in NPV as compared to the voidage replacement scheme (Figure 7-14). This can be alleviated by performing production optimisation.

The oscillation that sometime is observed in the pressure maintenance water injection scheme (e.g. Figure 7-9 b, c) is due to its use of proportional control. Therefore, the change in the volume of injected water to each region at the next time step is determined by the difference between the region pressure and the defined target pressure at the current time step. This can result in oscillations when the dynamics of the system is very fast (e.g. region pressure increases significantly by extra injection).

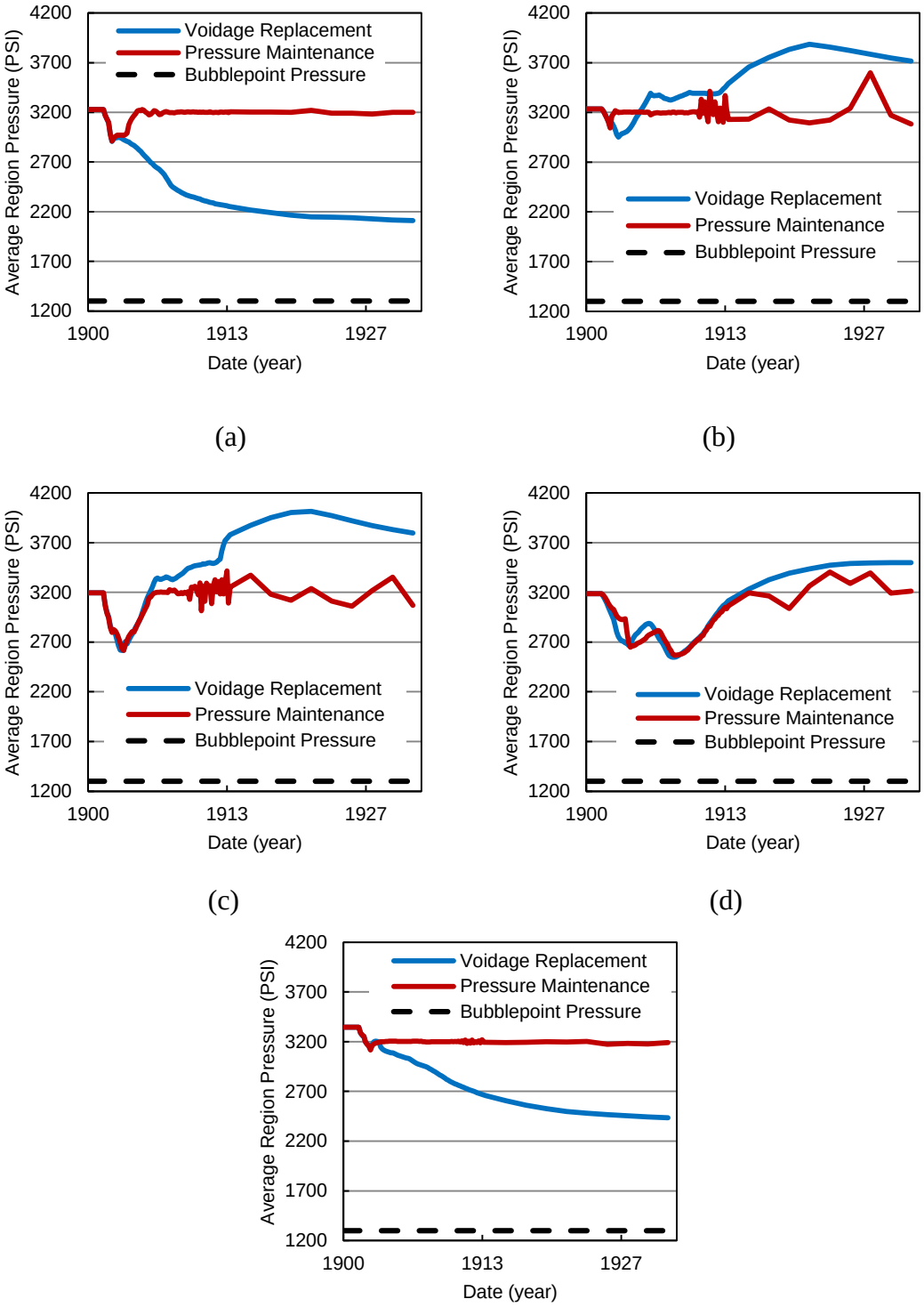

Figure 7-9: Bubblepoint pressure and average pressure of different injection regions (a) Region 1 (b) Region 2 (c) Region 3 (d) Region 4 (e) Region 5 when water injection is controlled using Voidage replacement or pressure maintenance scheme

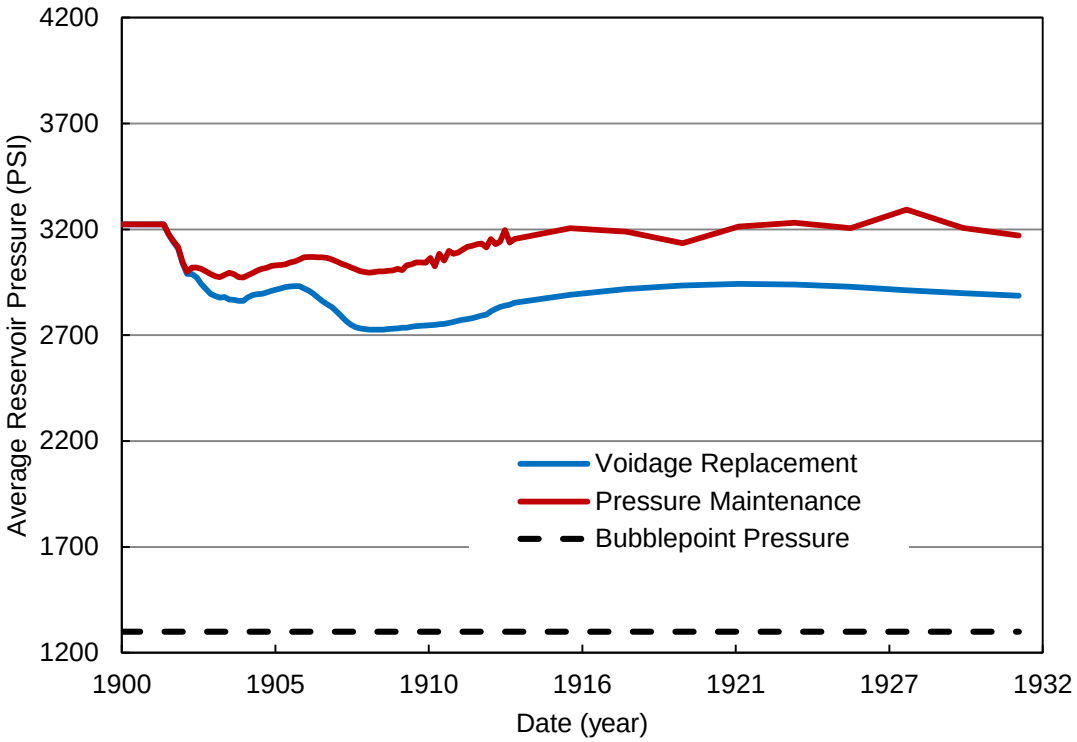

Figure 7-10: Average reservoir pressure when water injection is controlled using Voidage replacement or pressure maintenance scheme

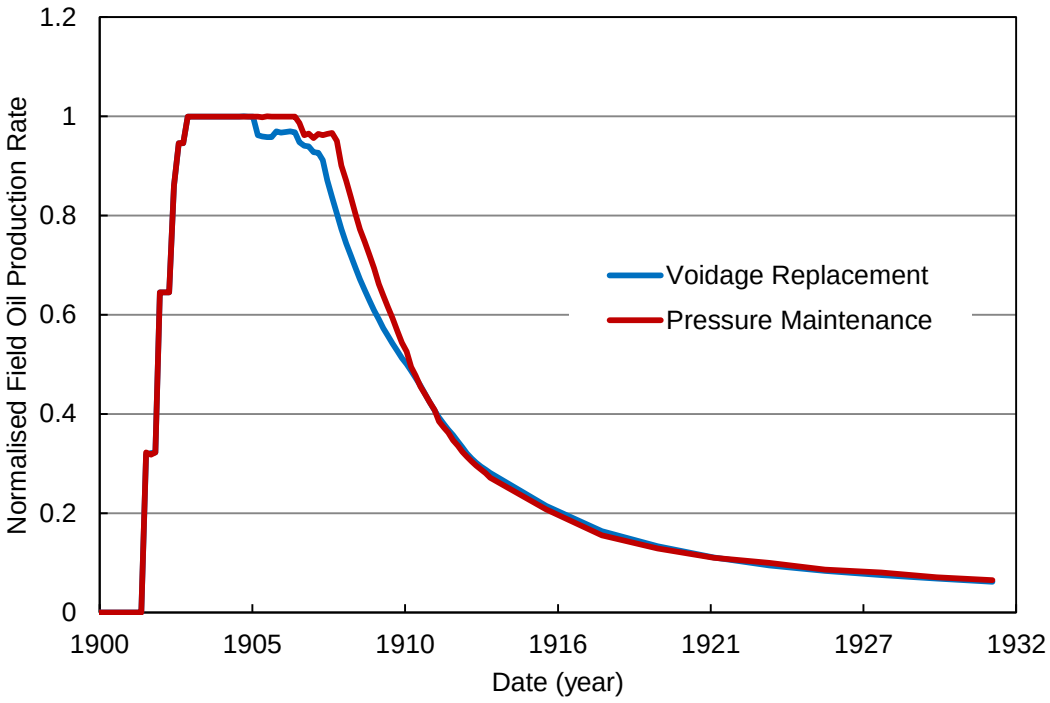

Figure 7-11: Normalised (to the plateau oil rate) field oil production rate when water injection is controlled using Voidage replacement or pressure maintenance scheme

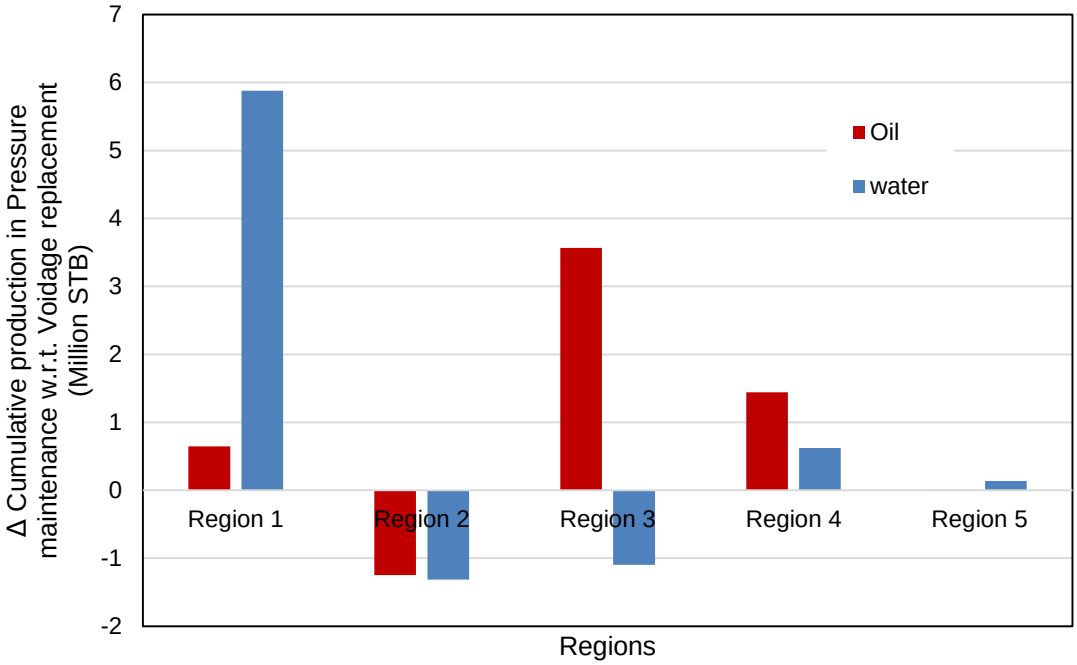

Figure 7-12: Change in cumulative oil and water production of the defined regions in the pressure maintenance w.r.t. Voidage replacement

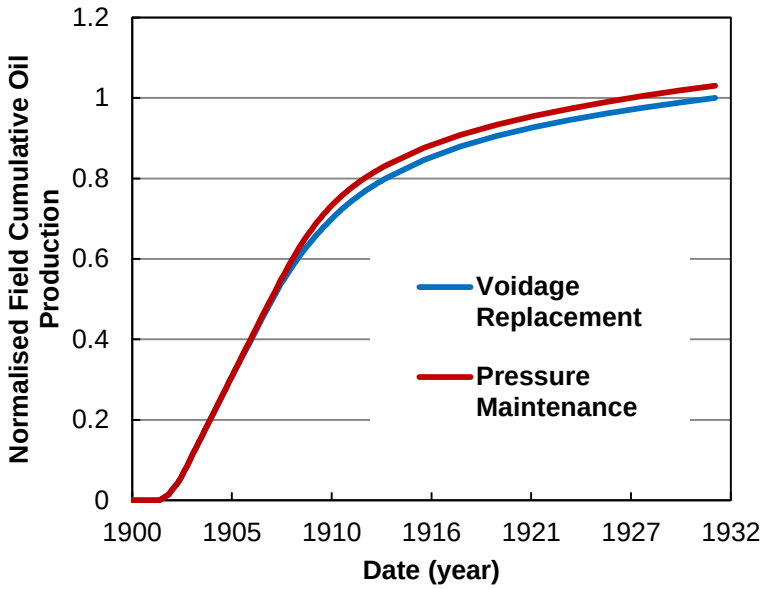

(a)

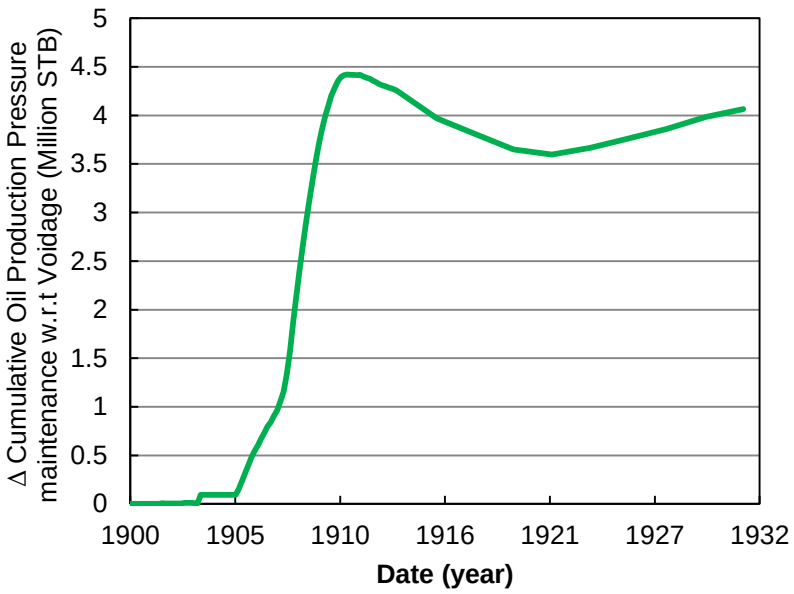

(b)

Figure 7-13: (a) Normalised Field cumulative oil production using Voidage replacement or pressure maintenance scheme (b) difference in Field cumulative oil production ($Q_{\text{pressure maintenance}} - Q_{\text{Voidage replacement}}$)

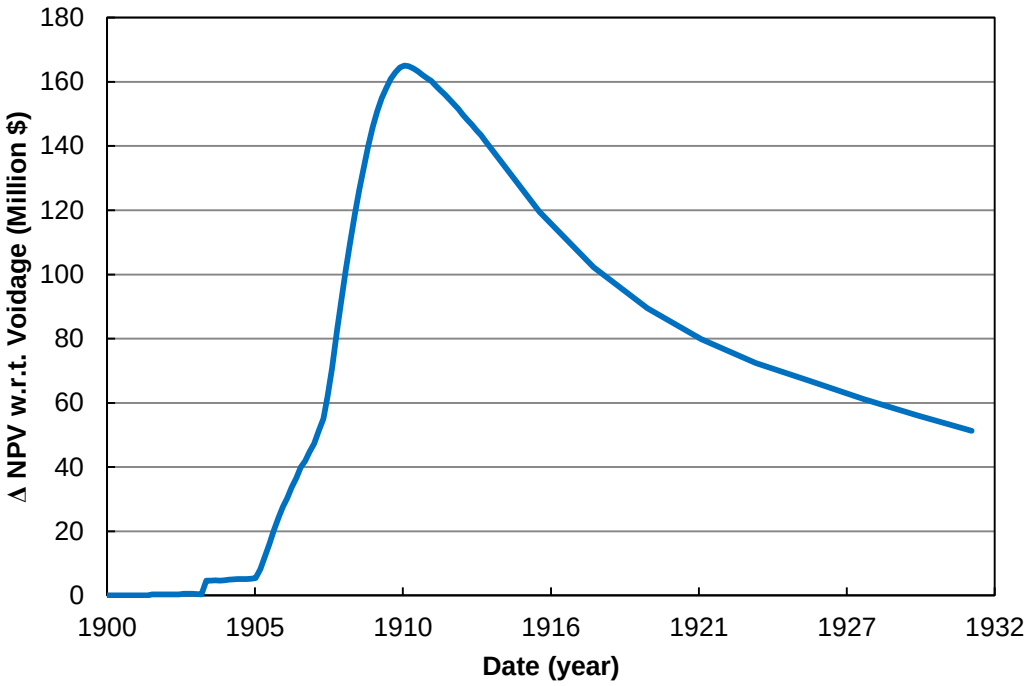

Figure 7-14: Difference in NPV ($NPV_{\text{pressure maintenance}} - NPV_{\text{Voidage replacement}}$)

7.5.1 Water injection schemes and proactive optimisation

Two cases are considered. In each case the proactive optimisation of ICVs is performed at 6 months control frequency while voidage replacement or pressure maintenance scheme is employed to control the water injection. Figure 7-15 compares the relative NPV of the optimised case w.r.t. the base-case with fully open ICVs. Proactive optimisation of ICVs provides a small improvement with a close to optimum injection scenario. However the importance of proactive optimisation increases when the water injection scheme deteriorates (which frequently occurs in practice). It should be noted that the pressure maintenance scheme for the N-field provided a better performance by keeping all region pressures close to the initial reservoir pressure and therefore can be considered as closer to the optimum injection scenario as compared to the employed voidage replacement scheme. The ultimate added-value is only achieved by a combined optimisation of production and injection (Figure 7-15) despite production well optimisation being able to alleviate the negative impacts of a non-optimum injection scenario.

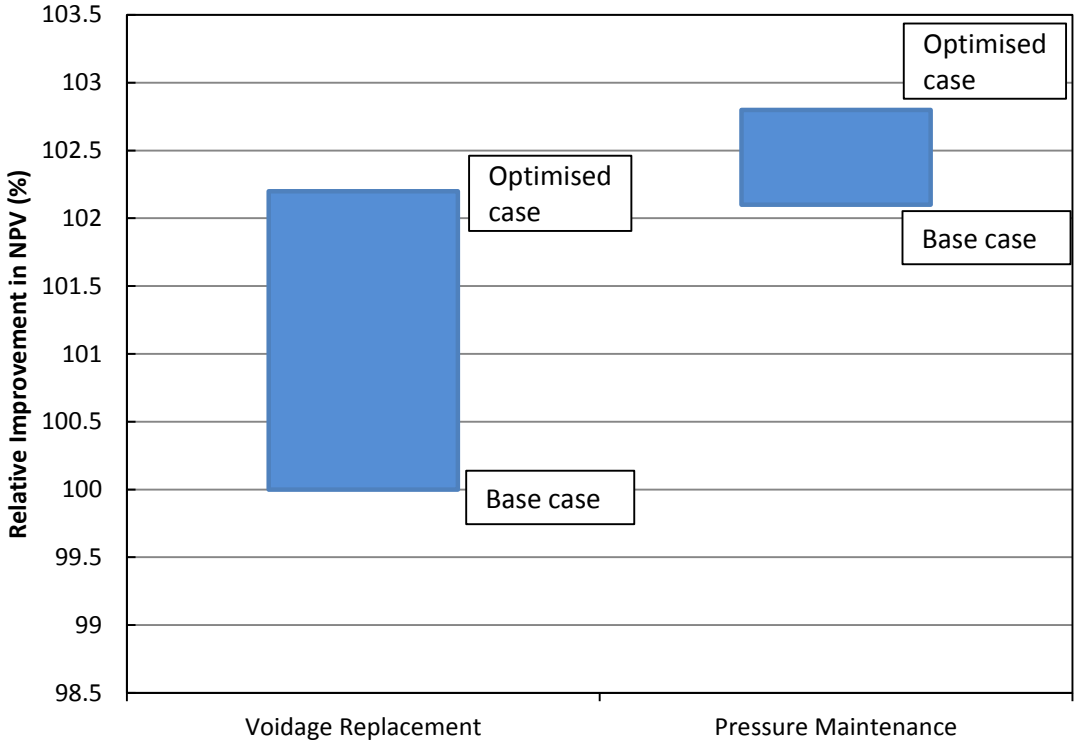

Figure 7-15: Comparison of the added-value of proactive optimisation of ICVs while water injection is controlled using voidage replacement or pressure maintenance

7.6. Robust proactive optimisation of ICVs under uncertainty

This section reports the results of robust proactive optimisation of ICV operation during the plateau and early decline periods using the workflow developed earlier with SPSA as the optimisation algorithm. ICVs are controlled once every 6 months. At the second level:

- The production optimisation allocates as much as possible the constrained total oil production rate to low potential wells using Group Rate Control (1/Qo).
- Gas lift operation is optimised using the gas lift optimisation facility in Eclipse.
- The water injection is controlled using voidage replacement.

7.6.1 Uncertainty in N-field

The reservoir uncertainty for the N-field was presented in the form of 3 model realizations. These had been provided by the operating company assuming that formation porosity and permeability, faults (locations and transmissibility), initial water saturation and reservoir net-to-gross were the major uncertainties. 3 different levels (minimum, most likely and maximum) are considered for all uncertain parameters to generate 3 realizations with pessimistic, most likely and optimistic performance. For the rest of this study these realizations are known as P10 (optimistic), P50 (base or most likely) and P90 (pessimistic). This should not be confused with the P10, P50 and P90 predictions of a probabilistic distribution. Figure 7-16 and Figure 7-17, the field oil production rate and NPV for these 3 model realizations produced with fully-open ICVs, record the impact of expected level of uncertainty in the response space. All 3 N-field realizations will be used for robust optimisation since the Chapter 6 realization selection stage is not required with the limited number of models available.

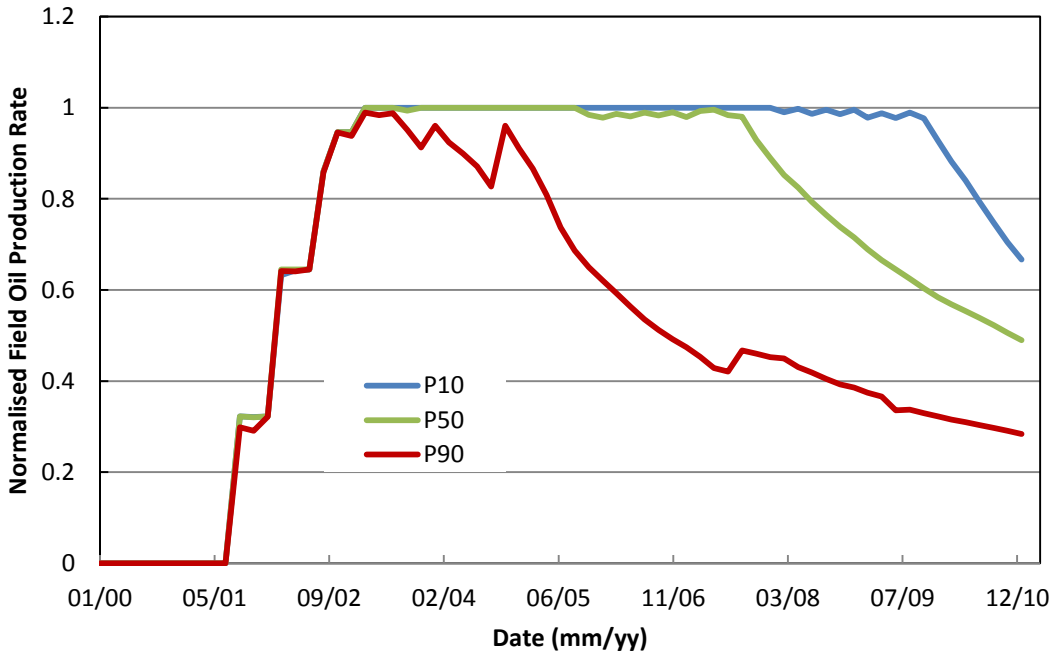

Figure 7-16: Normalised to the plateau rate early-time Field oil production rate for 3 N-field model realizations representative of the expected level of uncertainty

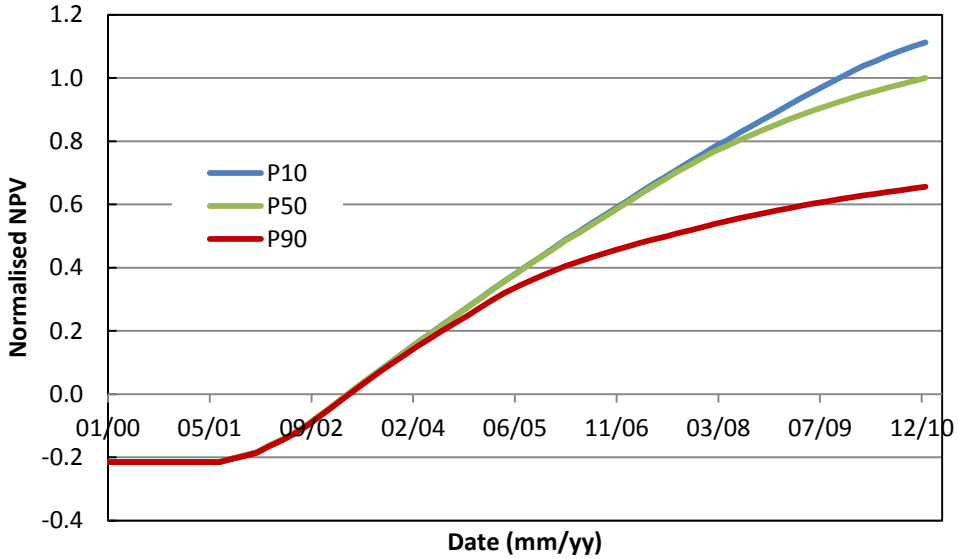

Figure 7-17: Relative NPV of early-time Field oil production for the N-field model realizations

7.6.2 Robust optimisation

Robust optimisation of N-field employed the "mean" approach (Equation 5-4, with *A=0*) using the 3 reservoir model realizations. SPSA is employed as the optimization algorithm with an ensemble size of 6 ($n_e = 6$), $\alpha_0 = 0.12$ and $c_{min} = 0.05$. Figure 7-18 shows the improvement w.r.t. the base-case versus iteration number for all realisations and for the objective function (i.e. the mean). The optimization algorithm increases the mean of the objective value of the 3 realizations (increasing trend of mean in Figure 7-18). The fluctuations in the mean value is due to the stochastic nature of the SPSA algorithm which might move in non-optimum direction during some iterations. Extra fluctuations in the objective value of individual realisations might also be observed due to a control scenario reducing one realization while providing greater increase in the other realizations and therefore improves the mean.

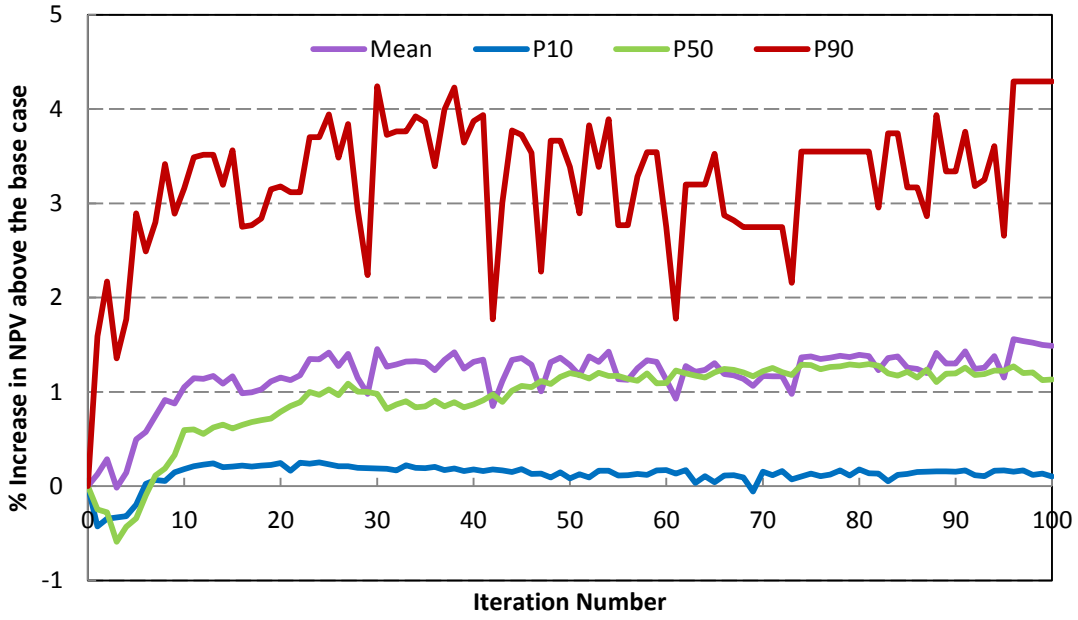

Figure 7-18: (%) NPV increase w.r.t. the base-case for all 3 N-field models employing the "mean" objective function

The optimisation was performed for 100 iterations at a computational cost of ~20 min/iteration using 21 CPUs of 3.2 GHz frequency of a HP-800 workstation (total run-time = 100×20 min ≈ 33 hr). Figure 7-18 indicates that 85% of the improvement was obtained after 10 iterations requiring only ~3.5 hours computation time.

Figure 7-19-b shows an improved mean implies a higher expected added-value while the reduced variance implies a higher reliability (lower risk) by applying the best ICV control scenario identified by robust proactive optimisation. The maximum improvement (~4%) is obtained for the pessimistic scenario (P90); with smaller improvements (~1.3 % and ~0.2 %) for the P50 and P10 realisations, respectively (Figure 7-19-a). As discussed in Section 6.7, the flexible zonal-flow control provided by I-well's ICVs improves the production performance compared to the equivalent base-case of fully open ICVs with no control. Experience shows that the optimisation generally delivers a greater improvement for the less favourable realisations. This effect inherently reduces the variance in the robust optimisation.

Figure 7-20 shows field oil production rates for the base control case with fully-open ICVs and the optimised-case for all 3 realisations. An extended oil plateau was observed for all realisations.

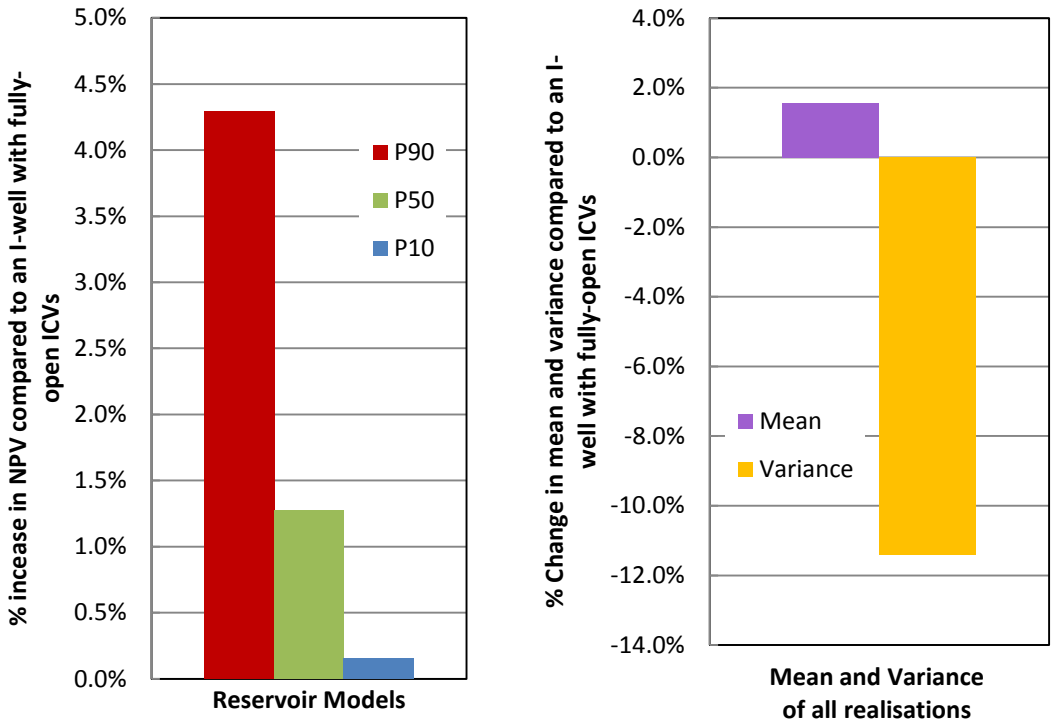

(a) (b)

Figure 7-19: (a) % Increase in NPV and (b) % change in the mean and variance for the best control scenario for all 3 N-field models

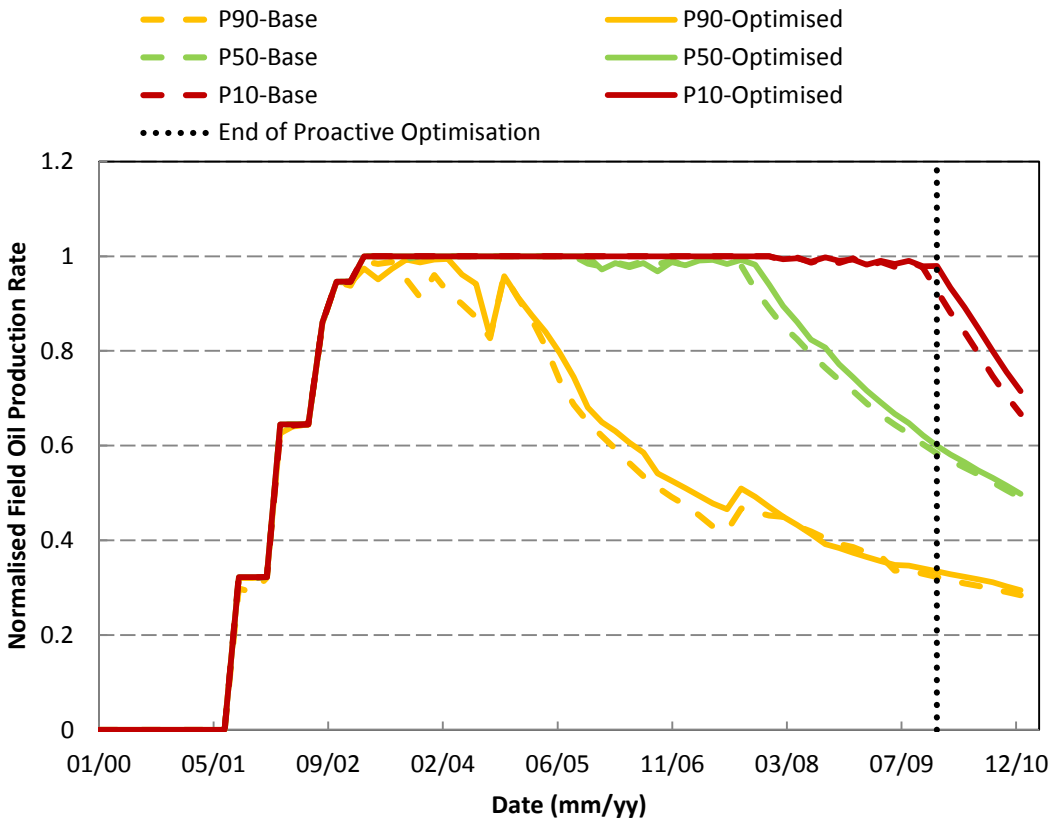

Figure 7-20: Normalised to the plateau rate Field oil production rate for base-case (fully-open ICVs) and optimised-case of different realisations

Figure 7-21, Figure 7-22 and Figure 7-23 compare the NPV for the conventional development plan (i.e. 14 conventional producers) versus the I-well version with a lower number of wells (i.e. 8 conventional and three 4-zone I-producers) with and without optimisation of ICV control in the P90, P50 and P10 realisations during the proactive optimisation period. It is assumed that the total drilling cost is invested at the beginning of the drilling campaign, hence the intelligent well case shows an initial improvement in NPV due to reducing the number of drilled wells. The drilling campaign continues after the start of production and ends on 07/05 (Figure 7-21b).

The I-well case with fully open ICVs and no optimisation showed improved production compared with the conventional well case for the P90 model (Figure 7-21b green line). This improvement is mainly due to accelerating the field's development by advancing the drilling schedule and not due to proactive optimisation of ICVs, the subject of this thesis. This drilling acceleration effect is not significant for the P50 and P10 realisations because all the drillings are completed during the plateau period; hence advancing the

drilling schedule cannot increase the current production due to the oil production rate constraint. Moreover, additional favourable effects were observed in the previous case studies when comingled production of zones without control was improving the production performance. This is achieved by allowing the stronger zone to keep the weaker zone flowing longer and/or changes in the downhole pressure profile which positively influence the recovery.

Robust proactive optimisation improves the production in the I-well controlled case in all realisations (section b of the figures show the difference in the NPVs). Proactive ICV optimisation was able to maintain the initial NPV gain by extending the oil production plateau while uncontrolled production via fully-open ICVs loses this advantage faster. It should be noted that, after this period the reactive control should be performed to improve the production by reducing the water production.

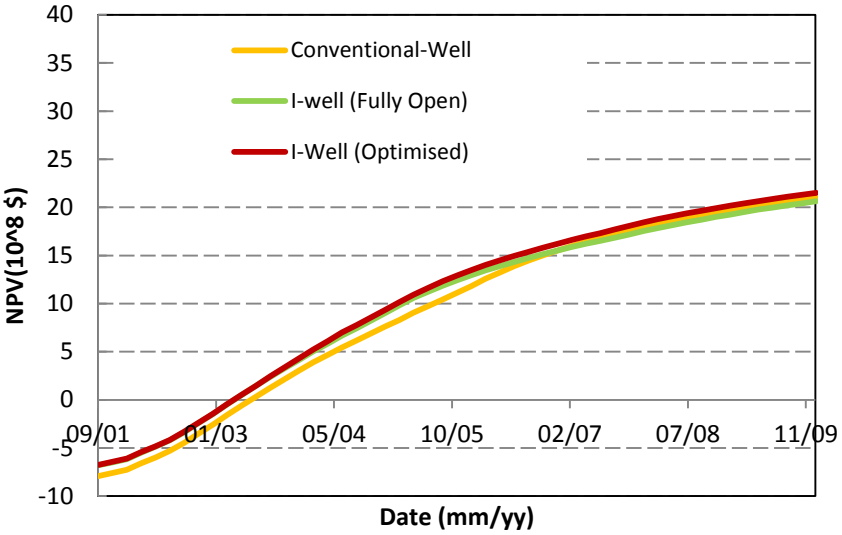

(a)

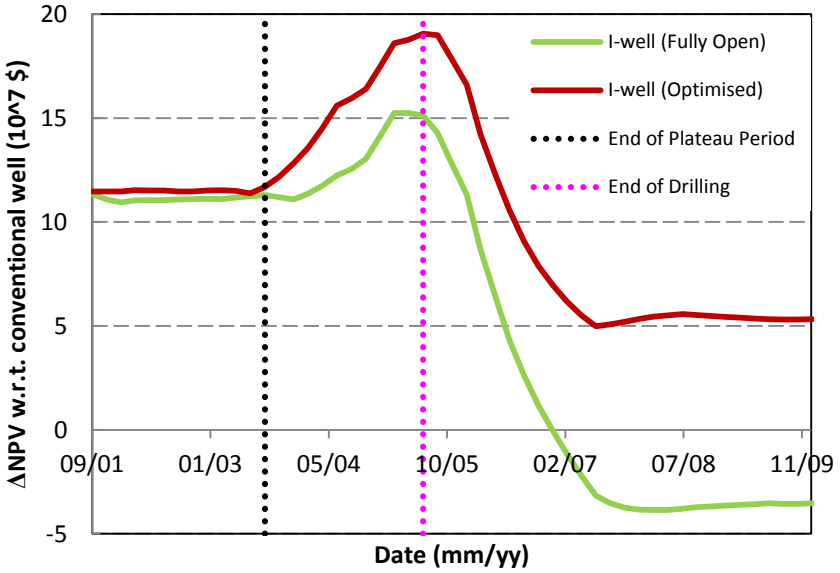

(b)

Figure 7-21: (a) NPV (b) ΔNPV for I-wells without optimisation and optimised I-wells w.r.t. conventional wells for the P90 reservoir model

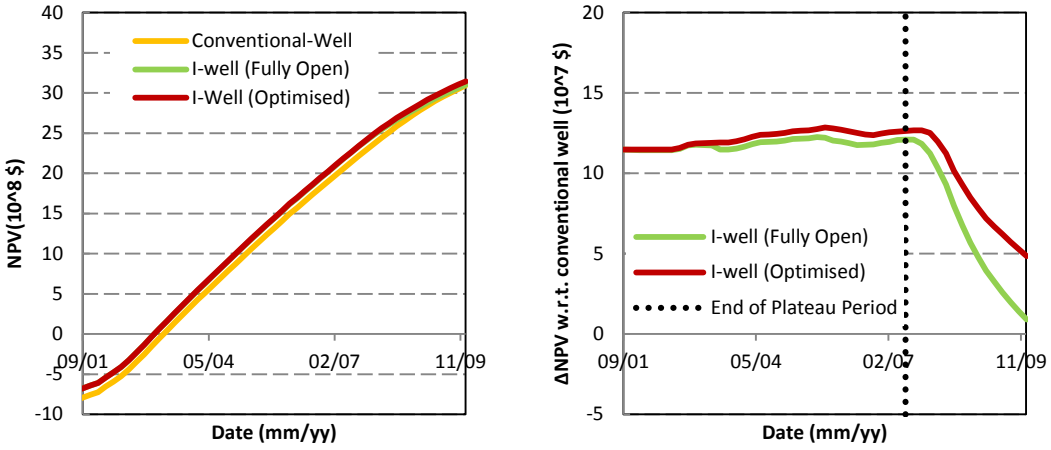

(a) (b)

Figure 7-22: (a) NPV (b) ΔNPV for I-wells without optimisation and optimised I-wells w.r.t. conventional wells for the P50 reservoir model

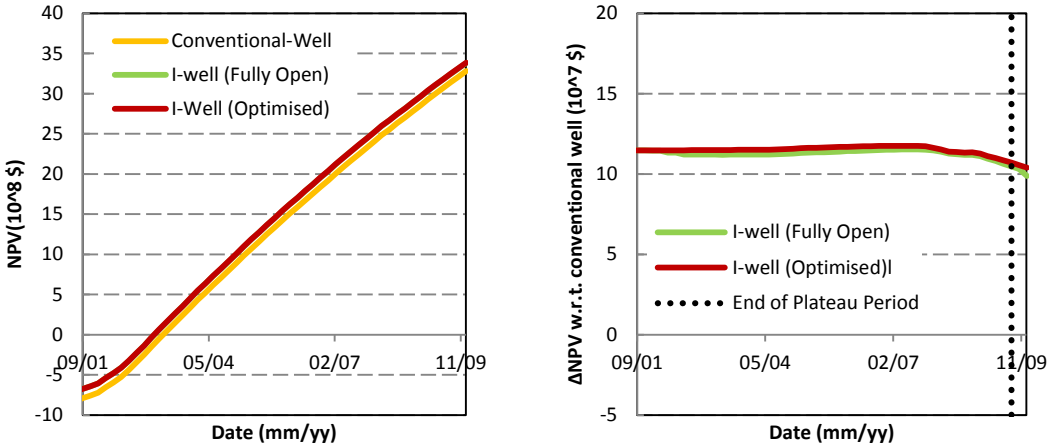

(a) (b)

Figure 7-23: (a) NPV (b) ΔNPV for I-wells without optimisation and optimised I-wells w.r.t. the conventional wells for the P10 reservoir model

7.6.3 Single-realisation optimisation (P50)

The advantage of robust optimisation can be shown by considering a non-robust optimisation performed using a single realisation (here P50). SPSA is employed with the ensemble size of 6 ($n_e = 6$), $\alpha_0 = 0.12$ and $c_{min} = 0.05$. The optimisation is performed for 100 iterations. Similar to the robust optimisation, the time taken is approximately 100xsingle_run, assuming parallel processing is available. Figure 7-24

shows the improvement in NPV w.r.t. the base-case (i.e. I-well with fully-open ICVs during the whole production period) versus iteration number.

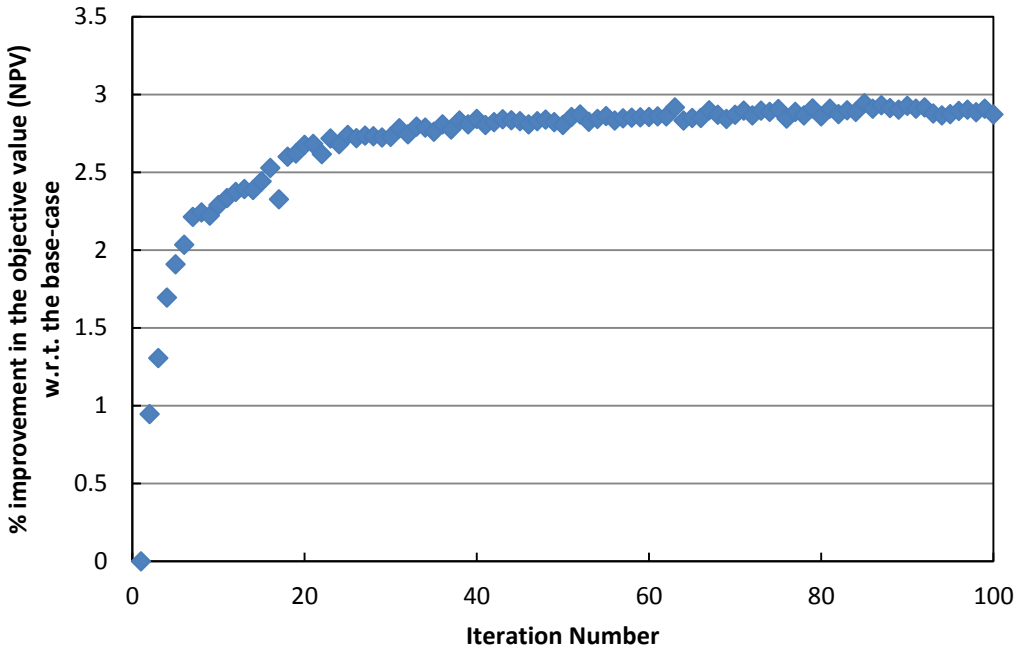

Figure 7-24: Improvement in NPV w.r.t. the base-case (i.e. I-well with fully-open ICVs) for realisation P50 versus iteration number

The best control scenario, which produced the maximum NPV, is applied to all realisations. Table 7-1 shows the percent improvement in NPV of each realisation and the percent change in the mean and variance of NPV, all calculated w.r.t. the base case. It is observed that single realisation optimisation, while providing the maximum improvement for that particular realisation, fails to provide optimal performance for other realisations. This behaviour results in a lower mean. Moreover, single realisation optimisation is unable to reduce the variance by ignoring the underlying uncertainty. For example, in this case an increase in variance is observed by single realisation optimization which means higher uncertainty compared to the base-case (Table 7-1). Robust optimization provides the control strategy of ICVs with the maximum expected added-value (i.e. increasing mean) while reducing the uncertainty in the operation (i.e. reducing the variance) in this full-field case study (Table 7-1).

Table 7-1: Changes in the NPV of each realisation, mean and variance w.r.t. the base-case when the control scenario is obtained using single-realisation optimisation or robust optimisation

% Change	NPV (P10)	NPV (P50)	NPV (P90)	Mean	Variance
Robust optimisation	+0.2	+1.3	+4.3	+1.6	-12
Single-realisation (P50)	+0.05	+2	+0.3	+0.8	+2.8

7.7. Conclusions

- Production allocation needs to be performed among all producers to respect the defined rate constraint when limiting the proactive optimisation of ICVs to the plateau period. The two-level approach, proposed in this study, enhances the robust proactive optimisation process of large real-field models by reducing the number of control variables associated with each stage.
- The ultimate improvement is only obtained by optimizing both production and injection.
- The developed framework can efficiently handle a large number of control variables, the high computation time and the instabilities due to several simultaneous optimizations, frequently experienced in proactive optimisation of large real-field models.
- The proposed robust proactive optimisation approach provides the control strategy of ICVs with the maximum expected added-value (i.e. increasing mean) while reducing the uncertainty in the operation (i.e. reducing the variance) in this full-field case study.
- The flexible and optimal control provided by ICVs inherently reduces the variance during the mean optimisation approach which provides a relatively fast process (mean is a relatively smooth function). The developed mean-variance (utility function) approach can be applied to achieve a larger reduction in the variance (i.e. low-risk control scenario). The mean-variance approach would result in a more complicated search space which theoretically would increase the computation time (Section 6.7).

Chapter 8 – Conclusions and recommendations for future study

8.1. Conclusions

Proactive optimisation of ICVs under reservoir uncertainty is investigated in this thesis and a novel, fast, efficient and robust framework is developed. The main results of this thesis can be grouped into following areas.

8.1.1 Impact of I-well modelling on proactive optimisation problem

Realistic modelling of advanced well completions is required to evaluate their performance and define an optimum well control strategy (Coats et al., 2004, Holmes, 2011). This can be achieved by detailed modelling of the outflow (wellbore model) coupled with the inflow (reservoir model). This approach is known as multi-segment well model (Holmes et al., 1998) and is available in several commercial reservoir simulators (e.g. Eclipse Reservoir Simulator (ECLIPSE, 2012)). The realistic interaction between the zonal productions (i.e. control variables) is captured by such detailed modelling which generally results in a more difficult optimisation problem compared to the case with independent zonal production especially using gradient-based optimisation algorithms.

8.1.2 Simplifying the proactive optimisation problem

Ideal proactive optimisation should be able to find the optimum control scenario prescribed for the whole production period to provide the maximum long-term objective value. However, the proactive optimisation problem often needs to be simplified in order to employ commercially available optimisation algorithms and/or reduce the computational cost. The following criteria are suggested for simplifying the proactive optimisation problem (i.e. without significant loss in the long-term objective value) by including engineering and mathematical understanding of the problem based on performed case studies.

a. Proactive optimisation is essential during early production period (defined by an oil production plateau) due to excess fluid inflow capacity and interaction between the control variables during this period. A simpler reactive control strategy is generally sufficient after the plateau period, satisfying short-term (production improvement) objectives. Reactive control is expected to provide a close to optimum long-term (NPV) objective during this stage while improving the objective function by reducing production of unfavourable phase(s) or improving tubing outflow performance.
b. Frequent control provides more flexible control of well production, potentially leading to an increase in the added-value. This is true up to a frequency. However after this point more frequent optimisation does not improve the results. This can be explained by the slow reservoir dynamics, mainly controlling the proactive optimization added-value, in contrast to the fast well dynamics which is generally the most important in the reactive optimization process. The control frequency should thus be carefully selected for a cost effective, reservoir management process with a reduced number of control variables.

8.1.3 Choosing an optimisation algorithm for proactive optimisation of ICVs

a. The search space in the proactive optimisation of ICVs is characterised by several local optima with objective values close to the global optimum. This was confirmed by (1) visualising the search space of a proactive optimisation problem and (2) identifying multiple control scenarios with the objective values close to each other using SPSA and EnOpt. Search space of similar topography was previously observed in a high-dimensional history matching study by (Oliver et al. (2008), Oliver and Chen (2011)) and in the production optimization of conventional wells by Fonseca et al. (2014). Jansen et al. (2009) and van Essen et al. (2011) observed similar behaviour during multi-objective short-term and long-term optimization, where Degree Of Freedom (DOF) exists to improve one objective without sacrificing the other.
b. Gradient-based algorithms are a suitable candidates for proactive optimisation of ICVs. Methods based on stochastic approximation of the gradient by simultaneous perturbation of all control variables provide a sufficiently accurate

estimate of the gradient. Furthermore, these methods are independent of the choice of the reservoir simulator.

c. SPSA and EnOpt, two popular stochastic gradient estimation algorithms, have shown good performance in proactive optimization case studies. Previously published tuning guidelines have been modified to make them more suited to proactive optimization of ICVs. Case studies demonstrated that, the two approaches not only gave differing levels of production improvement, but also the characteristics of the resulting optimal control strategies were different. SPSA tends to outperform EnOpt with a larger ensemble size and is recommended when greater parallel processing is available. No correlation in time is considered for the SPSA and EnOpt employed in this study and therefore fluctuations are observed in the optimum control of ICVs. A smoother control can be obtained by multiplying the gradient by a covariance matrix with a defined correlation length (e.g. (Do and Reynolds, 2013, Zhao et al., 2013)). EnOpt tends to be recommended in this condition.

8.1.4 Robust proactive optimisation of ICVs under reservoir description uncertainty

a. The control scenario obtained based on optimization of a single model realization provided the maximum improvement for that particular realization, but normally resulted in sub-optimal performance when applied to the full ensemble of possible realizations.

b. Robust optimized ICV controls are obtained by substituting the above objective function with an augmented function evaluated using an ensemble of realizations. It was confirmed that the control scenario obtained using robust mean-only optimization provided a greater expectation of the objective value as well as a lower variance compared to a single realization-based optimization (also reported by (van Essen et al., 2013)). Flexible, optimal control provided by ICVs generally provides a greater improvement of reservoir realizations with poorer base case performance and a smaller improvement of realizations with a good base case performance. This inherently reduces the variance to some extent; despite the variance term not playing a role in the objective function's definition (also reported by (van Essen et al., 2013)). Alternatively, the utility function, by considering both mean and variance of the ensemble of realizations

with adjustable weight, allows control of the manner in which the optimization provides robustness to the control scenario. The observed drawbacks of the mean-variance approach is the symmetric nature of the variance, therefore variance might be reduced by penalising the upper tail (good cases) instead of increasing the lower tail (bad cases) of the objective function distribution. The reduction in the mean value during the mean-variance optimization is also observed by Capolei et al. (2015). An asymmetric approach (Siraj et al., 2015) is expected to achieve better performance by providing higher improvement of the poor cases without reducing the improvement in the good cases.

c. Employing the full ensemble of model realizations for robust optimisation is the ideal approach that can be expected to provide the ultimate value, assuming the existing uncertainty is quantified by the full ensemble of model realizations. However, its use significantly increases the computational costs. A small ensemble of randomly selected realisations does not fully guarantee capturing the underlying model uncertainties. A systematic clustering of all the realisations followed by selection of representative realisation(s) from each cluster has been developed. Use of a connectivity distance measure defined in response space and tailored to the objective of the subsequent optimization is recommended as a measure of the similarity/dissimilarity of the different realizations prior to clustering. Moreover, the developed framework reduced the adverse effect of random realization selection which is theoretically preferred while independent runs are often computationally expensive.

8.1.5 Application to the full-field model

The developed concepts have been successfully employed to find the optimum I-well development scenario of a full-field model in a reasonable time using limited computational resources. The developed framework can efficiently handle a large number of control variables, high computation time and the instabilities due to several simultaneous optimizations, frequently experienced in proactive optimisation of large real-field models. The chosen simplified approach is expected to result in a sub-optimal solution however, the developed workflow ensures to achieve maximum added-value in a reasonable time with limited computational resources.

The proposed robust proactive optimisation approach provides the control strategy of ICVs with the maximum expected added-value while reducing the uncertainty in the operation. Reducing the number of wells to be drilled via a partial I-well development scenario resulted in an increased, early-time, NPV. Proactive optimisation of ICVs ensured that the early NPV gain was maintained by extending the oil production plateau.

8.2. Recommendations for future study

1- Apply the proposed proactive followed by reactive approach to a realistic full-field study and compare the computation time and added-value with proactive during whole production period.
2- Investigate the relation between optimum control frequency and reservoir dynamics (e.g. transient time obtained from well testing).
3- A numerical comparison of the prior realizations selection followed by robust optimisation (developed in this thesis) with the alternative approach of estimating the gradient using an ensemble of all realizations (Section 5.3.2) particularly the modified ensemble-based robust formulation proposed by Fonseca et al. (2015).
4- Propose surveillance techniques to validate and update (if necessary) the obtained proactive control decisions.
5- The developed framework can be extended to simultaneous injection and production or simultaneous advanced completion design and control optimisation.
6- Integration into a closed loop management workflow.
7- Investigate the impact of a different geology on the developed workflow and obtained conclusions.

Appendix A - Production Allocation

Various production rate limits can be imposed on a group of wells or the whole field when simulating the different stages of the field's production life. The limits can be total liquid production rate and/or production rate of one or more individual phases. The higher production rate potential of the system must now be reduced within the defined limit by a production cut-back from a single or multiple wells. This control, normally performed using the surface choke, provides the opportunity to add short and/or long-term value by optimal allocation of the production. The approaches available within the Eclipse (ECLIPSE, 2012) reservoir simulator are:

a. Optimisation

This approach follows the same logic as proactive optimisation of ICVs while the control variables are contribution to production from different wells. The maximum added-value is obtained in this approach if robust optimisation is performed using a suitable algorithm. However, similar to proactive optimisation, it is associated with a large scale optimisation with a computationally demanding and uncertain objective function. Optimising wells' production contribution has been studied previously (e.g. (Do and Reynolds, 2013)) and can be addressed using the developed optimisation framework in this thesis.

b. Prioritisation

Prioritisation uses a built-in feature in Eclipse (ECLIPSE, 2012) to reduce the computational time compared to the above "optimisation" approach. It speeds up the decision making process and/or invests computational resources to optimise other parts of the system (e.g. optimum downhole control of ICVs).

A priority coefficient (P) is defined for each well,

$$P = \frac{A + BQ_o + CQ_w + DQ_g}{E + FQ_o + GQ_w + HQ_g}, \qquad \text{A-1}$$

where Q_o, Q_w and Q_g are potential oil, water and gas production rate of the well which is the production rate that a well would achieve in the absence of any rate constraints at

the current grid block conditions. Coefficients (A-H) are user-defined quantities to prioritise wells' production based on the produced phases. Figure A1 shows the flow diagram of the algorithm. The majority of wells are either fully open or shut when production allocation is performed using prioritisation approach. This ON/OFF control is not preferred from an operational point of view due to the problems associated with well shut-in (well start-up, cross-flow during shut-in from surface, etc.). Calculation of the priority coefficient and subsequent allocation is repeated at a pre-defined frequency. The use of potential rate calculated using the near wellbore region eliminates the control oscillation problems and accounts for longer-term performance as compared to reactive control employing current production rates.

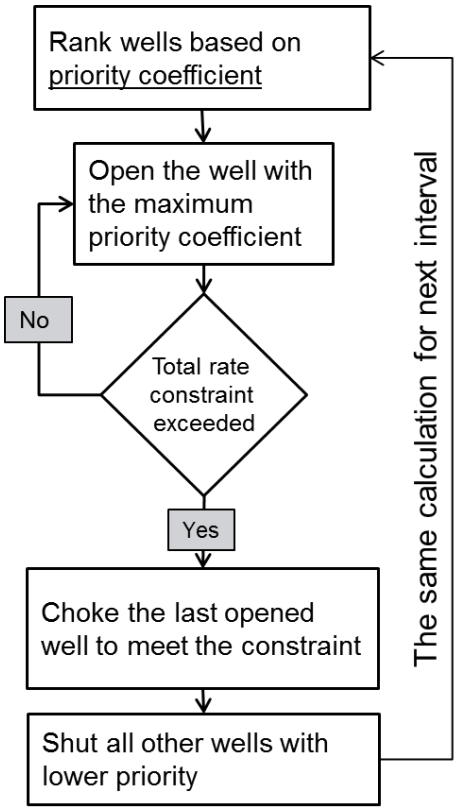

Figure A1: Flow diagram of the production allocation among several wells using the "Prioritisation" option in Eclipse

c. Guide-rate control

This approach, also a built-in feature in Eclipse (ECLIPSE, 2012), provides an alternative to prioritisation. The target rate is allocated to individual wells in proportion to each well's specified guide rate (GR):

$$GR = \frac{{Q_o}^A}{B + C(Q_w/Q_o)^D + E(Q_g/Q_o)^F}, \qquad \text{A-2}$$

where oil is considered as the favourable phase (for a general formula see (ECLIPSE, 2012)). Coefficients (A-F) are user-defined quantities.

d. Case-study (PUNQ-S3)

The above three approaches to production allocation were tested on PUNQ-S3 (Section 4.5.2) developed with 4 conventional producers (Figure A2). The field was constrained by total oil production rate of 1000 sm^3/day and a minimum BHP of 100 bar for production wells (Figure A3) during the 12 year production period. Figure A4 shows the individual cumulative oil and water production for all 4 wells producing at the minimum BHP and without limit on total filed oil production rate.

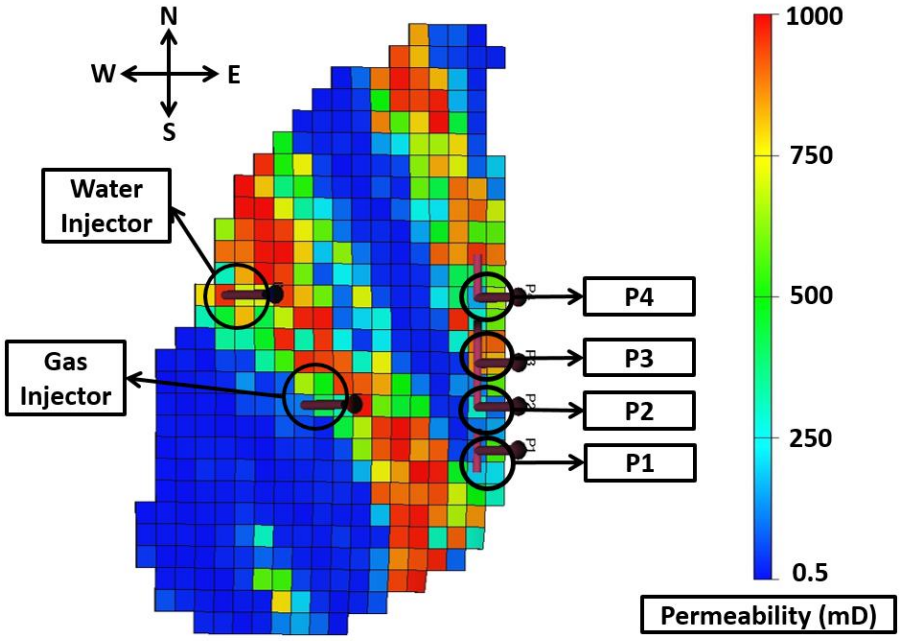

Figure A2: PUNQ-S3 developed with 4 conventional wells

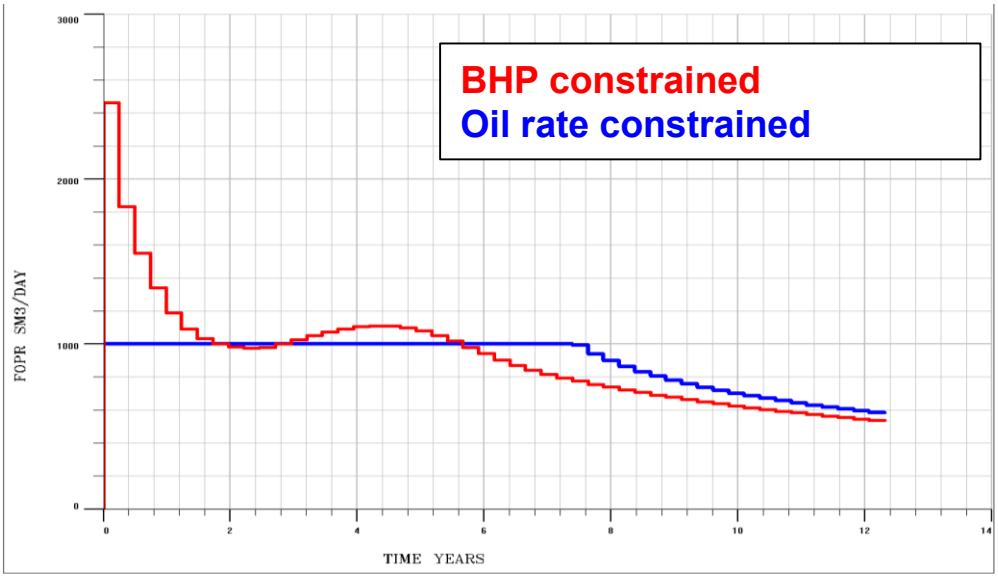

Figure A3: Field oil production rate (BHP and oil production rate constrained)

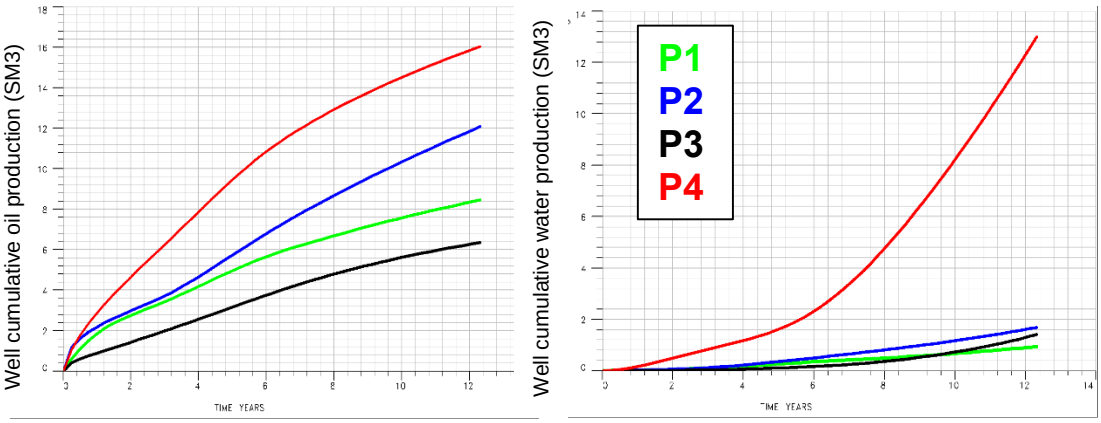

Figure A4: Individual well cumulative oil and water production in BHP constrained case from Figure A3

Table A1 describes five tests performed to allocate the defined total oil production rate among the 4 producers. A control frequency of 6 months in test-1 resulted in 96 control variables while "Prioritisation" and "guide-rate control" was performed at 1 month intervals. Figure A5 compares the field cumulative oil production. Optimisation approach provides the maximum value at the cost of 1100 simulation runs (N.B. the optimisation was performed for 100 iterations using central difference formulation and n_e=10). Initiating the production from low oil rate potential wells (i.e. Prioritisation ($1/Q_o$) and Guide-rate ($1/Q_o$)) increases production from reservoir areas with a lower sweep potential; resulting in an improved sweep of the reservoir (Figure A5). Only simple sets of coefficients are employed in this study to represent initiating production

from low or high potential wells. However, the coefficients in guide rate can also be optimized (e.g. (Asadollahi et al., 2012)).

Moreover, Figure A5 shows that the continuous control delivered by Guide-rate provides greater flexibility and a higher cumulative oil production in both cases (Qo and 1/Qo). A greater difference observed between Prioritization (Qo) and Guide-rate Control (Qo) compared to the difference between Prioritization (1/Qo) and Guide-rate Control (1/Qo) shows the value of greater flexibility in non-optimum and uncertain cases. It should be noted that in this case study initiating the production from high oil rate potential wells (i.e. directly proportional to Q_o) is non-optimum due to a lower cumulative oil production.

Table A1: Production allocation test descriptions

#	**Method**	**Description**
1	Optimisation	SPSA (Section 4.4.1), control every 6 months
2	Prioritisation (Q_o)	Equation A-1: $B = 1, E = 1, A, C, D, F, G, H = 0$
3	Prioritisation ($1/Q_o$)	Equation A-1: $A = 1, F = 1, B, C, D, E, G, H = 0$
4	Guide-rate (Q_o)	Equation A-2: $A = 1, B = 1, C, D, E, F = 0$
5	Guide-rate ($1/Q_o$)	Equation A-2: $A = -1, B = 1, C, D, E, F = 0$

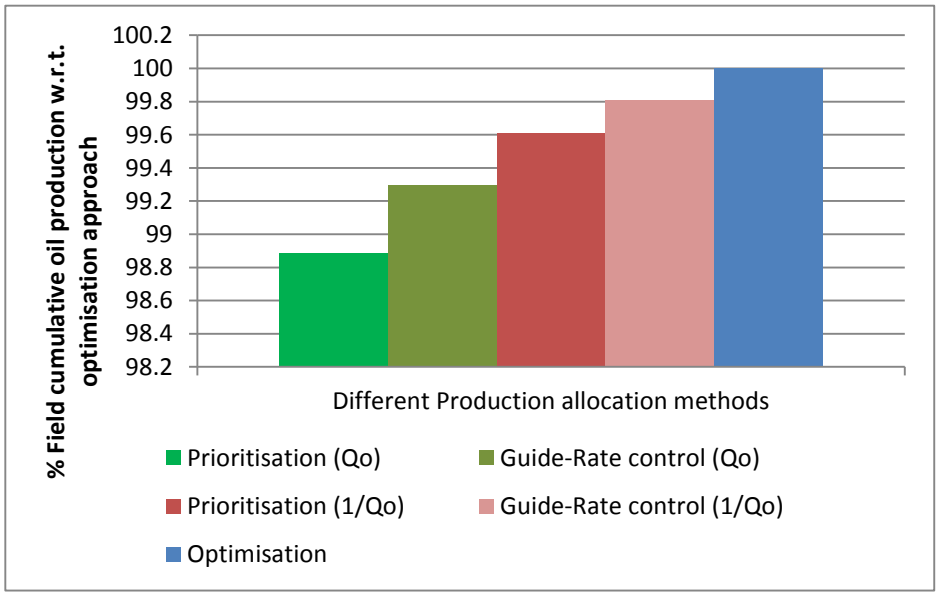

Figure A5: Percent cumulative field oil production (w.r.t. optimisation approach) when production allocation is performed using different approaches

Individual well production rates for Prioritisation ($1/Q_o$) and Guide-rate ($1/Q_o$) control are compared in Figure A6. Reduced production from high oil potential wells P2 and P4 (Figure A4) and ON/OFF control in Prioritisation are recorded. Figure A7 compares Guide-rate ($1/Q_o$) control with the optimisation approach. The greater cumulative oil production in the optimisation approach is due to:

1. No prior assumption on the control type: a continous control of well rates is assumed which can operate at 0 (shut) or 1 (fully-open) if it is optimum at some control steps. By contrast guide-rate control or prioritisation approach consider the prior assumption that only a continous control or an ON/OFF control is suitable during the whole prduction period, respectivley.
2. Recongnise long-term objectives and correlation between control variables: for example, well P3 is prone to early water breakthrough if production from P4 is chocked back significantly. This is alleviated in the optimum solution by higher production from P4 and stopping production from P3, resulting in higher production from P2 and a better sweep as compared to Guide-rate ($1/Q_o$) control.

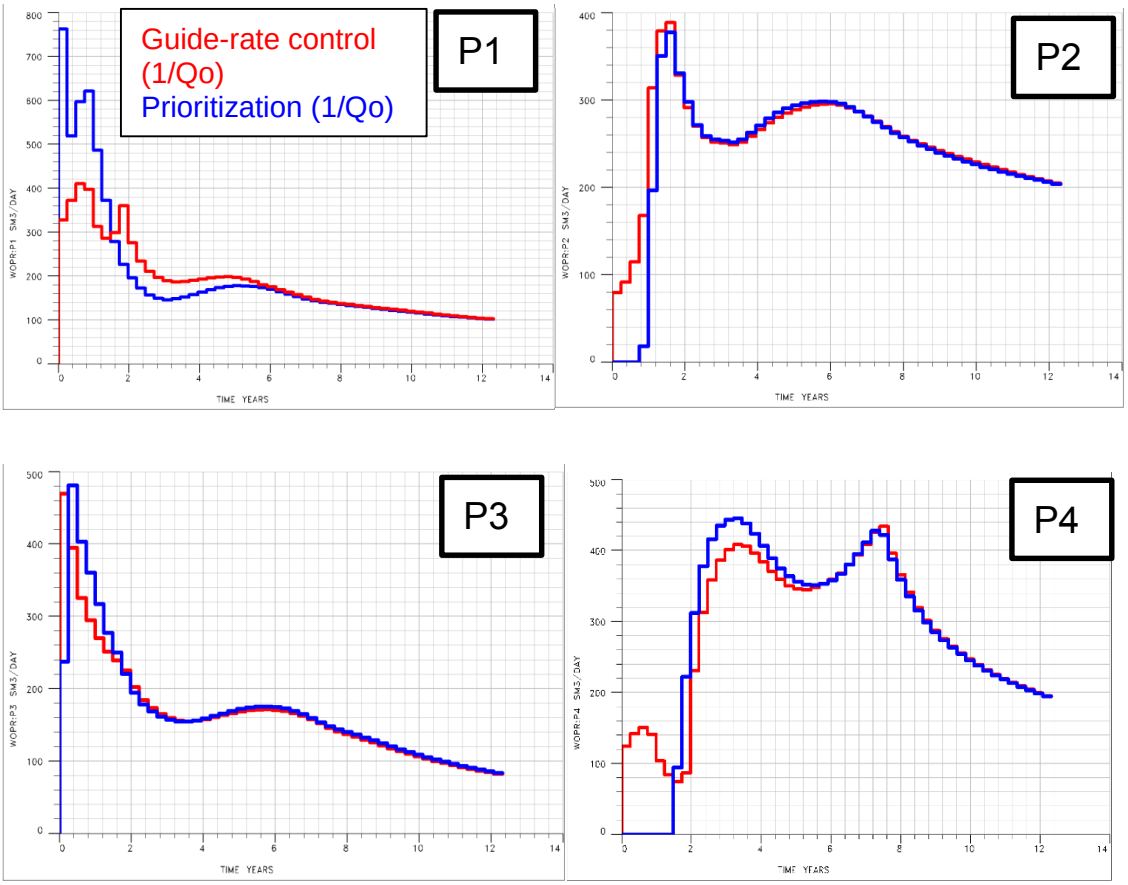

Figure A6: Individual well production rate in Prioritisation $(1/Q_o)$ and Guide-rate $(1/Q_o)$ control

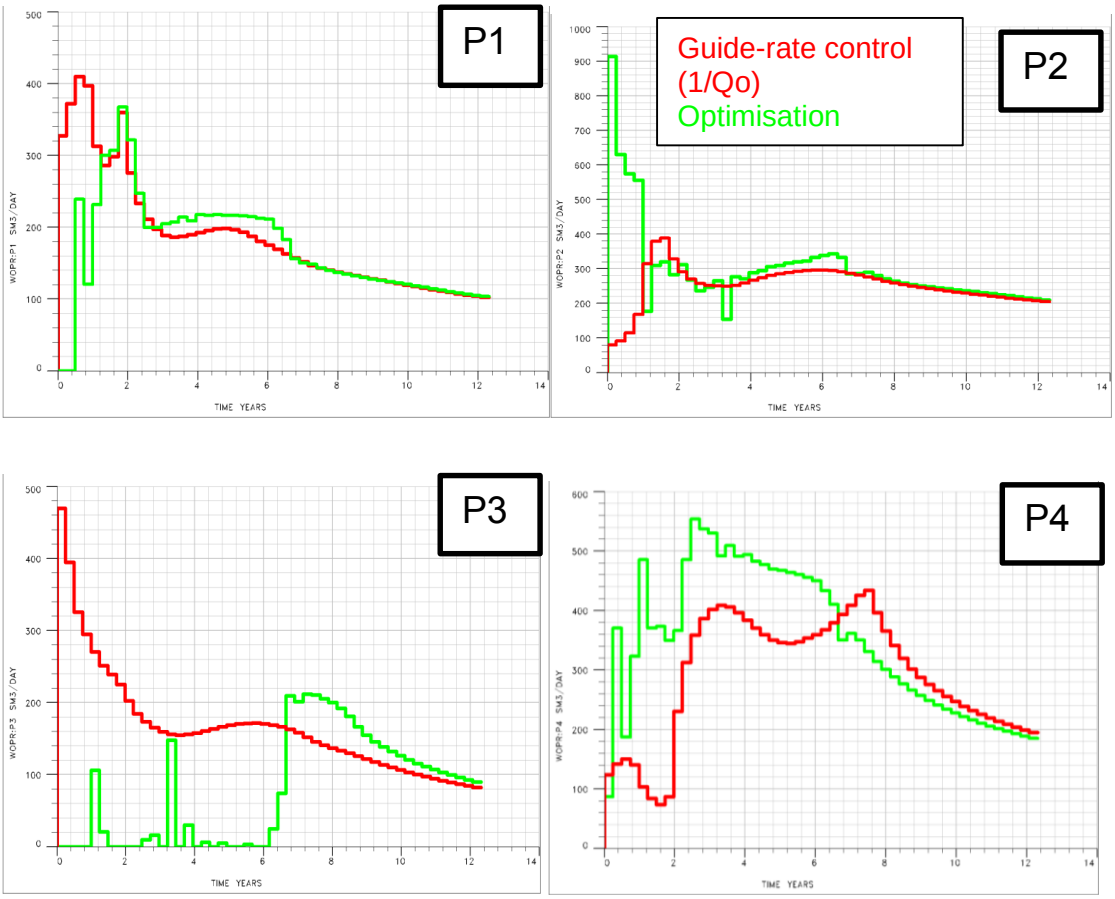

Figure A7: Individual well production rate in optimum control and Guide-rate ($1/Q_o$) control

Appendix B – Comparison of SPSA and a commercially available GA for proactive optimisation of ICVs

The MEPO software package (SPTGroup, 2012) provides a convenient implementation of GA for use with various commercial reservoir simulators. Proactive optimisation of ICVs with the I-well located at an optimum well location within the PUNQ-S3 reservoir model (Section 4.5.2) was performed using GA in MEPO and compared with the SPSA optimisation results. Further comparisons are available in (Haghighat Sefat et al., 2013).

Several sensitivity studies were performed together with the use of available "rule of thumb" to find the best values of the tuning parameters of GA. A population size of 80 with a 50% replacement gave the best performance. Iterations in GA and SPSA cannot be directly compared since they require a different number of objective function evaluations. The same computational power, equal to 1000 objective function evaluations, is assigned to both algorithms. Both algorithms are stochastic, hence random effects play an important role in the optimisation and a comparison based on a single run of each algorithm is incorrect. Five independent runs were performed in order to eliminate these random effects originating from the random number generator and the average results area shown in Figure C1. The use of stochastically estimated gradient in SPSA can result in stepping in a non-optimum direction during some iterations, decreasing the objective function value. Blocking is performed to plot the results of SPSA (i.e. if the value of the objective function decreases at some iteration previous maximum value is shown). The optimisation starts from the initial point with fully open ICVs during the whole production period in both algorithms.

Figure C1 shows that SPSA outperforms GA due to a faster improvement in the objective function. The complex search space in this example is characterised by several local optima (Section 4.5). Moreover, the I-well's optimum location together with the use of liquid rate constraints reduces the value of the production optimisation i.e. the value of the optimised objective function is close to that of the base case with no-control (Table 4-2). This is a difficult situation for GA due to the global search behaviour of the algorithm. By contrast, it is favourable to SPSA due to its fast local movement using gradient.

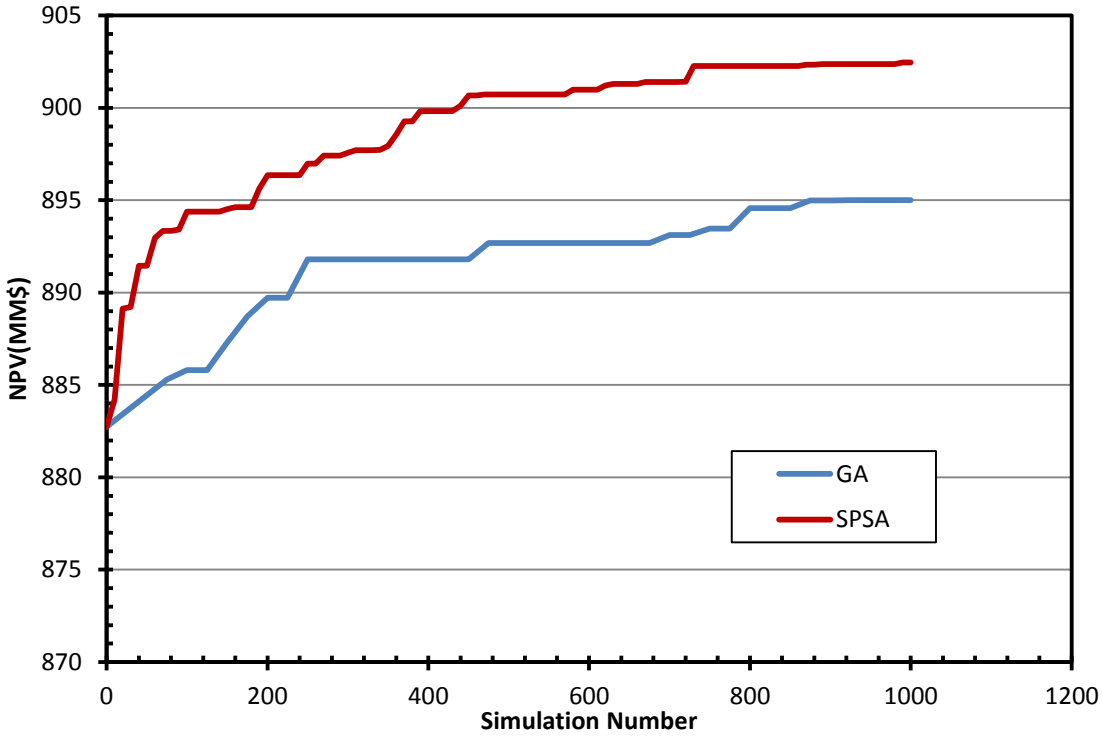

Figure C1: Comparison of the performance of SPSA and GA versus the number of simulation runs

References

Al-Khelaiwi, F. T. 2013. *A Comprehensive Approach to the Design of Advanced Well Completions.* PhD, Heriot-Watt University.

Alghareeb, Z., Horne, R. N., Yuen, B. B. W. & Shenawi, S. H. 2009. Proactive Optimization of Oil Recovery in Multilateral Wells Using Real Time Production Data. *SPE Annual Technical Conference and Exhibition.* New Orleans, Louisiana: Society of Petroleum Engineers.

Alhuthali, A. H. H., Datta-Gupta, A., Yuen, B. B. W. & Fontanilla, J. P. 2008. Optimal Rate Control Under Geologic Uncertainty. *SPE/DOE Improved Oil Recovery Symposium.* Tulsa, Oklahoma, U.S.A.: Society of Petroleum Engineers.

Almeida, L. F., Vellasco, M. M. B. R. & Pacheco, M. a. C. 2010. Optimization system for valve control in intelligent wells under uncertainties. *Journal of Petroleum Science and Engineering,* 73**,** 129-140.

Asadollahi, M. & Naevdal, G. 2009. Waterflooding Optimization Using Gradient Based Methods. *SPE/EAGE Reservoir Characterization and Simulation Conference.* Abu Dhabi, UAE: Society of Petroleum Engineers.

Asadollahi, M., Nævdal, G. & Shafieirad, A. 2012. Efficient workflow for optimizing well controls. *Journal of Petroleum Science and Engineering,* 82–83**,** 66-74.

Asadollahi, M., Nævdal, G., Dadashpour, M. & Kleppe, J. 2014. Production optimization using derivative free methods applied to Brugge field case. *Journal of Petroleum Science and Engineering,* 114**,** 22-37.

Bailey, W. J. & Couet, B. 2005. Field Optimization Tool for Maximizing Asset Value. *SPE Reservoir Evaluation & Engineering,* 8**,** 7-21.

Ben-Hur, A., Elisseeff, A. & Guyon, I. A stability based method for discovering structure in clustered data. Pacific symposium on biocomputing, 2001. 6-17.

Birchenko, V. M., Demyanov, V., Konopczynski, M. R. & Davies, D. R. 2008. Impact of Reservoir Uncertainty on Selection of Advanced Completion Type. *SPE Annual Technical Conference and Exhibition.* Denver, Colorado, USA: Society of Petroleum Engineers.

Borg, I. & Groenen, P. J. 2005. *Modern multidimensional scaling: Theory and applications*, Springer.

Bowman, A. W. & Azzalini, A. 1997. *Applied Smoothing Techniques for Data Analysis : The Kernel Approach with S-Plus Illustrations: The Kernel Approach with S-Plus Illustrations*, OUP Oxford.

Brekke, K. & Lien, S. C. 2013. New and Simple Completion Methods for Horizontal Wells Improve the Production Performance in High-Permeability, Thin Oil Zones. *SPE Drilling & Completion,* 9**,** 205-209.

Brouwer, D. R. & Jansen, J.-D. 2004. Dynamic Optimization of Waterflooding With Smart Wells Using Optimal Control Theory. *SPE Journal,* 9**,** 391-402.

Caers, J. & Park, K. A distance-based representation of reservoir uncertainty: the metric EnKF. ECMOR XI-11th European Conference on the Mathematics of Oil Recovery, 2008.

Campbell, J. R. All-Electric Intelligent Well System. SPE Aberdeen 2nd Inwell Flow Surveillance and Control Seminar, 2015 Aberdeen, UK. SPE.

Capolei, A., Suwartadi, E., Foss, B. & Jørgensen, J. B. 2013. Waterflooding optimization in uncertain geological scenarios. *Computational Geosciences,* 17**,** 991-1013.

Capolei, A., Suwartadi, E., Foss, B. & Jørgensen, J. B. 2015. A mean–variance objective for robust production optimization in uncertain geological scenarios. *Journal of Petroleum Science and Engineering,* 125**,** 23-37.

Carvajal, G. A., Boisvert, I. & Knabe, S. 2014. A Smart Flow for SmartWells: Reactive and Proactive Modes. *SPE Intelligent Energy Conference and Exhibition.* Utrecht, The Netherlands: Society of Petroleum Engineers.

Chen, C., Li, G. & Reynolds, A. C. 2011. Robust Constrained Optimization of Short and Long-Term NPV for Closed-Loop Reservoir Management. *SPE Reservoir Simulation Symposium.* The Woodlands, Texas, USA: Society of Petroleum Engineers.

Chen, W., Wiecek, M. M. & Zhang, J. 1999. Quality Utility—A Compromise Programming Approach to Robust Design. *Journal of Mechanical Design,* 121**,** 179-187.

Chen, Y. & Oliver, D. S. 2009. Ensemble-Based Closed-Loop Optimization Applied to Brugge Field. *SPE reservoir Simulation Symposium.* The Woodland, Texas, U.S.A.: Society of Petroleum Engineers.

Chen, Y., Oliver, D. S. & Zhang, D. 2009. Efficient Ensemble-Based Closed-Loop Production Optimization. *SPE Journal,* 14**,** 634-645.

Chen, Y., Wiesel, A., Eldar, Y. C. & Hero, A. O. 2010. Shrinkage Algorithms for MMSE Covariance Estimation. *IEEE Transactions on Signal Processing,* 58**,** 5016-5029.

Christie, M., Demyanov, V. & Erbas, D. 2006. Uncertainty quantification for porous media flows. *Journal of Computational Physics,* 217**,** 143-158.

Coats, B. K., Fleming, G. C., Watts, J. W., Rame, M. & Shiralkar, G. S. 2004. A Generalized Wellbore and Surface Facility Model, Fully Coupled to a Reservoir Simulator. *SPE Reservoir Evaluation & Engineering,* 7**,** 132-142.

Da Silva, M. F., Muradov, K. M. & Davies, D. R. 2012. Review, Analysis and Comparison of Intelligent Well Monitoring Systems. *SPE Intelligent Energy International.* Utrecht, The Netherland: Society of Petroleum Engineers.

Das, O. P., Al-Enezi, K., Aslam, M., El-Gezeeri, T., Ziyab, K., Fipke, S. R. & Ewens, S. 2012. Novel Design and Implementation of Kuwait's First Smart Multilateral Well with Inflow Control Device and Inflow Control Valve for Life-cycle Reservoir Management in High Mobility Reservoir, West Kuwait. *SPE Annual Technical Conference and Exhibition.* San Antonio, Texas, USA: Society of Petroleum Engineers.

Demyanov, V., Gopa, K., Arnold, D. & Elfeel, M. A. 2014. Production Optimisation under Uncertainty in Fractured Reservoirs. *ECMOR XIV - 14th European conference on the mathematics of oil recovery.* Italy: EAGE.

Do, S. & Reynolds, A. 2013. Theoretical connections between optimization algorithms based on an approximate gradient. *Computational Geosciences,* 17**,** 959-973.

Eberhart, R. & Kennedy, J. A new optimizer using particle swarm theory. Micro Machine and Human Science, 1995. MHS '95., Proceedings of the Sixth International Symposium on, 4-6 Oct 1995 1995. 39-43.

Eclipse 2012. ECLIPSE Reference Manuals. *Technical Description, Chapter 49.* Abingdon, U.K.: Schlumberger.

Eltaher, E. K., Muradov, K., Davies, D. R. & Grebenkin, I. M. 2014. Autonomous Inflow Control Valves - their Modelling and "Added Value&quot. *SPE Annual Technical Conference and Exhibition.* Amsterdam, The Netherlands: Society of Petroleum Engineers.

Floris, F. J. T., Bush, M. D., Cuypers, M., Roggero, F. & Syversveen, A.-R. 2001. Methods for quantifying the uncertainty of production forecasts: a comparative study. *Petroleum Geoscience,* 7**,** S87-S96.

Fonseca, R., Stordal, A., Leeuwenburgh, O., Van Den Hof, P. & Jansen, J. Robust ensemble-based multi-objective optimization. ECMOR XIV-14th European conference on the mathematics of oil recovery, 2014.

Fonseca, R. M., Kahrobaei, S. S., Van Gastel, L. J. T., Leeuwenburgh, O. & Jansen, J. D. 2015. Quantification of the Impact of Ensemble Size on the Quality of an Ensemble Gradient Using Principles of Hypothesis Testing. *SPE Reservoir Simulation Symposium.* Houston, Texas, USA: Society of Petroleum Engineers.

Forouzanfar, F., Li, G. & Reynolds, A. C. 2010. A Two-Stage Well Placement Optimization Method Based on Adjoint Gradient. *SPE Annual Technical Conference and Exhibition.* Florence, Italy: Society of Petroleum Engineers.

Forouzanfar, F., Poquioma, W. E. & Reynolds, A. C. 2015. A Covariance Matrix Adaptation Algorithm for Simultaneous Estimation of Optimal Placement and Control of Production and Water Injection Wells. *SPE Reservoir Simulation Symposium.* Houston, Texas, USA: Society of Petroleum Engineers.

Fripp, M., Zhao, L. & Least, B. 2013. The Theory of a Fluidic Diode Autonomous Inflow Control Device. *SPE Middle East Intelligent Energy Conference and Exhibition.* Dubai, UAE: Society of Petroleum Engineers.

Gao, G., Li, G. & Reynolds, A. C. 2007. A Stochastic Optimization Algorithm for Automatic History Matching. *SPE Journal,* 12**,** pp. 196-208.

Geman, S., Bienenstock, E. & Doursat, R. 1992. Neural Networks and the Bias/Variance Dilemma. *Neural Computation,* 4**,** 1-58.

Giles, M. & Pierce, N. 2000. An Introduction to the Adjoint Approach to Design. *Flow, Turbulence and Combustion,* 65**,** 393-415.

Golzari, A., Haghighat Sefat, M. & Jamshidi, S. 2015. Development of an Adaptive Surrogate Model for Production Optimization. *Journal of petroleum Science and Engineering,* 133**,** 677-688.

Grebenkin, I. & Davies, D. R. 2010. Analysis of the Impact of an Intelligent Well Completion on the Oil Production Uncertainty. *SPE Russian Oil and Gas Conference and Exhibition.* Moscow, Russia: Society of Petroleum Engineers.

Grebenkin, I. M. & Davies, D. R. 2012. A Novel Optimisation Algorithm for Inflow Control Valve Management. *SPE Europec/EAGE Annual Conference.* Copenhagen, Denmark: Society of Petroleum Engineers.

Grebenkin, I. M. 2013. *A New Optimisation Procedure for Uncertainty Reduction by Intelligent Wells during Field Development Planning.* PhD Thesis, Heriot-Watt University.

Guyaguler, B. & Byer, T. J. 2008. A New Rate-Allocation-Optimization Framework. *SPE Production & Operations,* 23**,** 448 - 457.

Haghighat Sefat, M., Muradov, K. M. & Davies, D. R. 2013. Field Management by Proactive Optimisation of Intelligent Wells - A Practical Approach. *SPE Middle East Intelligent Energy Conference and Exhibition.* Dubai, UAE.

Haghighat Sefat, M., Muradov, K. M., Elsheikh, A. H. & Davies, D. R. 2014. Reservoir Uncertainty-tolerant, Proactive Control of Intelligent Wells. *ECMOR XIV - 14th European conference on the mathematics of oil recovery* Italy: EAGE

Haghighat Sefat, M., Muradov, K. M., Elsheikh, A. H. & Davies, D. R. 2015. Proactive Optimization of Intelligent Well Production Using Stochastic Gradient-Based Algorithms. *SPE Reservoir Evaluation & Engineering*.

Hajizadeh, Y., Amorim, E. & Sousa, M. C. 2012. Building Trust in History Matching: The Role of Multidimensional Projection. *SPE Europec/EAGE Annual Conference.* Copenhagen, Denmark: Society of Petroleum Engineers.

Halvorsen, M., Elseth, G. & Naevdal, O. M. 2012. Increased oil production at Troll by autonomous inflow control with RCP valves. *SPE Annual Technical Conference and Exhibition.* San Antonio, Texas, USA: Society of Petroleum Engineers.

Haug, B. T. 1992. The Second Long-Term Horizontal Well Test in Troll: Successful Production From a 13-in. Oil Column With the Well Partly Completed in the Water Zone. *Annual Technical Conference and Exhibition.* Washington, DC: Society of Petroleum Engineers.

Holland, J. H. 1992. *Adaptation in Natural and Artificial Systems: An Introductory Analysis with Applications to Biology, Control and Artificial Intelligence*, MIT Press.

Holmes, J. A., Barkve, T. & Lund, O. 1998. Application of a Multisegment Well Model to Simulate Flow in Advanced Wells. *SPE European Petroleum Conference.* Netherlands: Society of Petroleum Engineers.

Holmes, J. A. 2011. Modeling Advanced Wells in Reservoir Simulation. *Journal of Petroleum Technology,* 53.

Jansen, J.-D., Brouwer, R. & Douma, S. G. 2009. Closed Loop Reservoir Management. *SPE Reservoir Simulation Symposium.* The Woodlands, Texas, USA: Society of Petroleum Engineers.

Jansen, J. D., Wagenvoort, A. M., Droppert, V. S., Daling, R. & Glandt, C. A. 2002. Smart Well Solutions for Thin Oil Rims: Inflow Switching and the Smart Stinger Completion. *In:* Engineers, S. O. P. (ed.) *SPE Asia Pacific Oil and Gas Conference and Exhibition.* Melbourne, Australia: Society of Petroleum Engineers.

Jansen, J. D. 2011. Adjoint-based optimization of multi-phase flow through porous media – A review. *Computers & Fluids,* 46**,** 40-51.

Jolliffe, I. T. 2002. *Principal Component Analysis,* Springer.

Kawaguchi, K., Takekawa, M., Ohtani, T. & Wada, H. 2013. Optimal Sensor Placement for Multi-Phase Flow Rate Estimation Using Pressure and Temperature Measurements. *SPE Digital Energy Conference.* The Woodlands, Texas, USA: Society of Petroleum Engineers.

Kernler, D. 2014. CC BY-SA 4.0: Creative Commons. Available: https://commons.wikimedia.org/w/index.php?curid=36506025.

Kiefer, J. & Wolfowitz, J. 1952. Stochastic Estimation of the Maximum of a Regression Function. *The Annals of Mathematical Statistics,* 23**,** 462-466.

Kourounis, D., Durlofsky, L. J., Jansen, J. D. & Aziz, K. 2014. Adjoint formulation and constraint handling for gradient-based optimization of compositional reservoir flow. *Computational Geosciences,* 18**,** 117-137.

Least, B., Greci, S., Konopczynski, M. & Thornton, K. 2013. Inflow Control Devices Improve Production in Heavy Oil Wells. *SPE Middle East Intelligent Energy Conference and Exhibition.* Dubai, UAE: Society of Petroleum Engineers.

Li, G. & Reynolds, A. 2011. Uncertainty quantification of reservoir performance predictions using a stochastic optimization algorithm. *Computational Geosciences,* 15**,** 451-462.

Li, L., Jafarpour, B. & Mohammad-Khaninezhad, M. R. 2013. A simultaneous perturbation stochastic approximation algorithm for coupled well placement and control optimization under geologic uncertainty. *Computational Geosciences,* 17**,** 167-188.

Lien, M. E., Brouwer, D. R., Mannseth, T. & Jansen, J.-D. 2008. Multiscale Regularization of Flooding Optimization for Smart Field Management. *SPE Journal,* 13**,** 195-204.

Lien, S. C., Seines, K., Havig, S. O. & Kydland, T. 1991. The First Long-Term Horizontal-Well Test in the Troll Thin Oil Zone. *Journal of Petroleum Technology,* 43.

Lorentzen, R. J., Berg, A., Naevdal, G. & Vefring, E. H. 2006. A New Approach For Dynamic Optimization Of Water Flooding Problems. *SPE Intelligent Energy Conference and Exhibition.* Amsterdam, The Netherlands: Society of Petroleum Engineers.

Malakooti, R. 2015. *Remote Soft Sensing.* PhD, Heriot-Watt University.

Mckay, M. D., Beckman, R. J. & Conover, W. J. 1979. A Comparison of Three Methods for Selecting Values of Input Variables in the Analysis of Output from a Computer Code. *Technometrics,* 21**,** 239-245.

Mohaghegh, S. 2000. Virtual-Intelligence Applications in Petroleum Engineering: Part 2—Evolutionary Computing. *Journal of Petroleum Technology,* 52**,** 40-46.

Mohaghegh, S. D., Liu, J. S., Gaskari, R., Maysami, M. & Olukoko, O. A. 2012. Application of Surrogate Reservoir Models (SRM) to am Onshore Green Field in Saudi Arabia; Case Study. *North Africa Technical Conference and Exhibition.* Cairo, Egypt: Society of Petroleum Engineers.

Moradidowlatabad, M., Muradov, K. M. & Davies, D. 2014. Novel Workflow to Optimise Annular Flow Isolation in Advanced Wells. *International Petroleum Technology Conference.* Kuala Lumpur, Malaysia: International Petroleum Technology Conference.

Mulvey, J. M., Vanderbei, R. J. & Zenios, S. A. 1995. Robust optimization of large-scale systems. *Operations research,* 43**,** 264-281.

Muradov, K. 2010. *Temperature Modelling and Real-time Flow Rate Allocation in Wells with Advanced Completion.* PhD, Heriot-Watt University.

Naus, M. M. J. J., Dolle, N. & Jansen, J. D. 2006. Optimization of commingled production using infinitely variable inflow control valves. *Spe Production & Operations,* 21**,** 293-301.

Neyman, J. & Pearson, E. S. 1933. On the Problem of the Most Efficient Tests of Statistical Hypotheses. *Philosophical Transactions of the Royal Society of London A: Mathematical, Physical and Engineering Sciences,* 231**,** 289-337.

Nikravesh, M., Zadeh, L. A. & Aminzadeh, F. 2003. *Soft computing and intelligent data analysis in oil exploration,* Elsevier.

Oliveira, D. F. & Reynolds, A. C. 2015. Hierarchical Multiscale Methods for Life-Cycle-Production Optimization: A Field Case Study. *SPE Journal,* 20**,** 896-907.

Oliver, D. & Chen, Y. 2011. Recent progress on reservoir history matching: a review. *Computational Geosciences,* 15**,** 185-221.

Oliver, D. S., Reynolds, A. C. & Liu, N. 2008. *Inverse theory for petroleum reservoir characterization and history matching,* Cambridge University Press.

Olken, F. 1993. *Random sampling from databases.* University of California at Berkeley.

Park, K. 2011. *Modeling Uncertainty in Metric Space.* PhD PhD Thesis, Stanford University.

Peters, L., Arts, R., Brouwer, G. & Geel, C. 2010. Results of the Brugge Benchmark Study for Flooding Optimisation and History Matching. *SPE Reservoir Evaluation & Engineering,* 13**,** 391-405.

Petvipusit, K., Elsheikh, A., Laforce, T., King, P. & Blunt, M. 2014. Robust optimisation of CO2 sequestration strategies under geological uncertainty using adaptive sparse grid surrogates. *Computational Geosciences,* 18**,** 763-778.

Pinto, M. a. S., Barreto, C. E. & Schiozer, D. J. 2012. Optimization of Proactive Control Valves of Producer and Injector Smart Wells under Economic Uncertainty. *SPE Europec/EAGE Annual Conference.* Copenhagen, Denmark: Society of Petroleum Engineers.

Potiani, M. & Eduardo, M. 2014. A Review of IC Installations: Lessons Learned from Electric-Hydraulic, Hydraulic and All-Electric Systems. *Offshore Technology Conference.* Houston, Texas, USA: SPE.

Rahman, J. U., Allen, C. & Bhat, G. 2012. Second Generation Interval Control Valve (ICV) Improves Operational Efficiency and Inflow Performance in Intelligent Completions. *North Africa Technical Conference and Exhibition.* Cairo, Egypt: Society of Petroleum Engineers.

Raniolo, S., Dovera, L., Cominelli, A., Callegaro, C. & Masserano, F. History Match and Polymer Injection Optimization in a Mature Field Using the Ensemble Kalman Filter. IOR 2013-From Fundamental Science to Deployment, 2013.

Ratterman, E. E., Augustine, J. R. & Voll, B. A. 2005. New Technology Applications to Increase Oil Recovery by Creating Uniform Flow Profiles in Horizontal Wells: Case Studies and Technology Overview. *International Petroleum Technology Conference h.* Doha, Qatar: International Petroleum Technology Conference.

Robinson, M. 2003. Intelligent well completions. *Journal of Petroleum Technology,* 55**,** 57-59.

Rousseeuw, P. J. 1987. Silhouettes: A graphical aid to the interpretation and validation of cluster analysis. *Journal of Computational and Applied Mathematics,* 20**,** 53-65.

Rousset, M. H., Huang, C., Klie, H. & Durlofsky, L. 2014. Reduced-order modeling for thermal recovery processes. *Computational Geosciences,* 18**,** 401-415.

Rubbo, R. & Littleford, S. J. 1998. [2]4 New Completion Technology for Interventionless Reservoir Management. *World Petroleum Congress.* World Petroleum Congress.

Sadegh, P. & Spall, J. C. 1998. Optimal random perturbations for stochastic approximation using a simultaneous perturbation gradient approximation. *Automatic Control, IEEE Transactions on,* 43**,** 1480-1484.

Sarma, P., Chen, W. H., Durlofsky, L. J. & Aziz, K. 2006. Production Optimization With Adjoint Models Under Nonlinear Control-State Path Inequality Constraints. *Intelligent Energy Conference and Exhibition.* Amsterdam, The Netherlands: Society of Petroleum Engineers.

Scheidt, C. & Caers, J. 2013. Uncertainty Quantification in Reservoir Performance Using Distances and Kernel Methods--Application to a West Africa Deepwater Turbidite Reservoir. *SPE Journal,* 14**,** 680-692.

Seber, G. a. F. 2004. *Multivariate Observations*, Wiley.

Sharpe, W. F. 1994. The sharpe ratio. *The journal of portfolio management,* 21**,** 49-58.

Shaw, J. 2011. Comparison of Downhole Control System Technologies for Intelligent Completions. *Canadian Unconventional Resources Conference.* Calgary, Alberta, Canada: Society of Petroleum Engineers.

Siraj, M. M., Hof, P. M. J. V. D. & Jansen, J. D. Risk management in oil reservoir water-flooding under economic uncertainty. 2015 54th IEEE Conference on Decision and Control (CDC), 15-18 Dec. 2015 2015. 7542-7547.

Snider, P. & Fraley, K. 2007. Marathon, partners adapt RFID technology for downhole drilling, completion applications. *Drilling Contractor,* March/April 2007**,** 40-42.

Spall, J., Hill, S. & Stark, D. 2006. Theoretical Framework for Comparing Several Stochastic Optimization Approaches. *In:* Calafiore, G. & Dabbene, F. (eds.) *Probabilistic and Randomized Methods for Design under Uncertainty.* Springer London.

Spall, J. C. 1992. Multivariate stochastic approximation using a simultaneous perturbation gradient approximation. *Automatic Control, IEEE Transactions on,* 37**,** 332-341.

Spall, J. C. 1997. Accelerated second-order stochastic optimization using only function measurements. *Decision and Control, 1997., Proceedings of the 36th IEEE Conference on,* 2**,** 1417-1424.

Spall, J. C. 1998. Implementation of the simultaneous perturbation algorithm for stochastic optimization. *Aerospace and Electronic Systems, IEEE Transactions on,* 34**,** 817-823.

Spall, J. C. 2003. *Introduction to stochastic search and optimization: Estimation, Simulation, and Control*, John Wiley and Sons.

Speyer, J. L. & Jacobson, D. H. 2010. *Primer on Optimal Control Theory*, Society for Industrial and Applied Mathematics.

Sptgroup 2012. MEPO User Manual Version 4.1.

Stordal, A. S., Szklarz, S. & Leeuwenburgh, O. A Closer Look at Ensemble-based Optimization in Reservoir Management. ECMOR XIV-14th European conference on the mathematics of oil recovery, 2014.

Suwartadi, E., Krogstad, S. & Foss, B. A. 2009. On State Constraints of Adjoint Optimization in Oil Reservoir Waterflooding. *SPE/EAGE Reservoir Characterization and Simulation Conference.* Abu Dhabi, UAE: Society of Petroleum Engineers.

Tavakoli, R., Srinivasan, S. & Wheeler, M. F. 2014. Rapid Updating of Stochastic Models by Use of an Ensemble-Filter Approach. *SPE Journal,* 19**,** 500-513.

Tendeka. 2013. *SigNet™ wireless intelligent completion technology* [Online]. Available: http://www.tendeka.com/product-ranges/wireless-technologies/.

Thiele, M. R., Batycky, R. P., Blunt, M. J. & Orr, F. M., Jr. 1996. Simulating Flow in Heterogeneous Systems Using Streamtubes and Streamlines. *SPE Reservoir Engineering,* 5.

Thorndike, R. 1953. Who belongs in the family? *Psychometrika,* 18**,** 267-276.

Tiwari, A. & Roy, R. 2002. Variable dependence interaction and multi-objective optimisation. *Proceedings of the 4th Annual Conference on Genetic and Evolutionary Computation.* New York City, New York: Morgan Kaufmann Publishers Inc.

Vachon, G. P. & Lee, J. 2007. Production Optimization Through a Well-Centric Intelligent System. *Asia Pacific Oil and Gas Conference and Exhibition.* Jakarta, Indonesia: Society of Petroleum Engineers.

Van Doren, J. F. M., Markovinović, R. & Jansen, J.-D. 2006. Reduced-order optimal control of water flooding using proper orthogonal decomposition. *Computational Geosciences,* 10**,** 137-158.

Van Essen, G., Hof, P. V. D. & Jansen, J.-D. 2011. Hierarchical Long-Term and Short-Term Production Optimization. *SPE Journal,* 16**,** pp. 191-199.

Van Essen, G., Zandvliet, M., Van Den Hof, P., Bosgra, O. & Jansen, J.-D. 2013. Robust Waterflooding Optimization of Multiple Geological Scenarios. *SPE Journal,* 14**,** 202-210.

Wang, C., Li, G. & Reynolds, A. C. 2009. Production Optimization in Closed-Loop Reservoir Management. *SPE Journal,* 14**,** pp. 506-523.

Wang, H., Echeverría-Ciaurri, D., Durlofsky, L. & Cominelli, A. 2012. Optimal Well Placement Under Uncertainty Using a Retrospective Optimization Framework. *Spe Journal,* 17**,** 112-121.

Wilson, K. C. & Durlofsky, L. J. 2013. Optimization of shale gas field development using direct search techniques and reduced-physics models. *Journal of Petroleum Science and Engineering,* 108**,** 304-315.

Yeten, B., Durlofsky, L. J. & Aziz, K. 2003. Optimization of Nonconventional Well Type, Location, and Trajectory. *SPE Journal,* 8**,** 200-210.

Zandvliet, M., Handels, M., Van Essen, G., Brouwer, R. & Jansen, J.-D. 2013. Adjoint-Based Well-Placement Optimization Under Production Constraints. *SPE Journal,* 13**,** 392-399.

Zhao, H., Chen, C., Do, S. T., Li, G. & Reynolds, A. C. 2011a. Maximization of a Dynamic Quadratic Interpolation Model for Production Optimization. *SPE*

Reservoir Simulation Symposium. The Woodlands, Texas, USA: Society of Petroleum Engineers.

Zhao, H., Li, Y., Yao, J. & Zhang, K. 2011b. Theoretical research on reservoir closed-loop production management. *Science China Technological Sciences,* 54**,** 2815-2824.

Zhao, H., Chen, C. H., Do, S., Oliveira, D., Li, G. M. & Reynolds, A. C. 2013. Maximization of a Dynamic Quadratic Interpolation Model for Production Optimization. *Spe Journal,* 18**,** 1012-1025.

Zingg, D. W., Nemec, M. & Pulliam, T. H. 2008. A comparative evaluation of genetic and gradient-based algorithms applied to aerodynamic optimization. *European Journal of Computational Mechanics/Revue Européenne de Mécanique Numérique,* 17**,** 103-126.

Zuber, N. & Findlay, J. A. 1965. Average Volumetric Concentration in Two-Phase Flow Systems. *Journal of Heat Transfer,* 87**,** 453-468.